University of Cape Town,
Department of Geological Sciences

The Metamorphic Evolution of an Ancient Accretionary Prism in the Southern Zone of the Damara Belt in Namibia

Clayton Cross

Dissertation submitted in total fulfilment of the requirements of the degree Master of Science

Supervised by
Dr J. F. A. Diener & Dr A. Fagereng

16 October 2013

The financial assistance of the National Research Foundation (NRF) towards this research is hereby acknowledged. Opinions expressed and conclusions arrived at, are those of the author and are not necessarily to be attributed to the NRF.

Abstract

The Southern Zone of the Damara Belt in central Namibia has an apparent stratigraphic thickness that exceeds 100 km and is comprised of highly strained, metamorphosed clastic sedimentary rocks that are intercalated with slices of metamorphosed basalt and gabbro. One of the only modern geological environments in which such vast amounts of sediments can be accumulated, with intercalated mafic rocks, is in an accretionary prism above a subduction zone, where the accreted material is also subjected to high pressure – low temperature metamorphic conditions and deformation to high strains. This has been suggested as the origin of the Southern Zone.

Samples collected from two localities within and immediately adjacent to the Southern Zone include representative rocks of both metapelitic and metamafic compositions. The inferred peak mineral assemblage in the metapelitic rocks consists of weak to moderately zoned garnet, staurolite and in some cases, kyanite porphyroblasts set in a fine-grained matrix of chlorite, biotite, muscovite, paragonite, epidote, ilmenite and quartz. The matrix exhibits a penetrative foliation that is defined by the alignment of the micaceous minerals. The garnet, staurolite and kyanite porphyroblasts overprint this fabric. By contrast, the metamafic rocks are very fine-grained with an inferred peak mineral assemblage of zoned amphibole, epidote, rutile, quartz, biotite and in some cases, chlorite and sphene. The amphibole and micaceous minerals define a distinct fabric. None of the minerals occur as porphyroblasts that overprint this fabric.

The results of thermodynamic modelling using THERMOCALC indicate that the inferred peak mineral assemblages (*M1b*) in the metapelites and metamafics formed at temperatures of ~ 600 °C and pressures of ~ 9.8 kbar in the Gaub Canyon, and temperatures of ~ 605 °C and pressures of ~ 10.5 kbar in the Kuiseb Canyon. These P-T conditions correspond to geothermal gradients of ~ 18.5 °C/km and ~ 17.3 °C/km, respectively, assuming a density of 2.7 g/cm^3. However, it is evident that fabric formation in the rocks from the Gaub and Kuiseb Canyons may have formed at consistent pressures, but at significantly lower temperatures. In rocks from the Gaub Canyon, the early, syn-tectonic fabric-forming mineral assemblages (*M1a*) record P-T conditions of ~ 8.4 to 11.8 kbar and ~ 535 to 550 °C, whereas in the rocks from the Kuiseb Canyon, they record P-T conditions of 10.5 to 10.8 kbar and ~ 540 to 545 °C. These P-T conditions equate to lower geothermal gradients of ~ 16.6 °C/km and ~ 15.1 °C/km, repsectively. The recorded pressure conditions for the Gaub (~ 9.8 kbar) and Kuiseb (~ 10.5 kbar) Canyons correspond to the burial of the accreted material to depths of ~ 30 km and ~ 33 km, respectively.

The likely P-T path for these rocks involves a near-isobaric increase in temperature of ~ 60 °C in the Gaub and Kuiseb Canyons while the rocks were near peak pressure. The apparent lack of deformation and rotation of the porphyroblasts that overprint the penetrative foliation in the metapelites and the fact that the pressure range at which fabric formation (*M1a*) occured overlaps with the pressures at which the inferred peak mineral assemblages (*M1b*) are stable, implies that the increase in temperature occured in a static environment, without concomitant deformation or changes in differential strain and was probably as a result of a fairly rapid heat pulse.

It is speculated that the increase in temperature is most likely to have been due to the subduction of a heat source, perhaps the spreading ridge that had once formed the Khomas Sea. This is substantiated by four key findings: Firstly, by the refutation of long-lived convergence, a change in the angle of subduction and continental crust collision as alternative geodynamic factors potentially responsible for the increase in temperature; secondly, by the resemblance of the metamorphic evolution of the Gaub and Kuiseb Canyons to those of other known HP-LT metamorphic terranes in which the increases in temperature have been attributed to the subduction of very young, very hot oceanic crust and/or a spreading ridge; thirdly, by the ability of the subduction of a spreading ridge to effectively explain the near-isobaric, rapid heat pulse suggested by the fabric relations in the rocks of the Southern Zone; and fourthly, by the existence of the Matchless Amphibolite Member, a narrow, linear, ~ 350 km long and < ~ 3 km wide belt of metamafic rock of MORB composition that is interbedded within the accreted metapsammopelitic schists of the Southern Zone, as a plausible representation of this spreading ridge.

The combined absence of retrograde features, such as alteration rims around the overprinting porphyroblasts, the euhedral-subhedral shape of the porphyroblasts and their lack of deformation and/or rotation within the matrix provides compelling evidence that the rocks from the Gaub and Kuiseb Canyons did not experience any post-peak, collision- and exhumation-related deformation and/or fluid infiltration. This apparent lack of recognition of the collision between the Congo and Kalahari Cratons by the rocks of Gaub and Kuiseb Canyons implies that the rocks of the Southern Zone were exhumed as discrete segments with the petrographic and thermobarometric changes relating to the collisional event being concentrated along discrete exhumation thrust faults around these segments.

While the subduction of a heat source has been suggested as the geodynamic factor responsible for the metamorphic evolution of a few HP-LT terranes, it is proposed that the change in metamorphic evolution resulting from the subduction of a spreading ridge is more widespread in HP-LT terranes than is currently recognised. The subduction of a spreading ridge is most likely in those HP-LT terranes where convergence was followed by collision. This is primarily due to the fact that in order for collision to occur, the entire

intervening (oceanic-) slab, including the spreading ridge, has to be completely consumed. Unfortunately, in many orogenic belts, the extensive overprinting of the HP-LT rocks during collision, or an equivalent change in tectonics, makes it challenging to distinguish the prograde increase in temperature caused by the subduction of a spreading ridge.

Department of Geological Sciences

Master of Science Dissertation: The Metamorphic Evolution of an Ancient Accretionary Prism in the Southern Zone of the Damara Belt in Namibia.

UCT

Plagiarism Declaration

According to the Merriam-Webster Online Dictionary, to "plagiarize" means

- to steal and pass off (the ideas or words of another) as one's own
- to use (another's production) without crediting the source
- to commit literary theft
- to present as new and original an idea or product derived from an existing source.

In other words, plagiarism is an act of fraud. It involves both stealing someone else's work and lying about it afterwards.

Please read this and sign:

1. Plagiarism is to use another's work and to pretend that it is one's own. I know that plagiarism is wrong.

2. I have used a standard (Harvard) referencing convention for citation and referencing. Each significant contribution to, and quotation in, this submission from the work, or works of other people, has been attributed, and has been cited and referenced.

3. This submission is my own work.

4. I have not allowed, and will not allow anyone to copy my work with the intention of passing it off as his or her own work.

I know the meaning of Plagarism and declare that all of the work in the document, save of that which is properly acknowledged, is my own.

Name: CLAYTON

Surname: CROSS

Student No: CRSCLA002

Course: GEO5001W (MSc Geochemistry)

Date: 16 October 2013

Signature:

Table of Contents

Page

List of Figures

Page

List of Tables

Page

1. Introduction

The Southern Zone of the Damara Belt in central Namibia has an apparent stratigraphic thickness that exceeds 100 km and is comprised of highly strained, metamorphosed clastic sedimentary rocks that are intercalated with slices of metamorphosed basalt and gabbro, all of which are immaculately preserved in a multitude of exposures (Miller, 1983; Kukla, 1992; Miller, 2008). One of the only modern geological environments in which such vast amounts of sediments could be accumulated with intercalated mafic rocks and subsequently subjected to deformation and metamorphism is in an accretionary prism. This was first suggested as the origin of the Southern Zone by Kukla & Stanistreet (1991).

Accretionary prisms form above subduction zones during the collision of two plates and are therefore composed of sediments derived from the top of the subducting oceanic crust, sediments supplied from the leading edge of the over-riding continental crust – including arc derived material, and slices of oceanic crust broken off the under-riding slab (Miyashiro, 1961; Ernst, 1973; Marshak, 2005; Maruyama *et al.*, 2010). The majority of known accretionary prisms in the rock record are younger than the early-Palaeozoic, circa 550 Ma (Ernst, 1973; Ernst, 1988). They contain intercalated metapsammopelitic and metamafic rocks that have a penetrative fabric that formed by deformation to high strain and mineral assemblages that record both high pressure – low temperature (HP-LT) metamorphic conditions and geothermal gradients that are colder than the stable continental geothermal gradient (~ 15.0 to 25.0 °C/km), typically between about 8.0 and 15.0 °C/km (Oxburgh & Turcotte, 1971; Ernst, 1973; Willner, 2005; Ernst, 2010). They are commonly separated from an adjacent terrane of high temperature – low pressure (HT-LP) metamorphism by a major structural feature, such as a prominent fault (Miyashiro, 1961; Oxburgh & Turcotte, 1971).

1.1. The Significance of this Study

Kukla & Stanistreet (1991) proposed that the convergence and subsequent collision of the Congo and Kalahari Cratons at ~ 542 Ma resulted in the closing of the Khomas Sea, a small ocean that had formed during a period of spreading between ~ 750 and ~ 600 Ma, and the formation of an accretionary prism. This suggestion is based on the correspondence of the characteristics of the Southern Zone to those observed in known accretionary prisms, such as the suggestion by Ernst (1973) that the presence of a high pressure – low temperature metamorphic terrane within present day continental crust is indicative of the position at which two continental slabs once converged through the consumption of an intervening ocean floor. However, to date, the specifics as to how exactly the supposed convergent margin evolved and the geodynamic factor/s responsible for its metamorphic evolution remain largely undetermined.

The metamorphic evolution of an accretionary prism may be influenced by a host of geodynamic factors, including the rate of convergence (Oxburgh & Turcotte, 1971; Ernst, 1988; Peacock, 2003; Willner, 2005; Maruyama *et al.*, 2010), the angle of subduction (Oxburgh & Turcotte, 1971; Ernst, 1973, 1988, 2010; Peacock, 2003; Willner, 2005), the age (warmth) of subducting material (Ernst, 1988; Iwamori, 2000; Peacock, 2003; Phillips *et al.*, 2008), the depth of subduction (Peacock, 2003; Willner, 2005; Ernst, 2010), the thickness of the subducting oceanic slab (Ernst, 1988; Peacock, 2003), the duration of subduction (Peacock, 2003; Ernst, 2010), the rate of mantle convection under the subducting oceanic slab (Oxburgh & Turcotte, 1971; Ernst, 1988, 2010), fluid infiltration (Ernst, 1973, 1988; Willner, 2005), the rate of exhumation (Ernst, 1988, 2010, Maruyama *et al.*, 2010) and the occurrence of continental crust collision post convergence (Ernst, 1988, 2010; Maruyama *et al.*, 2010).

The effect of these geodynamic factors on the prograde and retrograde metamorphic evolution of a prism can be constrained through the examination of their influence in several known modern and exhumed accretionary prisms. Importantly, the interplay of these geodynamic factors, all of which may be operational in any given prism, may either have a complementary effect or a non-complementary effect on the metamorphic evolution of the prism. In the case of the former, all of the operational geodynamic factors promote either the attainment and/or preservation of HP-LT conditions and cooler geothermal gradients, or HT-LP conditions and warmer geothermal gradients. For example, the interplay of fast convergence, a high angle of subduction and the subduction of old (cold) oceanic crust lead to HP-LT conditions and cooler geothermal gradients. By contrast, in the case of the latter, some of the operational geodynamic factors promote the attainment and/or preservation of HP-LT conditions and cooler geothermal gradients, whereas others promote HT-LP conditions and warmer geothermal gradients. An example of this is the interplay of the three aforementioned geodynamic factors, which support HP-LT conditions and cooler geothermal gradients, with long-lived subduction, a low rate of mantle convection under subducting oceanic slab and continental crust collision post-convergence, all of which support HT-LP conditions and warmer geothermal gradients.

By constructing pressure-temperature (P-T) paths and assessing the influence of the relevant, aforementioned geodynamic factors on the rocks of the Southern Zone, the metamorphic evolution of these rocks and the most likely geodynamic factor/s responsible for their evolution can be established. Constraints on the metamorphic evolution of the rocks of the Southern Zone may provide further evidence for Kukla & Stanistreet's (1991) suggestion and explore the possibility that the Southern Zone represents one of the oldest, largest and best-preserved examples of an accretionary prism in the rock record. Moreover, insight into the effect of the geodynamic factor/s on the metamorphic evolution of the Southern Zone may help to better constrain how the specific factor/s influence(s) the evolution of

accretionary prisms and by doing so, aid in the identification of accretionary prisms with similar metamorphic evolution histories in other HP-LT convergent margins.

1.2. The Objectives of this Study

The objectives of this study are to:

- Gain an understanding of the key characteristics of accretionary prisms, in particular how the various geodynamic factors influence their metamorphic evolution.
- Determine the mineral assemblages present in the rocks of the Southern Zone and the kinematic history of the rocks.
- Determine the P-T conditions that the Southern Zone was subjected to during metamorphism.
- Establish the metamorphic evolution of the Southern Zone through the construction of P-T paths.
- Potentially add evidence to the recognition of the Southern Zone as an accretionary prism by comparing the geothermal gradients recorded by the rocks of the Southern Zone to those in other known HP-LT metamorphic terranes.
- Assess and determine the most likely geodynamic factor/s responsible for the metamorphic evolution.
- Discuss the implications for the Southern Zone and the recognition of accretionary prisms with a similar metamorphic evolution in other HP-LT convergent margins.

2. *The Characteristics of an Accretionary Prism*

Metamorphism is defined as the mineralogical changes that take place in a rock due to changes in the pressure and temperature of the environment in which the rock resides (Bates & Jackson, 1984). Regional metamorphism occurring within different geological environments is discernible by different metamorphic conditions, the details and outcomes of which are preserved by the rocks that were subjected to the metamorphism (Miyashiro, 1961; Oxburgh & Turcotte, 1971; Peacock, 2003; Maruyama *et al.*, 2010). In other words, rocks that experienced regional metamorphism within an accretionary prism environment above a subduction zone will display a certain set of characteristics that enables them to be distinguished from rocks that underwent metamorphism in a different geological environment (Peacock, 2003; Ernst, 2010). For example, in *Figure 1*, which provides an overview of the geology of a convergent margin, those rocks metamorphosed close to the high heat flow domain, specifically the magmatic (volcanic) arc overlying the mantle wedge, are likely to record higher temperatures than those metamorphosed close to the low heat flow domain, specifically the old, cold under-riding slab and accreted sediments.

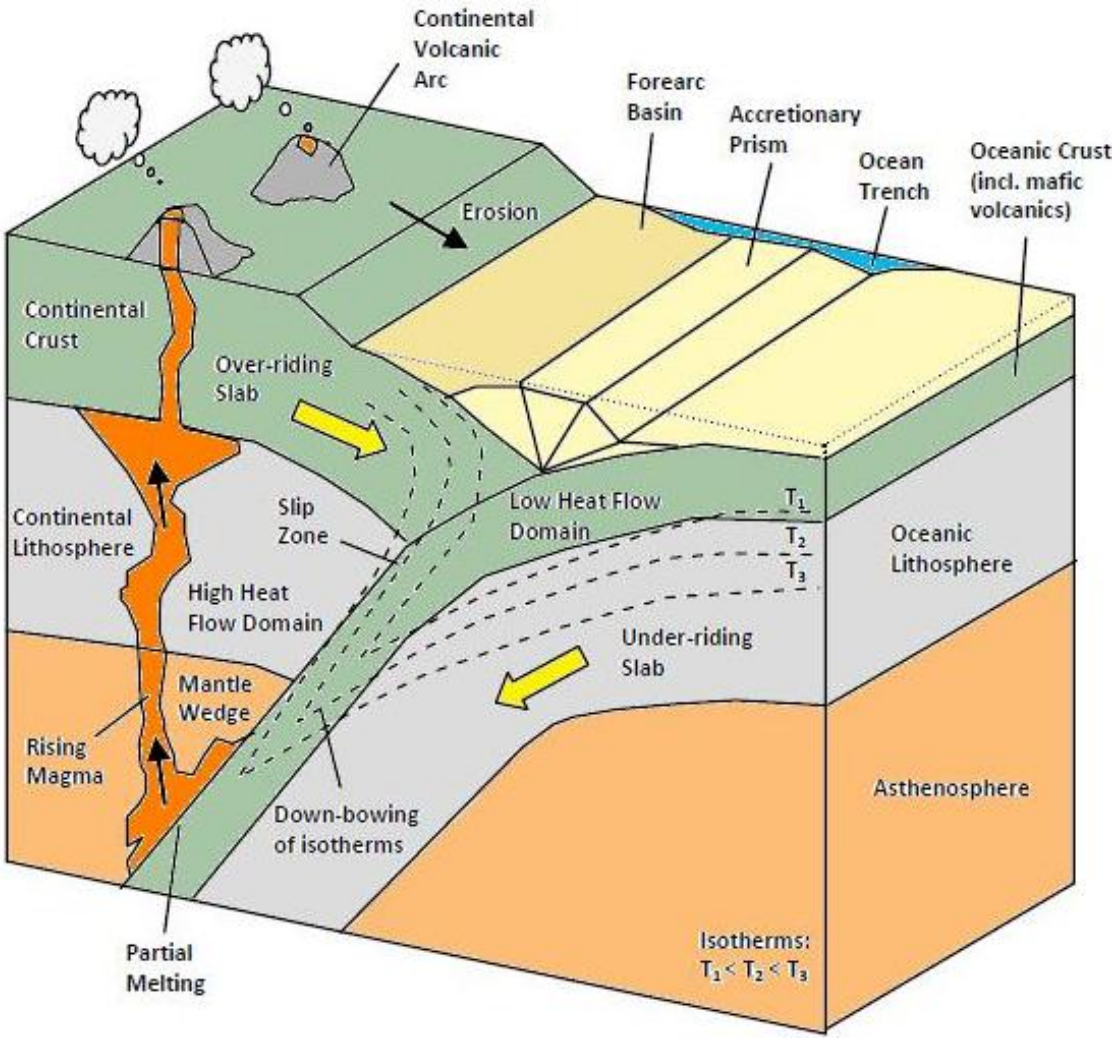

(Adapted from Marshak, 2005)

Figure 1: The geology of a convergent margin.

However, the exact details of the metamorphic evolution of the rocks within any given accretionary prism may vary depending on the specific geodynamic factor/s experienced by that prism (Ernst, 1973; Peacock, 2003; Ernst, 2010; Maruyama *et al.*, 2010). Examination of the rocks preserved in numerous known modern and exhumed accretionary prisms, as well as the geodynamic factor/s attributed to their metamorphic evolution, both facilitates the establishment of key characteristics by which the identification of accretionary prisms within the rock record can occur and allows for the assessment and understanding of the variability in the metamorphic evolution of accretionary prisms. The key characteristics of accretionary prisms and the variability therein are discussed below.

2.1. Intercalated metapsammopelites and metamafics with a high strain fabric

The protoliths for the metamorphosed rocks in an accretionary prism consist of trench-fill deposits that have both a terrigenous, turbiditic, sedimentary component derived primarily from the erosion of the over-riding slab and a volcanic, mafic, igneous component derived from the off-scraping of the uppermost part of under-riding slab during subduction. Oxburgh & Turcotte (1971), Peacock (2003) and Ernst (2010) noted that the accretion of these components into a prism may occur by over-plating, whereby new material is added to the leading edge of the over-riding slab (*Figure 2a*), or by under-plating, whereby new material is added to the underside of the over-riding slab (*Figure 2b*).

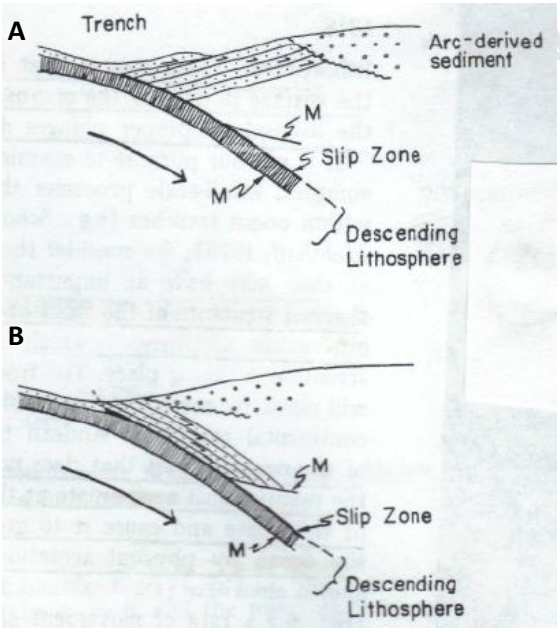

Figure 2: The methods of accretion by which an accretionary prism may form. Over-plating (*A*) involves the addition of new material to the front of the over-riding slab, whereas under-plating (*B*) involves the addition of new material to the base of the over-riding slab.

(Oxburgh & Turcotte, 1971)

Both of these methods of accretion allow for the sedimentary and igneous components to be periodically sliced off the surface of the under-riding slab as thrust sheets and become intimately intercalated with one another. The metamorphism of this mechanically intercalated material, which results in a change in mineral assemblages, gives rise to intercalated metapsammopelites and metamafics (Moore & Byrne, 1987).

Deformation to high strain during accretion results in the formation of a well-defined fabric within some of the metamorphosed lithologies (Ernst, 1988; Willner, 2005; Ernst, 2010; Maruyama *et al.*, 2010). The fabric is usually best preserved within the metapsammopelitic rocks, with the alignment of various phyllosilicate minerals (chlorite, biotite, muscovite, paragonite, phengite, etc.) facilitating the formation of a penetrative foliation (Ernst, 1988; Willner, 2005; Ernst, 2010; Maruyama *et al.*, 2010). In most cases, the fabric is sporadically disrupted and/or paralleled by quartz veins of variable thickness (Ernst, 1988; Willner, 2005; Ernst, 2010; Maruyama *et al.*, 2010).

Despite deformation, the metapsammopelites may exhibit remnant, deformed sedimentary features, such as distorted bedding, ripple marks and flute casts (Willner, 2005; Ernst, 2010; Maruyama *et al.*, 2010). Similarly, the metamafics, which usually have a compositional affinity to mid-ocean ridge basalt (MORB) and/or ocean island basalt (OIB), may display relic, weakly to moderately deformed igneous features, such as flattened pillow structures, in areas where deformation is less concentrated (Willner, 2005; Ernst, 2010; Maruyama *et al.*, 2010).

For example, the Western Belt of the Coastal Cordillera in Chile consists of metapsammopelitic schists and metapelitic garnet-mica schists that contain numerous blueschist and greenschist facies metabasite intercalations (Willner, 2005). The protoliths for the metapsammopelites and metabasites are thought to be terrigenous turbidite deposits and basaltic rocks of MORB composition, respectively (Willner, 2005). Relic igneous pillow structures are recognisable in some of the greenschist metabasite intercalations, whereas the metapsammopelitic schists have parallel bands of alternating quartz- and phyllosilicate-rich layers, with the alignment of the minerals in the latter forming a penetrative foliation (Willner, 2005). Similarly, in the Sanbagwa Belt in Japan, the metamorphism of basaltic rocks of MORB composition with intercalated terrigenous, turbidite deposits resulted in the formation of metamafic schists that contain metapelitic, garnet-rich pods (Aoki *et al.*, 2009). Moreover, the metasediments that are intercalated with metabasalts of MORB and OIB affinity in the Otago Schist Belt in New Zealand are likely to have formed from a trench-fill deposit consisting of sediments and volcanic rocks (Fagereng & Cooper, 2010). Primary sedimentary bedding and a prominent foliation that is defined by the alignment of chlorite and phengite and is readily cross-cut by quartz veins is observable within the fine-grained metasediments, whereas the metabasalts exhibit primary igneous textures (Fagereng & Cooper, 2010). In the exhumed Hongan Belt of the Qinling-Dabie Complex in China, abundant eclogite and amphibolite facies metamafic layers of volcanic origin are intercalated with metamorphosed quartzo-feldspathic schists of sedimentary origin (Zhou *et al.*, 1993).

2.2. Structurally adjacent to a high temperature – low pressure (HT-LP) metamorphic terrane

Miyashiro (1961) first recognised the existence of paired metamorphic belts, whereby a metamorphic terrane with a HP-LT mineral assemblage is situated immediately adjacent to a metamorphic terrane with a HT-LP mineral assemblage. Furthermore, the HP-LT and HT-LP terranes are commonly separated by a major structural feature, such as a prominent fault (Oxburgh & Turcotte, 1971; Maruyama *et al.*, 2010).

For example, the HP-LT Western Belt of the Coastal Cordillera in Chile is separated from the adjacent HT-LP Eastern Belt by the prominent, brittle, reverse Pichilemu Vichuquen fault (Willner, 2005). Similarly, the Pell-Manning fault separates the HP-LT Tablelands Complex of the southern New England Fold Belt in Australia from the adjacent, inland HT-LP Tamworth Belt (Phillips *et al.*, 2008).

2.3. Younger than early-Palaeozoic Age

Ernst (1973, 1988) noted that the majority of known accretionary prisms occur in orogenies that experienced metamorphism during the Mesozoic and Cenozoic, such as those in the circum-Pacific and Alpine-Himalayan areas, whereas accretionary prisms in older orogenies that experienced metamorphism in the Palaeozoic are rare.

One of the oldest known ages for metamorphism within an accretionary prism comes from the exhumed Tablelands Complex of the southern New England Belt in Australia, where metamorphism of the trench-fill deposits occurred in the mid-Palaeozoic between 407 to 340 Ma (Korsch *et al.*, 2008). Similarly, metamorphism within the Western Belt of the Coastal Cordillera in Chile occurred in the late-Palaeozoic between 365 and 250 Ma (Willner *et al.*, 2005). The Diahot Terrane in New Caledonia and the Otago Schist Belt in New Zealand are younger, with metamorphism only having occur in the early- to mid-Cenozoic (55 to 40 Ma) and late-Mesozoic (115 to 65 Ma), respectively (Ghent *et al.*, 1994; Nishimura *et al.*, 2000).

Based on the findings by Ernst (1973, 1988) and the examples given above, it is evident that regional metamorphism within accretionary prisms may be constrained to ages younger than the early-Palaeozoic, circa 550 Ma.

2.4. High pressures, low temperatures and a low geothermal gradient

The fragmentary nature of accretion dictates the preservation of a segmented metamorphic sequence that ranges from zeolite facies through prehnite-pumpellyite, prehnite-actinolite, blueschist, upper greenschist and upper amphibolite (epidote-amphibolite) facies to eclogite facies (Ernst, 1973; Ernst, 1988). As such, the peak pressure and temperature conditions experienced within an accretionary prism may vary greatly depending on the grade of metamorphism that was achieved – for example, the high grade conditions in Dora-Maira, Monte Rosa and Gran Paradiso Massifs in the Alps (Gasco *et al.*, 2013) versus the low grade conditions in the Otago Schist Belt in New Zealand (Fagereng & Cooper, 2010). Nevertheless, the metamorphosed rocks that are preserved are typically comprised of mineral assemblages that are indicative of high pressures of above ~ 5 kbar (usually 7 to 14 kbar) and low temperatures of below ~ 600 °C (usually 300 to 600 °C). The peak P-T conditions and P-T paths for numerous known high pressure – low temperature terranes is illustrated in *Figure 3* below.

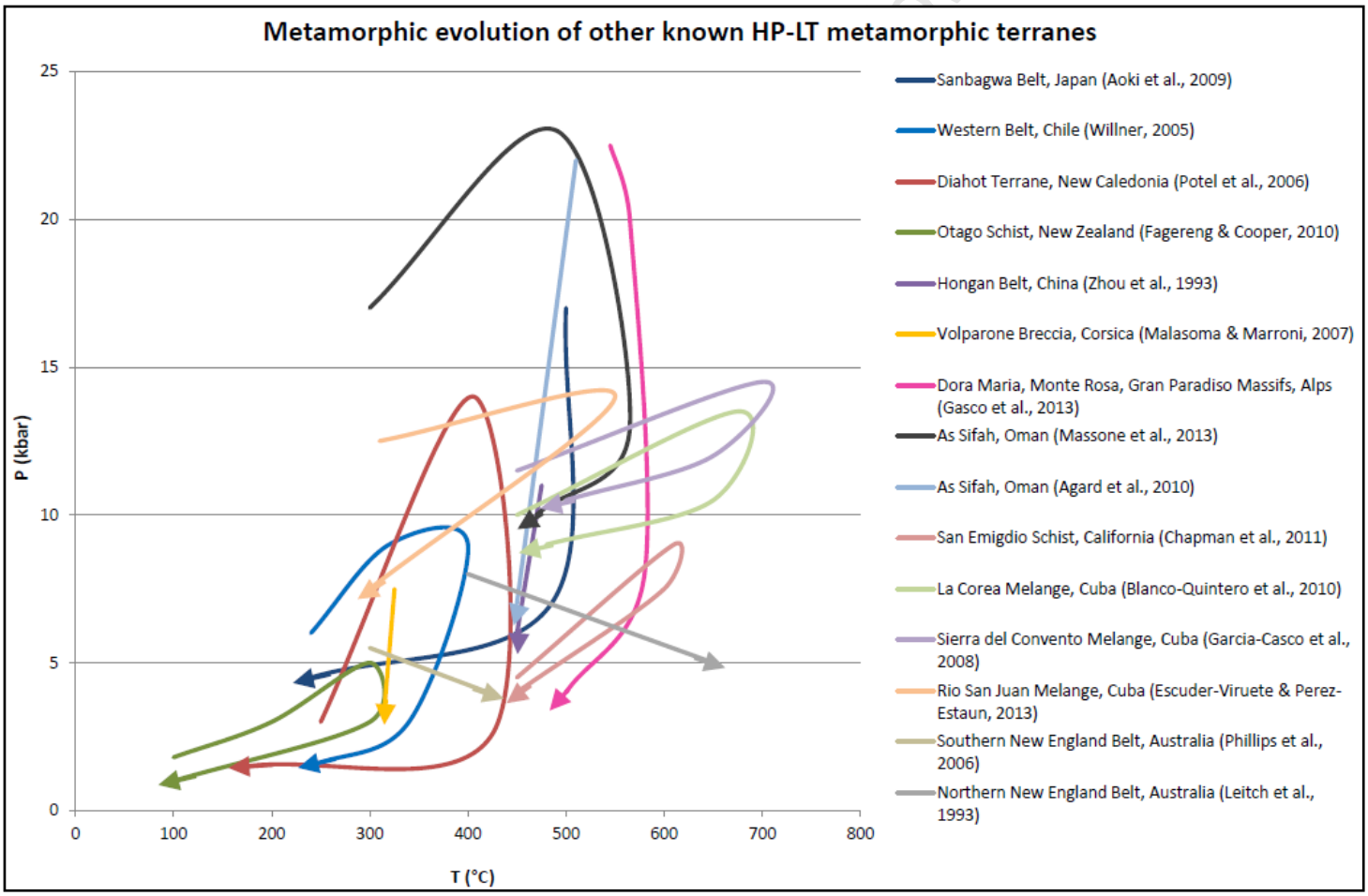

Figure 3: Variation in the peak P-T conditions and metamorphic evolution (P-T paths) of known high pressure – low temperature (HP-LT) metamorphic terranes.

A far less grade-dependent means by which regional metamorphism within an accretionary prism can be recognised is by examining the geothermal gradient at which the rocks were metamorphosed. The down-bowing of the isotherms in the vicinity of the cold, wet under-riding slab (*Figure 1)* results in an area of low heat flow (Oxburgh & Turcotte, 1971; Ernst, 1973, 1988; Peacock, 2003; Maruyama *et al.*, 2010). Geothermal gradients within this low heat flow area, including within an accretionary prism, are colder than the stable continental geothermal gradient (~ 15.0 to 25.0 °C/km), typically between ~ 8.0 and 15.0 °C/km.

For example, the metapsammopelites, the metamafic greenschists, the metamafic blueschists and the metapelitic garnet-mica schists in the Western Belt of the Coastal Cordillera in Chile record geothermal gradients of 11.0 to 22.5 °C/km, 12.0 to 18.0 °C/km, 9.5 to 12.0 °C/km and 13.5 to 15.0 °C/km, respectively (Willner, 2005). In the Sanbagwa Belt in Japan, the peak P and T conditions of the metapelitic garnet-rich pods equates to a geothermal gradient of 8.0 to 10.5 °C/km, whereas the peak P and T conditions of the metamafic schists equates a geothermal gradients of and 12.5 to 22.0 °C/km (Aoki *et al.*, 2009). A geothermal gradient of 6.5 to 11 °C/km is recorded for the metapelitic blueschists of the Diahot Terrane in New Caledonia (Potel *et al.*, 2008). The eclogite and amphibolite facies metamafic layers in the exhumed Hongan Belt of the Qinling-Dabie Complex in China have a geothermal gradient of 11.0 to 16.5 °C/km (Zhou *et al.*, 1993), whereas the metamafic schists in the Tablelands Complex of the southern New England Belt in Australia have a geothermal gradient of 12.5 to 17.5 °C/km (Phillips *et al.*, 2008).

As alluded to previously, the metamorphic evolution (P-T path) of subducted material, and consequently the realization and preservation of HP-LT metamorphic conditions and low geothermal gradients, is governed by a host of geodynamic factors. *Table 1* below summarises the observed variation in the metamorphic evolution of subducted material seen in *Figure 3* by examining the most likely effect of the various geodynamic factors on any given P-T path.

Table 1: Geodynamic factors affecting the metamorphic evolution (P-T paths) of subducted material. Compiled using information from Oxburgh & Turcotte (1971); Ernst (1973); Ernst (1988); Willner (2005); Peacock (2003); Phillips *et al.* (2008); Ernst (2010) and Maruyama *et al.* (2010), and using examples from several HP-LT metamorphic terranes.

Geodynamic factor	***Explanatory notes***	***Most likely change in geothermal gradient***	***Example/s of known HP-LT terranes in which geodynamic factor has been suggested to have been operational/influential***
Rate of convergence	***Predominantly influences prograde P-T evolution***		
Fast	Subduction at > ~ 50 mm/year: less time for heating of cold, subducting oceanic slab to occur.	Attainment and/or preservation of cooler geothermal gradient.	Sanbagwa Belt, Japan (Aoki *et al.*, 2009).
Slow	Subduction at < ~ 50 mm/year: more time for heating of cold, subducting oceanic slab to occur.	Attainment and/or preservation of warmer geothermal gradient.	Western Belt, Chile (Willner, 2005).
Angle of subduction	***Predominantly influences prograde P-T evolution***		
High	Subduction at > ~ 25 - 30 °: only minor horizontal movement of subducted material away from low heat flow domain (i.e. cold under-riding slab); less shear heating.	Attainment and/or preservation of cooler geothermal gradient.	
Low	Subduction at < ~ 25 - 30 °: major horizontal movement of subducted material towards high heat flow domain (i.e. magmatic arc overlying the mantle wedge); more shear heating.	Attainment and/or preservation of warmer geothermal gradient.	Western Belt, Chile (Willner, 2005).
Age (warmth) of subducting oceanic slab	***Predominantly influences prograde P-T evolution***		
Old	Subduction of > ~ 10 - 25 Ma old slab: subduction of cold oceanic crust.	Attainment and/or preservation of cooler geothermal gradient.	Sanbagwa Belt, Japan (Aoki *et al.*, 2009).
Young	Subduction of < ~ 10 - 25 Ma old slab: subduction of warm oceanic crust and possibly a heat source (very young and very hot oceanic crust and/or a spreading ridge). The latter creates a window in the under-riding slab through which heat from asthenosphere may directly alter the accreted material.	Attainment and/or preservation of warmer geothermal gradient.	Northern New England Belt, Australia (Leitch *et al.*, 1993); Sierra del Convento, La Corea and Rio San Juan melanges, Cuba (Garcia-Casco *et al.*, 2008; Blanco-Quintero *et al.*, 2010; Escuder-Viruete & Perez-Estaun, 2013).
Depth of subduction	***Predominantly influences prograde P-T evolution***		
Deep	Subduction to > ~ 50 km depth: major interaction with high heat flow domains (i.e. mantle wedge and asthenosphere) promotes heating of subducted material.	Attainment and/or preservation of warmer geothermal gradient.	Sanbagwa Belt, Japan (Aoki *et al.*, 2009); Dora-Maira, Monte Rosa and Gran Paradiso massifs, Alps (Gasco *et al.*, 2013).

Shallow	Subduction to < ~ 50 km depth: minor interaction with high heat flow domains (i.e. mantle wedge and asthenosphere) hinders heating of subducted material.	Attainment and/or preservation of cooler geothermal gradient.	Volparone Breccia, Corsica (Malasoma & Marroni, 2007); San Emigdio Schist, California (Chapman *et al.*, 2011).
Thickness of the subducting oceanic slab	***Predominantly influences prograde P-T evolution***		
Thick	Heating of the margins of the subducted oceanic slab only.	Attainment and/or preservation of cooler geothermal gradient.	Western Belt, Chile (Willner, 2005).
Thin	Possible heating of the entire subducted oceanic slab.	Attainment and/or preservation of warmer geothermal gradient.	
Duration of subduction	***Predominantly influences prograde P-T evolution***		
Long-lived	Subduction for > ~ 30 - 40 Ma: progressive seaward accretion causes the effective horizontal, landward movement of subducted material closer to high heat flow domain (i.e. magmatic arc overlying the mantle wedge).	Attainment and/or preservation of warmer geothermal gradient.	Northern and southern New England Belt, Australia (Leitch *et al.*, 1993; Phillips *et al.*, 2008); Otago Schist, New Zealand (Fagereng & Cooper, 2010); San Emigdio Schist, California (Chapman *et al.*, 2011).
Short-lived	Subduction for < ~ 30 - 40 Ma: limited seaward accretion hinders the effective horizontal, landward movement of subducted material closer to high heat flow domain (i.e. magmatic arc overlying the mantle wedge).	Attainment and/or preservation of cooler geothermal gradient.	Western Belt, Chile (Willner, 2005).
Rate of mantle convection under subducting oceanic slab	***Predominantly influences retrograde P-T evolution***		
High	Efficient removal of heat from the subducting oceanic slab.	Attainment and/or preservation of cooler geothermal gradient.	
Low	Inefficient removal of heat from the subducting oceanic slab.	Attainment and/or preservation of warmer geothermal gradient.	
Fluid Infiltration	***Predominantly influences retrograde P-T evolution***		
Does occur	Fluid (water) addition through extension faults: promotes retrogression to lower temperature conditions.	Attainment and/or preservation of cooler geothermal gradient.	Western Belt, Chile (Willner, 2005); Sanbagwa Belt, Japan (Aoki *et al.*, 2009).
Does not occur	Absence of fluid (water) addition: discourages retrogression to lower temperature conditions.	Attainment and/or preservation of warmer geothermal gradient.	

Rate of exhumation	***Predominantly influences retrograde P-T evolution***		
Rapid	Exhumation at > 10 mm/year: results from high rates of erosion, effective corner flow, large buoyancy contrasts, major extensional tectonics, and/or plate divergence (e.g. extensive slab roll-back).	Attainment and/or preservation of warmer geothermal gradient.	Dora-Maira massif, Alps (Gebauer *et al.*, 1997); Diahot Terrane, New Caledonia (Potel *et al.*, 2006); San Emigdio Schist, California (Chapman *et al.*, 2011).
Slow	Exhumation at ~ 3 mm/year: results from low rates of erosion, ineffective corner flow, small buoyancy contrasts, minor extensional tectonics and/or negligible plate divergence.	Attainment and/or preservation of cooler geothermal gradient.	
Continental crust collision post convergence	***Predominantly influences retrograde P-T evolution***		
Does occur	Continental slab collision following the complete consumption of the intervening oceanic crust: results in crustal thickening and possible heating.	Attainment and/or preservation of warmer geothermal gradient.	Hongan Belt, China (Zhou *et al.*, 1993); Dora-Maira, Monte Rosa and Gran Paradiso massifs, Alps (Gebauer *et al.*, 1997; Gasco *et al.*, 2013); Diahot Terrane, New Caledonia (Potel *et al.*, 2006); Volparone Breccia, Corsica (Malasoma & Marroni, 2007); As Sifah, Oman (Agard *et al.*, 2010; Massone *et al.*, 2013).
Does not occur	Cessation of convergence prior to the collision between the continental slabs: results from a change in tectonics.	Attainment and/or preservation of cooler geothermal gradient.	Northern and southern New England Belt, Australia (Leitch *et al.*, 1993; Phillips *et al.*, 2008); Western Belt, Chile (Willner, 2005); Sierra del Convento, La Corea and Rio San Juan melanges, Cuba (Garcia-Casco *et al.*, 2008; Blanco-Quintero *et al.*, 2010; Escuder-Viruete & Perez-Estaun, 2013); San Emigdio Schist, California (Chapman *et al.*, 2011).

The interplay and overprinting relations of all, or at least several of these influential geodynamic factors in any given subduction environment explains much of the variability in P-T conditions and P-T paths observed in *Figure 3*. The lack of complete quantitative constraint of some of these factors makes it is difficult to predict the exact metamorphic evolution that subducted material will follow. Nonetheless, there are a few general observations that appear to hold true in most subduction zones.

Firstly, thermal modelling of subduction zones has shown that the subduction of warm oceanic crust, younger than ~ 10 to 25 Ma, results in a gradual increase in temperature with a relatively insignificant change in pressure over time – i.e. a near-isobaric increase in temperature and hence, an increase in the recorded geothermal gradient (Iwamori, 2000; Peacock, 2003). Moreover, the subduction of a heat source, namely very hot and very young oceanic crust or a spreading ridge (~ 0 Ma years in age), results in a rapid increase in temperature that is comparatively faster than that attainable during the subduction of young, warm oceanic crust and with little or no change in differential strain (Iwamori, 2000).

Specific examples of the change in P-T evolution resulting from the subduction of a heat source come from the Sierra del Convento, La Corea and Rio San Juan mélanges in Cuba, where very young, very hot, proto-Caribbean oceanic crust in close proximity to a spreading ridge was subducted under the Caribbean plate, resulting in a fairly rapid temperature increase of in excess of ~ 150 °C over an increase in pressure of less than ~ 3 to 4 kbar - refer to *Figure 3* (Garcia-Casco *et al.*, 2008; Blanco-Quintero *et al.*, 2010; Escuder-Viruete & Perez-Estaun, 2013). Further examples come from the Shoalwater and Wandilla terranes in the northern New England Belt in Australia, where the subduction of a spreading ridge during the concluding stages of accretion resulted in the accreted material experiencing a temperature increase of in excess of ~ 150 °C over a decrease in pressure of less than ~ 3 kbar – refer to *Figure 3* (Leitch *et al.*, 1993).

Secondly, a change in the angle subduction to < ~ 25 to 30 ° and long-lived subduction of > ~ 30 to 40 Ma may cause a pronounced step towards higher temperatures at a constant or only slightly increasing/decreasing pressure over time - i.e. a near-isobaric increase in temperature therefore an increase in the recorded geothermal gradient (Peacock, 2003; Ernst, 2010). Unlike the subduction of a heat source, which as shown by Iwamori (2000), results in a rapid increase in temperature, the thermobarometric changes derived from a changes in the angle of subduction and duration of subduction only become noticeable over more extended periods of time – i.e. they produce a gradual increase in temperature over time (Peacock, 2003; Ernst, 2010). This is primarily because the angle at which the under-riding slab is subducted beneath the over-riding slab is unlikely to change rapidly with time, hence resulting in fairly constant P-T conditions over a short period of time (Ernst, 1988, 2010; Peacock, 2003; Willner, 2005). Similarly, the heating of accreted material as a result of the effective horizontal, landward movement of the accreted material closer to the magmatic arc overlying the mantle wedge only becomes influential after > ~ 30 to 40 Ma of progressive seaward accretion (Peacock, 2003; Ernst, 2010). The continuation of underplating during this time dictates the continued deformation of the accreted material (Peacock, 2003; Ernst, 2010).

An example of the change in P-T evolution resulting from a change to low angle subduction comes from the Western Belt of the Coastal Cordillera in Chile, where the temperature increase of ~ 80 °C over a pressure increase of ~ 1.5 kbar observed in the greenschist facies metabasites has been attributed to a change in the angle of subduction of the under-riding slab to ~ 25 ° and the subsequent formation of long flat duplexes of accreted material, which were stretched horizontally towards the magmatic arc of the Eastern Belt (HT-LP terrane) – refer to *Figure 3* (Willner, 2005).

The Tablelands Complex in the southern New England Belt in Australia, where long-lived convergence and the subsequent landward movement of the accreted material closer to the magmatic arc of the Tamworth Belt (HT-LP terrane) caused an post-tectonic increase in temperature of in excess of ~ 100 °C over a pressure decrease of less than ~ 3 kbar, provides an example of the change in P-T evolution resulting from long-lived subduction – refer to *Figure 3* (Phillips *et al.*, 2006). A further example comes from the Otago Schist Belt in New Zealand, where the progressive seaward growth of the accretionary prism resulting from the long-lived subduction of palaeo-Pacific oceanic crust beneath Gondwana continental crust, caused a post-tectonic increase in temperature of nearly ~ 200 °C over a pressure increase of ~ 3 kbar – refer to *Figure 3* (Fagereng & Cooper, 2010).

Thirdly, the onset of continental crust collision post convergence and the rapid exhumation of subducted material result in major decompression at a constant or only slightly increasing/decreasing temperature over time – i.e. a near-isothermal decrease in pressure and hence a increase in the recorded geothermal gradient (Ernst, 1988, 2010; Maruyama *et al.* 2010).

This has been described in the Diahot Terrane in New Caledonia, where the pressure decrease of ~ 12 kbar over a temperature increase of ~ 25 °C has been attributed to the collision of a dispersed fragment off eastern Gondwana and an intraoceanic island arc system and the resulting rapid exhumation of accreted material – refer to *Figure 3* (Potel *et al.*, 2006). A further examples comes from the Dora-Maira, Monte Rosa and Gran Paradiso massifs in the Alps, where collision and rapid exhumation are thought to have been responsible for the ~ 35 °C increase in temperature during decompression of greater than ~ 14 kbar – refer to *Figure 3* (Gasco *et al.*, 2013).

2.4.1. Mechanisms for the exhumation and preservation of subduction-related (HP-LT) metamorphic rocks

The change in thermobarometric conditions resulting from the occurrence and/or change of certain geodynamic factors during subduction may cause the partial or complete alteration of the mineral assemblage that records evidence for metamorphism at high pressures and low temperatures (Ernst, 1988; Peacock, 2003; Ernst, 2010). In collisional orogens, where the intervening oceanic crust is completely consumed, the extent of deformation of the HP-LT rocks is highly dependent on the mechanism by which the rocks are exhumed prior to or during the collision (Platt, 1993).

However, the exact mechanism by which the HP-LT rocks that formed in an accretionary prism are exhumed and preserved within a collisional orogen is highly controversial, with no one mechanism being able to explain the exhumation and preservation of all HP-LT terranes (Platt, 1993; Malusa

et al., 2011). Nevertheless, as accurately stated by Platt (1993) and re-iterated by Ring *et al.* (1999), all mechanisms for the exhumation of HP-LT rocks require either the removal of the overburden or the transport of the HP-LT rocks through the overburden.

Early proposals for mechanisms by which this occurred relied almost exclusively on a high rate of mantle convection under the subducting oceanic slab, the cessation of prevailing convergent margin tectonics and the buoyant rise of subducted material (e.g. Oxburgh & Turcotte, 1971; Ernst, 1973, 1988). More recently proposed mechanisms, however, may be grouped into two categories, namely those in which the boundaries of the subduction zone are spatially fixed and those in which the boundaries are not spatially fixed (Malusa *et al.*, 2011). The former category includes exhumation by erosion, corner flow, buoyancy contrasts, entrainment and extension; whereas the latter category is comprised of exhumation by divergence.

The erosion of thickened crust over a significant period of geological time allows for the exposure of rocks buried at depth (Platt, 1993; Beaumont *et al.*, 2001). Exhumation by this mechanism only would result in little deformation of the HP-LT rocks (Platt, 1993; Malusa, 2011). However, it is unlikely that erosion is exclusively responsible for the exhumation of rocks buried to a depth of greater than ~ 20 km and more likely that it operates concurrently with one of the other mechanisms described below (Platt, 1993).

Corner flow, which is the forced circulation of low viscosity, intercalated material in a prism towards the surface, results from the detachment of new material at the basal corner where the under-riding and over-riding plates are in contact and the subsequent, uplift of relatively coherent blocks of the overlying accreted material along thrust faults within the prism (Platt, 1993; Beaumont *et al.*, 2001; Malusa *et al.*, 2011). Beaumont *et al.* (2001) showed that the corner flow of low viscosity material coupled with surface erosion lead to distribution of deformation relating to collision throughout an entire extruded accretionary prism in the Himalayas.

Buoyancy contrasts, which are as a result of density contrasts between the lower density subducting crust and the higher density mantle, may allow for the uplift of HP-LT rocks (Platt, 1993; Ernst *et al.*, 1997; Malusa *et al.*, 2011). However, as noted by Platt (1993) and Ernst (2010), this mechanism struggles to explain both the exhumation of higher density mafic HP-LT rocks, which would presumably have a density similar to that of the mantle, and how the HP-LT rocks are exhumed at higher structural levels - i.e. through crustal material of a similar, low density. Nonetheless, as suggested by Platt (1993) and Guillot *et al.* (2000), HP-LT rocks, regardless of their density, may also be exhumed as blocks entrained in buoyant, low density material, such as mud or serpentinite. Guillet *et al.* (2000) showed that in several collision orogenies the

exhumation of HP-LT material may have occurred through the entrainment of the HP-LT rocks in small blocks of low density serpentinites and that the deformation relating to the collision event is concentrated around these blocks.

Extension, driven primarily by differences in surface elevation and occurring in the upper portion of thickened, extruded crust may be a further mechanism to explain the unroofing of HP-LT rocks (Platt, 1993; Malusa *et al.*, 2011). Chemenda *et al.* (1995) showed by physical modelling that exhumation by extension may be responsible for the concentration of deformation relating to collision along the boundaries of accreted material, specifically along thrust faults, in certain areas of the Himalayas, Alps, New Caledonia, Oman and eastern Pamir orogenies.

Malusa *et al.* (2011) noted that there are two prominent mechanisms by which divergence in a subduction zone can occur. The first of these, namely slab rollback, involves the decoupling of the under-riding plate and the accretionary prism situated at the leading edge of the over-riding plate and the subsequent movement of the under-riding plate back up the subduction zone (Malusa *et al.*, 2011). This change in tectonics allows for HP-LT rocks low in the prism to migrate back up the subduction zone and be exhumed near the front (previously seaward) of the accretionary prism (Malusa *et al.*, 2011). Similarly, the movement of the over-riding plate away from the under-riding plate is likely to result in divergence along pre-existing discontinuities near the rear (previously landward) of the accretionary prism, which in turn provides a gap through which HP-LT rocks low in the prism may be exhumed (Malusa *et al.*, 2011). Both slab roll back and the movement of the over-riding plate away from the subduction zone are most likely to be induced as a response to far-field plate motions, for example subduction elsewhere (Malusa *et al.*, 2011).

Malusa *et al.* (2011) have suggested that the deformation relating to collision is concentrated in the front of the accretionary prism when divergence occurs through slab rollback and at the rear of the accretionary prism, along a re-activated discontinuity, when divergence is as a result of the motion of the upper plate away from the subduction zone. Examples of the latter come from the Alps, Western Gneiss Region in Norway, Dabie-Sulu in China and eclogite belt in eastern Papua New Guinea (Malusa *et al.*, 2011).

3. Geological Setting

3.1. Regional Geology of the Damara Belt

The Pan-African Damara Orogen in Namibia formed during the amalgamation of the Gondwana supercontinent (Miller, 1983; Kukla, 1992; Miller, 2008). The Orogen consists of three Proterozoic belts, namely the ~ 250 to 450 km wide, NE-trending Damara Belt that passes through central Namibia, the ~ 150 km wide NNW-trending Kaoko Belt that extends along the northern coast of Namibia, and the SSE-trending Gariep Belt that extends along the southern coast of Namibia (Miller, 1983; Kukla, 1992; Miller, 2008) – refer to *Figure 4* below. The three belts intersect at a palaeo-triple junction that was centred off the coast of Namibia near Swakopmund (Miller, 1983; Miller, 2008).

The Damara Belt has been subdivided into several tectonostratigraphic zones that are discernible on the basis of their stratigraphy, structural features, metamorphic character, geochronology, plutonic igneous intrusions and aeromagnetic expression (Miller, 1983; Kukla, 1992; Miller; 2008) – refer to *Figure 4* below. From north to south, these zones are the Northern or Otavi Platform (NP), the Northern Margin or Fransfontein Zone (NMZ), the Northern or Outjo Zone (NZ), the Central or Swakop Zone (CZ), the Okahandja Lineament Zone (OLZ), the Southern or Khomas Zone (SZ), the Southern Margin or Hakos Zone (SMZ) and the Southern or Nama Foreland (SF) (Miller, 2008). The boundaries between these zones are defined by major changes in stratigraphy and/or by prominent, linear, structural features, such as thrusts, lineaments and mylonite belts (Miller, 1983; Kukla, 1992; Miller, 2008).

The stratigraphy of the Damara Belt is comprised of a variety of metamorphosed lithologies ranging from felsic and mafic volcanic, igneous rocks (e.g. rhyollite, tuff and amphibolite) to calcareous and clastic sedimentary rocks (e.g. dolomite, limestone, quartzite, conglomerate, diamictite and micaceous schists) (Kukla, 1992). The stratigraphic groups into which these rocks are divided are separated by a series of local and regional unconformities (Kukla, 1992). In addition to the above lithologies, the Damara Belt is intruded by several late-stage, plutonic igneous bodies that occur predominantly within the CZ, but are also present within the NZ, OLZ and SMZ (Miller, 2008). An example is the Donkerhuk Granite, which intruded at the northern margin of the SZ at ~ 535 Ma (Kukla, 1992; Miller, 2008).

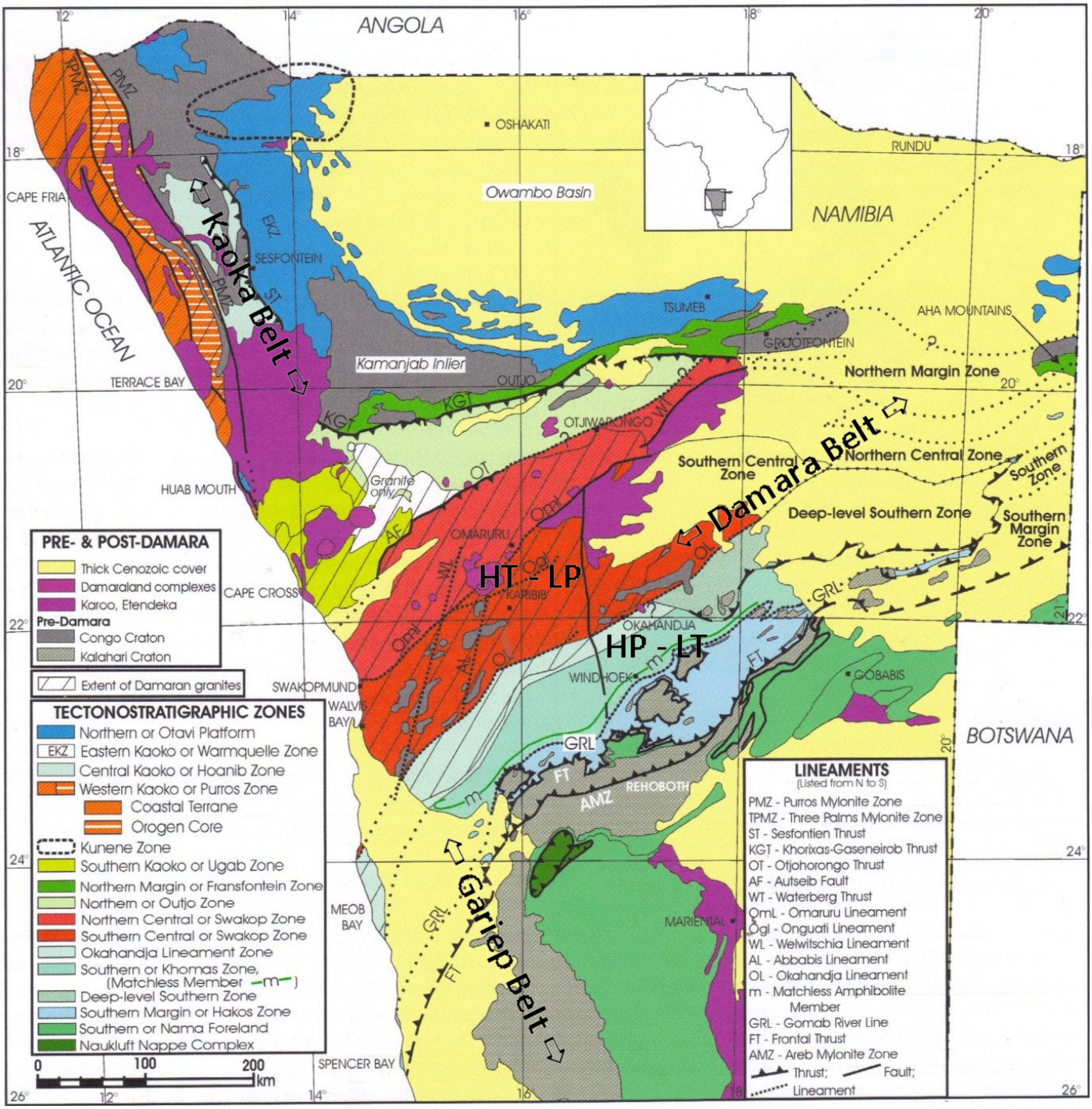

(Adapted from Miller, 2008)

Figure 4: The Proterozoic belts and tectonostratigraphic zones of the Damara Orogen. *HT – LP* = high temperature – low pressure; *HP – LT* = high pressure – low temperature.

Deformation within the Damara Belt resulted in the formation of a variety of macro-structures and associated fabric elements. Generally, the intensity of deformation within the northern (NP to NZ) and southern (OLZ to SMZ) portions of the Damara Belt increases southwards with folds gradually changing from open and upright to tight, isoclinal and locally recumbent or overturned (Kukla, 1992; Miller, 2008). By contrast, deformation within the central portion (CZ) is complicated by a mixture of large-scale, recumbent folds and doubly plunging domes in the southern CZ, and by the overprinting of early, tight,

upright folds by later, tight to isoclinal, locally recumbent folds and a certain degree of dextral strike-slip shearing in the northern CZ (Miller, 2008). Thrusting is most prevalent within the southern portion of the Damara Belt, with the frequency and magnitude of thrusts increasing towards the south and ultimately giving rise to complex thrust and nappe structures in the SMZ (Kukla, 1992; Miller, 2008). Other regional structural features within the Damara Belt vary from pre-Damaran granitic inliers to large-scale anticlines and thrusts, as well as a host of lineaments. One such example is the Okahandja Lineament, which is a highly linear, monocline-like structure at the southern margin of the CZ along which all of the rocks of the CZ are believed to have been downfolded to the south during the subduction of the Kalahari Craton beneath the Congo Craton (Kukla, 1992; Miller, 2008).

Metamorphism within the Damara Belt is believed to have been two-fold with the peak of the first and second metamorphic events occurring at ~ 555 Ma and ~ 535 Ma, respectively (Miller, 2008). The outcome of these events is defined by an increase in temperature and a decrease in pressure from the outer margins towards the centre of the Belt (Miller, 1983; Kukla, 1992; Miller, 2008). The central portion, or more specifically the southern CZ, contains rocks that were subjected to high temperature – low pressure (HT-LP) metamorphism, whereas the rocks of the SZ and SMZ experienced high pressure – low temperature (HP-LT) metamorphism (Kukla, 1992; Miller, 2008). These two metamorphic terranes are adjacent to one another and are structurally separated by the Okahandja Lineament.

3.2. Geology of the Southern Zone

The Southern Zone of the Damara Belt, which extends in a NE-SW orientation from the NE of Windhoek and Okahandja towards Meob Bay on the SW coast of Namibia, is a ~ 400 km long and up to ~ 100 km wide zone that is comprised predominantly of passive-margin schists of the Kuiseb Formation and active-margin schists of the Hureb Formation, both of which belong to the (upper-) Swakop Group (Kukla & Stanistreet, 1991; Kukla, 1992; Miller, 2008). In addition to these schists, a narrow, linear, ~ 350 km long and < ~ 3 km wide belt of metamafic rock of MORB composition, known as the Matchless Amphibolite Member, is intercalated within the Kuiseb Formation schists (Kukla & Stanistreet, 1991; Kukla, 1992; Miller, 2008). The boundaries of the Southern Zone are defined by the Okahandja Lineament in the north and by the Gomab River Line (GRL), including the Us Pass Lineament, in the south (Miller, 2008).

3.2.1. Stratigraphy

The Kuiseb Formation forms the lowermost stratigraphic unit within the Southern Zone and is comprised of metapsammopelitic schists that extend from the Gomab River Line to ~ 10 km north of the Matchless Amphibolite Member in the south of the Southern Zone (Miller, 2008). The schists of the Kuiseb Formation

are believed to have been deposited as greywackes and shales in a pre-tectonic, passive-margin environment during the spreading phase that lead to the formation of the Khomas Sea between ~ 750 Ma and ~ 600 Ma (Kukla & Stanistreet, 1991; Kukla, 1992; Miller, 2008). Intercalated within the southern third of the Kuiseb Formation is the Matchless Amphibolite Member, which is a dark green to black coloured, very fine- to medium-grained metamafic volcanic amphibolite of MORB composition (Kukla & Stanistreet, 1991; Kukla, 1992; Miller, 2008). In addition to these lithologies, the Kuiseb Formation also contains minor calc-silicates, which usually occur as thin layers within the metapsammopelitic schists (Kukla, 1992).

Miller (2008) classified the lithologies immediately south of the GRL in the SMZ, namely those belonging to the Haris, Mahonda, Melrose and Samara Formations, as part of the (upper-) Hakos Group. However, these formations display a remarkable resemblance to the Kuiseb Formation in the southern third of the SZ. Not only are they composed of intercalated metapsammopelitic schists, calc-silicates and narrow, metamafic volcanic amphibolite bodies, such as the ~ 50 to 150m wide Mohlatetsi Amphibolite Member, but they also exhibit deformation structures and fabric elements comparable to those present in the Kuiseb Formation (Kukla, 1992; Miller, 2008). Moreover, they record metamorphic conditions that closely parallel those recorded by the rocks of the Kuiseb Formation (Kasch, 1981; Miller, 2008). *Figure 5* below provides an overview of the stratigraphy of the Southern and Southern Margin Zones.

Conformably overlying the schists of the Kuiseb Formation are pale grey to whitish coloured metapsammopelitic schists that contain an abundance of thin (up to 2 m thick), sporadic layers, lenses, veins and nodules of calc-silicate (Kukla, 1992; Miller, 2008). These rocks constitute the Hureb Formation, which extends from ~ 10 km north of the Matchless Amphibolite Member to the Okahandja Lineament in the north of the Southern Zone and may be subdivided on the basis of sedimentary grading and deformation into the Upper and Lower Hureb Formations, with the former encompassing those schists immediately south of the Okahandja Lineament that have upward-thinning sedimentary cycles and show evidence for only one phase of deformation (Miller, 2008). The schists of the Hureb Formation are thought to have been deposited in a syn-tectonic, active-margin environment during the closure of the Khomas Sea, which occurred as a result of the subduction of the Kalahari Craton beneath the Congo Craton between ~ 580 Ma and ~ 535 Ma (Miller, 2008).

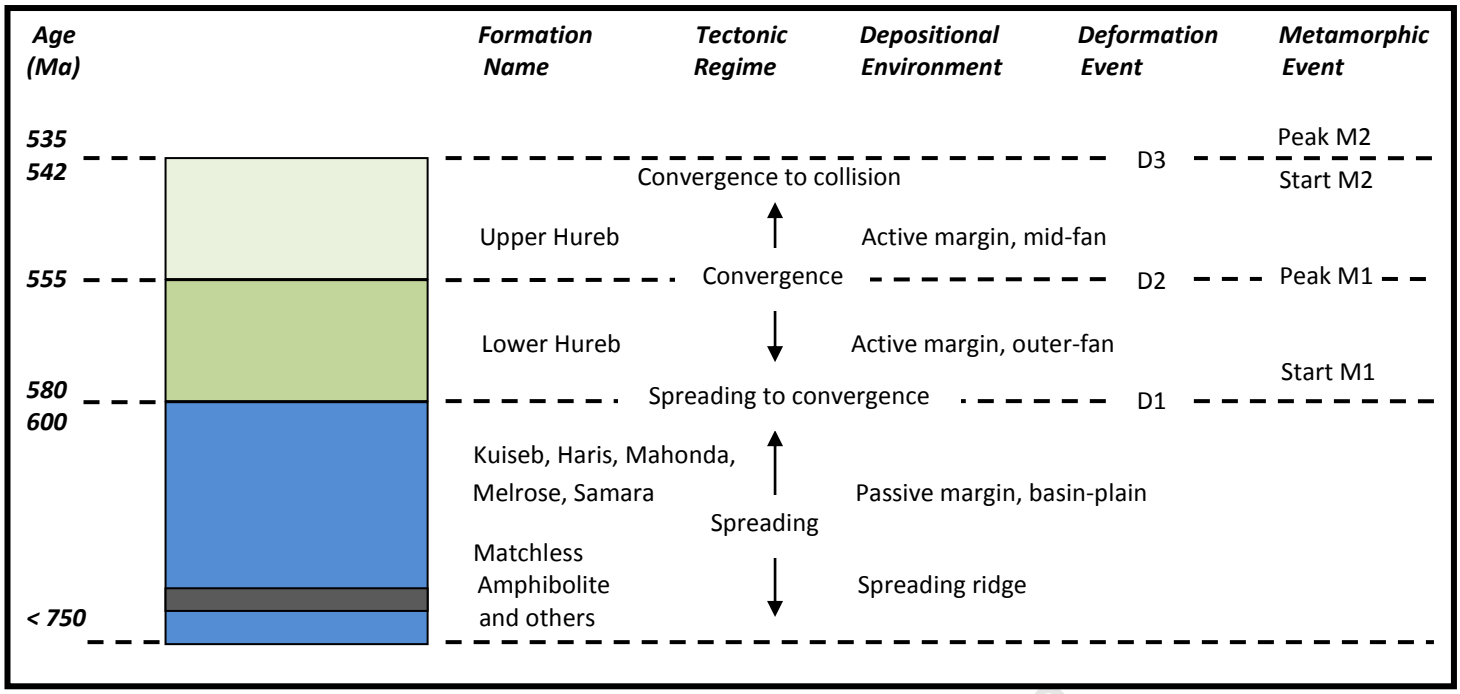

Figure 5: The stratigraphy of the Southern and Southern Margin Zones (after Kukla, 1992; Miller, 2008). D1, D2 and D3 denote the first, second and third deformation events, whereas M1 and M2 symbolise the first and second metamorphic events.

The schists of the Kuiseb and Hureb Formations contain an abundance of remnant sedimentary features, including cyclic, graded bedding with complete and semi-complete Bouma sequences, laterally extensive sedimentary marker units, scour and flame structures, ball-and-pillow structures, laminations, rip-up clasts and a multitude of palaeocurrent indicators, such as cross-bedding, ripple marks and flute casts (Kukla, 1992). Examination of the well preserved Bouma sequences and interpretation of the palaeocurrent indicators has allowed for the proposition that the protoliths to schists of the Kuiseb and Hureb Formation were deposited by several turbidity currents that propagated in a SW direction along a longitudinal submarine-fan that paralleled the margins of the Congo and Kalahari Cratons (Kukla & Stanistreet, 1991; Kukla, 1992; Miller, 2008). The protoliths to the schists of the Kuiseb Formation are believed to have been greywackes and shales that were deposited in a distal, deep-water, basin-plain environment beyond the outer-reaches of the sub-marine fan (Kukla & Stanistreet, 1991; Kukla, 1992; Miller, 2008). By contrast, the protoliths to the schists of the Hureb Formation are thought to have been deposited on the sub-marine fan, with the upward-thickening Bouma sequences of the Lower Hureb Formation indicating deposition in the outer-reaches of the fan and the upward-thinning Bouma sequences present in the Upper Hureb Formation signifying deposition in the mid-reaches of fan (Kukla & Stanistreet, 1991; Kukla, 1992; Miller, 2008). The presence of the calc-silicate bodies suggests that in addition to the turbiditic deposition processes, pelagic or at least hemi-pelagic deposition also occurred (Kukla, 1992; Miller, 2008).

Relic igneous features within the Matchless Amphibolite Member include abundant, flattened pillow structures that have medium-grained cores and fine-grained, chilled rims; sporadic bodies of coarse-grained metagabbro, some of which are undifferentiated and have chilled margins; and several dolerite dykes that also have chilled margins and are present as intrusions within the metagabbros (Kukla, 1992; Miller, 2008).

3.2.2. Deformation

Macro-structures and fabric elements present within the lithologies of the Southern Zone indicate that at least three deformation events occurred (Miller, 2008). The schists of the Kuiseb Formation display evidence for all three of these deformation events (D1, D2 and D3) (Miller, 2008). By contrast, the schists of the Hureb Formation exhibit evidence for only two of the deformation events that correlate to the second and third deformation events recognisable within the schists of the Kuiseb Formation (Miller, 2008). Furthermore, while the Lower Hureb Formation records both of these events (D2 and D3), the Upper Hureb Formation only records the last event (D3) (Miller, 2008). In other words, there is an observed decrease in structural complexity with increasing stratigraphic height, such that the youngest, overlying Upper Hureb Formation has evidence of one less deformation event than older, underlying Lower Hureb Formation, which in turn has evidence of one less deformation event than the oldest, lower most stratigraphic schists of the Kuiseb Formation.

The first deformation event (D1) involved the formation of fold and thrust structures, as well as an axial planar foliation, that were subsequently overprinted by the structural features of the later deformation events and are therefore only recognisable in a minor amount of the exposed Kuiseb Formation, specifically those to the south-east of Okahandja in the deepest stratigraphic levels (Miller, 2008).

The second deformation event (D2) resulted in SE-vergent folds with large amplitudes, large-scale thrusts and an axial planar foliation (Miller, 2008). The intensity of deformation increase southwards, such that the folds gradually change from being open and upright within the Lower Hureb Formation to tight and isoclinal within the Kuiseb Formation (Kukla, 1992; Miller, 2008). Moreover, the abundance of thrusts increases from only a sporadic few within the Lower Hureb Formation to a plenitude within the Kuiseb Formation (Kukla, 1992; Miller, 2008). The axial planar foliation, which is present as a slaty cleavage in the pelitic schists and as a metamorphic banding cleavage within the semipelitic schists, is more pronounced within the Kuiseb Formation than in the Lower Hureb Formation (Miller, 2008). In addition to these structures and fabric elements, S2-parallel quartz veins and a stretching lineation that plunges to the NW,

thus indicating transport and thrusting to the SE, may be observed within the pelitic schists of the Kuiseb Formation (Kukla, 1992; Miller, 2008).

The third deformation event (D3) is evidenced by the presence of isoclinal, SE-vergent folds and a NW-dipping axial planar foliation that is defined by the reorientation of mica within the Kuiseb and Lower Hureb Formations, and by open, upright folds and an axial planar foliation that is present as a metamorphic banding cleavage within the Upper Hureb Formation (Kukla, 1992; Miller, 2008). Additionally, a second lineation that plunges to the NW, thus indicating transport and thrusting to the SE, may be recognised within the Kuiseb Formation (Miller, 2008).

As a result of the intensity of deformation in the Southern Zone increasing southwards, a composite foliation that is comprised of all of the axial planar foliations that formed during all three deformation events (S0,1,2,3) exists in the southernmost schists of the Kuiseb Formation (Miller, 2008).

Deformation within the Matchless Amphibolite Member is limited relative to the surrounding schists of the Kuiseb Formation (Kukla, 1992; Miller, 2008). This is presumably due to ductility contrasts between the metamafic amphibolite and the metapsammopelitic schist (Miller, 2008). Nevertheless, deformation within the Matchless Amphibolite Member has been intense and includes local breccias, flattened pillow structures, sporadic thrusts and isoclinal folds that are overturned to the SE and seldom display fold closures (Kukla, 1992; Miller, 2008). Additionally, many of the metagabbro bodies have been deformed into lozenge-shaped pods that are elongated parallel to the penetrative foliation in the surrounding schists (Miller, 2008).

3.2.3. Metamorphism

Miller (2008) showed that for most of the Southern Zone the minerals muscovite, chlorite, biotite, garnet, staurolite and kyanite are present within metapsammopelitic schists. Thermobarometric measurements of the conditions at which these minerals equilibrated and the interpretation of the fabric relations between these minerals suggests that the rocks of the Southern Zone may have been subjected to two high pressure – low temperature metamorphic events (Kukla & Stanistreet, 1991; Kukla, 1992; Miller, 2008). The peak of the first metamorphic event (M1) occurred at ~ 555 Ma and was syn-tectonic (syn-D2), whereas the peak of the second metamorphic event (M2) occurred at ~ 535 Ma and was post-tectonic (post-D3) (Miller, 2008). According to Miller (2008), metamorphism relating to the gradual closure of the Khomas Sea during the convergence of the Congo and Kalahari Cratons between ~ 580 Ma and ~ 542 Ma corresponds to the

first metamorphic event, whereas the final closure of the Khomas Sea and collision of the two cratons at ~ 542 Ma relates to the second metamorphic event.

Work by Kasch (1981) on garnet-biotite and garnet-plagioclase pairs in garnet, staurolite and kyanite bearing assemblages in the Omitara and Gamsberg-Kuiseb River showed that the rocks of the Southern Zone record pressures of ~ 9 to 10 kbar and temperatures of ~ 574 to 590 °C for the first metamorphic event, and pressures of ~ 7.6 to 8.4 kbar and temperatures of ~ 532 to 570 °C for the second metamorphic event. Similar P-T conditions were recorded by Sawyer (1981) for peak mineral assemblages in the vicinity of the Gorob Mine. These conditions equate to a geothermal gradient of ~ 17 to 19.5 °C/km and ~ 19.0 to 22.5 °C/km, respectively (Miller, 2008).

4. *Field Relations and Petrography*

Field work was conducted during November 2011 and involved the collection of samples along two sections of the Gaub and Kuiseb Canyons (*Figure 6*). The canyons are approximately 150 km south-west of Windhoek and are in excess of 15 km apart from each other across strike. The Kuiseb Canyon is located in the southern third of the SZ, whereas the Gaub Canyon is located immediately adjacent to the GRL in the SMZ. These localities were chosen due to the comparatively higher availability of fresh exposures and uninterrupted sections within the canyons, along the periphery of dry river beds, as opposed to areas outside of the canyons that are extensively covered by recent calcrete.

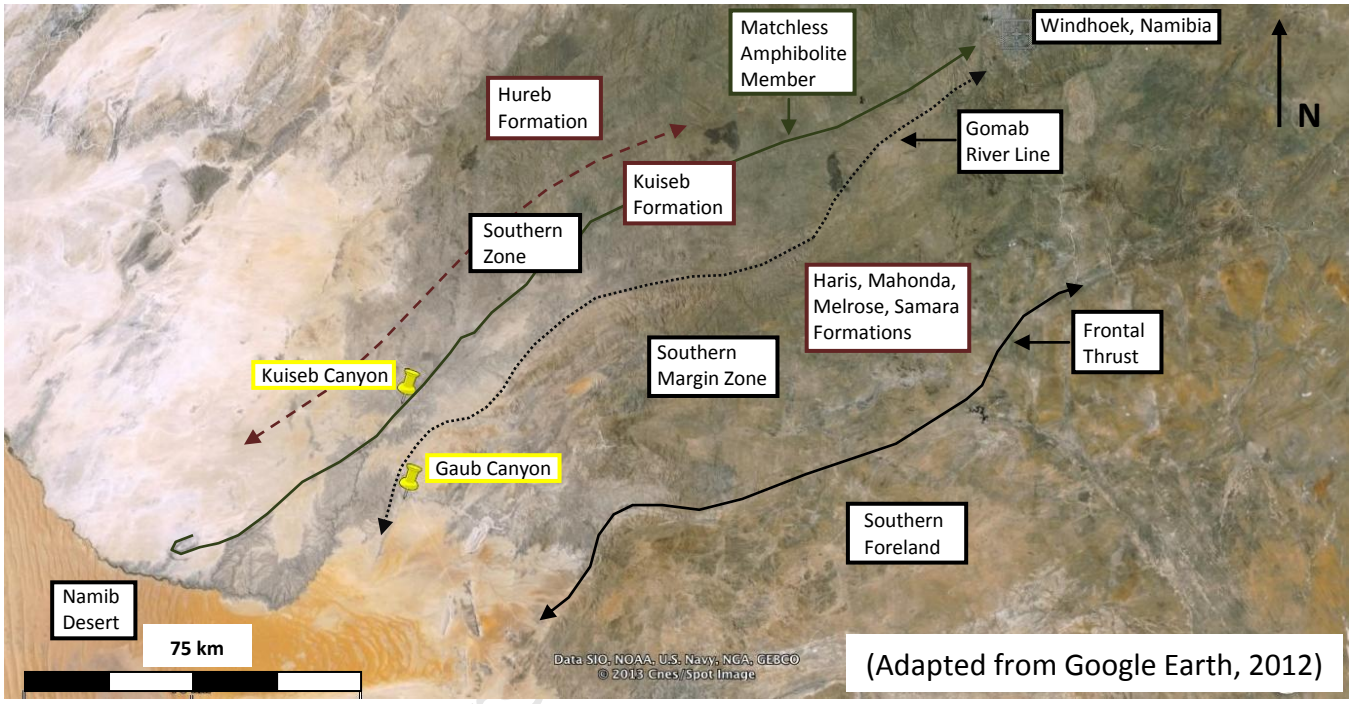

Figure 6: Sampling localities. Samples were collected from two pre-determined localities, ~ 15 km apart across strike, in the SZ and SMZ (yellow). The approximate location of tectonostratigraphic zones and boundaries (*black*) and the main stratigraphic formations (*red* & *green*) are also shown.

The main rock types present in both of these localities are metapelites, metapsammites, metamafics and calc-silicates. All of these rocks have an observed dip of approximately 45° to the north-west. The sample from the Gaub Canyon (*Figure 7)* was comprised of six metapelites (specimens GB-6, GB-7, GB-8, GB-10, GB-12 and GB-13), six metamafics (specimens GB-1, GB-2, GB-3, GB-4, GB-5 and GB-11) and one calc-silicate (specimen GB-9). Similarly, the sample from the Kuiseb Canyon (*Figure 8*) consisted of eight metapelites (specimens MA-29, MA-31, MA-35, MA-38, MA-39, MA-40, MA-41 and MA-42), two metapsammites (specimens MA-30 and MA-36), five metamafics (specimens MA-32, MA-33, MA-34, MA-43 and MA-44) and one calc-silicate (specimen MA-37). The compositional diversity of the collected specimens ensured the greatest potential for the establishment of the metamorphic evolution (P-T path/s) of the SZ, whereas the spatial distance between the two sampling localities ensured that the possibility of an internal field gradient in the SZ could be easily recognised.

Figure 7: Sample collection in the Gaub Canyon. Specimens GB-6, GB-7, GB-8, GB-10, GB-12 and GB-13 are metapelites, specimens GB-1, GB-2, GB-3, GB-4, GB-5 and GB-11 are metamafics, specimen GB-9 is a calc-silicate. The distance between GB-3 and GB-8 is ~ 2.05 km.

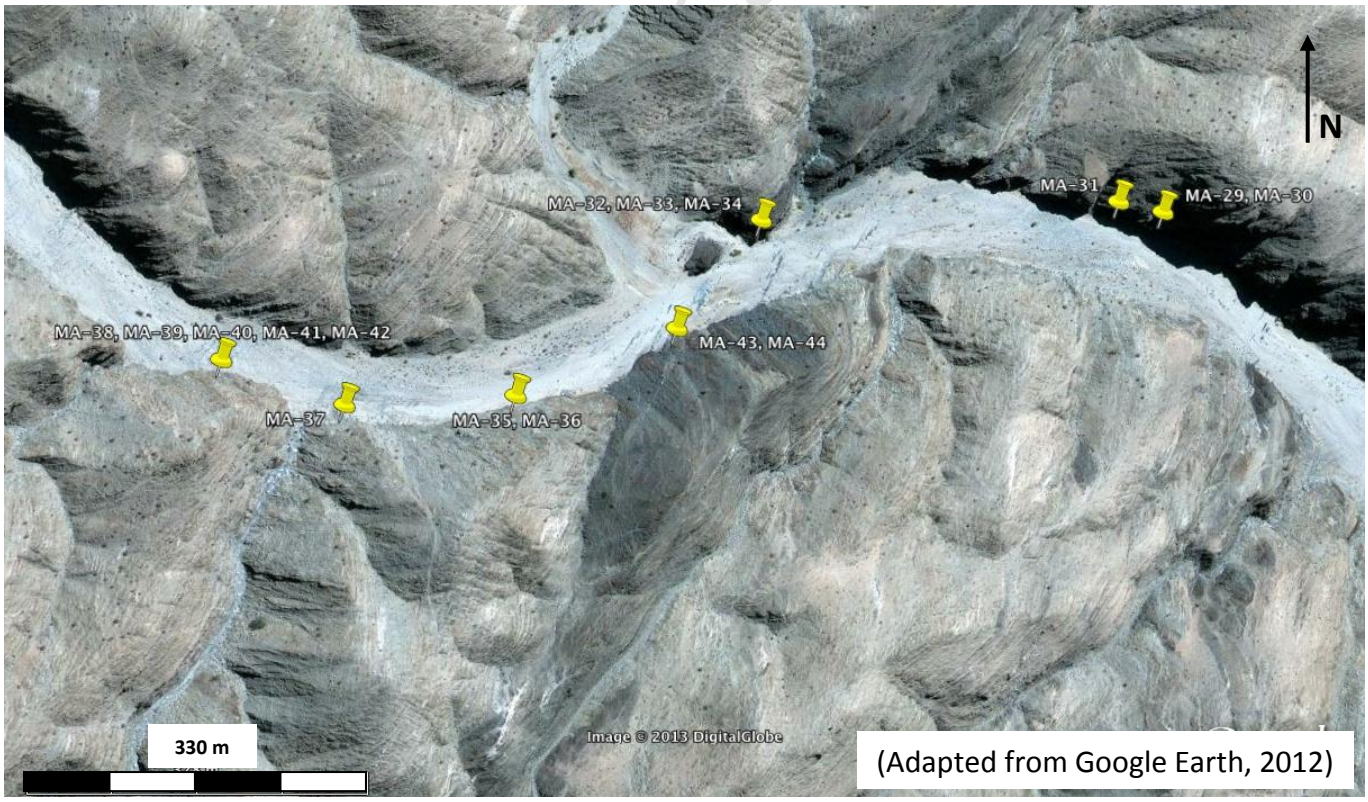

Figure 8: Sample collection in the Kuiseb Canyon. Specimens MA-29, MA-31, MA-35, MA-38, MA-39, MA-40, MA-41 and MA-42 are metapelites, specimens MA-30 and MA-36 are metapsammites, specimens MA-32, MA-33, MA-34, MA-43 and MA-44 are metamafics, specimen MA-37 is a calc-silicate. The distance between MA-30 and MA-38 is ~ 0.95 km.

4.1. Field Relations

In both the Gaub and Kuiseb Canyons, the metapelites and metapsammites are intimately intercalated with the metamafics (*Figure 9a & b*). Individual metapelitic, metapsammitic and metamafic layers range in width from tens of centimetres to a few metres. The metamafic Matchless Amphibolite Member in the Kuiseb Canyon displays the greatest spatial continuation without disruption by metapelites and metapsammites. In places, calc-silicates occur as thin (less than 30 cm thick) layers within the metapelites and metapsammites (*Figure 9c*). The metamafics contain an abundance of discrete gabbro pods that are up to tens of centimetres in length (*Figure 9d*).

All of the rocks are highly deformed, with prevalent evidence for high strain observed at a variety of scales. One such example comes from the gabbro pods in the metamafics. The elongated oval shape of these pods and in some cases, the apparent shearing of the pods – whereby portions of a pod have been drawn out relative to other portions, therefore giving the pod an irregular, jagged shape – are symptomatic of deformation to high strain (*Figure 10*). Moreover, strongly dismembered quartz veins of variable thickness (up to 20 cm thick) occur throughout all of the rock types. Where these quartz veins occur in large gabbro pods, they are often surrounded by a zone of alteration (*Figure 11*).

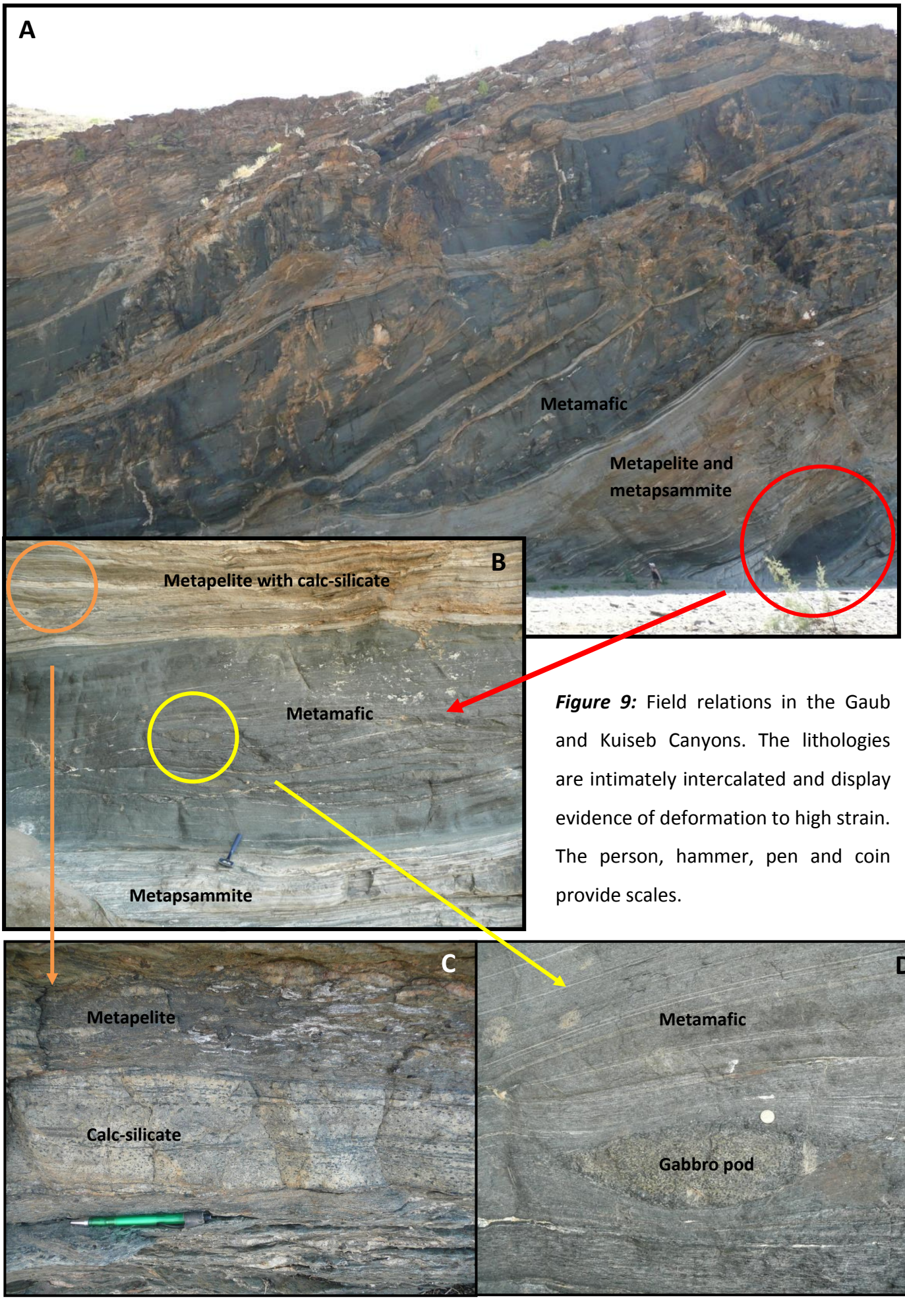

Figure 9: Field relations in the Gaub and Kuiseb Canyons. The lithologies are intimately intercalated and display evidence of deformation to high strain. The person, hammer, pen and coin provide scales.

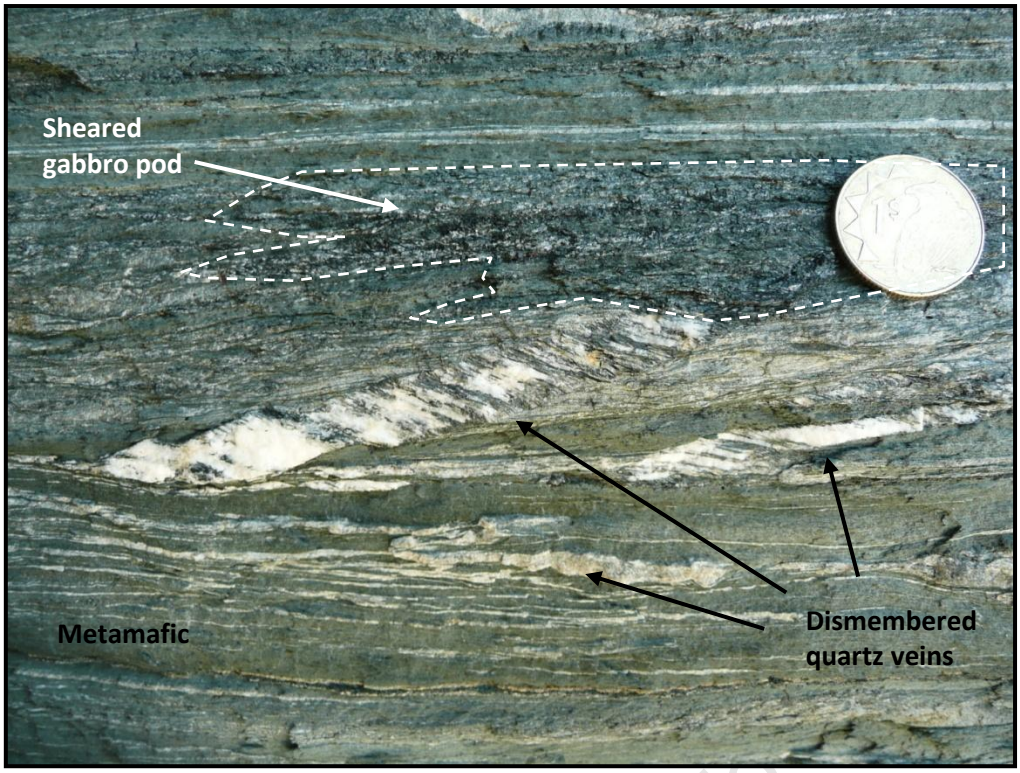

Figure 10: Deformation in the metamafic layers in the Gaub and Kuiseb Canyons. Sheared gabbro pods (*dashed white*) and strongly dismembered quartz veins provide evidence for deformation to high strain. The coin for scale is 2.3 cm across.

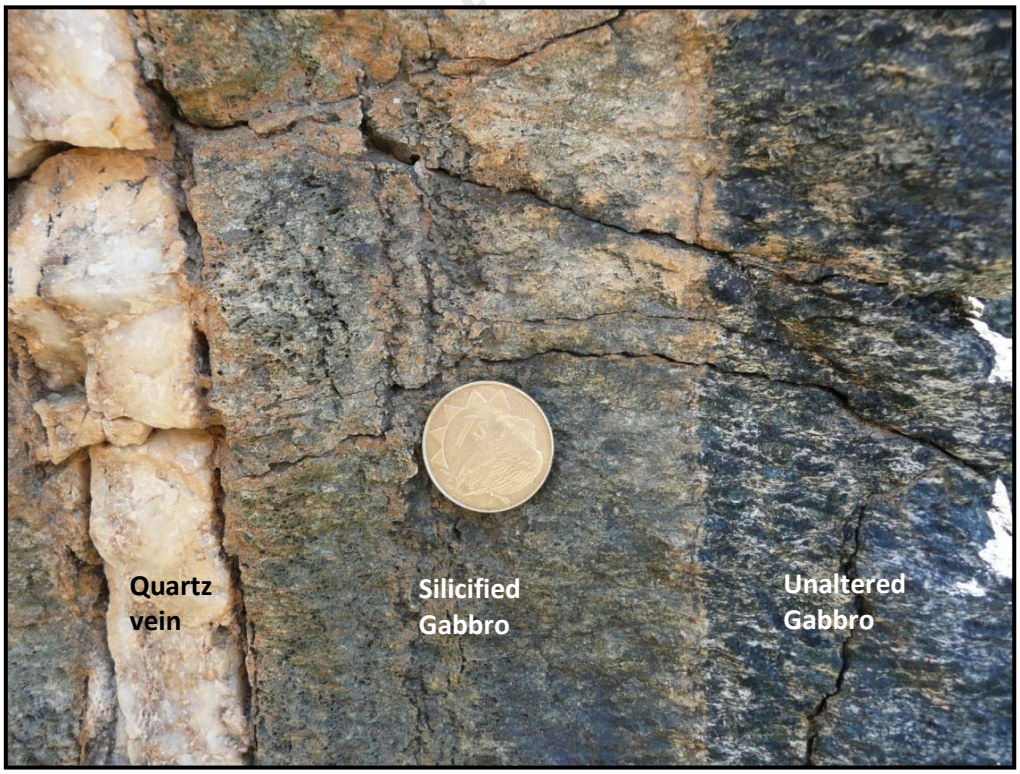

Figure 11: Alteration of the gabbro pods in the metamafic layers in the Gaub and Kuiseb Canyons. Quartz veins in large gabbro pods are often surrounded by a zone of silicification. The coin for scale is 2.3 cm across.

4.2. Metapelitic Rocks from the Gaub Canyon

In hand specimen, these rocks have a prominent schistose appearance and a distinct fabric that is defined by the alignment of very shiny, fine- to very fine-grained, silver - grey - green muscovite and chlorite, as well as biotite. The fabric is sporadically overprinted by two types of porphyroblasts, namely medium-grained, dark brown - black laths and blobs of staurolite that are up to 0.3 cm in length (typically ~ 0.15 cm) and have no preferred orientation or are weakly parallel to the fabric; and coarse- to very coarse-grained, red - brown, circular grains of garnet that are up to 0.9 cm across and have no preferred orientation (*Figure 12 & Figure 13*). In places, the laths are grouped together to form rosettes. The relative abundance of staurolite is greatest in specimens GB-8 and GB-10, whereas garnet is most prominent in specimen GB-13. In addition to these minerals, abundant, creamy white - pale brown quartz veins of variable thickness, but commonly greater than 1.5 cm, extend parallel to the fabric. Many of these quartz veins are strongly dismembered (*Figure 13*). Pale brown - orange surface weathering occurs in some areas on these rocks.

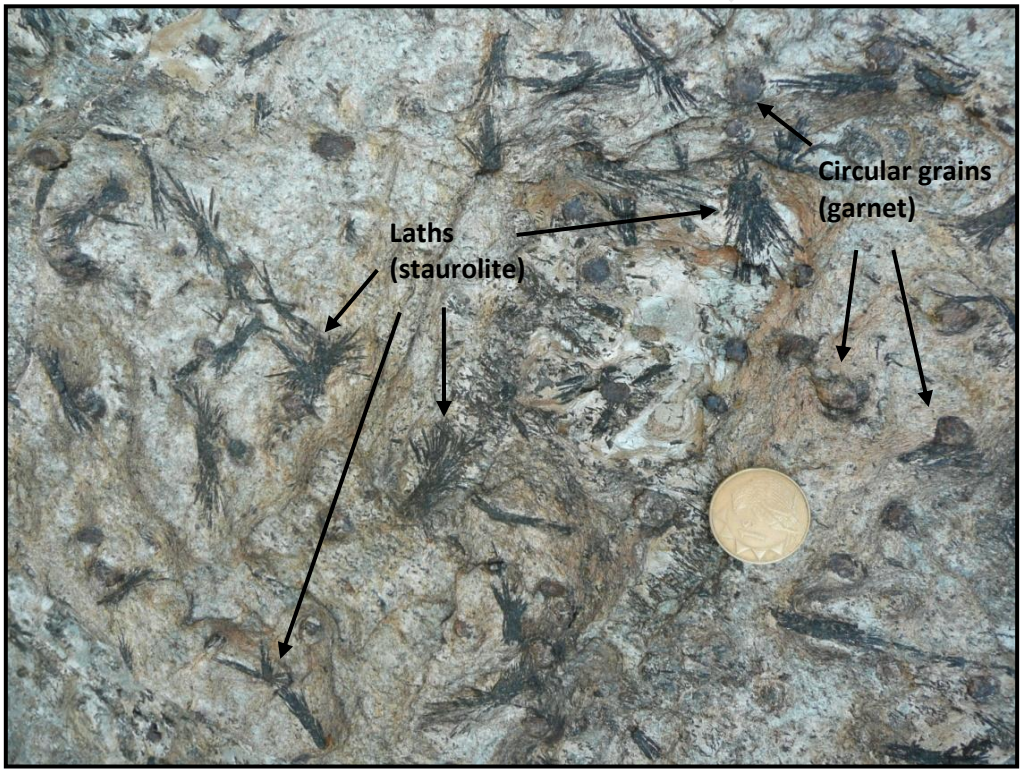

Figure 12: Outcrop of metapelitic specimen GB-13. The rock has a schistose appearance, with a silver - grey (- green) coloured matrix being overprinted by medium-grained, dark brown - black laths (staurolites) and very coarse-grained, red - brown, circular grains (garnets). Some of the laths are grouped together to form rosettes. The coin for scale is 2.3 cm across; view on foliation plane.

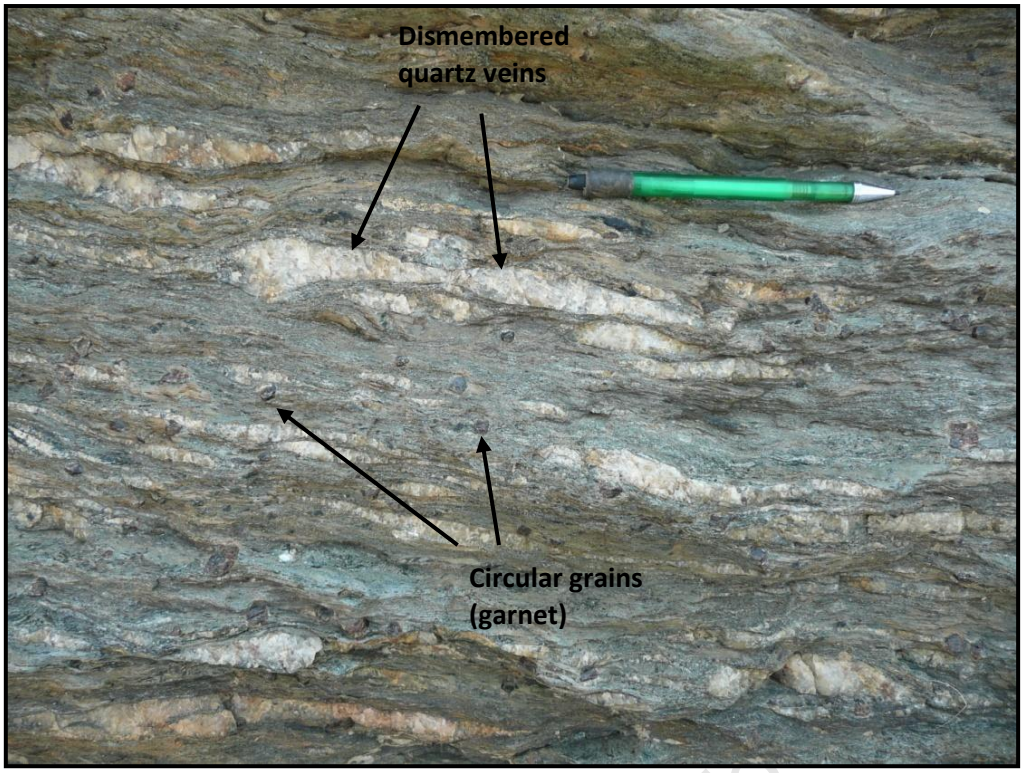

Figure 13: Outcrop of metapelitic specimen GB-8. Very coarse-grained, red - brown, circular grains (garnets) overprint the grey - green (- silver) fabric, whereas dismembered quartz veins of variable thickness extend parallel to the fabric. The pen for scale is 15 cm long; view is perpendicular to S2 foliation.

In thin section, the observed mineral assemblage in these rocks is comprised of garnet and staurolite porphyroblasts set in a fine- to very fine-grained matrix of chlorite, biotite, muscovite, paragonite, epidote, ilmenite and quartz. Additionally, plagioclase and magnetite are present in some of the specimens as very minor matrix minerals that were not observed in thin-section, but were detected by EMP analyses of the specimens. The matrix exhibits a strong penetrative foliation that is defined by the alignment of the micaceous minerals, chlorite, biotite and muscovite. The garnet and staurolite porphyroblasts overprint this fabric and are not preferentially oriented. *Figure 14* provides a representative set of photomicrographs of the metapelitic rocks the Gaub Canyon.

The garnet porphyroblasts are euhedral to subhedral in shape and range in size from 2 mm to 9 mm, with the majority being greater than 3.5 mm in diameter. The staurolite porphyroblasts, which in some cases overgrow the edges of the garnet porphyroblasts, are mainly subhedral in shape and smaller in size than the garnet porphyroblasts, with most of the porphyroblasts ranging in size from 0.4 mm to 3 mm. Both the garnet and staurolite porphyroblasts are undeformed and unrotated relative to the matrix. The garnet porphyroblasts, and to a lesser extent, the staurolite porphyroblasts, often contain inclusions of quartz and ilmenite that are less than 0.6 mm and 0.3 mm in size, respectively.

The chlorite, biotite and muscovite grains have predominant elongated, lath-like shapes that are of a highly variable length that ranges from 0.1 mm to 2.5 mm. Typically, the chlorite and biotite grains are larger than the muscovite grains, which seldomly exceed 1 mm. However, it must be noted that some of the larger chlorite and biotite grains are in fact amalgamations of multiple grains. In most cases, it appears that the biotite grains overgrow the chlorite and muscovite grains. A few of the biotite grains cross-cut the foliation. Epidote exists as sparse, tiny (less than 0.2 mm), crudely circular grains within the matrix. They are usually located along or close to a boundary between quartz and a micaceous mineral, and are distinguished from the surrounding matrix minerals by their high relief and high birefringence under cross-polarised light. Ilmenite occurs both as a sporadic, 0.5 mm to 2.5 mm blobs within the matrix and as smaller, less than 0.2 mm inclusions within the porphyroblasts. In places, quartz, which is a prominent matrix mineral, exists as large pockets composed of multiple grains – these presumably represent the quartz veins that were observed in hand specimen. The garnet and staurolite porphyroblasts account for ~ 25 to 30 % and ~ 10 to 25 % of the modal abundance in the specimens, respectively, with the matrix minerals constituting the remaining ~ 40 to 65 %. Of the matrix minerals, chlorite, biotite and quartz are the most abundant, whereas muscovite, ilmenite and epidote are less abundant.

The most prevalent textural feature observed in hand specimen and in thin section is the overprinting of the fabric, which is defined by the micaceous minerals muscovite, chlorite and biotite, by non-preferentially orientated garnet and staurolite porphyroblasts, and some biotite grains.

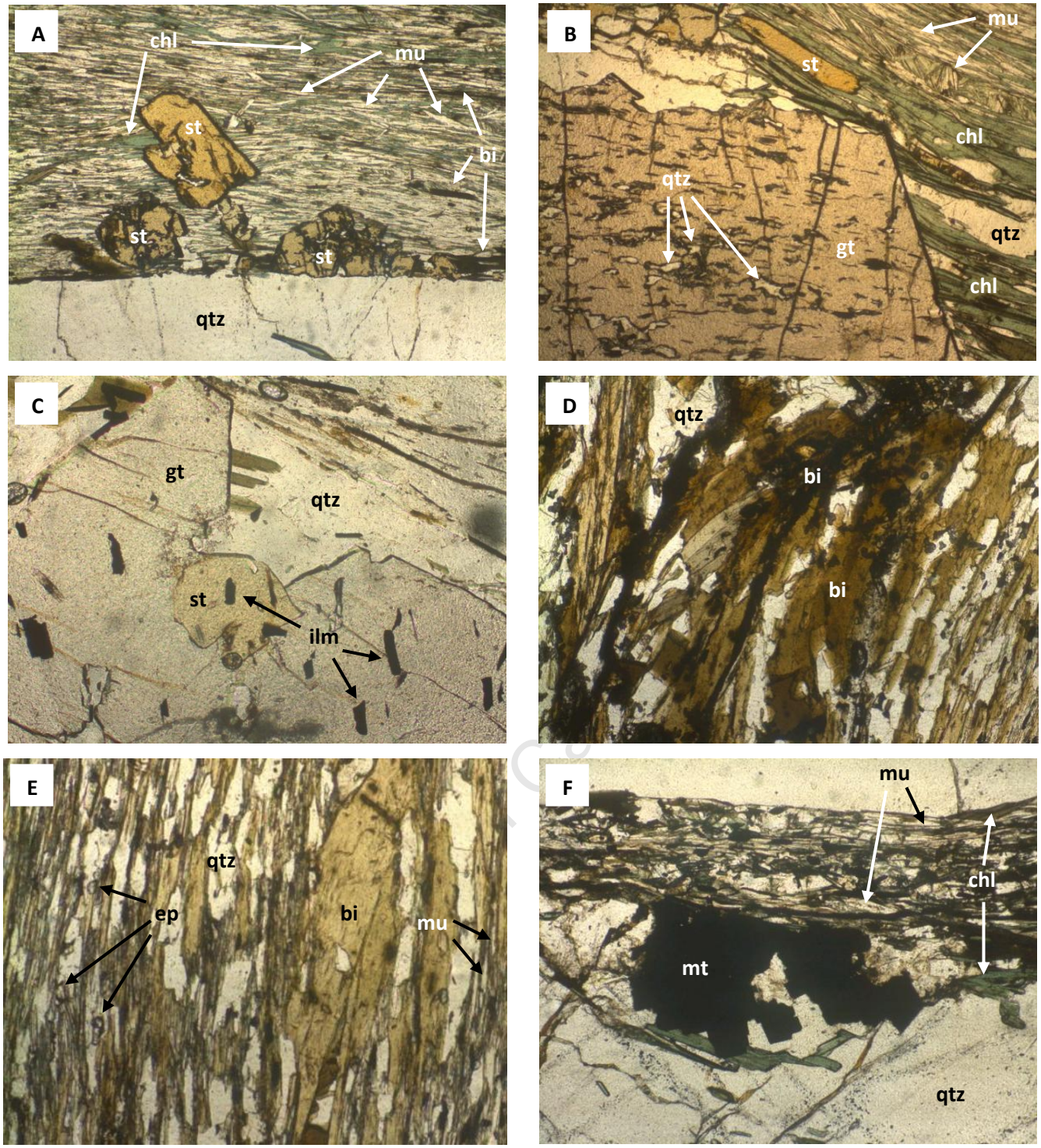

Figure 14: Photomicrographs of the metapelitic rocks from the Gaub Canyon. *A*: Staurolite porphyroblasts overprinting micaceous foliation (*GB-10*). *B*: Garnet porphyroblast with quartz inclusions overprinting micaceous foliation (*GB-10*). *C*: Staurolite porphyroblast overprinting rim of garnet porphyroblast, both with ilmenite inclusions (*GB-10*). *D*: An amalgamation of biotite grains (*GB-13*). *E*: Sparse, tiny epidote grains adjacent quartz in micaceous foliation (*GB-13*). *F*: A rare magnetite grain adjacent quartz and micaceous foliation (*GB-8*). *St* = staurolite, *gt* = garnet, *bi* = biotite, *chl* = chlorite, *mu* = muscovite, *ep* = epidote, *ilm* = ilmenite, *mt* = magnetite, *qtz* = quartz. Photomicrographs *A*, *B*, *D*, *E*, *F* were taken in PPL at 50X magnification, FOV = 3.5 mm; photomicrograph *C* was taken in PPL at 100X magnification, FOV = 2 mm.

4.3. Metapelitic Rocks from the Kuiseb Canyon

In hand specimen, these rocks are darker in colour, coarser grained and have a less prominent schistose appearance than the metapelitic rocks from the Gaub Canyon (*Figure 15 & 16*). They also contain a more abundant amount of porphyroblasts, as well as additional mineral phases. The specimens have a well-defined fabric that is composed of moderately shiny, fine- to very fine-grained, grey-white muscovite and chlorite, as well as biotite. The biotite occurs as prominent black flakes that are up to 0.6 cm (typically 0.25 cm) in length. The fabric is overprinted by three types of porphyroblasts that have no preferred orientation. These porphyroblasts are medium- to coarse-grained, orange - brown laths and blobs of staurolite that are up to 0.8 cm (typically 0.1 to 0.3 cm) in length; coarse-grained, crudely circular garnet grains that are red - brown in colour and up to 0.5 cm (typically 0.3 cm) across; and coarse-grained, pale blue patches of kyanite that are up to 0.7 cm across. The only exception is in specimen MA-29 where the staurolite is moderately parallel to the fabric. The garnet grains are best observed in specimen MA-29, whereas the kyanite is most obvious in specimen MA-31. Specimen MA-40 contains less garnet and is the only specimen that has a schistose appearance that is broadly similar to that observed in the metapelitic rocks from the Gaub Canyon. In addition to the fabric minerals and overprinting porphyroblasts, several thin, creamy white - orange - pale brown quartz veins of thickness commonly less than 0.25 cm exist parallel to fabric. As in the metapelitic rocks from the Gaub Canyon, many of these quartz veins are strongly dismembered. Orange - pale brown surface weathering is present in some areas on these rocks.

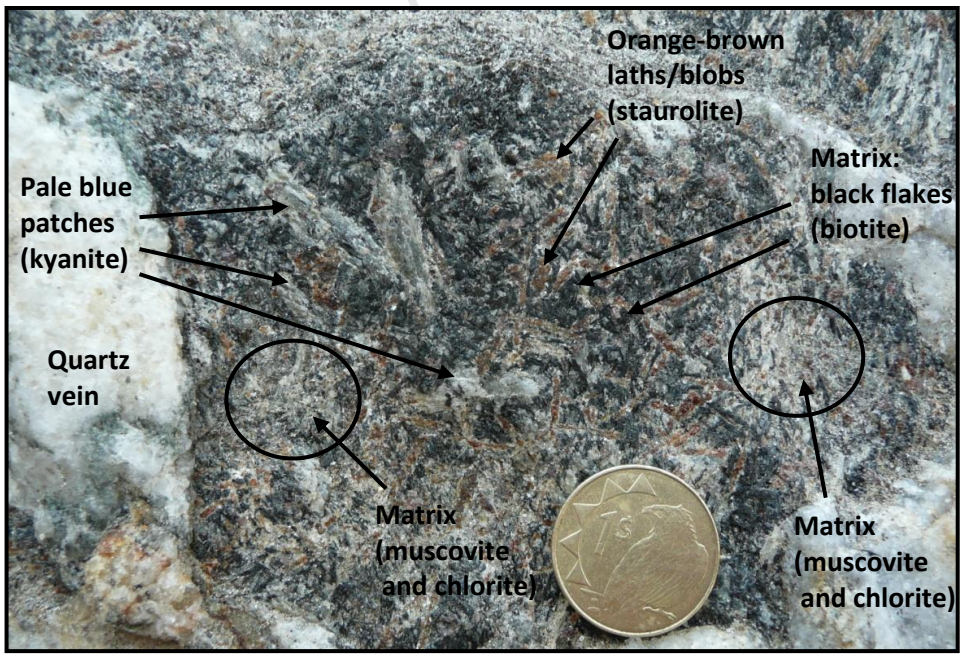

Figure 15: Outcrop of metapelitic specimen MA-38. The rock has a less prominent schistose appearance than the metapelitic rocks from the Gaub Canyon, with a grey-white coloured matrix (muscovite and chlorite) with abundant black flakes (biotites) being overprinted by medium- to coarse-grained, orange-brown laths/blobs (staurolites); coarse, circular grains that are red - brown in colour (garnets); and coarse pale blue patches (kyanites). The coin for scale is 2.3 cm across.

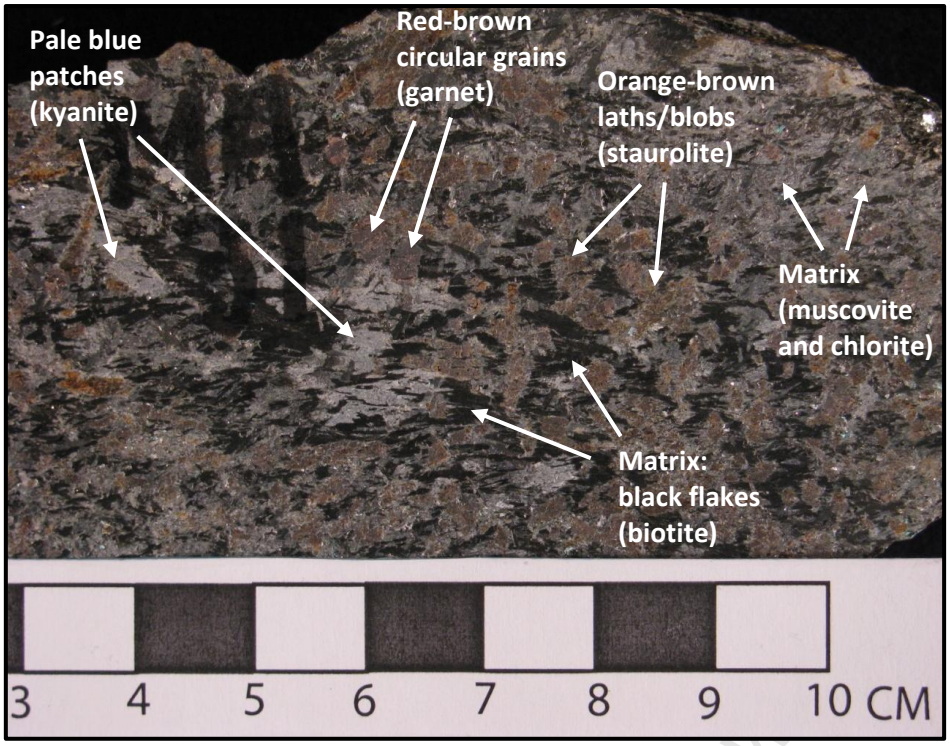

Figure 16: Metapelitic hand specimen MA-31. The matrix, which is grey-white in colour (muscovite and chlorite), contains prominent black flakes (biotites) and is overprinted by coarse, circular grains that are red - brown in colour (garnets); medium- to coarse-grained, orange-brown laths/blobs (staurolites); and coarse pale blue patches (kyanites). As with specimen MA-38, the rock has a schistose appearance that is less apparent than in the metapelitic rocks from the Gaub Canyon.

In thin section, the metapelitic rocks from the Kuiseb Canyon may be distinguished from those from the Gaub Canyon by a slightly coarser matrix, the presence of additional porphyroblasts of kyanite, the local existence of rutile in the matrix and the absence of magnetite. The observed mineral assemblage in these rocks is comprised of garnet, staurolite and kyanite porphyroblasts set in a fine- to very fine-grained matrix of chlorite, biotite, muscovite, paragonite, epidote, ilmenite and quartz. The only exception is in specimen MA-29, where no kyanite was observed. Rutile and plagioclase are present in some of the specimens as very minor matrix minerals that were not observed in thin-section, but were detected by EMP analyses of the specimens. As in the metapelitic rocks from the Gaub Canyon, the matrix exhibits a strong penetrative foliation that is defined by the alignment of the micaceous minerals, chlorite, biotite and muscovite. The garnet, staurolite and kyanite porphyroblasts overprint this fabric and have no preferential orientation. *Figure 17* below provides a representative set of photomicrographs of the metapelitic rocks the Kuiseb Canyon.

The garnet porphyroblasts are euhedral to subhedral in shape and range in size from 1 mm to 5 mm, with the most common size being ~ 3 mm. Most of the staurolite porphyroblasts are subhedral in shape and range in size from 1 mm to 3 mm, however certain porphyroblasts, specifically some of those in specimen

MA-29, are more anhedral in shape and are up to 8 mm across. The kyanite porphyroblasts are subhedral to anhedral in shape and are easily identified by their characteristic brick-work pattern. They have a broad size range from 1 mm to 7 mm, but are typically greater than 3.5 mm in diameter. All three of the porphyroblasts are undeformed and unrotated relative to the matrix. Additionally, they contain a variable amount of inclusions of quartz and ilmenite.

The fabric-forming minerals, biotite and chlorite are present as both elongated, anhedral patches and elongated laths, with the latter shape being primarily defined by the biotite grains. The chlorite grains have a narrow size range of between 1 mm and 2 mm, whereas the biotite grains range from 0.5 mm to 6 mm in length, with a common size of ~ 2.5 mm. Amalgamations of multiple grains of biotite or chlorite are present in some areas. Muscovite, the third fabric-forming mineral, typically exhibits an elongated lath-like shape and is much smaller than the biotite and chlorite grains, with all of the laths being less than 1 mm in length and the majority not exceeding 0.2 mm in length. In most cases, it appears that the chlorite and muscovite grains are overgrown by the biotite grains. Furthermore, a few of the biotite grains cross-cut the foliation. Epidote exists in the matrix as sparse, small (less than 0.2 mm), crudely circular grains that have a high relief and a high birefringence. They are usually located along or close to a boundary between quartz and a micaceous mineral. Ilmenite, which exists as small, often semi-circular grains that do not exceed 0.4 mm, occurs intermittently within the matrix and as inclusions within the porphyroblasts. Quartz exists as inclusions within the porphyroblasts, as sporadic grains distributed throughout the matrix and as large pockets composed of multiple grains. The garnet, staurolite and kyanite porphyroblasts account for ~ 25 to 35 %, ~ 25 to 35 % and ~ 5 to 15 % of the specimens, respectively, with the matrix minerals constituting the remaining ~ 15 to 45 %. Chlorite, biotite and quartz are the most abundant matrix minerals, whereas muscovite, ilmenite and epidote are less abundant.

The overprinting of the fabric, which is defined by the micaceous minerals muscovite, chlorite and biotite, by non-preferentially orientated garnet, staurolite and kyanite porphyroblasts, and some biotite grains, is the most obvious textural feature observed in hand specimen and in thin section.

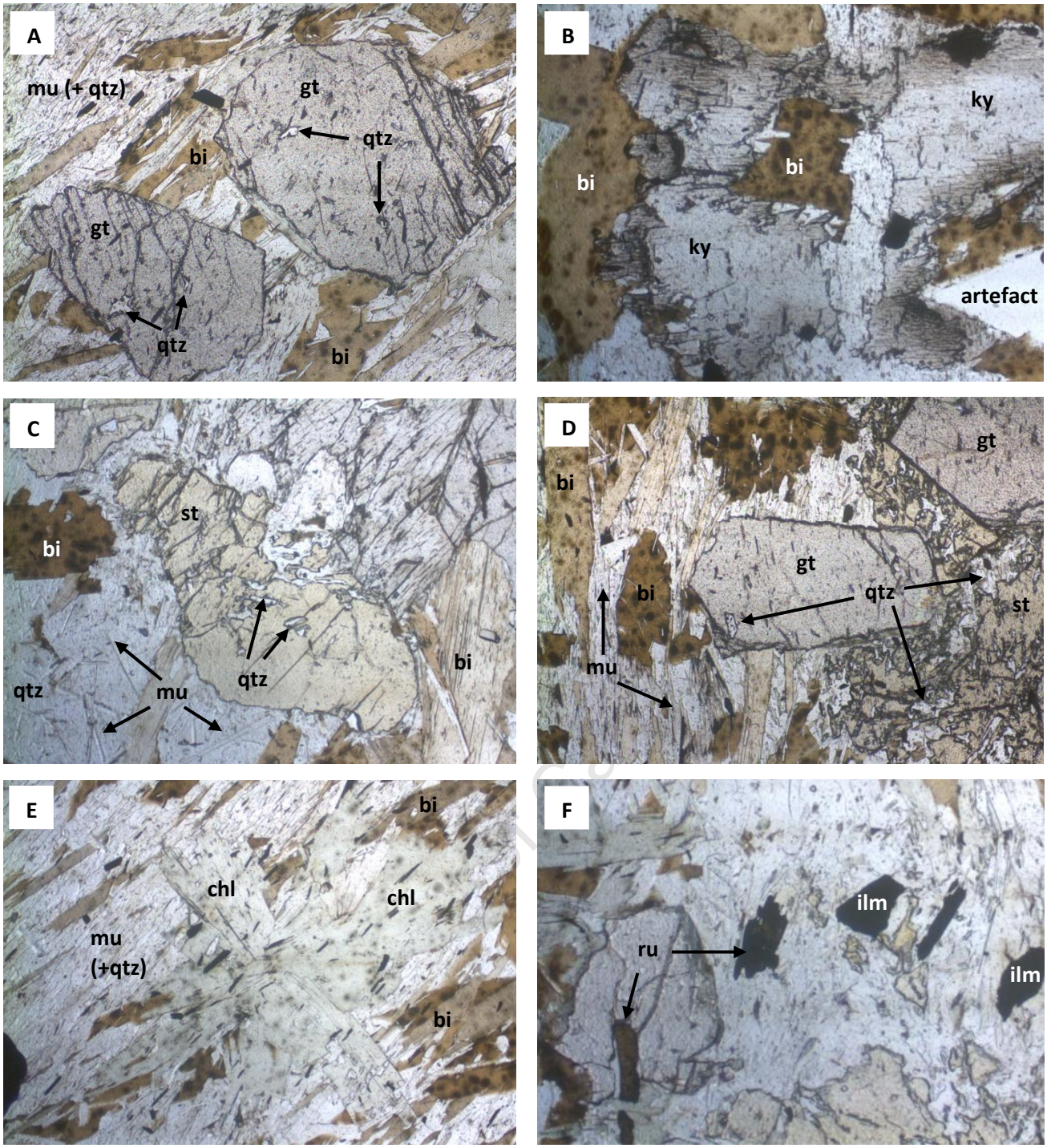

Figure 17: Photomicrographs of the metapelitic rocks from the Kuiseb Canyon. *A*: Garnet porphyroblasts with quartz inclusions overprinting micaceous foliation (*MA-29*). *B*: Kyanite porphyroblast/s, with distinct brickwork pattern at edges, overprinting biotite (MA-38). *C*: Staurolite porphyroblast with inclusions of quartz overprinting biotite, muscovite needles and quartz (*MA-31*). *D*: Garnet porphyroblasts overprinting rim of staurolite porphyroblast, both of which overprint micaceous foliation and have inclusions of quartz (*MA-31*). *E*: A radiating amalgamation of chlorite grains in micaceous foliation (*MA-29*). *F*: Rare rutile grains with ilmenite grains (*MA-40*). *St* = staurolite, *gt* = garnet, *bi* = biotite, *chl* = chlorite, *mu* = muscovite, *ep* = epidote, *ilm* = ilmenite, *qtz* = quartz, *arteface*t = hole or bubble in thin section. All of the photomicrographs were taken in PPL at 50X magnification. FOV = 3.5mm.

4.4. Metamafic Rocks from the Gaub and Kuiseb Canyons

In hand specimen, these rocks are grey - green in colour and are very fine- to fine-grained (*Figure 18*), with specimen GB-4 being only marginally coarser than specimen MA-44. Despite their grain size, a prominent schistose fabric may be observed. The fabric is disrupted by very thin veins of quartz of less than 0.15 cm. Orange - pale brown surface weathering is present in some areas on these rocks.

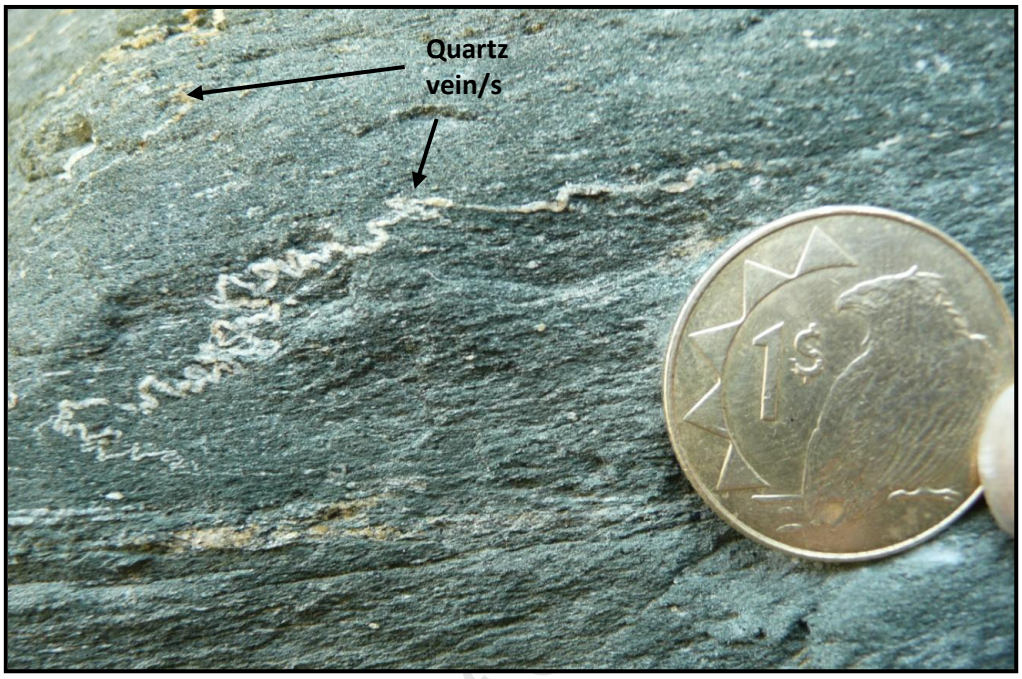

Figure 18: Outcrop of metamafic specimen MA-44. The rock is very fine- to fine-grained and grey - green in colour. Very thin quartz veins are observed. The coin for scale is 2.3 cm across.

In thin section, the observed mineral assemblage in these rocks is comprised of amphibole, epidote, rutile, quartz and minor mica, specifically biotite. In GB-4, the amphibole is hornblende, whereas in MA-44 both hornblende and actinolite exist. Additionally, specimen MA-44 contains sphene and minor chlorite. As with the metapelitic rocks from the Gaub and Kuiseb Canyons, plagioclase is also present in MA-44 as very minor matrix mineral that was not observed in thin-section, but was detected by EMP analysis of the specimen. The amphiboles and micas are aligned to form a distinct foliation within the rocks. No minerals occur as porphyroblasts that overprint the foliation. *Figure 19* below provides a representative set of photomicrographs of the metamafic rocks the Gaub and Kuiseb Canyons.

The amphiboles are pale brown-dark green in colour under plane-polarised transmitted light and are of a subhedral to anhedral shape, with some grains appearing slightly elongated and others being more semi-circular. All of the amphibole grains are less than 0.4 mm in size. Epidote is present as small, crudely circular grains that are less than 0.2 mm across and have a high relief and a high birefringence. Frequently, an irregular-shaped network of epidote resulting from the contact between multiple epidote grains exists

between the amphibole grains. In specimen GB-4, epidote is overgrown by hornblende. By contrast, in specimen MA-44, some the actinolite grains are overgrown by epidote and some of the epidote grains are overgrown by hornblende. Rutile, which occurs as infrequent amber-coloured anhedral blobs that have a high relief and are less than 0.3 mm across, often overgrows amphibole. Sphene forms small diamond-shaped grains that are less than 0.3 mm. The micas (biotite and chlorite), which are sparsely dispersed throughout the specimens, are subhedral to anhedral in shape and less than 0.5 mm in size. In both specimen GB-4 and MA-44, the micas are overgrown by epidote and amphibole. In specimen MA-44, narrow bands composed of multiple grains of quartz exist. These bands most probably represent the thin quartz veins that were observed in hand specimen. Amphibole has the greatest modal abundance within the specimens, accounting for ~ 40 to 45 % of the rocks. Epidote and quartz account for ~ 20 % and ~ 25 %, respectively, whereas the remaining ~ 10 to 15 % is comprised of rutile, sphene, chlorite and biotite.

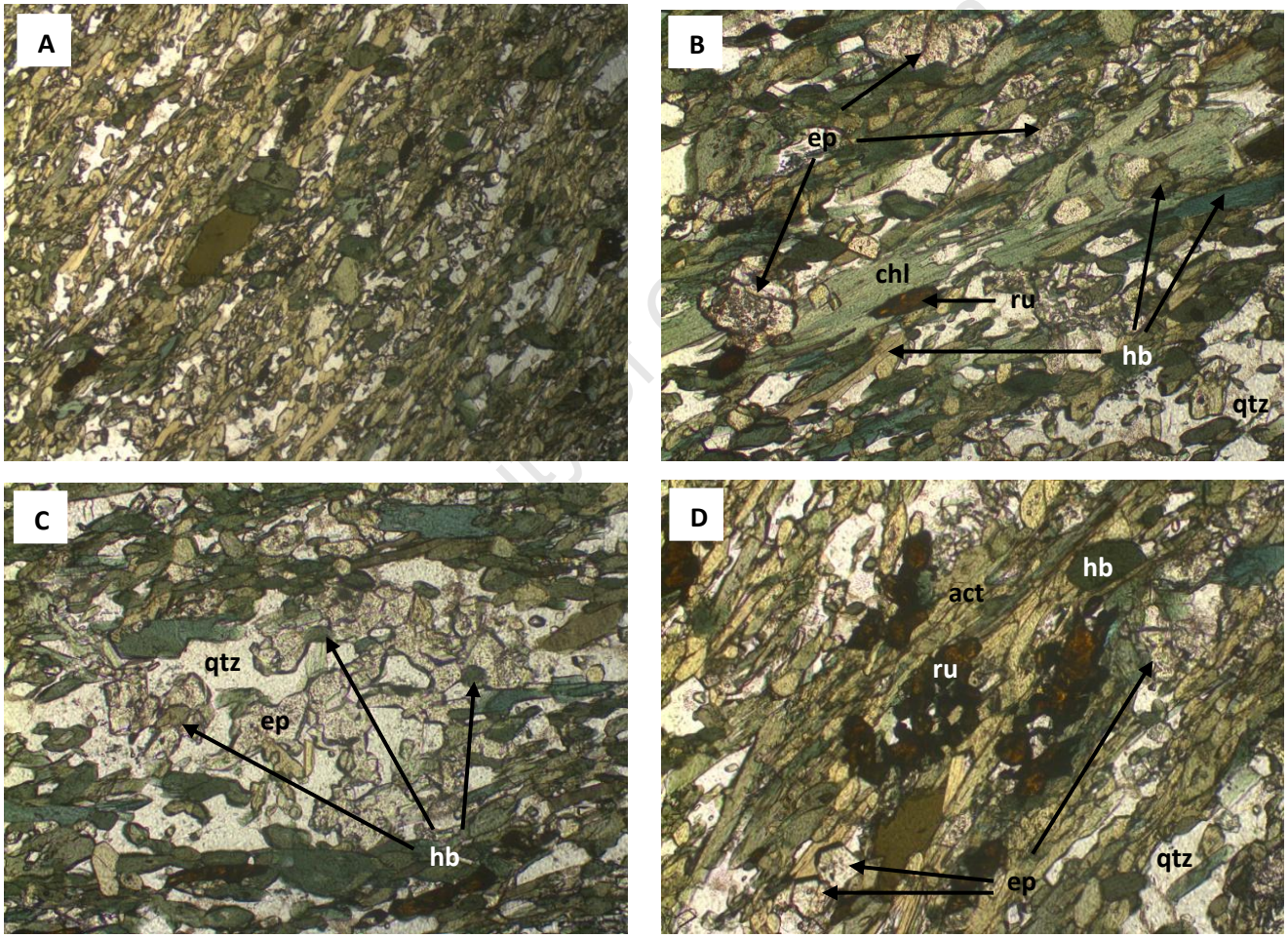

Figure 19: Photomicrographs of the metamafic rocks from the Gaub and Kuiseb Canyons. *A*: General very fine- to fine-grained, foliated appearance of the rocks in thin-section (*GB-4*). *B*: A rare, partially consumed chlorite grain overgrown by hornblende, epidote and rutile (*MA-44*). *C*: A network of epidote grains overgrown by hornblende (*GB-4*). *D*: Actinolite grains overgrown by rutile, epidote and hornblende (*MA-44*). *Hb* = hornblende, *act* = actinolite, *bi* = biotite, *chl* = chlorite, *ep* = epidote, *ru* = rutile, *qtz* = quartz. Photomicrograph *A* was taken in PPL at 50X magnification, FOV = 3.5 mm; photomicrographs *B – D* were taken in PPL at 100X magnification, FOV = 2 mm.

4.5. Metapsammitic Rocks from the Gaub and Kuiseb Canyons

In hand specimen, these rocks are quartz-rich and have a speckled, moderately schistose appearance that is defined by very fine-grained muscovite and fine- to medium-grained dark brown biotite flakes that are up to 0.15 cm (typically ~ 0.1 cm) in length (*Figure 20*). The former of these minerals are aligned to give the rock a distinct fabric, whereas the latter are weakly to moderately parallel to this fabric. Additionally, the fabric is overprinted by fine- to medium-grained, dark red – brown, circular garnet grains that are up to 0.25 cm across and by sporadic, medium-grained, brown staurolite needles that are up to 1 cm in length and often occur in clusters. Both of these minerals have no preferred orientation. In places, the fabric is cross cut by creamy white quartz veins, most of which are < 1 cm.

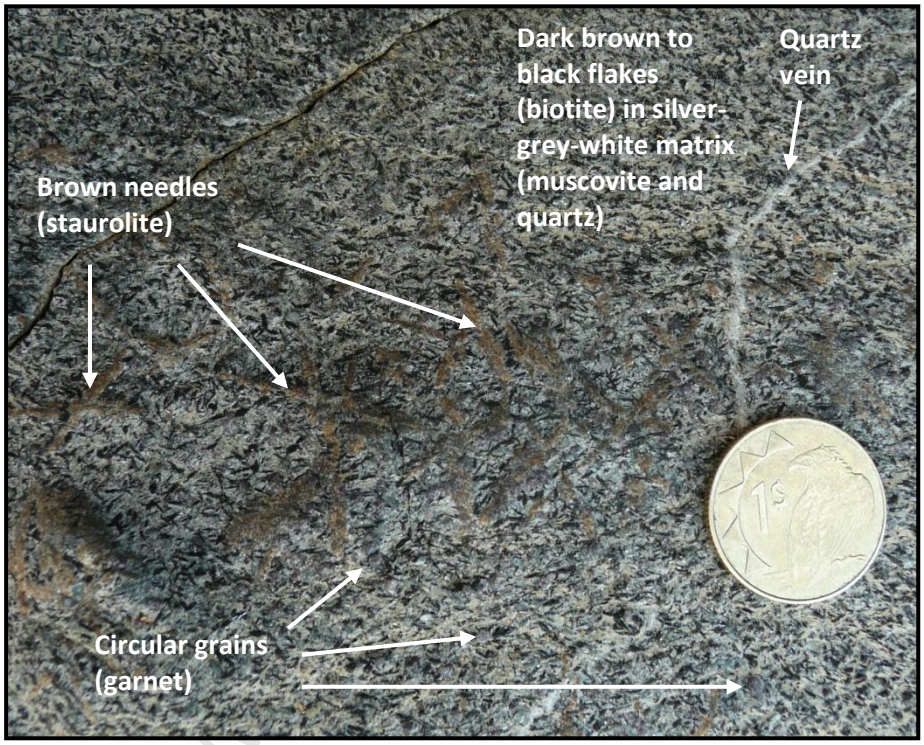

Figure 20: Outcrop of metapsammitic specimen MA-30. The rock has a speckled, schistose appearance defined by very fine-grained silver - grey - white grains (matrix: muscovite and quartz) and fine- to medium-grained dark brown to black flakes (biotite). The distinct fabric is overprinted by fine- to medium-grained, dark red - brown circular grains (garnets) and by sporadic, medium-grained, brown needles (staurolites) that often occur in clusters. Thin quartz veins cross-cut the fabric. The coin for scale is 2.3 cm across; view on foliation plane.

In thin section, these rocks have an observed mineral assemblage that is comprised of garnet porphyroblasts set in a matrix of biotite, muscovite, ilmenite and quartz. Additionally, specimen MA-30 contains a few, sporadically distributed staurolite porphyroblasts. *Figure 21* below provides a representative set of photomicrographs of the metapsammitic rocks the Gaub and Kuiseb Canyons. The garnet (and staurolite) porphyroblasts, which are subhedral to euhedral in shape and up to 2.5 mm in size (most are < 1.5 mm), overprint a penetrative foliation that is defined by the alignment of biotite and/or

muscovite in layers that alternate with quartz-rich layers. As in the metapelites, the porphyroblasts are undeformed and unrotated relative to the matrix.

The biotite and muscovite grains have an elongate lath-like shape, with the former typically ranging from 0.1 mm to 1 mm in length and the latter having a length of less than 0.15 mm. However, some of the biotite grains, specifically some of those in the thicker micaceous layers that are uninterrupted by quartz-rich layers, are not parallel to the overall fabric (in the rock), are less elongated and are coarser, up to 1.5 mm in length. These biotite grains overgrow muscovite and quartz. The quartz grains are composed of multiple sub-grains, all of which are subhedral to anhedral in shape and less than 0.5 mm. Ilmenite exists as small, anhedral grains. Unlike in the metapelites, no chlorite was observed in the metapsammites. On average, the garnet and staurolite porphyroblasts account for ~ 15 to 20 % and ~ 5 to 10 % of the modal abundance in the specimens, respectively. The biotite grains make up ~ 25 to 30 % of the modal abundance, whereas the muscovite and quartz constitute the remaining ~ 40 to 55 %.

In similarity to the metapelites from the Gaub and Kuiseb Canyons, the most notable textural feature observed in hand specimen and in thin section is the overprinting of the fabric, which is defined by the micaceous minerals muscovite and/or biotite, by non-preferentially orientated garnet and staurolite porphyroblasts, and some biotite grains.

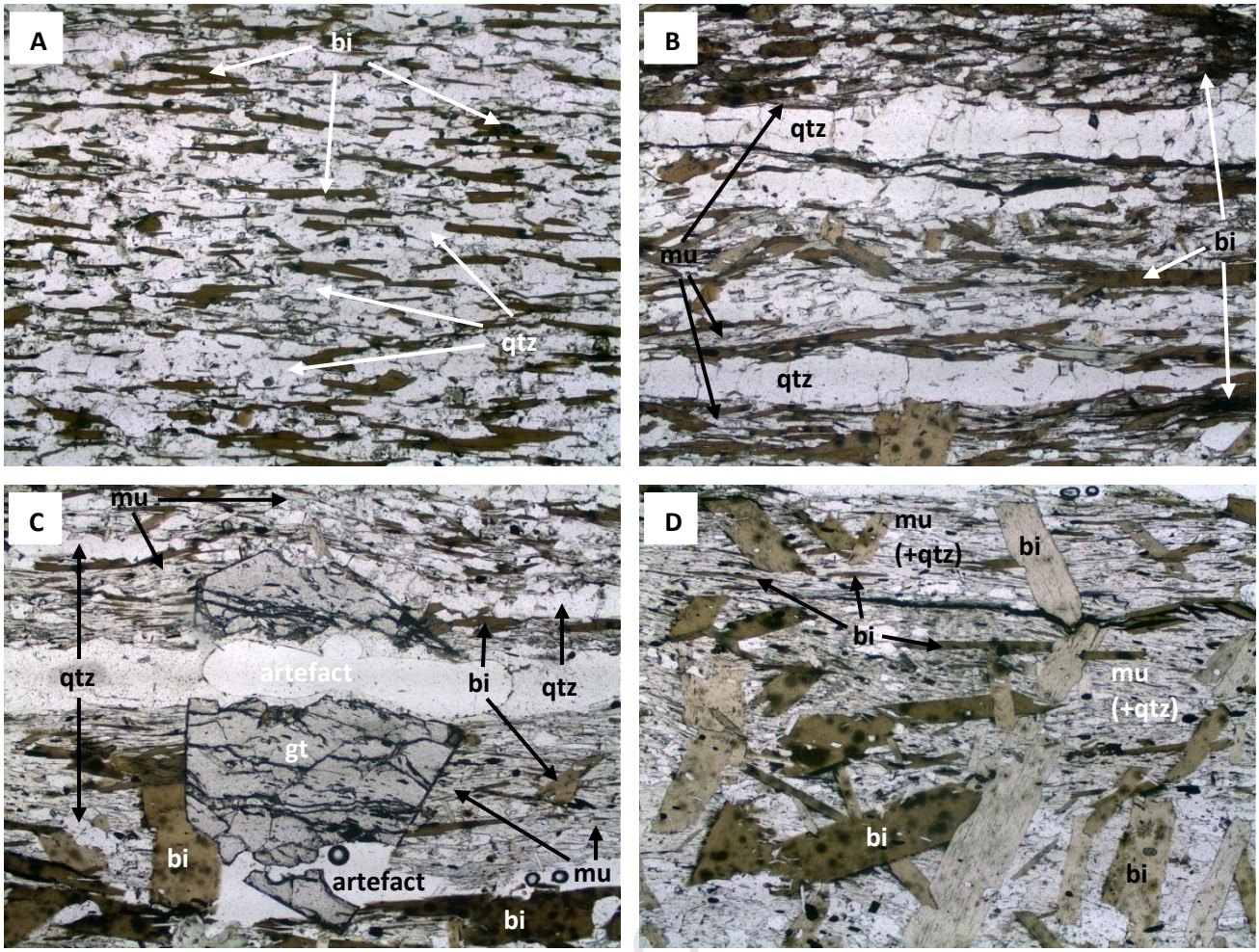

Figure 21: Photomicrographs of the metapsammitic rocks from the Gaub and Kuiseb Canyons. *A*: Biotite laths in quartz (*MA-36*). *B*: Alternating micaceous- and quartz-rich layers (*MA-36*). *C*: Garnet overprinting biotite, muscovite and quartz. Unfortunately, all of the observed garnet grains were disrupted by artefacts (*MA-36*). *D*: Coarse biotite grains cross-cutting a predominantly micaceous layer (*MA-36*). *Gt* = garnet, *bi* = biotite, *mu* = muscovite, *qtz* = quartz, *artefact* = bubble or hole in thin section. All of the photomicrographs were taken in PPL at 50X magnification, FOV = 3.5 mm.

4.6. Calc-silicate Rocks from the Gaub and Kuiseb Canyons

In hand specimen, these rocks are comprised of coarse-grained black hornblende needles and biotite flakes set in a medium-grained creamy white matrix (*Figure 22*). The black needles and flakes exhibit no preferred orientation and are frequently grouped together to form large rosettes. The flakes are up to 0.35 cm in length, whereas the needles appear to be up to 1.25 cm in length. In specimen GB-9, and to a lesser extent in specimen MA-37, these needles and flakes appear to be concentrated into discrete layers. This gives the rock an alternating light (creamy white) and dark (black) layered appearance when viewed in cross section. Specimen MA-37 contains additional medium-grained dark red – brown, circular garnet grains that are up to 0.3 cm across. These grains are absent in specimen GB-9.

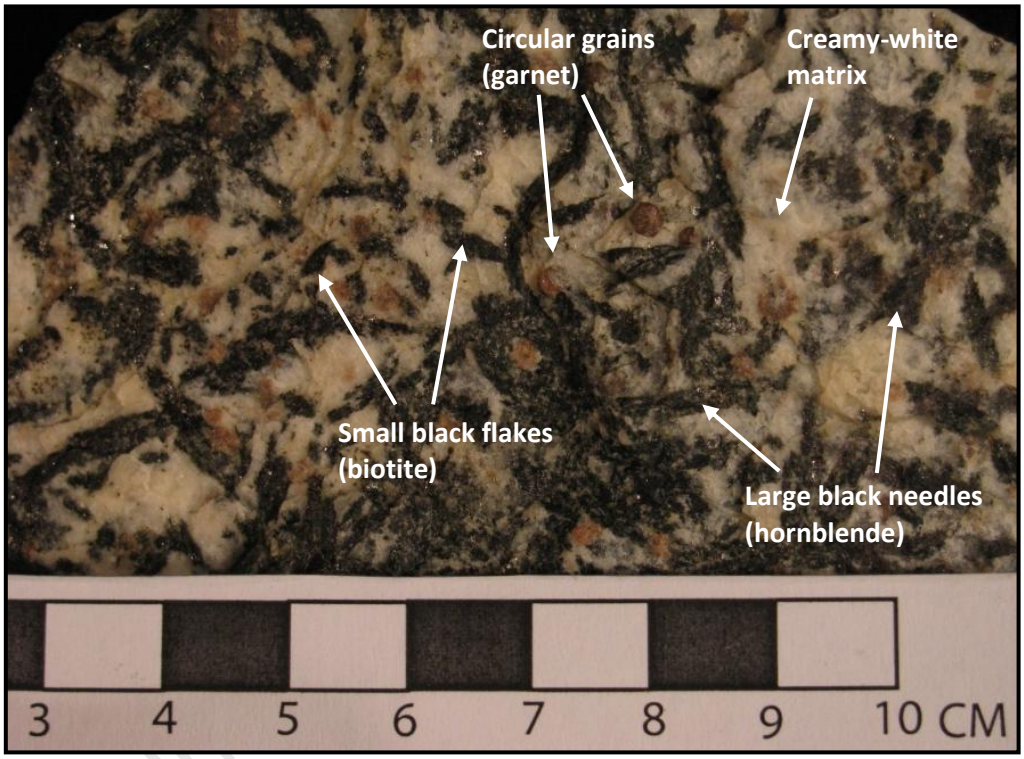

Figure 22: Calc-silicate hand specimen MA-37. The rock is comprised of coarse-grained black needles (hornblende) and flakes (biotite), and medium-grained dark red – brown circular grains (garnets) set in a medium-grained creamy white matrix. The coin for scale is 2.3 cm across.

In thin section, the observed mineral assemblage in these rocks is comprised of garnet, hornblende, biotite, epidote, carbonate (calcite), ilmenite and quartz. *Figure 23* below provides a representative set of photomicrographs of the metapelitic rocks the Gaub Canyon. The garnets, which are mostly subhedral, up to 3 mm across and contain inclusions of quartz and ilmenite, overgrow the hornblende, biotite and quartz. The hornblende typically forms an irregularly-shaped network of multiple grains that is interrupted by many inclusions and overgrowths of quartz. While it is difficult to determine the size of individual grains, the networks are typically greater than 3.5 mm in diameter. Similarly, the biotite grains, which are anhedral, crudely elongated and up to 3.5 mm in length (mostly ~ 1.5 mm), may occur as a network of

amalgamated grains. The epidote grains are anhedral in shape and are slightly coarser in specimen MA-37 (usually ~ 1 mm) than in specimen GB-9 (usually ~ 0.7 mm). In specimen GB-9, networks of epidote occur in epidote-quartz-rich layers that alternate with hornblende-quartz-epidote-rich layers. The carbonate (calcite) grains are less than 2 mm (typically ~ 1.5 mm) and anhedral in shape. Many of these grains are overgrown by hornblende. Ilmenite, which overgrows the hornblende and biotite, is anhedral and ~ 0.25 mm in size. Rare, coarse ilmenite grains that are up to ~ 1 mm in size also occur. In specimen MA-37, the hornblende and biotite grains account for ~ 40 % of the modal abundance, whereas the garnet grains constitute ~ 10 %. The minerals that comprise the creamy white matrix, namely epidote, carbonate, ilmenite and quartz make up the remaining ~ 50 %. By contrast, in specimen GB-9, where garnet is absent, the minerals that comprise the creamy white matrix make up ~ 60 % of the modal abundance.

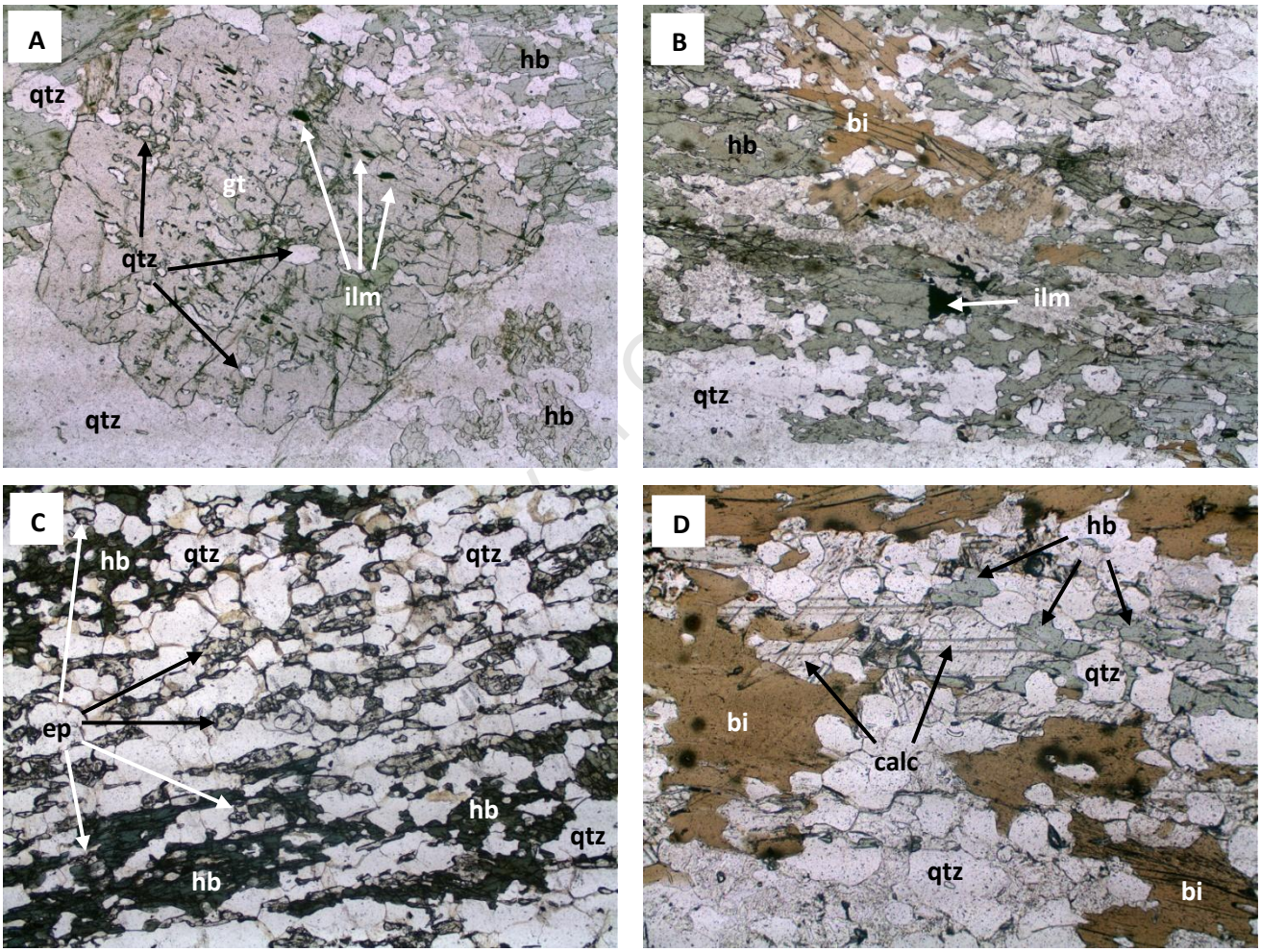

Figure 23: Photomicrographs of the calc-silicate rocks from the Gaub and Kuiseb Canyons. *A*: Garnet porphyroblast with inclusions of quartz and ilmenite overgrowing hornblende and quartz (*MA-37*). *B*: Networks of hornblende and biotite with quartz and a rare, coarse ilmenite grain (*MA-37*). *C*: Alternating epidote-quartz-rich and hornblende-epidote-quartz-rich layers (*GB-9*). *D*: Carbonate grain (calcite) with overgrowths of hornblende (*MA-37*). *Gt* = garnet, *hb* = hornblende, *bi* = biotite, *ep* = epidote, *calc* = carbonate (calcite), *ilm* = ilmenite, *qtz* = quartz. Photomicrographs *A* - *C* were taken in PPL at 50X magnification, FOV = 3.5 mm; photomicrograph *D* was taken in PPL at 100X magnification, FOV = 2 mm.

4.7. Inferred mineral assemblages and parageneses

In the metasedimentary (metapelitic and metapsammitic) rocks from the Gaub and Kuiseb Canyons, the inferred peak mineral assemblage is comprised of both an early, fabric-forming mineral assemblage and a later, overprinting mineral assemblage. The early mineral assemblage is defined primarily by those minerals that were concurrently aligned to form the penetrative foliation observed within the rocks, as well as those that are interbedded within the foliation. This mineral assemblage is constituted by the micaceous minerals chlorite, muscovite and biotite, together with paragonite, epidote, ilmenite and quartz in the metapelites; and by biotite, muscovite, ilmenite and quartz in the metapsammites. Importantly, the alignment of the micaceous minerals implies that this mineral assemblage must have formed during the main phase of deformation – i.e. syn-tectonically. In the metapelites, it appears that the biotite grains overgrow the chlorite and muscovite grains, suggesting that the chlorite and muscovite grains formed prior to the biotite grains. This is confirmed by a few of the biotite grains cross-cutting the foliation, which suggests that biotite growth was both (late-) syn-tectonic and post-tectonic. In the metapsammites, the overgrowth of muscovite and quartz by biotite indicates that the muscovite and quartz grew prior to the biotite. Due to their very minor abundance in the fabric, it was decided that plagioclase, magnetite and rutile would not be considered when constraining the P-T conditions at which fabric formation occurred and were therefore excluded from the early, fabric-forming mineral assemblage in the metapelites.

The later mineral assemblage is defined by those minerals that overprint the penetrative foliation. This mineral assemblage is constituted primarily by garnet and staurolite porphyroblasts in the metapelites from the Gaub Canyon, by garnet, staurolite and kyanite porphyroblasts in the metapelites from the Kuiseb Canyon and by garnet porphyroblasts in the metapsammites from the Gaub Canyon and by garnet and a few, sporadic staurolite porphyroblasts in the metapsammites from the Kuiseb Canyon. All of these porphyroblasts are not preferentially orientated within the matrix. In addition to the porphyroblasts, the post-tectonic biotite also forms part of this assemblage. The partial consumption of some of the minerals that define the early mineral assemblage would have facilitated the growth of these porphyroblasts. However, none of the minerals from the early mineral assemblage were entirely lost and are still present in the in the rocks. This suggests that the overprinting porphyroblasts are in equilibrium with the earlier, fabric-forming minerals. The lack of deformation and rotation of the overprinting porphyroblasts both provides further evidence that they are in equilibrium with the earlier, fabric-forming minerals and implies that the porphyroblasts grew in a relatively static environment after the main phase of deformation – i.e. post-tectonically. Moreover, the lack of alteration of the porphyroblasts suggests that the rocks do not record any obvious retrograde features. In the metapelites from the Gaub Canyon, the consistent overgrowth of some of the garnet porphyroblasts by staurolite porphyroblasts suggests that the garnets

formed prior to the staurolites. By contrast, the relations between the porphyroblasts in the metapelites from the Kuiseb Canyon are more complicated, with some of the metapelites exhibiting overgrowths of staurolite on garnet porphyroblasts and others having overgrowths of garnet on staurolite porphyroblasts.

In summary, the metapelitic rocks from the Gaub and Kuiseb Canyons are inferred to preserve two distinct mineral assemblages: an early, prograde assemblage (*M1a*) that defines the fabric and a peak metamorphic assemblage (*M1b*) that includes the fabric-forming minerals and later, overprinting porphyroblasts. The prograde assemblage consists of chlorite, muscovite, biotite, paragonite, epidote, ilmenite and quartz; whereas the peak assemblage consists of garnet, staurolite, kyanite (only in Kuiseb metapelites), chlorite, muscovite, biotite, paragonite, epidote, ilmenite and quartz.

Similarly, the metapsammitic rocks from the Gaub and Kuiseb Canyons are inferred to preserve an early, prograde mineral assemblage (*M1a*) that defines the fabric and a peak metamorphic assemblage (*M1b*) that is inclusive of the fabric-forming minerals and later, overprinting porphyroblasts. The prograde assemblage consists of biotite, muscovite, ilmenite and quartz; whereas the peak assemblage consists of garnet, staurolite (only in the Kuiseb metapsammites), biotite, muscovite, ilmenite and quartz.

By contrast to the metasedimentary rocks, the metamafic rocks from the Gaub and Kuiseb Canyons only have a single, foliated peak metamorphic assemblage and do not display any obvious post-tectonic features, such as overprinting porphyroblasts. This indicates that no new minerals formed subsequent to the prograde, fabric-forming event. However, it is possible that a mineral, or several minerals, may have been partially- or completely lost (consumed) from the early, prograde, fabric-forming mineral assemblage to produce the peak metamorphic assemblage. Based on the difference between the mineral assemblage observed in the metamafic rocks from the Gaub Canyon and that observed in the metamafic rocks from the Kuiseb Canyon, as well as the presence of relict, partially consumed chlorite in the metamafics from the Kuiseb Canyon (*Figure 19c*), it is plausible that the partial- or complete loss (consumption) of chlorite may have occurred during the post-tectonic, peak metamorphic event.

In the metamafic rocks from the Gaub Canyon, the early, prograde, fabric-forming mineral assemblage (*M1a*) is inferred to have been comprised of amphibole (hornblende), epidote, rutile, quartz, biotite and chlorite. The later, post-tectonic event most likely resulted in the complete loss (consumption) of chlorite and therefore an inferred peak mineral assemblage (*M1b*) constituted by amphibole (hornblende), epidote, rutile, quartz and biotite.

The existence of chlorite in the metamafic rocks from the Kuiseb Canyon, suggests that either these rocks did not experience the later, post-tectonic event or more probably, that only the partial loss of chlorite occurred. The observed mineral assemblage in these rocks (*M1a*) is inferred to be constituted by amphibole (hornblende and actinolite) epidote, rutile, quartz, biotite, sphene and chlorite. Due to its very minor abundance, it was decided that plagioclase would not be considered when constraining the P-T conditions at which the observed mineral assemblage formed and was therefore excluded from the assemblage.

In the metamafics from the Gaub Canyon, the overgrowth of epidote by hornblende indicates that the epidote formed prior to the hornblende grains. Similarly, in the metamafic from the Kuiseb Canyon, some of the actinolite grains are overgrown by epidote and some of the epidote grains are overgrown by hornblende. This suggests the actinolite was present prior to the epidote, which was in turn present prior to the growth of the hornblende. The micas are overgrown by epidote and amphibole, which indicates that they formed prior to the growth of epidote and amphibole.

The calc-silicates from the Gaub and Kuiseb Canyons do not display a penetrative foliation or any obvious post-tectonic features. The overgrowth of hornblende, biotite and quartz by garnet indicates that the garnet grew after the hornblende, biotite and quartz. Similarly, the overgrowth of the carbonate grains by hornblende indicates that the carbonate formed prior to the hornblende. The inferred peak mineral assemblage (*M1b*) in the calc-silicates from the Gaub and Kuiseb Canyons is constituted by garnet, hornblende, biotite, epidote, carbonate (calcite), ilmenite and quartz.

5. Mineral Chemistry

The following representative specimens were selected for mineral chemical analyses: metapelitic specimens GB-8, GB-10 and GB-13 from the Gaub Canyon, metapelitic specimens MA-29, MA-31, MA-38 and MA-40 from the Kuiseb Canyon, metamafic specimen GB-4 from the Gaub Canyon and metamafic specimen MA-44 from the Kuiseb Canyon. The specimens were chosen on the basis of their suitability as a representative rock in the location from which they were sampled, their mineral assemblages and fabric relations, their exhibition of sufficient interesting features and their lack of recent alteration.

Mineral composition analyses were performed using the Jeol JXA-8100 Electron Microprobe (EMP) at the University of Cape Town. A thin coating of carbon was applied to the normal thin sections prior to the samples being loaded into the EMP. The premeditated orientation of the normal thin sections, as well as the use of photomicrographs (from the catalogues of photomicrographs) and the demarcation of grains of analytical interest with a fine-tipped marker pen, provided a means by which the specific mineral grains were efficiently and accurately found under the EMP's very high magnification.

The beam of the microprobe was set to an accelerating voltage of 15 kV and a current of 20 µA. The analyses were calibrated using both natural and synthetic internal standards. The counting times for all elements was 10 seconds per peak, expect for iron (Fe) and nickel (Ni), which were counted for 30 seconds and 20 seconds per peak, respectively. Count rates were corrected using the Bence-Albee routine and full corrections for spectral line and background interferences, dead time and instrument drift were applied. The minerals analysed in this manner included garnet, staurolite, kyanite, chlorite, biotite, muscovite, epidote, hornblende, actinolite, ilmenite, magnetite, rutile, sphene and plagioclase. The results of the chemical analyses were computed into representative tables for each specimen and plotted on various graphs to illustrate zoning and other key features.

5.1. Metapelitic Rocks from the Gaub Canyon

The tables below provide representative compositions for minerals in each of the selected metapelitic specimens from the Gaub Canyon.

Table 2: Representative compositions for minerals in metapelitic specimen GB-8 from the Gaub Canyon.

Specimen	Gaub Metapelitic Specimen GB-8							
Mineral Probed	Garnet		Staurolite		Chlorite	Biotite	Muscovite	Magnetite
Mineral Position	Core	Rim	Core	Rim	Matrix	Matrix	Matrix	Matrix
Oxide conc. (wt%)								
SiO_2	37.59	37.66	28.31	28.32	25.75	37.15	47.00	~
TiO_2	0.06	0.02	0.47	0.48	0.08	1.62	0.31	0.09
Al_2O_3	21.64	21.86	54.83	54.87	24.35	19.31	36.55	0.19
Cr_2O_3	0.02	0.05	~	~	0.02	0.04	0.03	0.06
FeO	32.07	33.12	13.12	13.03	25.18	20.57	2.65	92.06
MnO	1.75	0.99	0.09	0.08	0.06	0.05	0.02	0.04
MgO	2.62	3.02	1.36	1.29	17.01	11.53	0.82	0.01
CaO	4.26	3.80	0.01	0.01	0.02	0.00	0.00	~
Na_2O	0.02	0.02	~	~	0.05	0.21	1.64	~
K_2O	0.00	0.00	~	~	0.02	9.44	9.01	~
ZnO	~	~	1.46	1.50	~	~	~	~
NiO	~	~	~	~	~	~	~	0.02
Total	100.02	100.53	99.63	99.58	92.55	99.92	98.03	92.48
Cations (a.p.f.u)								
Si	3.00	2.99	7.73	7.74	2.55	2.70	3.04	~
Ti	0.00	0.00	0.10	0.10	0.01	0.09	0.02	0.00
Al	2.04	2.04	17.65	17.67	2.84	1.65	2.79	0.01
Cr	0.00	0.00	~	~	0.00	0.00	0.00	0.00
Fe	2.14	2.20	3.00	2.98	2.09	1.25	0.14	3.97
Mn	0.12	0.07	0.02	0.02	0.00	0.00	0.00	0.00
Mg	0.31	0.36	0.55	0.53	2.51	1.25	0.08	0.00
Ca	0.36	0.32	0.00	0.00	0.00	0.00	0.00	~
Na	0.00	0.00	~	~	0.01	0.03	0.21	~
K	0.00	0.00	~	~	0.00	0.87	0.74	~
Zn	~	~	0.29	0.30	~	~	~	~
Ni	~	~	~	~	~	~	~	0.00
Total	7.98	7.99	29.35	29.33	10.03	7.84	7.02	3.99
Al(VI)	~	~	~	~	1.40	0.35	1.83	~
X_{Fe}	~	~	~	~	0.45	0.50	~	~
X_{Mg}	~	~	0.16	0.15	~	~	~	~
X_{Grss}	0.12	0.11	~	~	~	~	~	~
X_{Spss}	0.04	0.02	~	~	~	~	~	~
X_{Alm}	0.73	0.75	~	~	~	~	~	~
X_{Py}	0.11	0.12	~	~	~	~	~	~
X_{Pa}	~	~	~	~	~	~	0.22	~
X_{Mu}	~	~	~	~	~	~	0.78	~
X_{An}	~	~	~	~	~	~	~	~
X_{Ab}	~	~	~	~	~	~	~	~
X_{Or}	~	~	~	~	~	~	~	~

~ = Not analysed, not calculated or not applicable

Structural formulae calculated on the basis of 12 oxygens for garnet, 46 for staurolite, 14 for chlorite, 11 for biotite, 11 for muscovite and 4 for magnetite.

Table 3: Representative compositions for minerals in metapelitic specimen GB-10 from the Gaub Canyon.

Specimen	Gaub Metapelitic Specimen GB-10									
Mineral Probed	Garnet		Staurolite		Chlorite	Biotite	Muscovite	Ilmenite	Magnetite	Plagioclase
Mineral Position	Core	Rim	Core	Rim	Matrix	Matrix	Matrix	Matrix	Matrix	Matrix
Oxide conc. (wt%)										
SiO_2	37.53	37.53	27.95	28.04	25.27	37.35	46.19	~	~	59.81
TiO_2	0.09	0.03	0.44	0.46	0.07	1.40	0.33	46.71	0.04	0.02
Al_2O_3	21.52	21.65	54.09	54.20	24.51	19.76	35.96	0.02	0.19	26.84
Cr_2O_3	0.03	0.02	~	~	0.03	0.03	0.04	0.03	0.03	0.01
FeO	30.41	32.00	14.66	14.53	22.99	18.52	2.76	50.85	93.77	0.24
MnO	3.37	1.58	0.10	0.10	0.06	0.05	0.03	0.53	0.02	0.02
MgO	2.73	3.11	1.95	1.87	18.03	12.59	0.93	0.38	0.03	0.00
CaO	4.61	3.98	0.01	0.01	0.03	0.01	0.00	~	~	6.89
Na_2O	0.01	0.02	~	~	0.06	0.42	1.41	~	~	7.96
K_2O	0.00	0.00	~	~	0.04	9.13	9.26	~	~	0.07
ZnO	~	~	0.42	0.42	~	~	~	~	~	~
NiO	~	~	~	~	~	~	~	0.01	0.02	~
Total	100.30	99.93	99.63	99.63	91.09	99.25	96.91	98.51	94.11	101.86
Cations (a.p.f.u)										
Si	2.99	2.99	7.66	7.68	2.52	2.70	3.03	~	~	2.62
Ti	0.01	0.00	0.09	0.10	0.01	0.08	0.02	0.93	0.00	0.00
Al	2.02	2.04	17.48	17.50	2.88	1.68	2.78	0.00	0.01	1.39
Cr	0.00	0.00	~	~	0.00	0.00	0.00	0.00	0.00	0.00
Fe	2.03	2.14	3.36	3.33	1.92	1.12	0.15	1.12	3.97	0.01
Mn	0.23	0.11	0.02	0.02	0.01	0.00	0.00	0.01	0.00	0.00
Mg	0.32	0.37	0.80	0.76	2.68	1.36	0.09	0.01	0.00	0.00
Ca	0.39	0.34	0.00	0.00	0.00	0.00	0.00	~	~	0.32
Na	0.00	0.00	~	~	0.01	0.06	0.18	~	~	0.68
K	0.00	0.00	~	~	0.00	0.84	0.78	~	~	0.00
Zn	~	~	0.09	0.08	~	~	~	~	~	~
Ni	~	~	~	~	~	~	~	0.00	0.00	~
Total	7.99	7.99	29.51	29.47	10.04	7.84	7.04	2.07	3.99	5.02
Al(VI)	~	~	~	~	1.41	0.38	1.82	~	~	~
X_{Fe}	~	~	~	~	0.42	0.45	~	~	~	~
X_{Mg}	~	~	0.19	0.19	~	~	~	~	~	~
X_{Grss}	0.13	0.12	~	~	~	~	~	~	~	~
X_{Spss}	0.08	0.04	~	~	~	~	~	~	~	~
X_{Alm}	0.68	0.72	~	~	~	~	~	~	~	~
X_{Py}	0.11	0.13	~	~	~	~	~	~	~	~
X_{Pa}	~	~	~	~	~	~	0.19	~	~	~
X_{Mu}	~	~	~	~	~	~	0.81	~	~	~
X_{An}	~	~	~	~	~	~	~	~	~	0.32
X_{Ab}	~	~	~	~	~	~	~	~	~	0.68
X_{Or}	~	~	~	~	~	~	~	~	~	0.00

~ = Not analysed, not calculated or not applicable

Structural formulae calculated on the basis of 12 oxygens for garnet, 46 for staurolite, 14 for chlorite, 11 for biotite, 11 for muscovite, 3 for ilmenite, 4 for magnetite and 8 for plagioclase.

Table 4: Representative compositions for minerals in metapelitic specimen GB-13 from the Gaub Canyon.

Specimen	Gaub Metapelitic Specimen GB-13						
Mineral Probed	Garnet		Staurolite		Chlorite	Biotite	Muscovite
Mineral Position	Core	Rim	Core	Rim	Matrix	Matrix	Matrix
Oxide conc. (wt%)							
SiO_2	37.47	37.81	27.90	28.03	25.60	36.81	46.73
TiO_2	0.10	0.03	0.46	0.48	0.09	1.46	0.31
Al_2O_3	21.40	21.82	54.24	54.21	25.13	20.19	36.43
Cr_2O_3	0.02	0.02	~	~	0.00	0.03	0.02
FeO	29.92	32.61	14.51	14.40	22.95	18.26	1.93
MnO	3.83	0.97	0.09	0.08	0.07	0.05	0.01
MgO	2.24	3.23	1.97	1.90	18.07	12.31	1.01
CaO	5.36	3.92	0.01	0.01	0.03	0.00	0.00
Na_2O	0.03	0.03	~	~	0.04	0.36	1.20
K_2O	0.00	0.00	~	~	0.03	8.85	9.53
ZnO	~	~	0.60	0.58	~	~	~
NiO	~	~	~	~	~	~	~
Total	100.37	100.44	99.78	99.69	92.01	98.31	97.17
Cations (a.p.f.u)							
Si	2.99	3.00	7.64	7.67	2.52	2.68	3.05
Ti	0.01	0.00	0.10	0.10	0.01	0.08	0.01
Al	2.01	2.04	17.51	17.49	2.92	1.73	2.80
Cr	0.00	0.00	~	~	0.00	0.00	0.00
Fe	2.00	2.16	3.32	3.30	1.89	1.11	0.11
Mn	0.26	0.07	0.02	0.02	0.01	0.00	0.00
Mg	0.27	0.38	0.81	0.78	2.65	1.34	0.10
Ca	0.46	0.33	0.00	0.00	0.00	0.00	0.00
Na	0.01	0.00	~	~	0.01	0.05	0.15
K	0.00	0.00	~	~	0.00	0.82	0.79
Zn	~	~	0.12	0.12	~	~	~
Ni	~	~	~	~	~	~	~
Total	8.00	7.98	29.51	29.48	10.02	7.81	7.01
Al(VI)	~	~	~	~	1.44	0.41	1.85
X_{Fe}	~	~	~	~	0.42	0.45	~
X_{Mg}	~	~	0.19	0.19	~	~	~
X_{Grss}	0.15	0.11	~	~	~	~	~
X_{Spss}	0.09	0.02	~	~	~	~	~
X_{Alm}	0.67	0.73	~	~	~	~	~
X_{Py}	0.09	0.13	~	~	~	~	~
X_{Pa}	~	~	~	~	~	~	0.16
X_{Mu}	~	~	~	~	~	~	0.84
X_{An}	~	~	~	~	~	~	~
X_{Ab}	~	~	~	~	~	~	~
X_{Or}	~	~	~	~	~	~	~

~ = Not analysed, not calculated or not applicable

Structural formulae calculated on the basis of 12 oxygens for garnet, 46 for staurolite, 14 for chlorite, 11 for biotite and 11 for muscovite.

In the metapelitic rocks from the Gaub Canyon, the garnet porphyroblasts are almandine-rich and weakly zoned with an increase in Fe and Mg and a decrease in Mn and Ca from core to rim (*Figure 24*). The zoning is most prominent in specimen GB-13, where the garnets have a representative core composition of X_{Grss} = 0.15, X_{Spss} = 0.09, X_{Alm} = 0.67, X_{Py} = 0.09 and a representative rim composition of X_{Grss} = 0.11, X_{Spss} = 0.02, X_{Alm} = 0.73, X_{Py} = 0.13, and least prominent in specimen GB-8, where the garnets have a representative core composition of X_{Grss} = 0.12, X_{Spss} = 0.04, X_{Alm} = 0.73, X_{Py} = 0.11 and a representative rim composition of X_{Grss} = 0.11, X_{Spss} = 0.02, X_{Alm} = 0.75, X_{Py} = 0.12. The staurolite porphyroblasts have no prominent zoning and an X_{Mg} value that ranges from 0.13 to 0.22, mainly between different samples. The staurolites in specimens GB-10 and GB-13 have the highest X_{Mg} values of around 0.19, whereas the X_{Mg} value for staurolites in specimen GB-8 is around 0.15.

Biotite has an *Al*(VI) value that ranges from 0.28 to 0.50 a.p.f.u and an X_{Fe} value that ranges from 0.43 to 0.54. Biotite in specimen GB-13 has the highest *Al*(VI) values of around 0.41, whereas the X_{Fe} for biotite in specimen GB-8 is the highest, around 0.50. Chlorite has an *Al*(VI) value that ranges from 1.33 to 1.46 a.p.f.u and an X_{Fe} value that ranges from 0.40 to 0.48. Chlorite in specimen GB-13 has the highest *Al*(VI) values of around 1.44, whereas the X_{Fe} for chlorite in specimen GB-8 is the highest, around 0.45. Muscovite is of an intermediate composition with an X_{Mu} and X_{Pa} values ranging from 0.73 to 0.88 and 0.12 to 0.27, respectively. Muscovite in specimen GB-8 has the highest paragonite component, with a representative X_{Pa} value of 0.22, whereas muscovite in specimen GB-13 has the highest muscovite component, with a representative X_{Mu} value of 0.84. The *Al*(VI) value for muscovite ranges from 1.75 to 1.89 a.p.f.u, with muscovite in specimen GB-13 having the highest values of around 1.85 and muscovite in specimen GB-10 having the lowest values of around 1.82. Ilmenite has an Fe value of around 1.12 a.p.f.u and a Ti value of around 0.93 a.p.f.u; whereas magnetite has an Fe value of around 3.97 a.p.f.u. Plagioclase is not zoned and has a representative composition of X_{An} = 0.32.

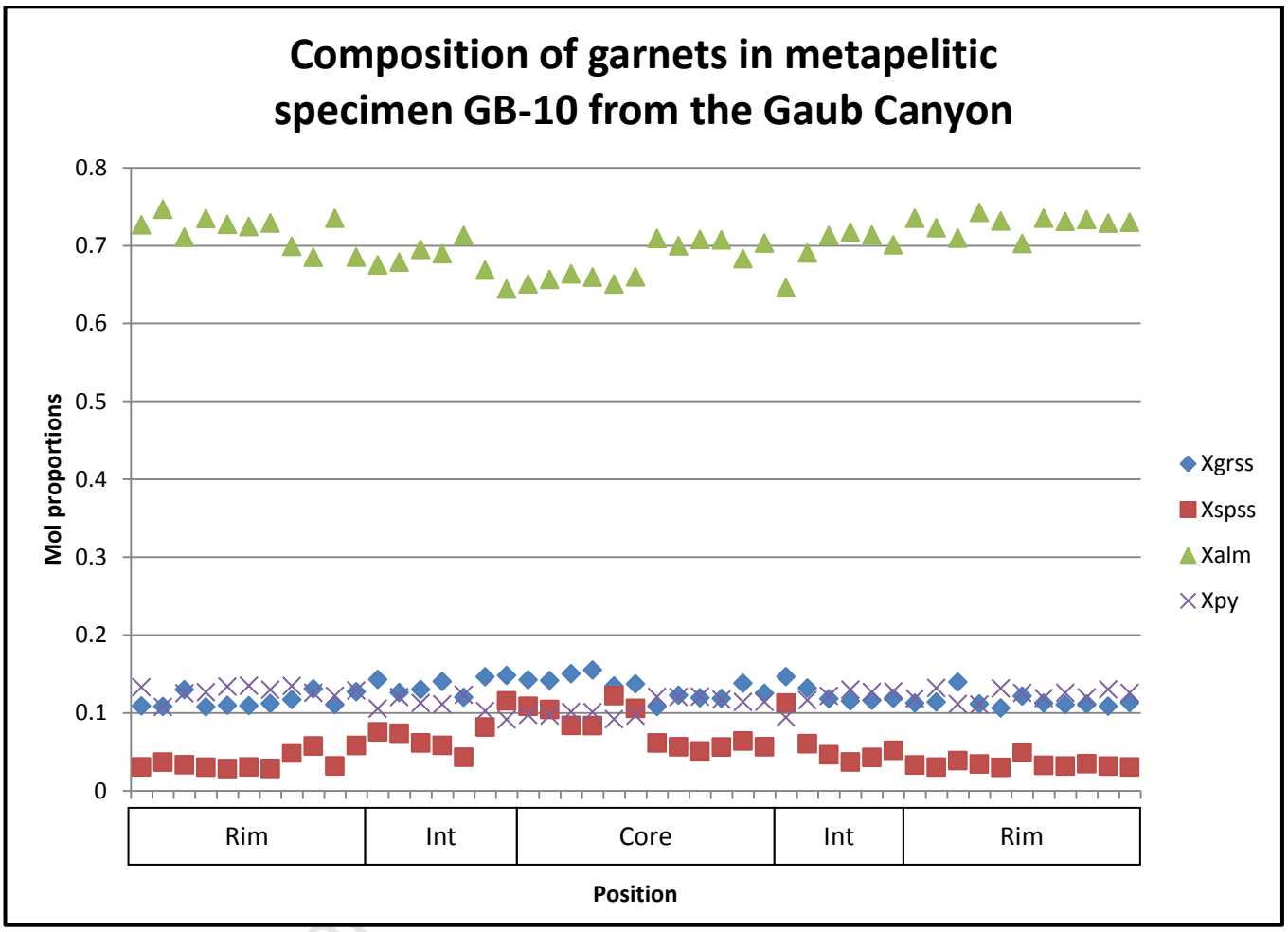

Figure 24: Weak zoning in garnet porphyroblasts in metapelitic specimen GB-10 from the Gaub Canyon. There is an increase in Fe (X_{Alm}) and Mg (X_{Py}) and a decrease in Mn (X_{Spss}) and Ca (X_{Grss}) from core to rim. X_{Grss} = Ca/(Ca+Fe+Mg+Mn); X_{Spss} = Mn/(Mn+Fe+Mg+Ca); X_{Alm} = Fe/(Fe+Mg+Mn+Ca); X_{Py} = Mg/(Mg+Mn+Ca+Fe).

5.2. Metapelitic Rocks from the Kuiseb Canyon

The tables below provide representative compositions for minerals in each of the selected metapelitic specimens from the Kuiseb Canyon.

Table 5: Representative compositions for minerals in metapelitic specimen MA-29 from the Kuiseb Canyon.

Specimen	Kuiseb Metapelitic Specimen MA-29								
Mineral Probed	Garnet		Staurolite		Chlorite	Biotite	Muscovite	Ilmenite	Plagioclase
Mineral Position	Core	Rim	Core	Rim	Matrix	Matrix	Matrix	Matrix	Matrix
Oxide conc. (wt%)									
SiO_2	37.49	37.63	27.52	27.70	25.54	36.71	47.06	~	61.79
TiO_2	0.09	0.05	0.59	0.58	0.08	1.50	0.37	51.74	0.02
Al_2O_3	21.61	21.77	54.72	54.93	24.72	20.24	37.51	0.01	25.69
Cr_2O_3	0.02	0.01	~	~	0.02	0.03	0.05	0.01	0.03
FeO	28.31	33.65	13.79	13.93	23.28	18.50	1.09	45.83	0.39
MnO	5.88	1.00	0.11	0.11	0.07	0.05	0.04	0.55	0.01
MgO	2.00	3.15	1.75	1.58	17.60	11.85	0.86	0.45	0.02
CaO	4.83	2.94	0.01	0.01	0.03	0.00	0.00	~	5.53
Na_2O	0.04	0.04	~	~	0.04	0.30	1.35	~	8.68
K_2O	0.00	0.00	~	~	0.03	8.84	9.31	~	0.08
ZnO	~	~	0.69	0.72	~	~	~	~	~
NiO	~	~	~	~	~	~	~	0.01	~
Total	100.25	100.23	99.19	99.56	91.41	98.02	97.62	98.60	102.24
Cations (a.p.f.u)									
Si	3.00	3.00	7.56	7.58	2.54	2.68	3.04	~	2.69
Ti	0.01	0.00	0.12	0.12	0.01	0.08	0.02	1.00	0.00
Al	2.03	2.04	17.72	17.72	2.90	1.74	2.85	0.00	1.32
Cr	0.00	0.00	~	~	0.00	0.00	0.00	0.00	0.00
Fe	1.89	2.24	3.17	3.19	1.94	1.13	0.06	0.98	0.01
Mn	0.40	0.07	0.03	0.03	0.01	0.00	0.00	0.01	0.00
Mg	0.24	0.37	0.71	0.65	2.61	1.29	0.08	0.02	0.00
Ca	0.41	0.25	0.00	0.00	0.00	0.00	0.00	~	0.26
Na	0.01	0.01	~	~	0.01	0.04	0.17	~	0.73
K	0.00	0.00	~	~	0.00	0.82	0.77	~	0.00
Zn	~	~	0.14	0.15	~	~	~	~	~
Ni	~	~	~	~	~	~	~	0.00	~
Total	7.98	7.98	29.46	29.44	10.01	7.80	6.99	2.00	5.02
Al(VI)	~	~	~	~	1.44	0.42	1.89	~	~
X_{Fe}	~	~	~	~	0.43	0.47	~	~	~
X_{Mg}	~	~	0.18	0.17	~	~	~	~	~
X_{Grss}	0.14	0.09	~	~	~	~	~	~	~
X_{Spss}	0.14	0.02	~	~	~	~	~	~	~
X_{Alm}	0.64	0.76	~	~	~	~	~	~	~
X_{Py}	0.08	0.13	~	~	~	~	~	~	~
X_{Pa}	~	~	~	~	~	~	0.18	~	~
X_{Mu}	~	~	~	~	~	~	0.82	~	~
X_{An}	~	~	~	~	~	~	~	~	0.26
X_{Ab}	~	~	~	~	~	~	~	~	0.74
X_{Or}	~	~	~	~	~	~	~	~	0.00

~ = Not analysed, not calculated or not applicable

Structural formulae calculated on the basis of 12 oxygens for garnet, 46 for staurolite, 14 for chlorite, 11 for biotite, 11 for muscovite, 3 for ilmenite and 8 for plagioclase.

Table 6: Representative compositions for minerals in metapelitic specimen MA-31 from the Kuiseb Canyon.

Specimen	Kuiseb Metapelitic Specimen MA-31											
Mineral Probed	Garnet		Staurolite		Kyanite		Chlorite	Biotite	Muscovite	Ilmenite	Rutile	Plagioclase
Mineral Position	Core	Rim	Core	Rim	Core	Rim	Matrix	Matrix	Matrix	Matrix	Matrix	Matrix
Oxide conc. (wt%)												
SiO_2	37.65	37.70	27.91	28.03	36.68	36.70	25.80	36.95	46.18	~	~	59.65
TiO_2	0.12	0.04	0.52	0.80	0.02	0.01	0.09	1.49	0.41	51.54	95.71	0.00
Al_2O_3	21.50	21.72	54.87	55.27	62.63	62.46	24.66	20.44	37.87	0.02	0.01	25.95
Cr_2O_3	0.02	0.03	~	~	0.04	0.02	0.02	0.03	0.03	0.01	0.08	0.01
FeO	26.14	31.17	13.61	13.70	0.16	0.22	21.86	17.37	0.94	45.65	0.55	0.19
MnO	6.85	2.00	0.14	0.15	0.02	0.03	0.09	0.08	0.03	0.94	0.06	0.02
MgO	1.86	3.23	1.87	1.90	0.02	0.01	18.09	12.13	0.68	0.31	0.00	0.02
CaO	6.01	4.20	0.00	0.02	0.01	0.01	0.02	0.00	0.05	~	~	6.35
Na_2O	0.02	0.04	~	~	0.01	0.01	0.03	0.29	1.43	~	~	7.92
K_2O	0.00	0.00	~	~	0.01	0.00	0.02	8.96	8.83	~	~	0.06
ZnO	~	~	0.19	0.26	~	~	~	~	~	~	~	~
NiO	~	~	~	~	~	~	~	~	~	0.01	0.01	~
Total	100.17	100.14	99.12	100.10	99.60	99.46	90.69	97.73	96.46	98.48	96.43	100.16
Cations (a.p.f.u)												
Si	3.00	3.00	7.64	7.60	0.99	1.00	2.57	2.69	3.01	~	~	2.65
Ti	0.01	0.00	0.11	0.16	0.00	0.00	0.01	0.08	0.02	0.99	1.00	0.00
Al	2.02	2.03	17.70	17.67	2.00	2.00	2.89	1.76	2.91	0.00	0.00	1.36
Cr	0.00	0.00	~	~	0.00	0.00	0.00	0.00	0.00	0.00	0.00	0.00
Fe	1.74	2.07	3.12	3.11	0.00	0.00	1.82	1.06	0.05	0.98	0.01	0.01
Mn	0.46	0.13	0.03	0.03	0.00	0.00	0.01	0.01	0.00	0.02	0.00	0.00
Mg	0.22	0.38	0.76	0.77	0.00	0.00	2.68	1.32	0.07	0.01	0.00	0.00
Ca	0.51	0.36	0.00	0.01	0.00	0.00	0.00	0.00	0.00	~	~	0.30
Na	0.00	0.01	~	~	0.00	0.00	0.01	0.04	0.18	~	~	0.68
K	0.00	0.00	~	~	0.00	0.00	0.00	0.83	0.73	~	~	0.00
Zn	~	~	0.04	0.05	~	~	~	~	~	~	~	~
Ni	~	~	~	~	~	~	~	~	~	0.00	0.00	~
Total	7.98	7.99	29.40	29.40	3.00	3.00	9.99	7.78	6.97	2.01	1.00	5.01
Al(VI)	~	~	~	~	~	~	1.46	0.45	1.92	~	~	~
X_{Fe}	~	~	~	~	~	~	0.40	0.45	~	~	~	~
X_{Mg}	~	~	0.20	0.20	~	~	~	~	~	~	~	~
X_{Grss}	0.17	0.12	~	~	~	~	~	~	~	~	~	~
X_{Spss}	0.16	0.05	~	~	~	~	~	~	~	~	~	~
X_{Alm}	0.59	0.70	~	~	~	~	~	~	~	~	~	~
X_{Py}	0.08	0.13	~	~	~	~	~	~	~	~	~	~
X_{Pa}	~	~	~	~	~	~	~	~	0.20	~	~	~
X_{Mu}	~	~	~	~	~	~	~	~	0.80	~	~	~
X_{An}	~	~	~	~	~	~	~	~	~	~	~	0.31
X_{Ab}	~	~	~	~	~	~	~	~	~	~	~	0.69
X_{Or}	~	~	~	~	~	~	~	~	~	~	~	0.00

~ = Not analysed, not calculated or not applicable

Structural formulae calculated on the basis of 12 oxygens for garnet, 46 for staurolite, 5 for kyanite, 14 for chlorite, 11 for biotite, 11 for muscovite, 3 for ilmenite, 2 for rutile and 8 for plagioclase.

Table 7: Representative compositions for minerals in metapelitic specimen MA-38 from the Kuiseb Canyon.

Specimen	Kuiseb Metapelitic Specimen MA-38										
Mineral Probed	Garnet		Staurolite		Kyanite		Chlorite	Biotite	Muscovite	Ilmenite	Rutile
Mineral Position	Core	Rim	Core	Rim	Core	Rim	Matrix	Matrix	Matrix	Matrix	Matrix
Oxide conc. (wt%)											
SiO_2	37.37	37.63	27.33	27.69	36.69	36.54	25.82	37.71	46.62	~	~
TiO_2	0.11	0.10	0.45	0.60	0.03	0.03	0.10	1.48	0.32	51.68	95.09
Al_2O_3	21.58	21.67	55.55	55.17	62.63	62.54	24.92	20.72	38.70	0.02	0.03
Cr_2O_3	0.00	0.00	~	~	0.04	0.04	0.04	0.04	0.03	0.02	0.14
FeO	29.24	31.51	13.84	13.78	0.15	0.23	20.53	15.96	0.97	45.96	0.48
MnO	5.88	3.04	0.19	0.18	0.02	0.03	0.09	0.07	0.01	0.66	0.03
MgO	2.49	3.26	2.05	2.01	0.01	0.01	18.22	12.78	0.58	0.39	0.02
CaO	3.40	2.78	0.01	0.01	0.01	0.01	0.02	0.01	0.00	~	~
Na_2O	0.02	0.06	~	~	0.02	0.01	0.06	0.37	1.63	~	~
K_2O	0.00	0.00	~	~	0.01	0.01	0.03	8.57	7.68	~	~
ZnO	~	~	0.19	0.18	~	~	~	~	~	~	~
NiO	~	~	~	~	~	~	~	~	~	0.01	0.01
Total	100.10	100.05	99.59	99.60	99.59	99.43	89.83	97.70	96.54	98.74	95.80
Cations (a.p.f.u)											
Si	2.99	3.00	7.46	7.55	0.99	0.99	2.57	2.72	3.01	~	~
Ti	0.01	0.01	0.09	0.12	0.00	0.00	0.01	0.08	0.02	0.99	1.00
Al	2.04	2.04	17.88	17.74	2.00	2.00	2.93	1.76	2.95	0.00	0.00
Cr	0.00	0.00	~	~	0.00	0.00	0.00	0.00	0.00	0.00	0.00
Fe	1.96	2.10	3.16	3.14	0.00	0.01	1.71	0.96	0.05	0.98	0.01
Mn	0.40	0.20	0.04	0.04	0.00	0.00	0.01	0.00	0.00	0.01	0.00
Mg	0.30	0.39	0.83	0.82	0.00	0.00	2.71	1.37	0.06	0.01	0.00
Ca	0.29	0.24	0.00	0.00	0.00	0.00	0.00	0.00	0.00	~	~
Na	0.00	0.01	~	~	0.00	0.00	0.01	0.05	0.20	~	~
K	0.00	0.00	~	~	0.00	0.00	0.00	0.79	0.63	~	~
Zn	~	~	0.04	0.04	~	~	~	~	~	~	~
Ni	~	~	~	~	~	~	~	~	~	0.00	0.00
Total	7.98	7.98	29.51	29.46	3.00	3.00	9.96	7.74	6.92	2.01	1.00
Al(VI)	~	~	~	~	~	~	1.50	0.48	1.96	~	~
X_{Fe}	~	~	~	~	~	~	0.39	0.41	~	~	~
X_{Mg}	~	~	0.21	0.21	~	~	~	~	~	~	~
X_{Grss}	0.10	0.08	~	~	~	~	~	~	~	~	~
X_{Spss}	0.14	0.07	~	~	~	~	~	~	~	~	~
X_{Alm}	0.66	0.72	~	~	~	~	~	~	~	~	~
X_{Py}	0.10	0.13	~	~	~	~	~	~	~	~	~
X_{Pa}	~	~	~	~	~	~	~	~	0.24	~	~
X_{Mu}	~	~	~	~	~	~	~	~	0.76	~	~
X_{An}	~	~	~	~	~	~	~	~	~	~	~
X_{Ab}	~	~	~	~	~	~	~	~	~	~	~
X_{Or}	~	~	~	~	~	~	~	~	~	~	~

~ = Not analysed, not calculated or not applicable

Structural formulae calculated on the basis of 12 oxygens for garnet, 46 for staurolite, 5 for kyanite, 14 for chlorite, 11 for biotite, 11 for muscovite, 3 for ilmenite and 2 for rutile.

Table 8: Representative compositions for minerals in metapelitic specimen MA-40 from the Kuiseb Canyon.

Specimen	Kuiseb Metapelitic Specimen MA-40										
Mineral Probed	Garnet		Staurolite		Kyanite		Chlorite	Biotite	Muscovite	Ilmenite	Plagioclase
Mineral Position	Core	Rim	Core	Rim	Core	Rim	Matrix	Matrix	Matrix	Matrix	Matrix
Oxide conc. (wt%)											
SiO_2	37.67	37.61	27.65	27.88	36.73	36.69	25.61	36.94	46.67	~	60.61
TiO_2	0.08	0.03	0.52	0.67	0.02	0.01	0.10	1.51	0.33	51.41	0.02
Al_2O_3	21.74	21.70	55.55	55.49	62.88	62.72	24.65	20.40	38.30	0.16	25.73
Cr_2O_3	0.02	0.02	~	~	0.02	0.03	0.04	0.04	0.03	0.02	0.00
FeO	28.91	32.80	13.23	13.20	0.15	0.18	22.49	17.70	0.99	45.74	0.06
MnO	5.00	2.09	0.15	0.16	0.02	0.03	0.09	0.06	0.02	0.79	0.03
MgO	2.31	3.16	1.55	1.35	0.02	0.01	17.55	11.97	0.66	0.28	0.02
CaO	4.62	2.61	0.01	0.02	0.01	0.01	0.03	0.00	0.01	~	6.04
Na_2O	0.02	0.02	~	~	0.01	0.00	0.03	0.25	1.37	~	7.99
K_2O	0.00	0.00	~	~	0.00	0.00	0.01	8.90	8.34	~	0.17
ZnO	~	~	0.55	0.53	~	~	~	~	~	~	~
NiO	~	~	~	~	~	~	~	~	~	0.01	~
Total	100.37	100.04	99.21	99.29	99.86	99.68	90.60	97.77	96.73	98.40	100.67
Cations (a.p.f.u)											
Si	3.00	3.00	7.56	7.61	0.99	0.99	2.56	2.69	3.02	~	2.68
Ti	0.00	0.00	0.11	0.14	0.00	0.00	0.01	0.08	0.02	0.99	0.00
Al	2.04	2.04	17.90	17.86	2.00	2.00	2.90	1.75	2.92	0.00	1.34
Cr	0.00	0.00	~	~	0.00	0.00	0.00	0.00	0.00	0.00	0.00
Fe	1.92	2.19	3.03	3.01	0.00	0.00	1.88	1.08	0.05	0.98	0.00
Mn	0.34	0.14	0.04	0.04	0.00	0.00	0.01	0.00	0.00	0.02	0.00
Mg	0.27	0.38	0.63	0.55	0.00	0.00	2.61	1.30	0.06	0.01	0.00
Ca	0.39	0.22	0.00	0.00	0.00	0.00	0.00	0.00	0.00	~	0.29
Na	0.00	0.00	~	~	0.00	0.00	0.01	0.04	0.17	~	0.68
K	0.00	0.00	~	~	0.00	0.00	0.00	0.83	0.69	~	0.01
Zn	~	7.98	0.11	0.11	~	~	9.98	~	~	~	~
Ni	~	~	~	~	~	~	~	~	~	0.00	~
Total	7.98	7.98	29.38	29.32	3.00	3.00	9.98	7.78	6.94	2.01	5.00
Al(VI)	~	~	~	~	~	~	1.46	0.45	1.94	~	~
X_{Fe}	~	~	~	~	~	~	0.42	0.45	~	~	~
X_{Mg}	~	~	0.17	0.15	~	~	~	~	~	~	~
X_{Grss}	0.13	0.08	~	~	~	~	~	~	~	~	~
X_{Spss}	0.12	0.05	~	~	~	~	~	~	~	~	~
X_{Alm}	0.66	0.75	~	~	~	~	~	~	~	~	~
X_{Py}	0.09	0.13	~	~	~	~	~	~	~	~	~
X_{Pa}	~	~	~	~	~	~	~	~	0.20	~	~
X_{Mu}	~	~	~	~	~	~	~	~	0.80	~	~
X_{An}	~	~	~	~	~	~	~	~	~	~	0.29
X_{Ab}	~	~	~	~	~	~	~	~	~	~	0.70
X_{Or}	~	~	~	~	~	~	~	~	~	~	0.01

~ = Not analysed, not calculated or not applicable

Structural formulae calculated on the basis of 12 oxygens for garnet, 46 for staurolite, 5 for kyanite, 14 for chlorite, 11 for biotite, 11 for muscovite, 3 for ilmenite and 8 for plagioclase.

In the metapelitic rocks from the Kuiseb Canyon, the garnet porphyroblasts are almandine-rich and moderately zoned with an increase in Fe and Mg and a decrease in Mn and Ca from core to rim (*Figure 25*). The zoning is most prominent in specimen MA-31, where the garnets have a representative core composition of X_{Grss} = 0.14, X_{Spss} = 0.14, X_{Alm} = 0.64, X_{Py} = 0.08 and a representative rim composition of X_{Grss} = 0.09, X_{Spss} = 0.02, X_{Alm} = 0.76, X_{Py} = 0.13, and least prominent in specimen MA-38, where the garnets have a representative core composition of X_{Grss} = 0.10, X_{Spss} = 0.14, X_{Alm} = 0.66, X_{Py} = 0.10 and a representative rim composition of X_{Grss} = 0.08, X_{Spss} = 0.07, X_{Alm} = 0.72, X_{Py} = 0.13. The staurolite porphyroblasts exhibit no prominent zoning and have X_{Mg} values that vary from 0.16 to 0.23. The staurolites in specimens MA-38 have the highest X_{Mg} values of around 0.21, whereas the X_{Mg} value for staurolites in specimen MA-40 is the lowest, around 0.17.

Biotite has an *Al*(VI) value that ranges from 0.36 to 0.49 a.p.f.u and an X_{Fe} value that ranges from 0.41 to 0.48. Biotite in specimen MA-38 has the highest *Al*(VI) values of around 0.48, whereas the X_{Fe} for biotite in specimen MA-29 is the highest, around 0.47. Chlorite has an *Al*(VI) value that ranges from 1.39 to 1.60 a.p.f.u and an X_{Fe} value that ranges from 0.38 to 0.43. Chlorite in specimen MA-38 has the highest *Al*(VI) values of around 1.50, whereas the X_{Fe} for chlorite in specimen MA-29 is the highest, around 0.43. Muscovite is of an intermediate composition with an X_{Mu} and X_{Pa} values ranging from 0.76 to 0.82 and 0.18 to 0.24, respectively. Muscovite in specimen MA-38 has the highest paragonite component, with a representative X_{Pa} value of 0.24, whereas muscovite in specimen MA-29 has the highest muscovite component, with a representative X_{Mu} value of 0.82. The *Al*(VI) value for muscovite ranges from 1.77 to 1.98 a.p.f.u, with muscovite in specimen MA-38 having the highest values of around 1.96 and muscovite in specimen MA-29 having the lowest values of around 1.89. Ilmenite has an Fe value of around 0.98 a.p.f.u and a Ti value of around 0.99 a.p.f.u. Similarly, rutile has a Ti value of around 1.00 a.p.f.u. Plagioclase is not zoned and has a representative composition of X_{An} = 0.26 to 0.31.

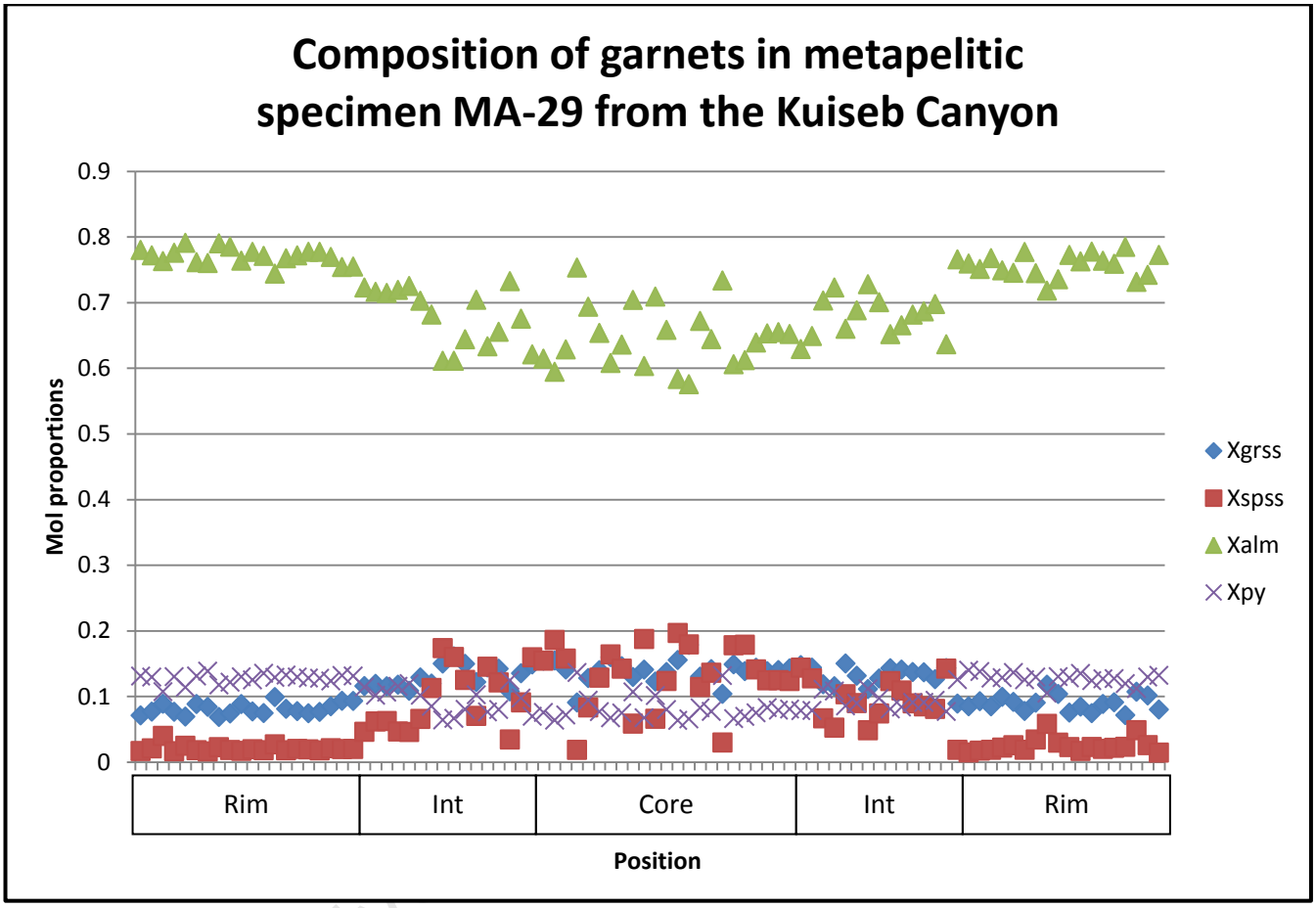

Figure 25: Moderate zoning in garnet porphyroblasts in metapelitic specimen MA-29 from the Kuiseb Canyon. There is an increase in Fe (X_{Alm}) and Mg (X_{Py}) and a decrease in Mn (X_{Spss}) and Ca (X_{Grss}) from core to rim. X_{Grss} = Ca/(Ca+Fe+Mg+Mn); X_{Spss} = Mn/(Mn+Fe+Mg+Ca); X_{Alm} = Fe/(Fe+Mg+Mn+Ca); X_{Py} = Mg/(Mg+Mn+Ca+Fe).

5.3. Metamafic Rocks from the Gaub and Kuiseb Canyons

Table 9 below provides representative compositions for minerals in the metamafic specimen GB-4 from the Gaub Canyon and in the metamafic specimen MA-44 from the Kuiseb Canyon.

Table 9: Representative compositions for minerals in the metamafic specimen GB-4 from the Gaub Canyon and the metamafic specimen MA-44 from the Kuiseb Canyon.

Sample	Gaub Metamafic Specimen GB-4			Kuiseb Metamafic Specimen MA-44					
Mineral Probed	Amphibole		Epidote	Amphibole		Plagioclase		Epidote	Sphene
Mineral Position	Matrix: Core (Hb)	Matrix: Rim (Hb)	Matrix	Matrix: Core (Act)	Matrix: Rim (Hb)	Matrix: Core	Matrix: Rim	Matrix	Matrix
Oxide conc. (wt%)									
SiO_2	43.94	42.79	37.34	51.51	43.63	59.63	57.81	36.91	29.59
TiO_2	0.40	0.50	0.09	0.11	0.38	0.01	0.01	0.14	38.11
Al_2O_3	13.12	14.07	24.99	3.82	12.66	24.90	26.21	26.94	1.16
Cr_2O_3	0.05	0.02	0.02	0.04	0.07	0.00	0.00	0.03	0.01
FeO	15.70	16.37	9.92	11.83	15.59	0.13	0.17	8.80	0.40
MnO	0.32	0.28	0.22	0.29	0.27	0.02	0.02	0.14	0.07
MgO	10.95	10.30	0.08	15.80	10.69	0.01	0.01	0.03	0.02
CaO	11.23	11.34	23.00	12.18	11.72	5.46	6.84	23.49	28.16
Na_2O	1.60	1.68	0.02	0.37	1.29	7.78	7.25	0.02	0.02
K_2O	0.35	0.42	0.00	0.04	0.09	0.03	0.04	0.01	0.01
Total	97.66	97.77	95.68	95.99	96.38	97.97	98.35	96.51	97.55
Cations (a.p.f.u)									
Si	6.51	6.37	6.13	7.54	6.54	2.70	2.62	5.98	0.99
Ti	0.04	0.06	0.01	0.01	0.04	0.00	0.00	0.02	0.96
Al	2.29	2.47	4.84	0.66	2.24	1.33	1.40	5.14	0.05
Cr	0.01	0.00	0.00	0.00	0.01	0.00	0.00	0.00	0.00
Fe	1.95	2.04	1.36	1.45	1.96	0.01	0.01	1.19	0.01
Mn	0.04	0.04	0.03	0.04	0.03	0.00	0.00	0.02	0.00
Mg	2.42	2.28	0.02	3.45	2.39	0.00	0.00	0.01	0.00
Ca	1.78	1.81	4.05	1.91	1.88	0.26	0.33	4.07	1.01
Na	0.46	0.48	0.01	0.11	0.38	0.68	0.64	0.01	0.00
K	0.07	0.08	0.00	0.01	0.02	0.00	0.00	0.00	0.00
Total	15.56	15.62	16.44	15.17	15.49	4.98	5.00	16.44	3.03
X_{Ps}	~	~	0.26	~	~	~	~	0.22	~
X_{An}	~	~	~	~	~	0.28	0.34	~	~
X_{Ab}	~	~	~	~	~	0.72	0.66	~	~
X_{Or}	~	~	~	~	~	0.00	0.00	~	~

~ = Not analysed, not calculated or not applicable

Structural formulae calculated on the basis of 23 oxygens for amphibole, 25 for epidote, 5 for sphene and 8 for plagioclase.

Amphibole within the metamafic specimen GB-4 exhibits no prominent zoning and is composed of pure hornblende with an Al value of around 2.36 a.p.f.u and a Na value of around 0.47 a.p.f.u. By contrast, some of the amphiboles in the metamafic specimen MA-44 are zoned, with cores of actinolite grading into rims of hornblende (*Figure 26*). For these amphiboles, the cores have an Al value of around 0.66 a.p.f.u and a Na value of around 0.11 a.p.f.u, whereas the rims have Al and Na values of around 2.24 a.p.f.u and 0.38 a.p.f.u, respectively. The X_{Ps} value for epidote in specimen GB-4 ranges from 0.23 to 0.32, whereas epidote in specimen MA-44 has an X_{Ps} value that ranges from 0.17 to 0.27. Plagioclase in specimen MA-44 is strongly zoned with a decrease in Na and an increase in Ca from core to rim (*Figure 27*). The plagioclase has a representative core composition of X_{An} = 0.28 and a representative rim composition of X_{An} = 0.34. Sphene in specimen MA-44 has a Ca value of around 1.01 a.p.f.u, a Si value of around 0.99 a.p.f.u and a Ti value of around 0.96 a.p.f.u.

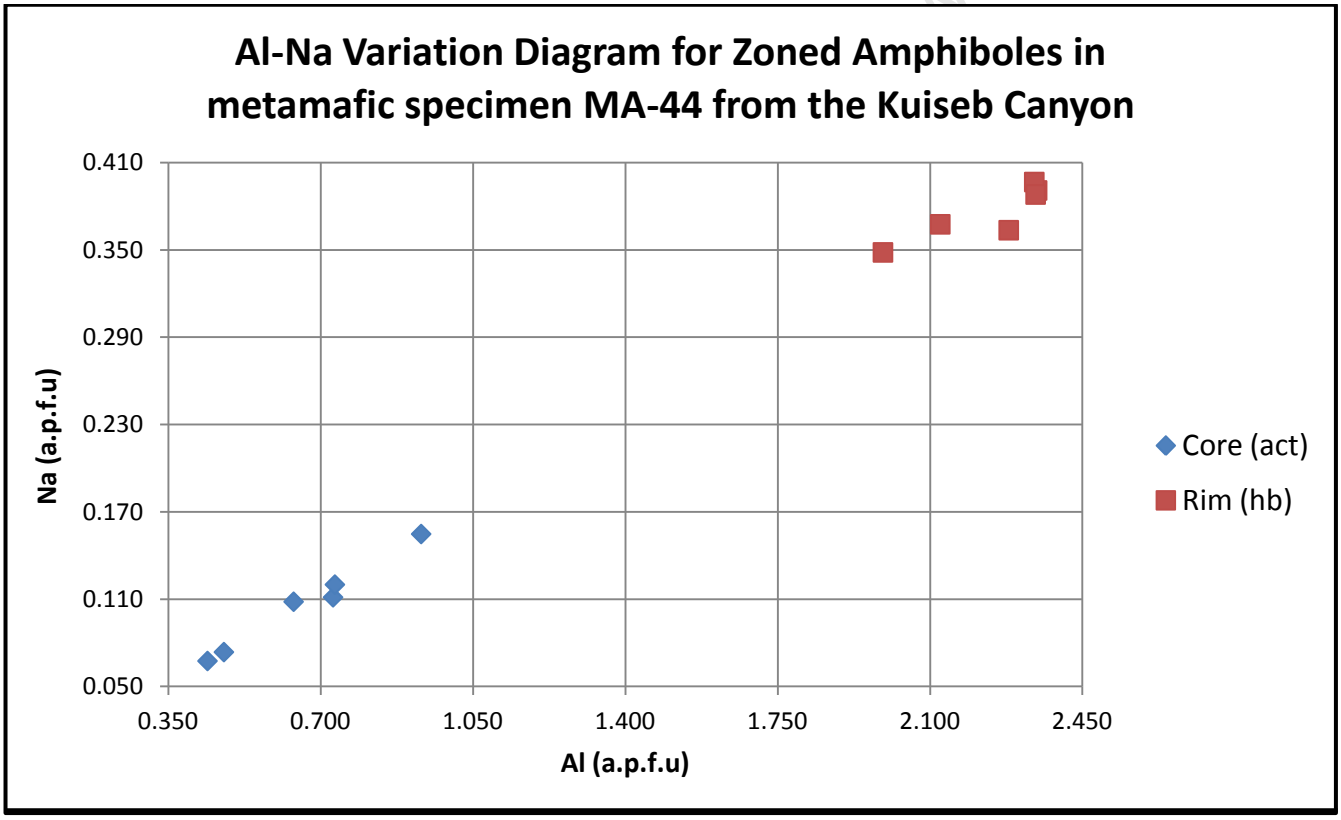

Figure 26: Strongly zoned amphiboles in metamafic specimen MA-44 from the Kuiseb Canyon. The amphiboles have cores that are depleted in Na and Al relative to the rims.

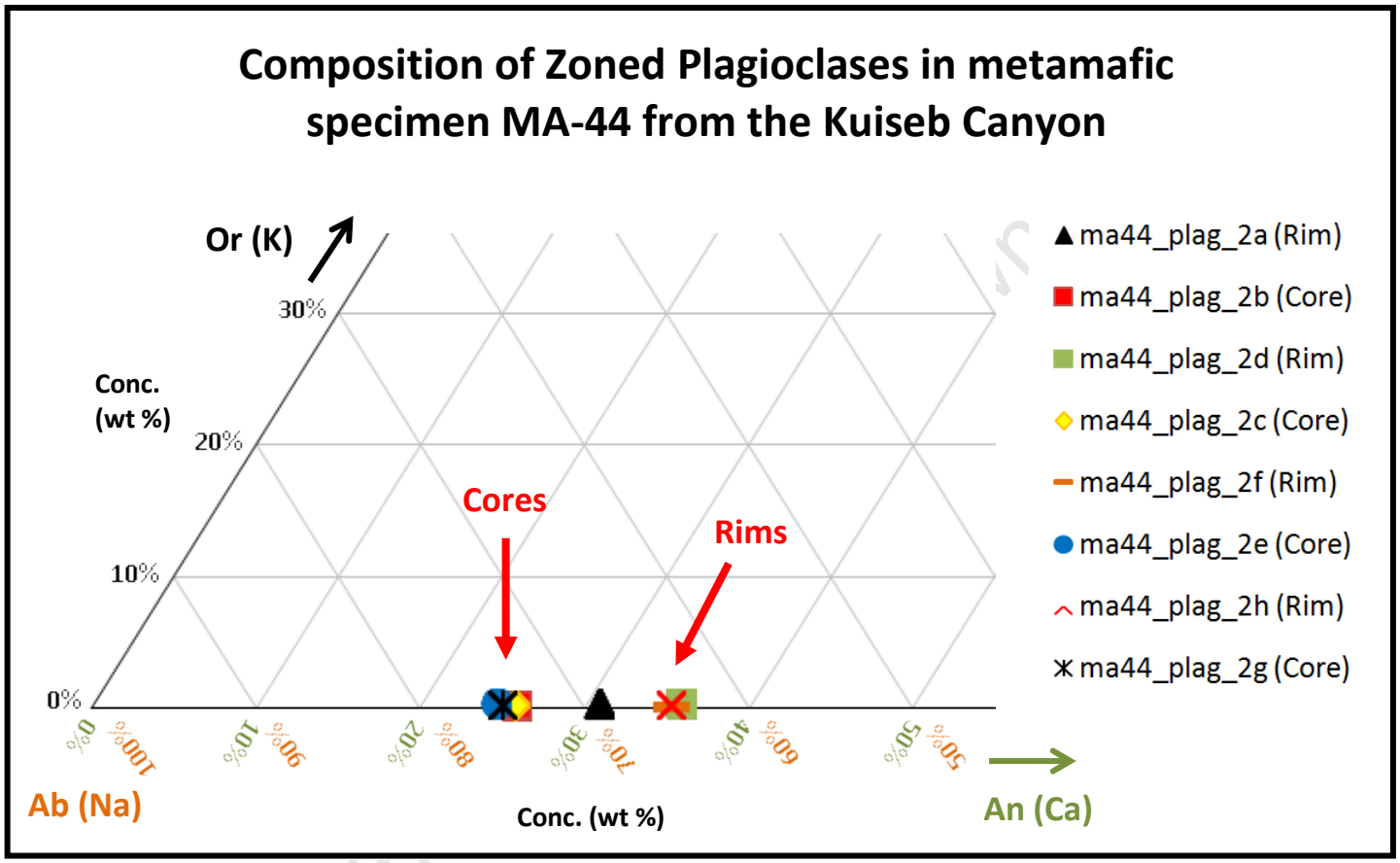

Figure 27: Strong zoning in plagioclases in metamafic specimen MA-44 from the Kuiseb Canyon. There is a notable decrease in Na (X_{Ab}) and increase in Ca (X_{An}) from core to rim. The K (X_{Or}) content remains largely unchanged.

6. Thermodynamic Modelling

The following specimens were selected for bulk rock geochemistry analyses: metapelitic specimens GB-8, GB-10 and GB-13 from the Gaub Canyon, metapelitic specimens MA-29, MA-31, MA-35, MA-38, MA-39 and MA-40 from the Kuiseb Canyon, metamafic specimens GB-4 and GB-5 from the Gaub Canyon, metamafic specimens MA-32 (altered and non-altered portions), MA-43 and MA-44 from the Kuiseb Canyon, and calc-silicate specimen MA-37 from the Kuiseb Canyon. As with the selection of specimens for mineral composition analyses, these specimens were chosen on the basis of their suitability as a representative rock in the location from which they were sampled, their mineral assemblages and fabric relations, their exhibition of sufficient interesting features and their lack of recent alteration.

The selected specimens were analysed for major oxides using X-ray Fluorescence Spectrometry (XRF). The initial preparation procedure for each specimen involved two stages of crushing into progressively finer size fragments and the subsequent milling of approximately 70 g of the specimen into a fine powder using a carbon Seib. 35 g of the fine powder for each of the specimens was then sent for analysis at the Department of Soil Sciences at the University of Stellenbosch. The major oxides were determined on a fusion disc consisting of 0.700 +/- 0.002 g of powdered specimen mixed with 6.000 +/- 0.002 g of Sigma Flux (57:43 Li Tetraborate:Li Metaborate). The XRF operating parameters and analytical data processing techniques are described by Willis (1999). The resulting weight percentage concentration of the major oxides Na_2O, CaO, K_2O, Fe_2O_3, MgO, Al_2O_3, SiO2 and TiO_2 were used as the basis for the thermodynamic modelling of some of the specimens.

Thermodynamic modelling was conducted using THERMOCALC version 3.33 and involved the construction of labelled P-T pseudosections for metapelitic specimens GB-8, GB-10 and GB-13 from the Gaub Canyon metapelitic specimens MA-29, MA-31, MA-38 and MA-40 from the Kuiseb Canyon, metamafic specimen GB4 from the Gaub Canyon and metamafic specimen MA44 from the Kuiseb Canyon. P-T pseudosections, which utilise mineral assemblages in the estimation of P-T conditions, are advantageous relative to other thermobarometric methods, such as conventional and optimal thermobarometry that utilise mineral compositions, in that mineral assemblages are more readily preserved than mineral compositions (Powell & Holland, 2008). The P-T pseudosections were modelled for a pressure and temperature interval of 4 to 13 kbar and 450 to 700 °C, respectively, and for the chemical system NCKFMASHTO (Holland & Powell, 2003), the data for which was obtained from the bulk rock geochemistry (XRF) analyses that were conducted for each specimen.

The phases considered in the calculations and references to the activity-composition models used are: hornblende, actinolite, cummingtonite, glaucophane (Diener *et al.*, 2007, updated by Diener and Powell, 2012), diopside, omphacite, jadeite (Green *et al.*, 2007, updated by Diener and Powell, 2012), garnet, biotite, silicate melt (White *et al*., 2007), epidote, staurolite, cordierite (Holland and Powell, 1998), plagioclase, alkali feldspar (Holland and Powell, 2003), orthopyroxene, spinel, magnetite (White *et al.*, 2002), muscovite, paragonite (Coggon and Holland, 2002), chlorite, chloritoid (Holland et al., 1998), ilmenite and hematite (White *et al.*, 2000). Rutile, sphene, albite, lawsonite, the aluminosilicates, quartz and aqueous fluid (H_2O) are pure end-member phases.

For all of the pseudosections produced, the following assumptions were made:

- The mineral assemblages in all of the modelled specimens only contain minerals that can be approximated by the elements Na, Ca, K, Fe, Mg, Al, Si, H_2O, Ti and O (NCKFMASHTO). If we consider that these elements probably constitute the majority, if not all, of the minerals present, then it is likely to be a reasonable assumption. However, there may be (very-) minor elements, and therefore possibly even minor mineral phases, that may not have been accounted for. The lack of these elements (and minor mineral phases) within the modelled pseudosections may have an (insignificant-) influence on the accuracy of the experimental pressures and temperatures obtained for the stability fields of the various mineral assemblages in the specimens. For example, the addition of Mn to the chosen chemical system would increase the P-T stability of garnet to lower temperatures by ~ 15 °C (Marmo *et al.*, 2002; Tinkham & Ghent, 2005). Similarly, the addition of Zn would increase the P-T stability of staurolite. The low Zn content of ~ 0.1 a.p.f.u in the rocks from the Gaub and Kuiseb Canyons reduces the influence of this element on the stability of staurolite.

- In all of the modelled specimens, fluid is assumed to be pure H_2O that is not inclusive of other phases, such as CO_2, and is in excess during metamorphism. The lack of carbonate minerals, for example calcite [$CaCO_3$] and dolomite [$CaMg(CO_3)_2$], in all of the modelled specimens supports the first part of this assumption. Note that carbonate minerals do exist in the calc-silicates from the Gaub and Kuiseb Canyons, but none of these rocks were chosen for thermodynamic modelling purposes. The second part of this assumption, which implies that H_2O was present during prograde to peak metamorphism, is only valid for first-cycle, subsolidus rocks (e.g. Guiraud *et al.*, 2001) – a criterion that all of the rocks from the Gaub and Kuiseb Canyons fulfil.

6.1. Metapelitic Rocks from the Gaub Canyon

The topology of the pseudosections for all of the metapelitic specimens from the Gaub Canyon (*Figures 28, 29 & 30*) are similar to one another and have the following characteristics:

Chlorite, which is stable at lower temperatures, is lost at ~ 590 °C at ~ 8 kbar, at ~ 600 °C at ~ 10 kbar and at ~ 610 °C at ~ 12 kbar. Muscovite is more pervasive across the modelled P-T range and is only absent at high temperatures of above ~ 565 to 625 °C at low pressures of below ~ 6.5 to 8.5 kbar. By contrast, paragonite is only stable in a narrow window that is defined by a lower limit of pressures of ~ 7.5 to 8 kbar and temperatures of ~ 585 °C, and an upper limit of pressures of ~ 9.5 to 13 kbar and temperatures of ~ 625 to 675 °C. Biotite, which is stable at higher temperatures, is introduced after chlorite and muscovite at temperatures of ~ 475 to 525 °C at ~ 8 kbar, at ~ 500 to 550 °C at ~ 10 kbar and at ~ 525 to 575 °C at ~ 12 kbar.

For the modelled P range, the introduction of the minerals garnet and staurolite occurs after the minerals chlorite, muscovite and biotite at temperatures of above ~ 540 to 575 °C. Additionally, the garnet is lost at pressures of below ~ 7.5 to 8.5 kbar at temperatures of below ~ 610 to 650 °C, whereas the staurolite is lost at pressures of above ~ 10.5 to 11 kbar and at temperatures of above ~ 625 to 650 °C. Between these pressures (~ 8 to 10.75 kbar), the garnet is introduced prior to (at lower temperatures) than the staurolite. Kyanite is stable at high temperatures of above ~ 560 °C at high pressures of above ~ 5 to 7 kbar. At lower pressures, the kyanite is replaced by andalusite and/or sillimanite.

Epidote is lost below ~ 4 kbar at ~ 550 °C, below ~ 6 to 7.5 kbar at ~ 600 °C and below ~ 7 to 9 kbar at ~ 650 °C. Ilmenite and quartz are stable across the entirety of the modelled P-T range. Similarly, water (H_2O) is only absent at high temperatures of > ~ 675 °C and at high pressures of > ~ 10.5 kbar, where the introduction of liquid melt occurs. Plagioclase is predominantly stable at lower pressures and higher temperatures. It is introduced at ~ 585 to 595 °C at ~ 8 kbar, at ~ 625 to 645 °C at ~ 10 kbar and at ~ 670 °C at ~ 12 kbar. In the same way, magnetite and cordierite are confined to high temperatures and low pressures of above ~ 600 °C and below ~ 6 kbar, respectively. Sphene, which is present over the whole modelled P range, is lost between ~ 500 and 550 °C. Both glaucophane and chloritoid only occur at high pressures and low temperatures of above ~ 8 to 10 kbar and below ~ 550 to 575 °C.

For all of the metapelitic specimens from the Gaub Canyon, the inferred peak mineral assemblage (*M1b*) consists of garnet, staurolite, chlorite, biotite, muscovite, paragonite, epidote, ilmenite and quartz. Importantly, the garnet and staurolite, which exist as undeformed and unrotated porphyroblasts, form a

later, post-tectonic mineral assemblage that overprinted an earlier, syn-tectonic, prograde, fabric-forming mineral assemblage. The earlier, prograde mineral assemblage (*M1a*) is characterised primarily by the concurrent alignment of micaceous minerals chlorite, biotite and muscovite into a penetrative foliation.

In each of the pseudosections presented below, the most likely stability field for the earlier, syn-tectonic, prograde, fabric-forming mineral assemblage (*M1a*) (i.e. the P-T conditions of fabric formation) is indicated in *green*; whereas the stability field for the inferred peak mineral assemblage (*M1b*) (i.e. the P-T conditions of peak metamorphism), which is inclusive of the earlier, syn-tectonic, prograde assemblage plus the later, post-tectonic, overprinting assemblage, is indicated in *red*.

In metapelitic specimen GB-8, the stability field for the inferred peak mineral assemblage is between pressures of ~ 8.8 and 10.5 kbar and temperatures of ~ 590 and 605 °C. The stability field at which the minerals that define the penetrative foliation are most likely to have first formed in the presence of one another occurs between pressures of ~ 4 and 11.8 kbar and temperatures of ~ 455 and 550 °C.

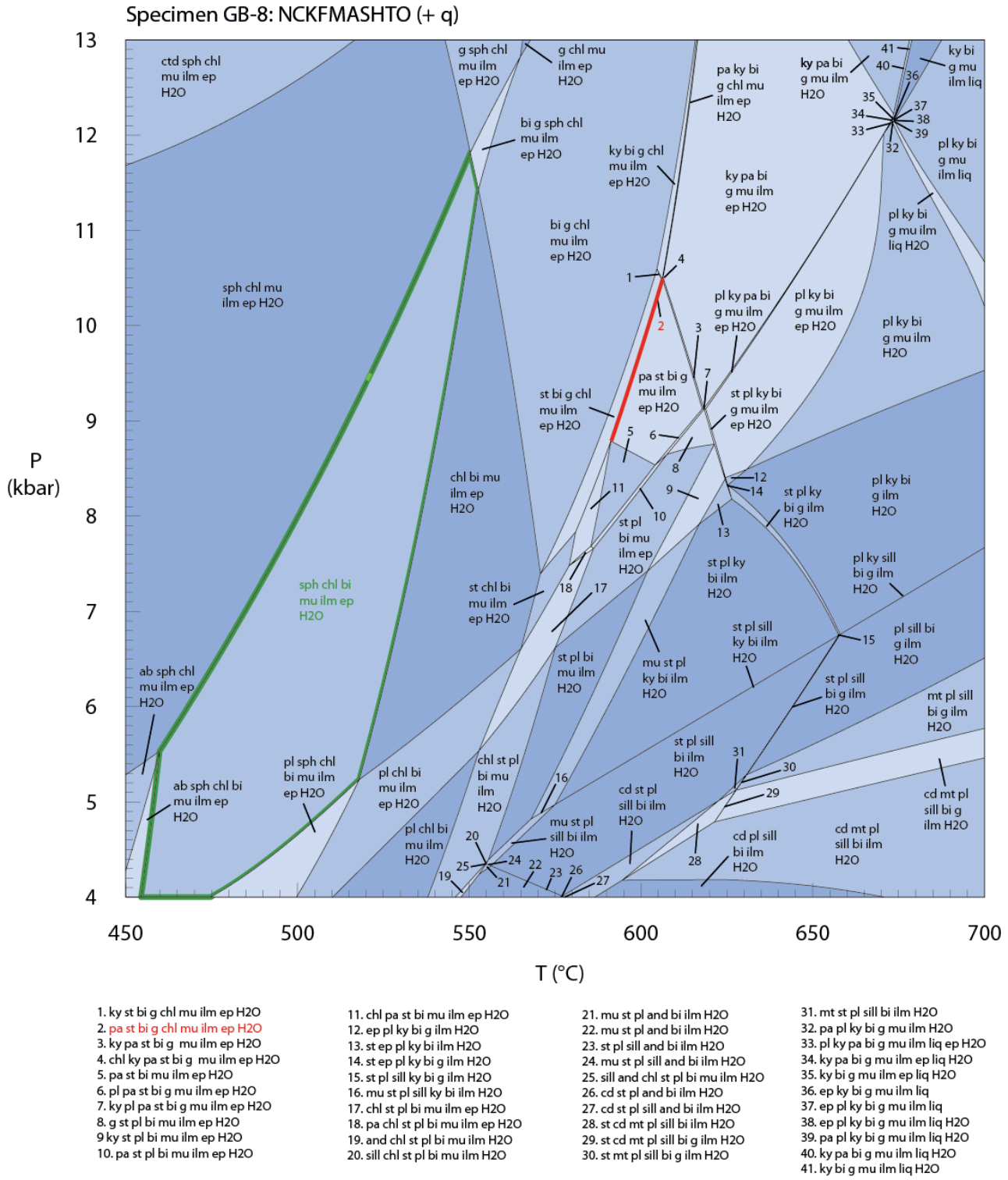

1. ky st bi g chl mu ilm ep H2O
2. pa st bi g chl mu ilm ep H2O
3. ky pa st bi g mu ilm ep H2O
4. chl ky pa st bi g mu ilm ep H2O
5. pa st bi mu ilm ep H2O
6. pl pa st bi g mu ilm ep H2O
7. ky pl pa st bi g mu ilm ep H2O
8. g st pl bi mu ilm ep H2O
9 ky st pl bi mu ilm ep H2O
10. pa st pl bi mu ilm ep H2O
11. chl pa st bi mu ilm ep H2O
12. ep pl ky bi g ilm H2O
13. st ep pl ky bi ilm H2O
14. st ep pl ky bi g ilm H2O
15. st pl sill ky bi g ilm H2O
16. mu st pl sill ky bi ilm H2O
17. chl st pl bi mu ilm ep H2O
18. pa chl st pl bi mu ilm ep H2O
19. and chl st pl bi mu ilm H2O
20. sill chl st pl bi mu ilm H2O
21. mu st pl and bi ilm H2O
22. mu st pl and bi ilm H2O
23. st pl sill and bi ilm H2O
24. mu st pl sill and bi ilm H2O
25. sill and chl st pl bi mu ilm H2O
26. cd st pl and bi ilm H2O
27. cd st pl sill and bi ilm H2O
28. st cd mt pl sill bi ilm H2O
29. st cd mt pl sill bi g ilm H2O
30. st mt pl sill bi g ilm H2O
31. mt st pl sill bi ilm H2O
32. pa pl ky bi g mu ilm H2O
33. pl ky pa bi g mu ilm liq ep H2O
34. ky pa bi g mu ilm ep liq H2O
35. ky bi g mu ilm ep liq H2O
36. ep ky bi g mu ilm liq
37. ep pl ky bi g mu ilm liq
38. ep pl ky bi g mu ilm liq H2O
39. pa pl ky bi g mu ilm liq H2O
40. ky pa bi g mu ilm liq H2O
41. ky bi g mu ilm liq H2O

Figure 28: A pseudosection modelled for specimen GB-8.

In metapelitic specimen GB-10, the inferred peak mineral assemblage is stable between pressures of ~ 9.7 and 9.8 kbar and at a temperature of ~ 600 °C, whereas the minerals that define the penetrative foliation are most likely to have first formed in the presence of one another is between pressures of ~ 4 and 10.2 kbar and temperatures of ~ 485 and 575 °C.

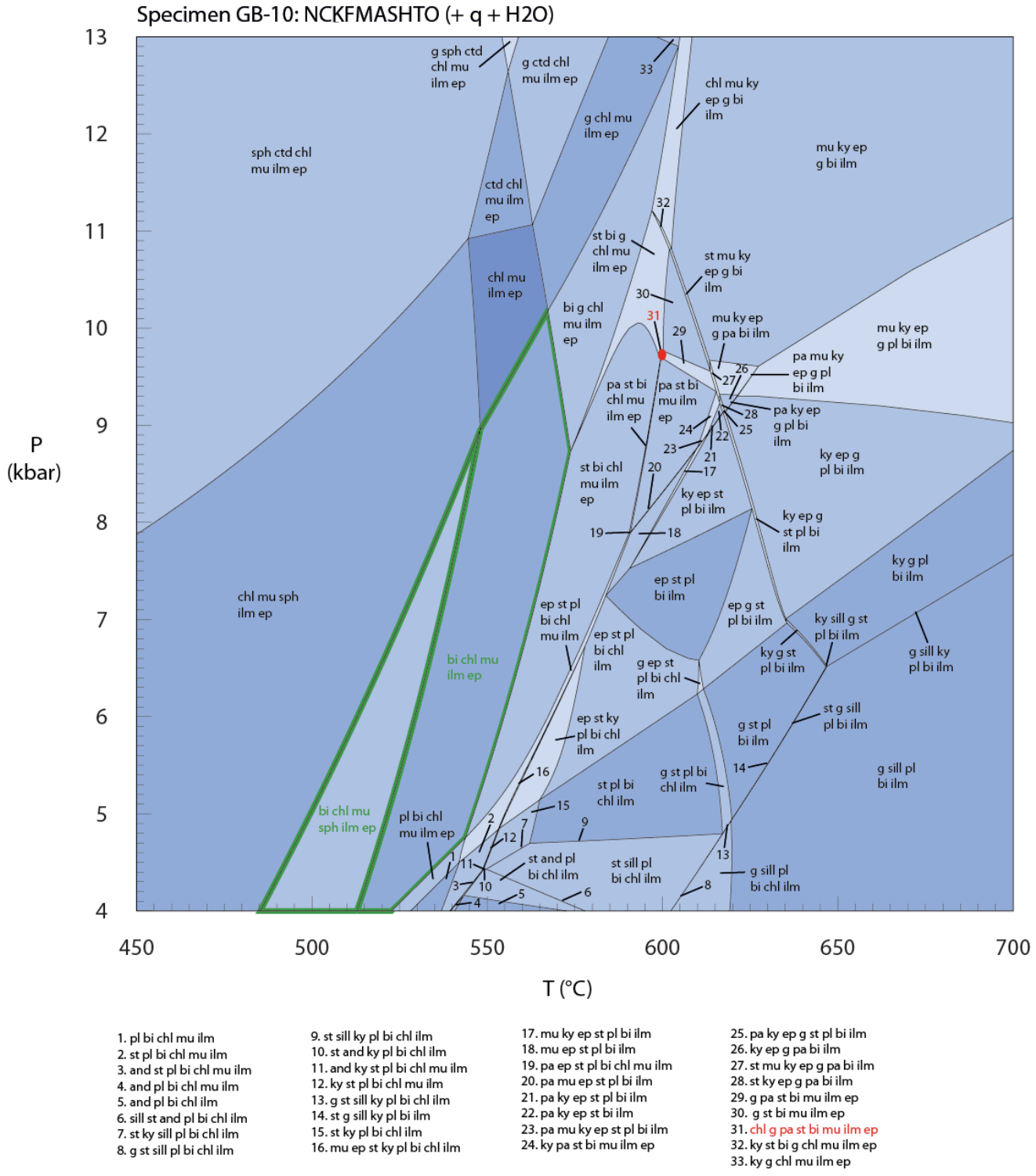

Figure 29: A pseudosection modelled for specimen GB-10.

In metapelitic specimen GB-13, the stability field for the inferred peak mineral assemblage is between pressures of ~ 9.4 and 10.5 kbar and temperatures of ~ 595 and 605 °C. The stability field at which the minerals that define the penetrative foliation are likely to have first formed in the presence of one another occurs between pressures of ~ 4 and 13 kbar and temperatures of ~ 450 and 555 °C.

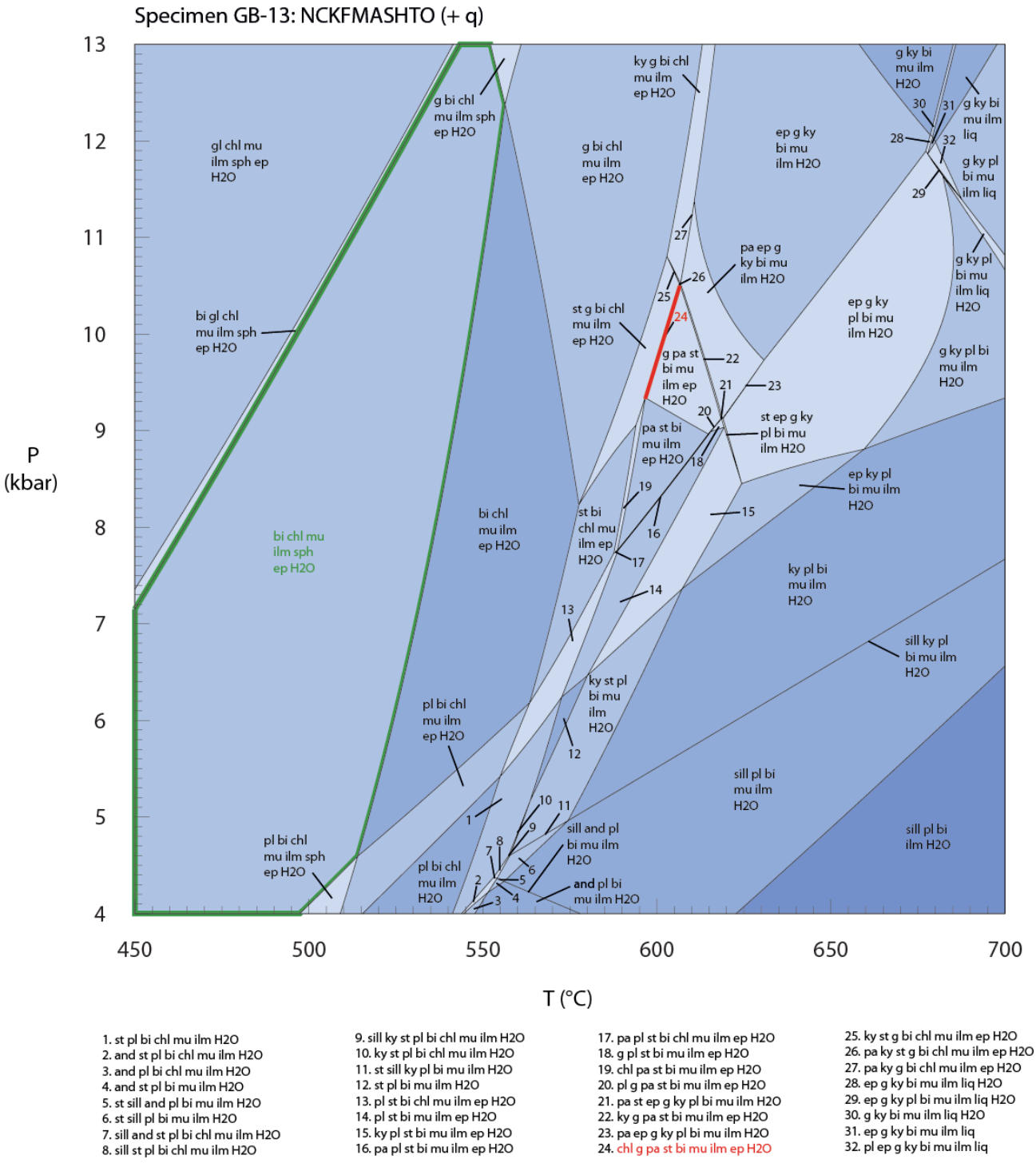

1. st pl bi chl mu ilm H2O
2. and st pl bi chl mu ilm H2O
3. and pl bi chl mu ilm H2O
4. and st pl bi mu ilm H2O
5. st sill and pl bi mu ilm H2O
6. st sill pl bi mu ilm H2O
7. sill and st pl bi chl mu ilm H2O
8. sill st pl bi chl mu ilm H2O
9. sill ky st pl bi chl mu ilm H2O
10. ky st pl bi chl mu ilm H2O
11. st sill ky pl bi mu ilm H2O
12. st pl bi mu ilm H2O
13. pl st bi chl mu ilm ep H2O
14. pl st bi mu ilm ep H2O
15. ky pl st bi mu ilm ep H2O
16. pa pl st bi mu ilm ep H2O
17. pa pl st bi chl mu ilm ep H2O
18. g pl st bi mu ilm ep H2O
19. chl pa st bi mu ilm ep H2O
20. pl g pa st bi mu ilm ep H2O
21. pa st ep g ky pl bi mu ilm H2O
22. ky g pa st bi mu ilm ep H2O
23. pa ep g ky pl bi mu ilm H2O
24. chl g pa st bi mu ilm ep H2O
25. ky st g bi chl mu ilm ep H2O
26. pa ky st g bi chl mu ilm ep H2O
27. pa ky g bi chl mu ilm ep H2O
28. ep g ky bi mu ilm liq H2O
29. ep g ky pl bi mu ilm liq H2O
30. g ky bi mu ilm liq H2O
31. ep g ky bi mu ilm liq
32. pl ep g ky bi mu ilm liq

Figure 30: A pseudosection modelled for specimen GB-13.

6.2. Metapelitic Rocks from the Kuiseb Canyon

The topology of the pseudosections for all of the metapelitic specimens from the Kuiseb Canyon (*Figures 31, 32, 33 & 34*) are both similar to one another and to those of the metapelitic specimens from the Gaub Canyon. They have the following characteristics:

Chlorite, which is stable at lower temperatures, is lost above ~ 590 °C at ~ 8 kbar, above ~ 600 °C at ~ 10 kbar and above ~ 610 °C at ~ 12 kbar. The only major exception is in the pseudosection for specimen MA-38, where chlorite is stable up to ~ 640 °C below ~ 9 kbar. If not pervasive across the entire modelled P-T range, muscovite is only absent at temperatures of above ~ 550 - 585 °C at pressures of below ~ 7 kbar, at temperatures of above ~ 585 to 610 °C at pressures of ~ 7 to 9 kbar and at temperatures of above ~ 610 °C at pressures of ~ 9.5 to 11.5 kbar. The stability of paragonite is more tightly confined in the pseudosections for specimens MA-31 and MA-38 than in those for specimens MA-29 and MA-40. In the former pseudosections, it is introduced between temperatures of ~ 595 and 615 °C at pressures above ~ 7.5 kbar and lost between ~ 595 and 625 °C from ~ 7.5 to 9 kbar, between ~ 625 and 675 °C from ~ 9 to 11.5 kbar and at > ~ 625 °C at > ~ 11.5 kbar. In the latter pseudosections, it is introduced between temperatures of ~ 450 and 550 °C at pressures of above ~ 5.5 kbar, however, it is not stable at pressures below ~ 7 kbar at ~ 460 °C to 550 °C, above ~ 10 kbar at ~ 500 °C and above ~ 11 kbar at ~ 525 °C. The loss of paragonite in these pseudosections occurs between ~ 550 and 600 °C from ~ 7 to 8 kbar, between ~ 600 and 650 °C from ~ 8 to 11 kbar and above ~ 650 °C at > ~ 11 kbar. Similarly, biotite is introduced at higher temperatures in the pseudosections for specimens MA-31 and MA-38 than in those for specimens MA-29 and MA-40. In the former pseudosections, it is introduced to after chlorite and muscovite between temperatures of ~ 545 and 585 °C from ~ 4 to 9 kbar, between ~ 585 and 600 °C from ~ 9 to 11 kbar and between ~ 600 and 615 °C from ~ 11 to 13 kbar. In the later pseudosections, it is stable across the entire modelled P-T range, except at pressures of above ~ 9.5 kbar at temperatures of ~ 450 to 500 °C and at pressures of above ~ 11.5 kbar at temperatures of ~ 500 to 550 °C.

For the modelled P range, the introduction of garnet and staurolite occurs after the minerals chlorite, muscovite and biotite at temperatures of between ~ 555 and 590 °C in the pseudosections for specimens MA-29 and MA-40 and between ~ 515 and 580 °C in the pseudosections for specimens MA-31 and MA-38. In the former pseudosections, the garnet is not stable at pressures of below ~ 9 kbar, whereas the staurolite is not stable at pressures of above ~ 10.5 kbar and lost at temperatures of above ~ 600 to 615 °C at pressures of between ~ 7 and 10.5 kbar. In the latter pseudosections, the garnet is lost at pressures of below ~ 8 to 8.5 kbar at temperatures below ~ 620 to 640 °C, whereas the staurolite is lost at pressures of above ~ 10 to 12 kbar at temperatures of ~ 575 to 610 °C and at temperatures of above ~ 610 to 650 °C

at pressures < ~ 10 kbar. In similarity to the garnet and staurolite, kyanite is introduced at temperatures of between ~ 570 and 600 °C in the pseudosections for specimens MA-29 and MA-40 and between ~ 555 and 600 °C in the pseudosections for specimens MA-31 and MA-38. In all cases, the kyanite is replaced by sillimanite and/or andalusite at pressures below ~ 5 to 7 kbar. An additional, narrow band of kyanite that extends from ~ 500 to 520 °C at ~ 4 kbar at ~ 570 °C at ~ 10 kbar occurs in the latter two pseudosections.

Epidote is lost at pressures of below ~ 4 to 4.5 kbar at ~ 500 °C, below ~ 5 to 6 kbar at ~ 550 °C, below ~ 8 kbar at ~ 600 °C and below ~ 10.5 to 11.5 kbar at ~ 650 °C. Ilmenite and quartz are stable across the entirety of the modelled P-T range, expect in the pseudosections for specimens MA-29 and MA-40, where ilmenite is absent at pressures of above ~ 8.5 kbar at temperatures of ~ 450 to 500 °C. Similarly, water (H_2O) is only absent at high temperatures of > ~ 665 °C, where the introduction of liquid melt occurs. Plagioclase is predominantly stable at lower pressures and higher temperatures. It is introduced at temperatures of above ~ 590 to 600 °C at ~ 8 kbar, at temperatures of above ~ 630 to 640 °C at ~ 10 kbar and at temperatures of above ~ 660 °C at ~ 12 kbar. In the same way, the magnetite and cordierite in the pseudosection for specimen MA-31 are confined to high temperatures and low pressures of above ~ 600 °C and below ~ 6 kbar, respectively. Sphene, which is present over the whole modelled P range, is lost between temperatures of ~ 490 and 560 °C in the pseudosections for specimens MA-31 and MA-38, and between of ~ 500 and 575 °C in the pseudosections for specimens MA-29 and MA-40. Similarly, chloritoid, which is present over the whole modelled P range in the former pseudosections, is lost between temperatures of ~ 505 and 580 °C. Glaucophane, in the latter pseudosections, only occurs at high pressures of above ~ 7 to 9 kbar and low temperatures of below ~ 525 °C.

For all of the metapelitic specimens from the Kuiseb Canyon, the inferred peak mineral assemblage (*M1b*) consists of garnet, staurolite, kyanite, chlorite, biotite, muscovite, paragonite, epidote, ilmenite and quartz. The only exception is in specimen MA-29, where no kyanite was observed. Importantly, the garnet, staurolite and kyanite, which exist as undeformed and unrotated porphyroblasts, form a later, post-tectonic mineral assemblage that overprinted an earlier, syn-tectonic, prograde, fabric-forming mineral assemblage. The earlier, prograde mineral assemblage (*M1a*) is characterised primarily by the concurrent alignment of micaceous minerals chlorite, biotite and muscovite into a penetrative foliation.

As in the pseudosections for the metapelitic rocks of the Gaub Canyon, the most likely stability field for the earlier, syn-tectonic, prograde, fabric-forming mineral assemblage (*M1a*) (i.e. the P-T conditions of fabric formation) is indicated in *green*; whereas the stability field for the inferred peak mineral assemblage (*M1b*) (i.e. the P-T conditions of peak metamorphism), which is inclusive of the earlier, syn-tectonic, prograde assemblage plus the later, post-tectonic, overprinting mineral assemblage, is indicated in *red*.

In metapelitic specimen MA-29, the stability field for the inferred peak mineral assemblage is between pressures of ~ 8.7 and 10.5 kbar and temperatures of ~ 590 and 605 °C. The stability field at which the minerals that define the penetrative foliation are most likely to have first formed in the presence of one another occurs between pressures of ~ 5.3 and 13 kbar and temperatures of ~ 455 and 565 °C.

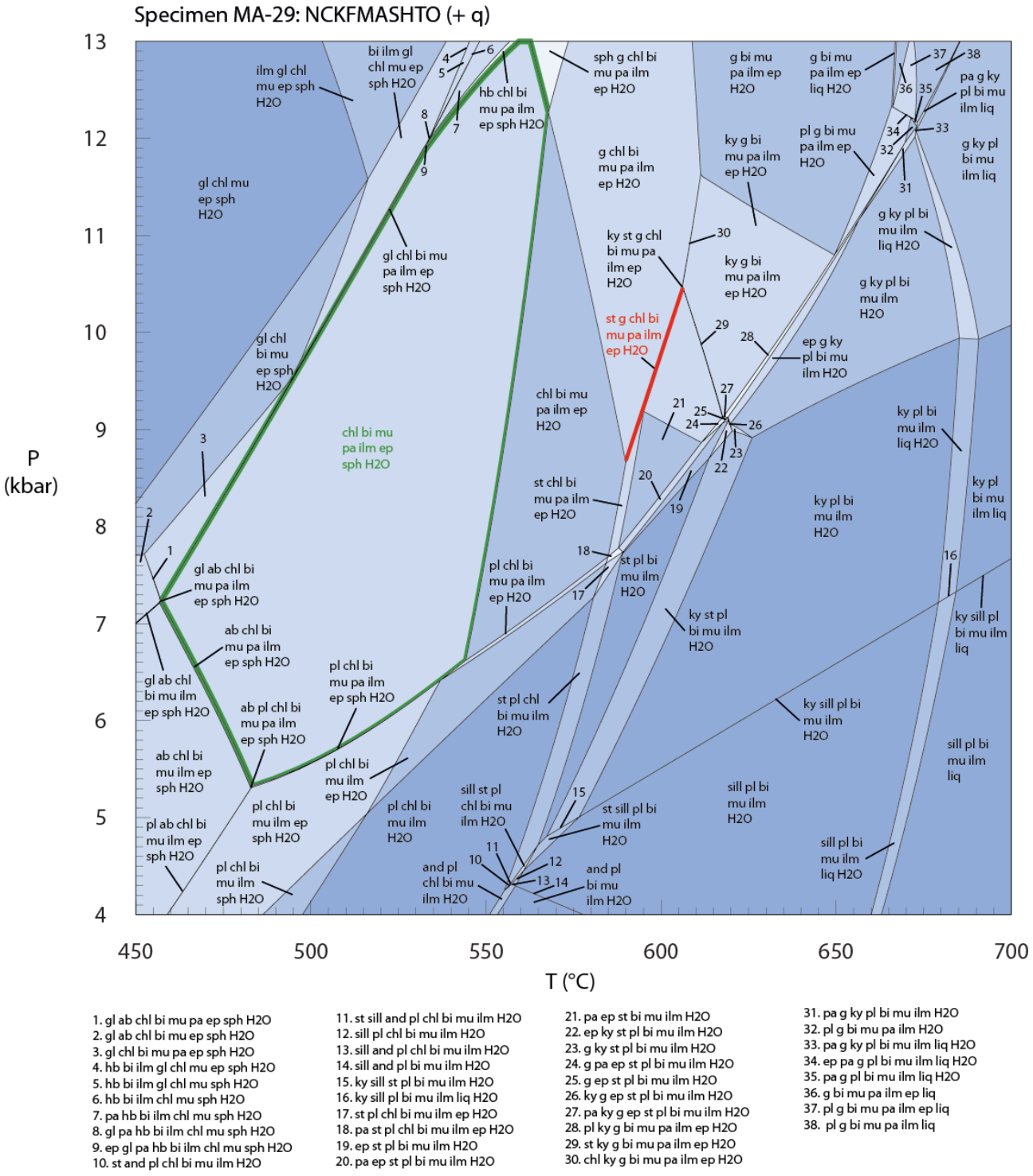

Figure 31: A pseudosection modelled for specimen MA-29.

In metapelitic specimen MA-31, the inferred peak mineral assemblage is stable at a pressure of ~ 10.5 kbar and at a temperature of ~ 605 °C. Unfortunately, there is no stability field that is inclusive of all of fabric-forming minerals prior to the P-T conditions at which the overprinting porphyroblasts (specifically staurolite) become stable. Nevertheless, the most likely stability field at which the penetrative foliation may have formed is between pressures of ~ 4 and 13 kbar and temperatures of ~ 450 and 555 °C. It is at these P-T conditions that the micaceous minerals that are always aligned within the foliation, namely chlorite and muscovite, first co-exist.

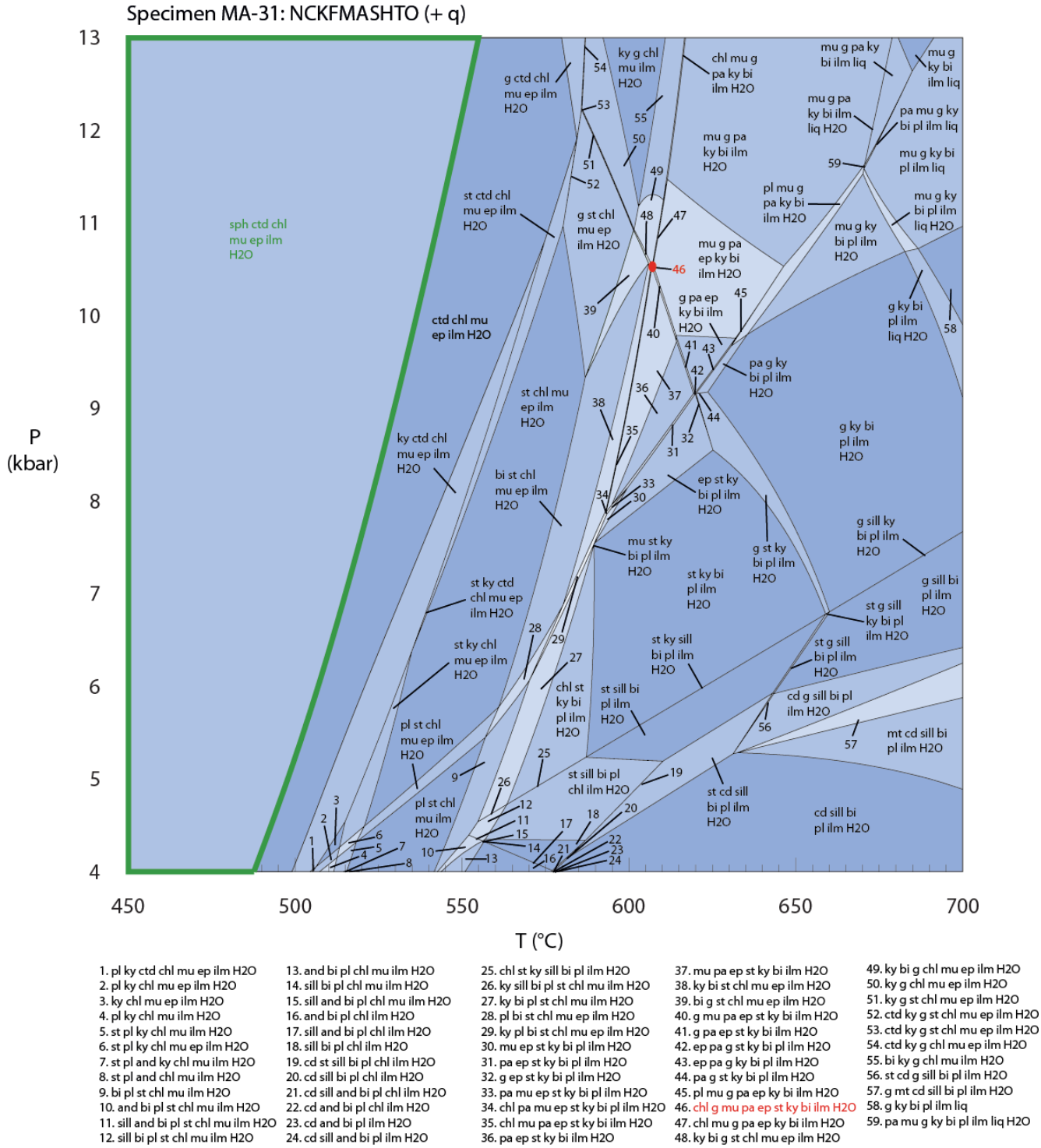

1. pl ky ctd chl mu ep ilm H2O
2. pl ky chl mu ep ilm H2O
3. ky chl mu ep ilm H2O
4. pl ky chl mu ilm H2O
5. st pl ky chl mu ilm H2O
6. st pl ky chl mu ep ilm H2O
7. st pl and ky chl mu ilm H2O
8. st pl and chl mu ilm H2O
9. bi pl st chl mu ilm H2O
10. and bi pl st chl mu ilm H2O
11. sill and bi pl st chl mu ilm H2O
12. sill bi pl st chl mu ilm H2O
13. and bi pl chl mu ilm H2O
14. sill bi pl chl mu ilm H2O
15. sill and bi pl chl mu ilm H2O
16. and bi pl chl ilm H2O
17. sill and bi pl chl ilm H2O
18. sill bi pl chl ilm H2O
19. cd st sill bi pl chl ilm H2O
20. cd sill bi pl chl ilm H2O
21. cd sill and bi pl chl ilm H2O
22. cd and bi pl chl ilm H2O
23. cd and bi pl ilm H2O
24. cd sill and bi pl ilm H2O
25. chl st ky sill bi pl ilm H2O
26. ky sill bi pl st chl mu ilm H2O
27. ky bi pl st chl mu ilm H2O
28. pl bi st chl mu ep ilm H2O
29. ky pl bi st chl mu ep ilm H2O
30. mu ep st ky bi pl ilm H2O
31. pa ep st ky bi pl ilm H2O
32. g ep st ky bi pl ilm H2O
33. pa mu ep st ky bi pl ilm H2O
34. chl pa mu ep st ky bi pl ilm H2O
35. chl mu pa ep st ky bi ilm H2O
36. pa ep st ky bi ilm H2O
37. mu pa ep st ky bi ilm H2O
38. ky bi st chl mu ep ilm H2O
39. bi g st chl mu ep ilm H2O
40. g mu pa ep st ky bi ilm H2O
41. g pa ep st ky bi ilm H2O
42. ep pa g st ky bi pl ilm H2O
43. ep pa g ky bi pl ilm H2O
44. pa g st ky bi pl ilm H2O
45. pl mu g pa ep ky bi ilm H2O
46. chl g mu pa ep st ky bi ilm H2O
47. chl mu g pa ep ky bi ilm H2O
48. ky bi g st chl mu ep ilm H2O
49. ky bi g chl mu ep ilm H2O
50. ky g chl mu ep ilm H2O
51. ky g st chl mu ep ilm H2O
52. ctd ky g st chl mu ep ilm H2O
53. ctd ky g st chl mu ep ilm H2O
54. ctd ky g chl mu ep ilm H2O
55. bi ky g chl mu ilm H2O
56. st cd g sill bi pl ilm H2O
57. g mt cd sill bi pl ilm H2O
58. g ky bi pl ilm liq
59. pa mu g ky bi pl ilm liq H2O

Figure 32: A pseudosection modelled for specimen MA-31.

In metapelitic specimen MA-38, the inferred peak mineral assemblage is stable at a pressure of ~ 10.5 kbar and a temperature of ~ 605 °C. As in metapelitic specimen MA-31, there is no stability field that is inclusive of all of fabric-forming minerals prior to the P-T conditions at which the overprinting porphyroblasts (specifically staurolite) become stable. Nonetheless, the most likely stability field at which the penetrative foliation may have formed is between pressures of ~ 4 and 12.6 kbar and temperatures of ~ 450 and 555 °C. It is at these P-T conditions that the micaceous minerals that are always aligned within the foliation, namely chlorite and muscovite, first co-exist.

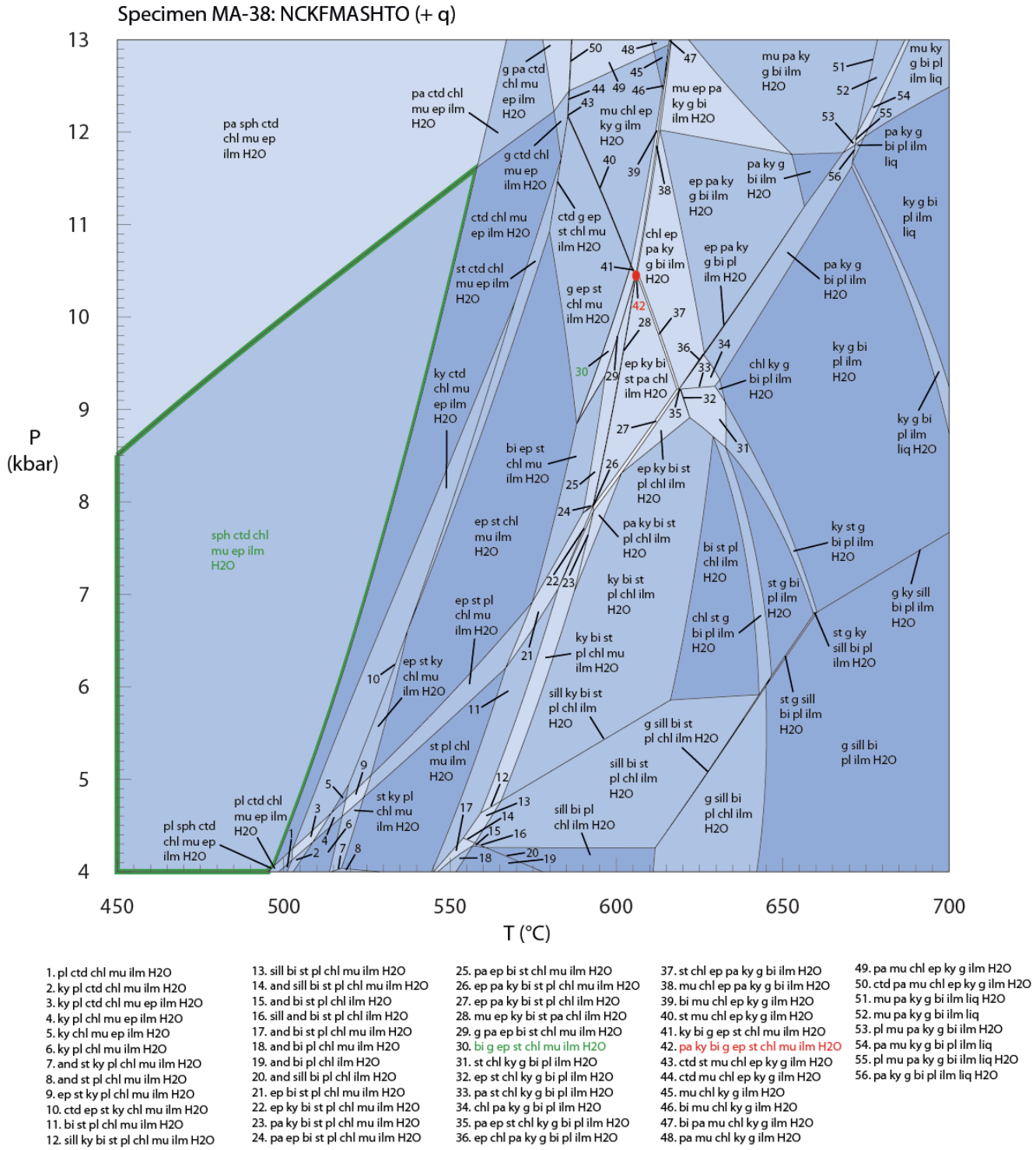

1. pl ctd chl mu ilm H2O
2. ky pl ctd chl mu ilm H2O
3. ky pl ctd chl mu ep ilm H2O
4. ky pl chl mu ep ilm H2O
5. ky chl mu ep ilm H2O
6. ky pl chl mu ilm H2O
7. and st ky pl chl mu ilm H2O
8. and st pl chl mu ilm H2O
9. ep st ky pl chl mu ilm H2O
10. ctd ep st ky chl mu ilm H2O
11. bi st pl chl mu ilm H2O
12. sill ky bi st pl chl mu ilm H2O
13. sill bi st pl chl mu ilm H2O
14. and sill bi st pl chl mu ilm H2O
15. and bi st pl chl ilm H2O
16. sill and bi st pl chl ilm H2O
17. and bi st pl chl mu ilm H2O
18. and bi pl chl mu ilm H2O
19. and bi pl chl ilm H2O
20. and sill bi pl chl ilm H2O
21. ep bi st pl chl mu ilm H2O
22. ep ky bi st pl chl mu ilm H2O
23. pa ky bi st pl chl mu ilm H2O
24. pa ep bi st pl chl mu ilm H2O
25. pa ep bi st chl mu ilm H2O
26. ep pa ky bi st pl chl mu ilm H2O
27. ep pa ky bi st pl chl ilm H2O
28. mu ep ky bi st pa chl ilm H2O
29. g pa ep bi st chl mu ilm H2O
30. bi g ep st chl mu ilm H2O
31. st chl ky g bi pl ilm H2O
32. ep st chl ky g bi pl ilm H2O
33. pa st chl ky g bi pl ilm H2O
34. chl pa ky g bi pl ilm H2O
35. pa ep st chl ky g bi pl ilm H2O
36. ep chl pa ky g bi pl ilm H2O
37. st chl ep pa ky g bi ilm H2O
38. mu chl ep pa ky g bi ilm H2O
39. bi mu chl ep ky g ilm H2O
40. st mu chl ep ky g ilm H2O
41. ky bi g ep st chl mu ilm H2O
42. pa ky bi g ep st chl mu ilm H2O
43. ctd st mu chl ep ky g ilm H2O
44. ctd mu chl ep ky g ilm H2O
45. mu chl ky g ilm H2O
46. bi mu chl ky g ilm H2O
47. bi pa mu chl ky g ilm H2O
48. pa mu chl ky g ilm H2O
49. pa mu chl ep ky g ilm H2O
50. ctd pa mu chl ep ky g ilm H2O
51. mu pa ky g bi ilm liq H2O
52. mu pa ky g bi ilm liq
53. pl mu pa ky g bi ilm H2O
54. pa mu ky g bi pl ilm liq
55. pl mu pa ky g bi ilm liq H2O
56. pa ky g bi pl ilm liq H2O

Figure 33: A pseudosection modelled for specimen MA-38.

In metapelitic specimen MA-40, the inferred peak mineral assemblage is stable at a pressure of ~ 10.5 kbar and at a temperature of ~ 605 °C, whereas the minerals that define the penetrative foliation are most likely to have first formed in the presence of one another is between pressures of ~ 5.4 and 13 kbar and temperatures of ~ 455 and 580 °C.

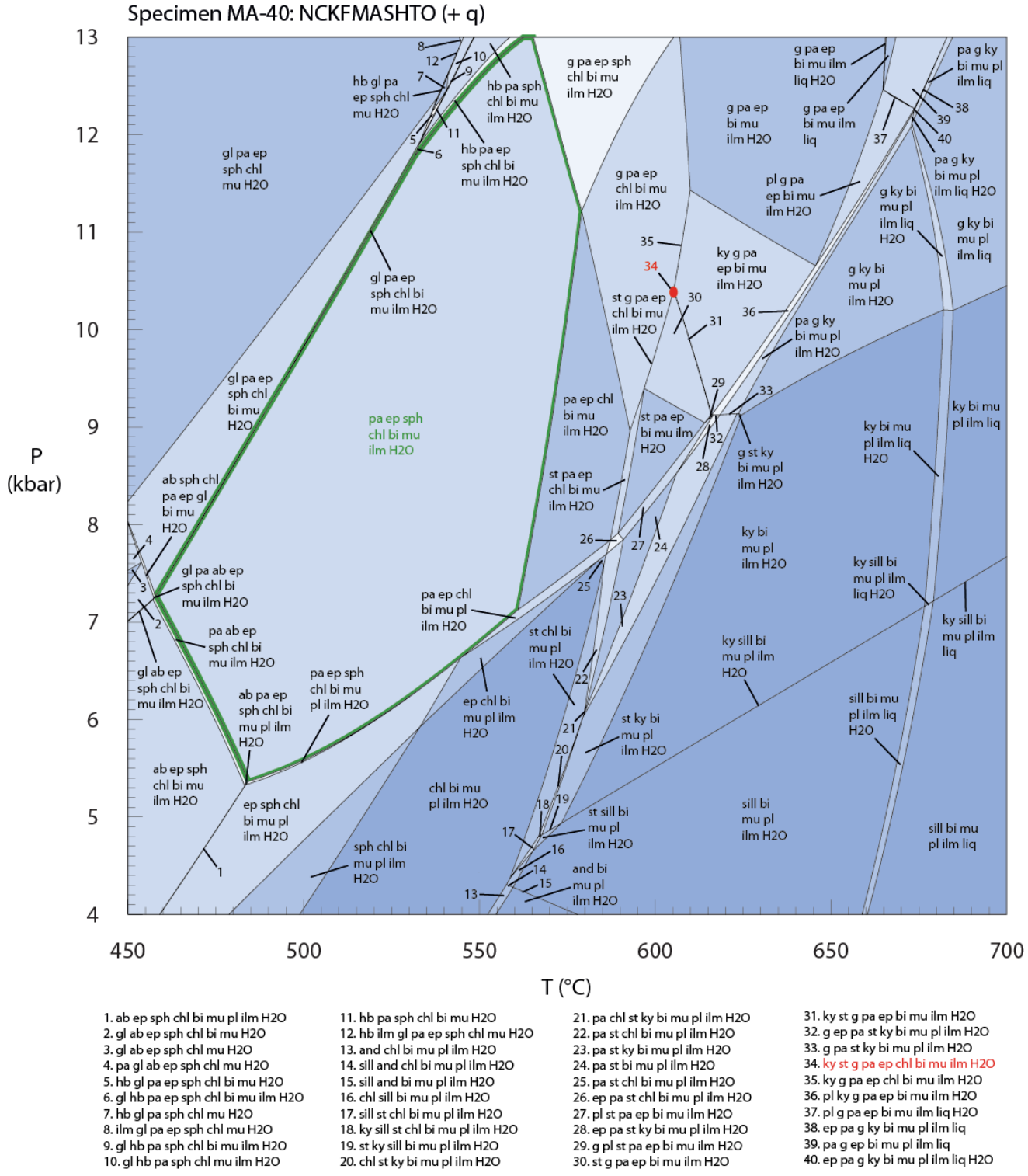

Figure 34: A pseudosection modelled for specimen MA-40.

6.3. Metamafic Rocks from the Gaub and Kuiseb Canyons

The topology of the pseudosection for metamafic specimen GB-4 from the Gaub Canyon (*Figure 35*) has the following characteristics:

Rutile is introduced between ~ 510 and 520 °C at the modelled P range and lost at above ~ 530 °C at ~ 4 kbar, above ~ 600 °C at ~ 6 kbar, above ~ 650 °C at ~ 7.5 kbar and above ~ 700 °C at ~ 9.5 kbar. Similarly, epidote is lost below ~ 4 kbar at ~ 500 °C, below ~ 4.5 kbar at ~ 550 °C, below ~ 6 kbar at ~ 600 °C, below ~ 7.5 kbar at ~ 650 °C and below ~ 9.5 kbar at ~ 700 °C. Chlorite, which is stable at low temperatures, is lost at ~ 530 °C below ~ 7 kbar, between ~ 530 and 575 °C from ~ 7 to 10 kbar and at ~ 575 °C above ~ 10 kbar. Biotite, quartz and water (H_2O) are present across the entirety of the modelled P-T range. Sphene is also present the majority of the modelled P-T range, except below ~ 5 to 6 kbar at temperatures above ~ 600 to 650 °C. The introduction of hornblende at ~ 475 °C below ~ 9 kbar and between ~ 490 and 525 °C from ~ 9 to 13 kbar, is closely followed by the loss of actinolite at ~ 490 °C below ~ 9 kbar and between ~ 500 and 545 °C from ~ 9 to 13 kbar. Plagioclase is introduced below ~ 4 kbar at ~ 500 °C, below ~ 6 kbar at ~ 600 °C and below ~ 8 kbar above ~ 650 °C. Ilmenite is introduced below ~ 5 kbar at ~ 550 °C, below ~ 6.5 kbar at ~ 600 °C and below ~ 8.5 kbar above ~ 650 °C. Garnet is only introduced above ~ 580 °C at ~ 8 to 10 kbar. Glaucophane is confined to high pressures of above ~ 8.5 to 9 kbar and low temperatures of below ~ 490 to 520 °C. Similarly, omphacite is only stable above ~ 11 kbar and below ~ 500 °C. Albite only occurs at low pressures of below ~ 9 kbar and low temperatures of below ~ 475 to 500 °C. By contrast, diopside is introduced at high temperatures of above ~ 675 °C between ~ 5.5 and 7.5 kbar.

In the metamafic specimen GB-4 from the Gaub Canyon, the early, syn-tectonic, prograde, fabric-forming mineral assemblage (*M1a*) is comprised of hornblende, epidote, rutile, quartz, biotite and chlorite. The stability field for this assemblage is between pressures of ~ 6.4 and 12.9 kbar and temperatures of ~ 535 and 580 °C (*green*). The inferred peak mineral assemblage (*M1b*), which came into existence after the later, post-tectonic event that may have resulted in the complete loss (consumption) of chlorite, consists of hornblende, epidote, rutile, quartz and minor biotite. The stability field for this assemblage is between pressures of ~ 6.5 and 10.1 kbar and temperatures of ~ 535 and 620 °C (*red*).

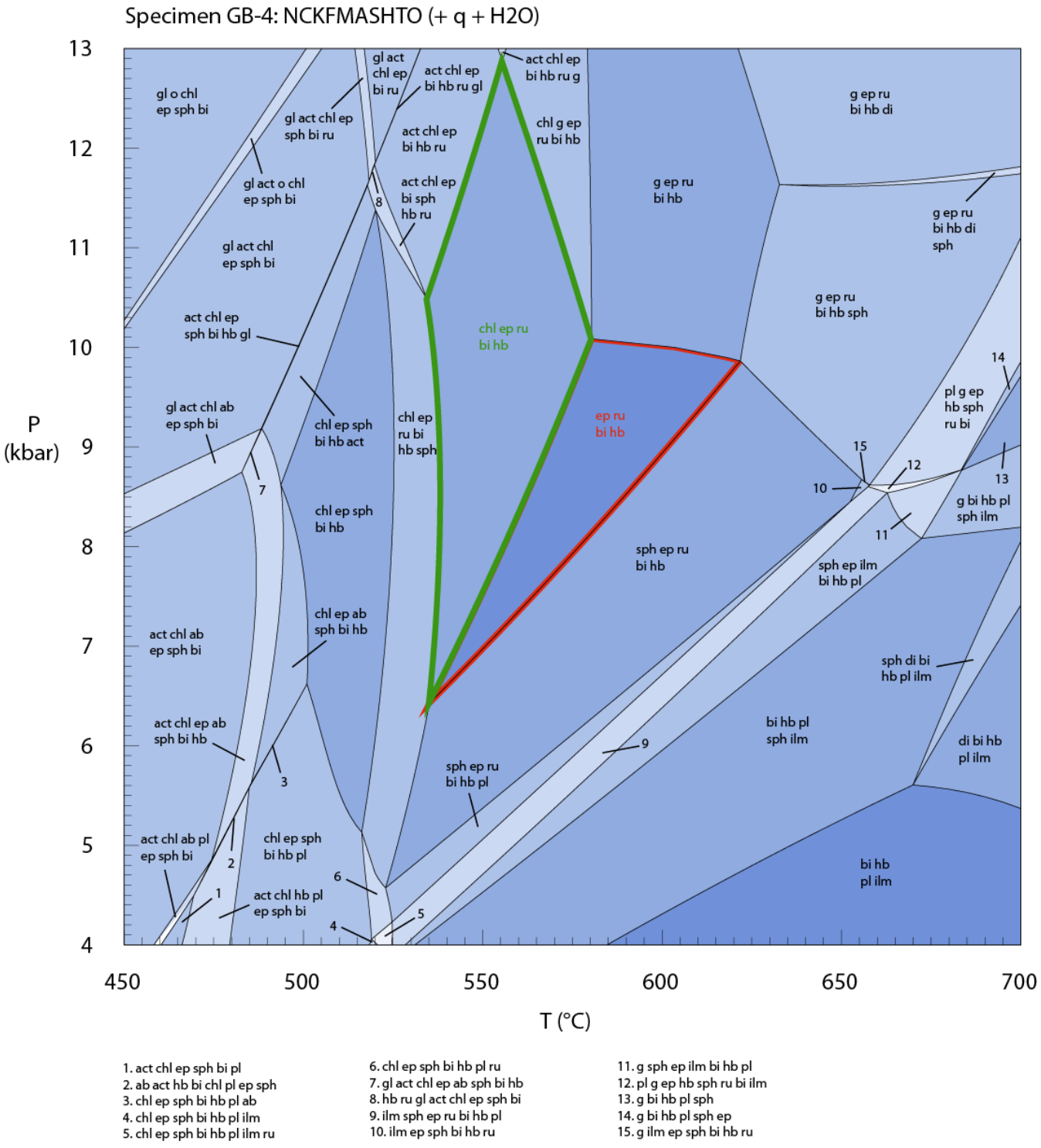

Figure 35: A pseudosection modelled for specimen GB-4.

The topology of the pseudosection for metamafic specimen MA-44 from the Kuiseb Canyon (*Figure 36*) has the following characteristics:

Sphene, biotite, quartz and water (H_2O) are present across the entirety of the modelled P-T range. Rutile is introduced at high pressures of above ~ 10 kbar at high temperatures of ~ 535 to 550 °C. It is lost at ~ 10 to 12 kbar between ~ 595 and 610 °C and above ~ 12 kbar at above ~ 610 °C. Epidote is lost at high temperatures of above ~ 620 to 650 °C at low pressures of below ~ 5 to 7 kbar. Chlorite, which is stable at low temperatures, is lost above ~ 525 to 555 °C at the modelled P range. Hornblende is introduced at ~ 485 °C below ~ 9 kbar, between ~ 485 and 540 °C at ~ 9 to 11.5 kbar and between ~ 540 and 580 °C above ~ 11.5 kbar. The loss of actinolite occurs shortly after the introduction of hornblende below ~ 550 °C at below ~ 6 kbar, between ~ 550 and 575 °C at ~ 6 to 10 kbar and above ~ 575 °C at above ~ 10 kbar. Garnet is introduced above ~ 11.5 kbar at ~ 530 to 545 °C, above ~ 10.5 to 11.5 kbar at ~ 545 to 590 °C and above ~ 6.5 to 7.5 kbar at above ~ 590 °C. Plagioclase is introduced below ~ 4.5 kbar at ~ 550 °C, below ~ 6 kbar at ~ 600 °C, below ~ 7.5 kbar at ~ 650 °C and below ~ 9.5 kbar at ~ 700 °C. Ilmenite is introduced below ~ 11 kbar at ~ 525 to 545 °C and lost at below ~ 575 °C at ~ 10 to 11 kbar and at ~ 575 to 615 °C at ~ 5 to 10 kbar. Glaucophane is confined to high pressures of ~ 8.5 to 10.5 kbar and low temperatures of below ~ 475 °C. Similarly, omphacite is only stable above ~ 10.5 kbar and below ~ 500 °C. Albite only occurs at low pressures of below ~ 8.5 kbar and low temperatures of below ~ 485 °C. By contrast, diopside is introduced at high temperatures of above ~ 600 °C at ~ 5 kbar and above ~ 675 °C at ~ 8.5 kbar.

In the metamafic specimen MA-44 from the Kuiseb Canyon, the observed mineral assemblage (*M1a*) is constituted by hornblende, actinolite, epidote, rutile, quartz, biotite, sphene and chlorite. The stability field for this mineral assemblage is between pressures of ~ 10.8 and 11.5 kbar and temperatures of ~ 540 and 545 °C (*green*).

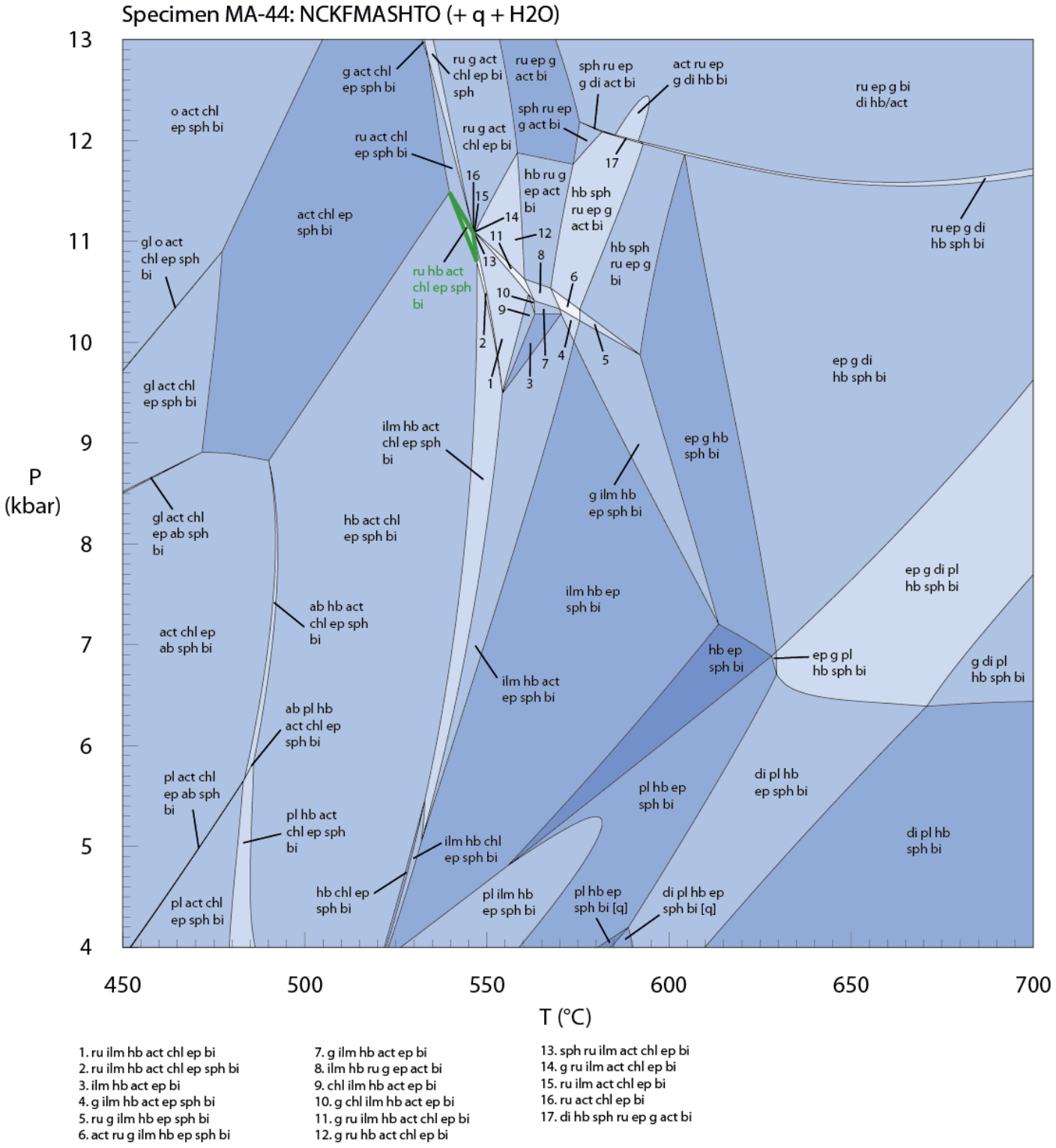

Figure 36: A pseudosection modelled for specimen MA-44.

7. Discussion

7.1. Inferred peak P-T conditions and depths of burial

In the Gaub Canyon, the stability fields for the inferred peak mineral assemblage (*M1b*) in the modelled metapelitic specimens (GB-8, GB-10 and GB-13) overlap at a well-constrained pressure of ~ 9.8 kbar and temperature of ~ 600 °C. The modelled metamafic specimen (GB-4) has an inferred peak mineral assemblage (*M1b*) that is stable over a large pressure (~ 6.5 to 10.1 kbar) and temperature (~ 535 to 620 °C) range that is consistent with the P-T estimates derived from the metapelites. Similarly, in the Kuiseb Canyon, the stability fields for the inferred peak mineral assemblage (*M1b*) in the modelled metapelitic specimens (MA-29, MA-31, MA-38 and MA-40) overlap at a tightly constrained pressure and temperature of ~ 10.5 kbar and ~ 605 °C, respectively. The observed mineral assemblage in the modelled metamafic specimen (MA-44) occurs at very similar peak pressures (~ 10.8 to 11.5 kbar) to the metapelitic specimens, but at lower temperatures (~ 540 to 545 °C). At the temperatures of ~ 605 °C inferred from the metapelites, the metamafic specimen is calculated to be garnet-bearing, however no garnet is present. This apparent discrepancy could be due to slow garnet nucleation (e.g. Carlson *et al.*, 1995) or perhaps an underestimation of the amount of Fe^{3+} in the bulk composition. Given the tight and consistent P-T estimates recorded by the metapelitic specimens, these are preferred as a representative estimate of peak metamorphic P-T conditions for the Kuiseb Canyon. The recorded peak pressure conditions for the Gaub (~ 9.8 kbar) and Kuiseb (~ 10.5 kbar) Canyons correspond to the burial of the accreted material to depths of ~ 30 km and ~ 33 km, respectively, assuming a density of 2.7 g/cm^3.

Evidently, the metapelitic and metamafic rocks from the Gaub and Kuiseb Canyons record inferred peak P-T conditions and depths of burial that are closely comparable to one another. The very minor thermobarometric differences between the two localities, specifically the documentation of slightly higher pressure (~ 0.5 to 1.5 kbar) and temperature (~ 5 °C) conditions by those rocks from the Kuiseb Canyon compared to those from the Gaub Canyon, are within the error of the thermodynamic modelling and are therefore considered to not be significant. The inferred peak P-T conditions for rocks from the Gaub and Kuiseb Canyons correspond fairly closely to the P-T conditions of ~ 9 to 10 kbar and ~ 574 to 590 °C recorded by Kasch (1981) for garnet-biotite and garnet-plagioclase pairs in garnet, staurolite and kyanite bearing assemblages in the Omitara and Gamsberg-Kuiseb River areas of the Southern Zone.

Given that the rocks of the SZ and SMZ have an observed dip of approximately 45 °, then the distance of ~ 15 km across strike between the Gaub and Kuiseb Canyons equates to a true tectonostratigraphic thickness of ~ 10 km, which in turn should correspond to a change in pressure of ~ 3 kbar between the two localities. The lack of a significant change in pressure between the two localities confirms that the Southern

Zone represents a disrupted structural sequence and suggests that the rocks of the Gaub and Kuiseb Canyons represent similar structural levels despite being tectonostratigraphically ~ 10 km apart from one another.

7.2. Constraints on the P-T paths

7.2.1. Prograde metamorphism in the rocks from the Gaub Canyon

In the modelled metapelitic and metamafic specimens GB-4, GB-8 and GB-13 from the Gaub Canyon, the stability fields for the early, syn-tectonic, prograde, fabric-forming mineral assemblage (*M1a*) overlap at pressures of ~ 8.4 to 11.8 kbar and temperatures of ~ 535 to 550 °C. These P-T conditions are consistent with the pressure (~ 9.8 kbar) at which the inferred peak mineral assemblages in these specimens (*M1b*) are stable, but at temperatures that are > ~ 50 °C lower. Between ~ 550 °C and ~ 600 °C in the modelled pseudosections, the addition of garnet and staurolite occurs in the metapelites, whereas the loss of chlorite occurs in the metamafics. These changes are consistent with the petrographic observations of post-tectonic garnet, staurolite and biotite in these specimens.

Evidently, for the rocks of the Gaub Canyon, the change from the P-T conditions at which fabric formation (*M1a*) occurred to the P-T conditions at which the inferred peak mineral assemblages (*M1b*) are stable involved a ~ 50 to 65 °C increase in temperature, seemingly without a concomitant change in pressure. The fact that the pressure conditions at which fabric formation (*M1a*) occurred overlaps with that of the inferred peak mineral assemblages (*M1b*) and the apparent lack of deformation and rotation of the overprinting porphyroblasts in the metapelites, suggests that the increase in temperature is likely to have been near-isobaric. *Figure 37* below illustrates the inferred P-T path for the rocks of the Gaub Canyon.

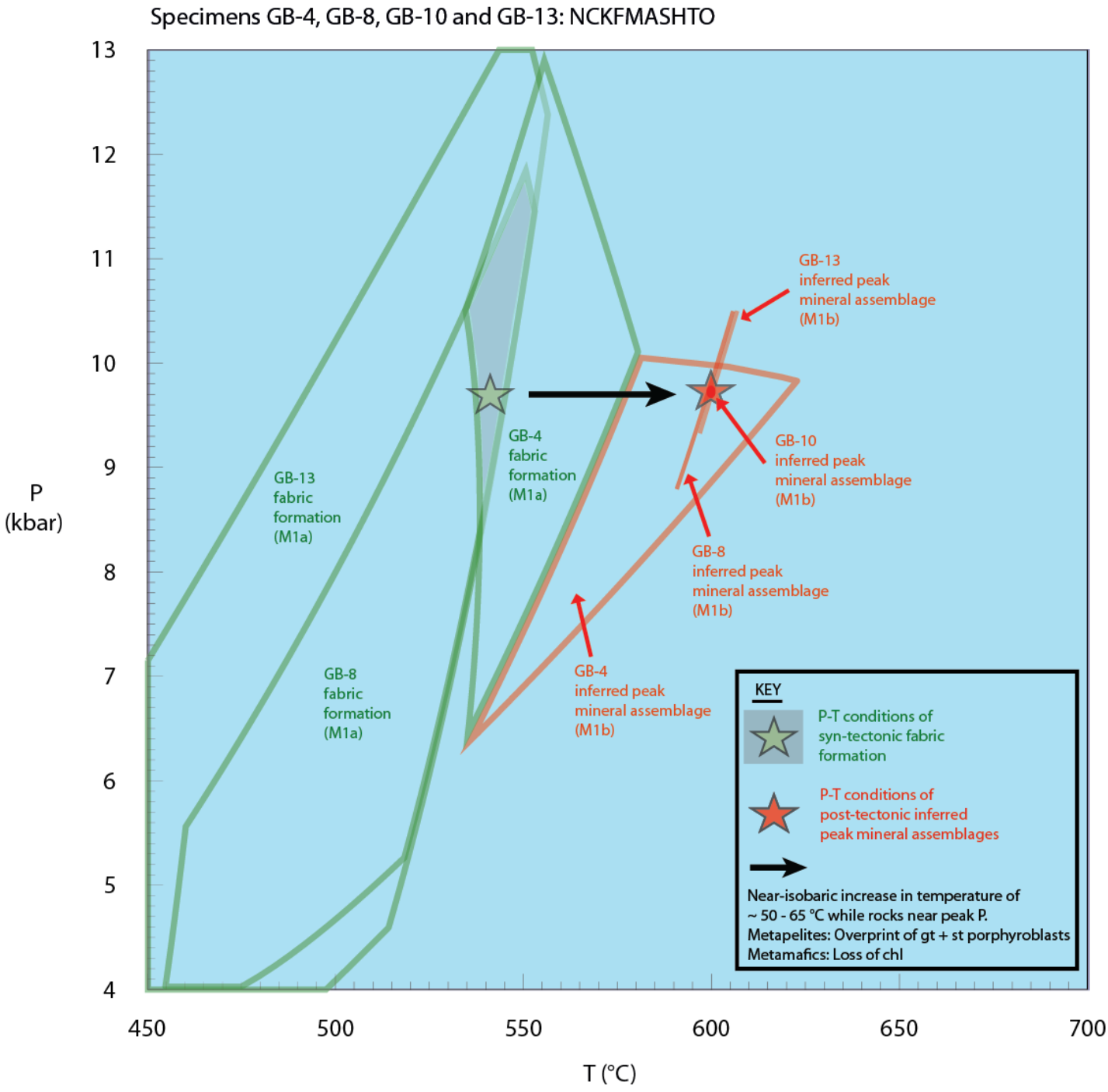

Figure 37: Inferred metamorphic evolution (P-T Path) from the rocks of the Gaub Canyon.

7.2.2. Prograde metamorphism in the rocks from the Kuiseb Canyon

In the modelled metapelitic and metamafic specimens MA-29, MA-40 and MA-44 from the Kuiseb Canyon, the stability fields for the early, syn-tectonic, prograde, fabric-forming mineral assemblage (*M1a*) overlap at pressures of ~ 10.8 to 11.5 kbar and temperatures of ~ 540 to 545 °C. These P-T conditions are fairly consistent with the pressure (~ 10.5 kbar) determined for the inferred peak mineral assemblage in the metapelites (*M1b*), but at temperatures that are > ~ 60 °C lower. Between ~ 545 °C and ~ 605 °C in the modelled pseudosections, the addition of garnet, staurolite and kyanite occurs in the metapelites, whereas the addition of garnet and loss of chlorite occurs in the metamafics. For the metapelites, these changes are consistent with the petrographic observations of post-tectonic garnet, staurolite, kyanite and biotite in these specimens. In the metamafics, only the partial loss of chlorite is apparent. Moreover, as mentioned previously, the lack of post-tectonic garnet in the metamafics may be due to the slow nucleation of garnet. Due to the lack of stability fields that perfectly match fabric formation in the modelled metapelitic specimens MA-31 and MA-38, these specimens were not used in determining P-T conditions at which fabric formation occurred.

Evidently, for the rocks of the Kuiseb Canyon, the change from the P-T conditions at which fabric formation (*M1a*) occurred to the P-T conditions at which the inferred peak mineral assemblage (*M1b*) is stable involved a ~ 60 to 65 °C increase in temperature, seemingly without a concomitant change in pressure. The fact that the pressure conditions at which fabric formation (*M1a*) occurred appear to overlap with that of the inferred peak mineral assemblage in the metapelites (*M1b*) and the apparent lack of deformation and rotation of the overprinting porphyroblasts in the metapelites, suggests that the increase in temperature is likely to have been near-isobaric. *Figure 38* below illustrates the inferred P-T path for the rocks of the Kuiseb Canyon.

Importantly, while the P-T path for the rocks of the Kusieb Canyon is not as well-constrained as the P-T path for the rocks of the Gaub Canyon, they are closely comparable, with both P-T paths illustrating that the development of the inferred peak mineral assemblages (*M1b*) from the fabric-forming mineral assemblages (*M1a*) involved a significant increase in temperature without a concomitant change in pressure or differential strain.

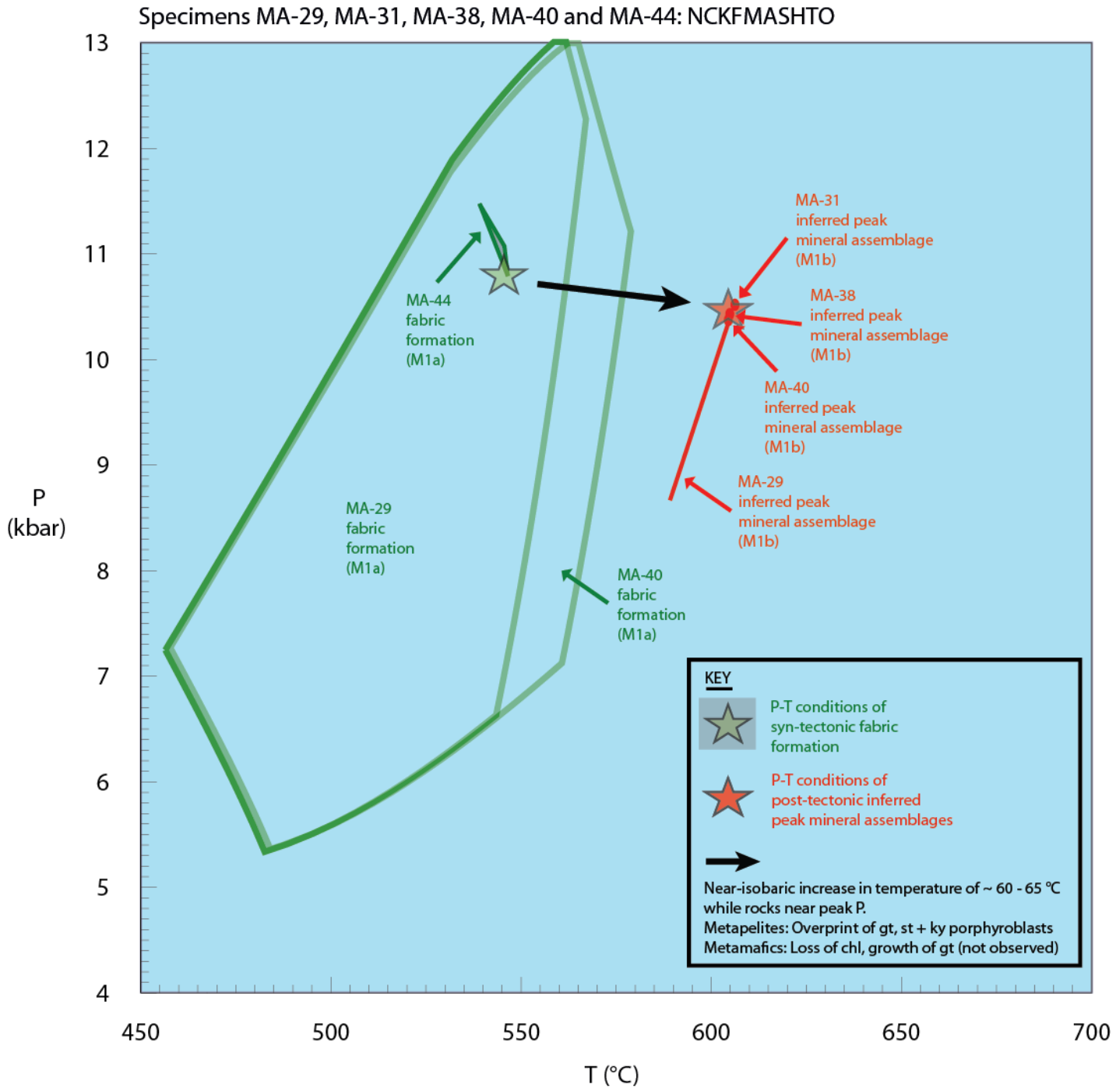

Figure 38: Inferred metamorphic evolution (P-T Path) from the rocks of the Kuiseb Canyon.

7.2.3. Retrograde metamorphism in the rocks from the Gaub and Kusieb Canyons

The euhedral-subhedral shape and lack of deformation and/or rotation of the porphyroblasts within the matrix of the inferred peak mineral assemblages (*M1b*) in the metapelites from the Gaub and Kuiseb Canyons, as well the absence of retrograde features, such as alteration rims around the porphyroblasts or overgrowths of new minerals, indicates that there was not any post-peak, collision- and exhumation-related deformation and/or fluid infiltration. Importantly, this suggests that these rocks were not subjected to the deformation resulting from the collision of the Congo and Kalahari Cratons at ~ 542 Ma.

7.3. The Southern Zone as an accretionary prism

Kukla & Stanistreet's (1991) recognition of the Southern Zone as an accretionary prism was founded on the similarities of the Southern Zone to the characteristics derived from known accretionary prisms. These characteristics are summarised below and elaborated on in light of the new metamorphic constraints presented in this study.

Firstly, the Southern Zone, like many known accretionary prisms, is comprised of intercalated metapsammopelites and metamafics with a high strain fabric. The Kuiseb and Hureb Formations of the (upper-) Swakop Group in the Southern Zone, as well as the stratigraphically identical Haris, Mahonda, Melrose and Samara Formations of the (upper-) Hakos Group in the Southern Margin Zone, consist predominantly of metapsammopelitic schists that display a multitude of relic sedimentary features, such as graded bedding with Bouma sequences and palaeocurrent indicators, and a penetrative foliation defined the alignment of the phyllosilicate minerals chlorite, biotite and muscovite and often paralleled by dismembered quartz veins of variable thickness. Intimately intercalated within these schists are a plenitude of relatively narrow, mafic, volcanic amphibolite bodies, such as the spatially extensive Matchless Amphibolite Member and the Mohlatetsi Amphibolite Member, both which have a compositional affinity to MORB, exhibit remnant igneous features, such as abundant flattened pillow structures and chilled margins around undifferentiated metagabbros and dolerite dykes, and have a distinct fabric defined by the alignment of amphibole and mica.

Secondly, the position of the HP-LT terrane of the Southern and Southern Margin Zones immediately adjacent to the HT-LP terrane of the southern Central Zone and the separation of these contrasting metamorphic terranes by the Okahandja Lineament, a prominent structural feature at the northern boundary of the Southern Zone (Miller, 1983; Kukla, 1992; Miller, 2008), is in agreement both with the concept of paired metamorphic belts recognised by Miyashiro (1961) and with the structural separation of a HP-LT accretionary prism from an adjacent HT-LP magmatic arc identified by Oxburgh &

Turcotte (1971) and re-iterated by Maruyama *et al.* (2010). Moreover, the observed arrangement corresponds to that seen in other known accretionary prisms, such as the HP-LT Western Belt of the Coastal Cordillera in Chile (Willner, 2005) and the HP-LT Tablelands Complex of the southern New England Fold Belt in Australia (Phillips *et al.*, 2008).

Thirdly, according to Kukla (1992) and Miller (2008) the metamorphism of the rocks of the Southern Zone is related to the convergence of the Congo and Kalahari Cratons from ~ 580 Ma to ~ 542 Ma and their subsequent collision and closure of the Khomas Sea at ~ 542 Ma. These ages for metamorphism overlap with the oldest ages of metamorphism recorded in known accretionary prisms, most of which are younger than the early-Palaeozoic (< 550 Ma) (Ernst, 1973, 1988 and various examples, e.g. Phillips *et al.*, 2008). Hence, the metamorphosed rocks of the Southern Zone may represent some of the oldest rocks to have undergone metamorphism within an accretionary prism environment.

Importantly, the geothermal gradients documented by rocks of the Southern Zone closely resemble those documented by rocks in known accretionary prisms and hence provide further evidence for Kukla & Stanistreet's (1991) recognition of the Southern Zone as an accretionary prism. As exemplified in *Chapter 2*, the ideal geothermal gradient within an accretionary prism is colder than the stable continental geothermal gradient, typically between ~ 8 and ~ 15 °C/km. While the P-T conditions for the inferred peak mineral assemblages (*M1b*) in the rocks from the Gaub and Kuiseb Canyons (~ 9.8 kbar, ~ 600 °C and ~ 10.5 kbar and ~ 605 °C) correspond to geothermal gradients of ~ 18.5 °C/km and ~17.3 °C/km, respectively (assuming a density of 2.7 g/cm^3), and are therefore too warm to be suggestive of metamorphism within an accretionary prism, the P-T conditions at which fabric formation (*M1a*) may have occurred (~ 9.8 kbar, ~ 540 °C and ~ 10.7 kbar, ~ 542 °C) equate to cooler geothermal gradients of ~ 16.6 °C/km and ~ 15.1 °C/km, respectively. These values are indicative of metamorphism within an accretionary prism, particularly if one considers additional factors that may affect the recorded geothermal gradients, such as heating due to the decay of radioactive elements between ~ 542 Ma and 0 Ma and the fact that the Earth was warmer and the lithosphere thinner at ~ 542 Ma (Brown, 2007). These factors could lower the geothermal gradient at which fabric formation occurred. Interestingly, the geothermal gradients obtained from the inferred peak P-T conditions correspond fairly closely to those geothermal gradients of ~ 17 to 19.5 °C/km calculated by Miller (2008) for the rocks of the Omitara and Gamsberg-Kuiseb River areas of the Southern Zone.

7.4. Geodynamic constraints on metamorphism

In the Gaub Canyon, fabric formation (*M1a)* occurred at P-T conditions of ~ 8.4 to 11.8 kbar and ~ 535 to 550 °C, whereas peak metamorphism (*M1b*) was at ~ 9.8 kbar and temperatures of ~ 600 °C. These P-T conditions correspond to geothermal gradients of ~ 16.6 °C /km and ~ 18.5 °C /km, respectively, and depths of burial of ~ 30 km. Similarly, in the Kuiseb Canyon, fabric formation (*M1a)* occurred at P-T conditions of ~ 10.8 to 11.5 kbar and ~ 540 to 545 °C, whereas peak metamorphism (*M1b*) was at ~ 10.5 kbar and ~ 605 °C. These conditions equate to geothermal gradients of ~ 15.1 °C/km and ~ 17.3 °C/km, respectively, and depths of burial of ~ 33 km.

The high pressures, low temperatures and low geothermal gradients recorded by the rocks from the Gaub and Kuiseb Canyons are indicative of subduction zone geodynamics. The most remarkable aspect in these rocks is the inferred near-isobaric increase in temperature of ~ 60 °C that they experienced while at high pressure conditions. Such a temperature change can possibly be attributed to several geodynamic factors, such as long-lived convergence, changes in the angle of subduction, continental crust collision post-convergence and the subduction of young, warm oceanic crust or a heat source. The various possibilities for the origin of this temperature increase are discussed and evaluated below.

According to Peacock (2003) and Ernst (2010), long-lived convergence of > ~ 30 to 40 Ma years enhances the seaward growth of an accretionary prism and by doing so promotes the effective horizontal, landward movement of underplated, accreted material further from the low heat flow domains of the cold under-riding slab and closer to the high heat flow domains of the magmatic arc overlying the mantle wedge, which in turn results in a pronounced increase in temperature and geothermal gradient over time. Examples of this come from the Otago Schist Belt in New Zealand and from the Tablelands Complex of the southern New England Belt, where the respective increases in temperature of nearly ~ 200 °C over a pressure increase of ~ 3 kbar and in excess of ~ 100 °C over a pressure decrease of less than ~ 3 kbar, have been ascribed to long-lived convergence (Fagereng & Cooper, 2010; Phillips *et al.*, 2008). Importantly, the thermobarometric changes derived from the heating of accreted material as a result of changes in proximity to high heat flow domains and distance away from low heat flow domains only become noticeable after extended periods of time of > 30 to 40 Ma – i.e. the increase in temperature occurs very slowly over time (Peacock, 2003; Ernst, 2010). Furthermore, the continuation of underplating during long-lived convergence dictates the continued deformation of the accreted material (Peacock, 2003; Ernst, 2010). For example, in the Tablelands Complex of the southern New England Belt, the above thermobarometric changes are constrained by the progressive deformation of the accreted material over time, whereby a HP-LT assemblage defining an early foliation is successively overprinted by and partially

consumed by two later foliations each defined by assemblages produced at successively higher temperature conditions (Phillips *et al.*, 2008).

In the Southern Zone of the Damara Belt, the convergence of the Congo and Kalahari lasted from ~ 580 Ma to ~ 542 Ma, a period of ~ 38 Ma years (Miller, 2008). While this could be regarded as long-lived convergence, its borderline value (close to ~ 30 to 40 Ma years) creates doubt as to the likelihood of long-lived convergence being one of the geodynamic factors responsible for the inferred increase in temperature. More importantly, however, the apparent lack of deformation and rotation of the porphyroblasts that overprint the penetrative foliation in the metapelites and the fact that the pressure range at which fabric formation (*M1a*) occured overlaps with the pressures at which the inferred peak mineral assemblages (*M1b*) are stable implies that the increase in temperature occured in a static environment, without concomitant deformation and changes in differential strain and was most probably due to a fairly rapid heat pulse. These observations do not fit with those that have been ascribed to heating due to long-lived convergence. It is therefore considered to be highly unlikely that long-lived convergence played a defining role in the metamorphic evolution of the Southern Zone, and does not appear to have been a geodynamic factor responsible for the inferred increase in temperature.

In similarity to long-lived convergence, a change in the angle of subduction to < 25° to 30° both enhances the horizontal, landward movement of accreted material away from low heat flow domains and towards high heat flow domains over time, and allows for a larger slip zone and therefore greater shear heating along the slip zone (Oxburgh & Turcotte, 1971; Peacock, 2003; Willner, 2005; Ernst, 2010). This causes a pronounced increase in temperature and geothermal gradient over time (Peacock, 2003, Ernst, 2010). An example comes from the Western Belt of the Coastal Cordillera in Chile, where an increase in temperature of ~ 80 °C over a pressure increase of ~ 1.5 kbar is observed in the greenschist facies metabasites (Willner, 2005). This gradual increase in temperature caused by the movement of accreted material towards the Eastern Belt (high heat flow magmatic arc of the Coastal Cordillera) resulted in the early, dominant foliation defined by a HP-LT mineral assemblage being overprinted by a later crenulation cleavage defined by a higher temperature assemblage; both of which were in turn overprinted by anhedral, rotated albite and garnet porphyroblasts (Willner, 2005). Importantly, the angle at which the under-riding slab is subducted beneath the over-riding slab is unlikely to change rapidly with time, hence resulting in fairly constant P-T conditions over a short period of time (Ernst, 1988, 2010; Peacock, 2003; Willner, 2005).

The lack of literature on the angle at which the Khomas Sea (under-riding oceanic crust) was subducted beneath the Congo craton (over-riding continental crust) prevents the accurate assessment of potential changes in the angle of subduction as a geodynamic factor responsible for the inferred increase in

temperature. Nonetheless, given that the angle of subduction remains fairly constant over a short period of time, it is considered to be highly unlikely that a change in the angle of subduction over < ~ 38 Ma years could have facilitated the increase in temperature responsible for the change from the lower temperature, fabric-forming mineral assemblages (*M1a*) to the higher temperature, peak mineral assemblages (*M1b*). Moreover, the higher temperature, peak mineral assemblages in the metapelitic rocks (*M1b)* from the Gaub and Kuiseb Canyons are not foliated like those in the greenschist facies metabasites in the Western Belt of the Coastal Cordillera in Chile. In other words, the gradual increase in temperature acheivable through changes in the angle of subduction does not fit the rapid heat pulse suggested by the aforementioned fabric relations and pressure constraints in the rocks of the Southern Zone.

As shown in *Chapter 2*, the onset of continental crust collision post-convergence and subsequent exhumation of subducted material is most likely to result in the formation of a relatively higher temperature mineral assemblage through major decompression at constant or only slightly increasing/decreasing temperatures over time (Ernst, 1988, 2010; Maruyama *et al.* 2010). This causes an increase in the recorded geothermal gradient (Ernst, 1988, 2010; Maruyama *et al.* 2010). For example, in the Diahot Terrane in New Caledonia, the pressure decrease of ~ 12 kbar over a temperature increase of ~ 25 °C has been attributed to the collision of continental crust with an intraoceanic island arc system and the resulting rapid exhumation of accreted material (Potel *et al.*, 2006). Similarly, in the Dora-Maira, Monte Rosa and Gran Paradiso massifs in the Alps, collision and rapid exhumation are thought to have been responsible for the ~ 35 °C increase in temperature during decompression of greater than ~ 14 kbar (Gasco *et al.*, 2013). In the latter, these thermobarometric changes are marked by an early, subduction-related foliation defined by a higher pressure assemblage being overprinted by a later, collision- and exhumation-related foliation defined by a higher temperature assemblage in metapelitic rocks (Gasco *et al.*, 2013). These textural relations have also been described in rocks from the Volparone Breccia, a subduction-to-collision HP-LT terrane in Corsica (Malasoma & Marroni, 2007).

Once again, the aformentioned fabric relations and pressure constraints in the rocks of the Southern Zone, indicate that the increase in temperature occurred in a static environment, without concomitant deformation and changes in differential stress. In other words, the fact that the overprinting, higher temperature porphyroblasts do not illustrate features pertaining to growth during decompression, such as their alignment into a second foliation that overprints the early, lower temperature, fabric-forming mineral assemblage, rules out any geodynamic factors that involve exhumation and heating during later continental crust collision.

The subduction of warm oceanic crust, younger than ~ 10 to 25 Ma, results in a gradual increase in temperature with a relatively insignificant change in pressure over time – i.e. a near-isobaric increase in temperature and geothermal gradient (Iwamori, 2000; Peacock, 2003). Moreover, Iwamori (2000) showed by thermal modelling that the subduction of a heat source, namely very young and very hot oceanic crust or a spreading ridge (~ 0 Ma years in age), results in a rapid increase in temperature that is comparatively faster than that achievable during the subduction of young, warm oceanic crust and with little or no change in differential strain. For example, in the Sierra del Convento, La Corea and Rio San Juan mélanges in Cuba, the subduction of very young, very hot oceanic crust in close proximity to a spreading ridge resulted in the accreted material being subjected to an increase in temperature of in excess of ~ 150 °C over an increase in pressure of less than ~ 3 to 4 kbar (Garcia-Casco *et al.*, 2008; Blanco-Quintero *et al.*, 2010; Escuder-Viruete & Perez-Estaun, 2013). In the former two mélanges, the above thermobarometric changes are constrained by the overprinting of an early foliation, defined by primarily the alignment of amphiboles, by large, weakly rotated, syn- to post-kinematic garnets in metamafic rocks (Garcia-Casco *et al.*, 2008; Blanco-Quintero *et al.*, 2010). Similarly, in the Shoalwater and Wandilla terranes in the northern New England Belt in Australia, the subduction of a spreading ridge resulted in the accreted material experiencing a temperature increase of in excess of ~ 150 °C over a decrease in pressure of less than ~ 3 kbar (Leitch *et al.*, 1993). This heating under relatively static, near-isobaric conditions is resolved, to a certain extent, by the overprinting of the well-developed, dominant micaceous fabric in some of the higher grade metapelitic rocks by unrotated biotite porphyroblasts (Leitch *et al.*, 1993).

Given that the Khomas Sea was relatively small compared to modern day oceans (Miller, 1983; Kukla & Stanistreet, 1991; Kukla, 1992; Miller, 2008), the oceanic crust would have been young and warm. The subduction of this oceanic crust, as opposed to older, colder oceanic crust may help to explain why the recorded geothermal gradients are slightly warmer than those recorded in other known HP-LT metamorphic terranes. However, the comparitively gradual increase in temperature resulting from the subduction of young, warm oceanic crust – as described by Iwamori (2000) – does not account for the rapid heat pulse suggested by the fabric relations and pressure constraints in the rocks of the Southern Zone.

Consequently, it is speculated that the near-isobaric increase in temperature is most likely to have been due to the subduction of a heat source, possibly the spreading ridge that had once formed the Khomas Sea. This is supported by several findings: Firstly, by the refutation of long-lived convergence, a change in the angle of subduction and continental crust collision as alternative geodynamic factors potentially responsible for the increase in temperature; secondly, by the similarity of the P-T paths of the Gaub and Kuiseb Canyons to those of other known HP-LT metamorphic terranes in which notable increases in temperature have been ascribed to the subduction of very young, very hot oceanic crust and/or a

spreading ridge – i.e. a prominent heat source (*Figure 39* below); thirdly, by the capacity of the subduction of a spreading ridge to explain the near-isobaric, rapid heat pulse suggested by the fabric relations in the rocks of the Southern Zone; and lastly, by the occurence of the Matchless Amphibolite Member, a laterally extensive mafic, volcanic igneous body of MORB composition that is interbedded within the accreted metapsammopelitic schists of the Southern Zone, which provides a feasible representation of this spreading ridge.

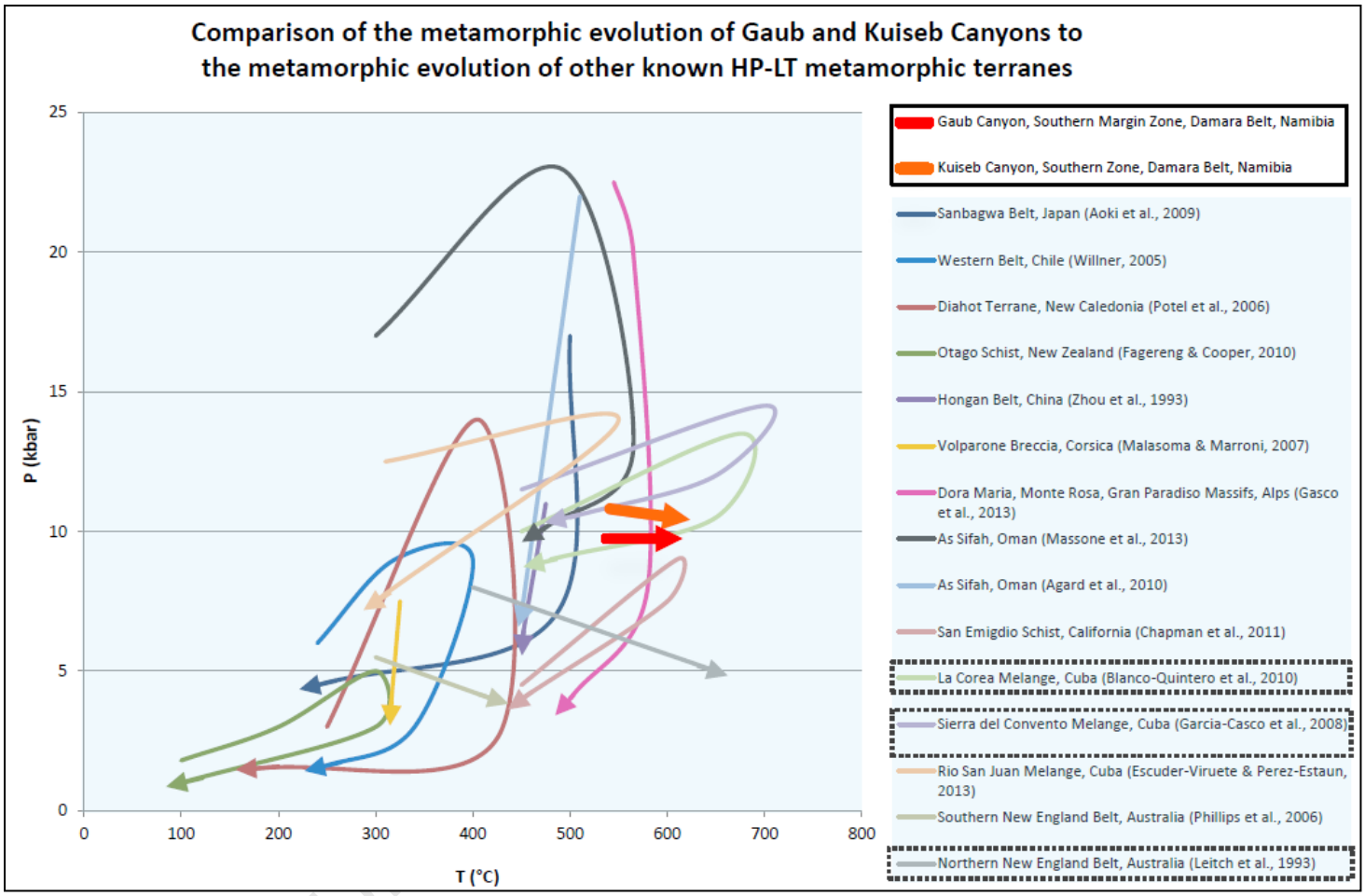

Figure 39: Comparison of the inferred metamorphic evolution (P-T paths) of the rocks from the Gaub and Kuiseb Canyons to the metamorphic evolution of other known HP-LT metamorphic terranes. The metamorphic evolution of the rocks from the Gaub and Kuiseb Canyons (*red* and *orange* coloured paths) most closely matches that of the La Corea and Sierra del Convento melanges in Cuba (*olive green* and *purple* coloured paths) and that of the northern New England Belt in Australia (*grey* coloured path), all of which involved the subduction of a heat source (very young, very hot oceanic crust and/or a spreading ridge).

Unlike in the rocks from the Sierra del Convento, La Corea and Rio San Juan mélanges in Cuba, which record a major increase in temperature with a minor concomitant increase in pressure of less than ~ 3 to 4 kbar (Garcia-Casco *et al.*, 2008; Blanco-Quintero *et al.*, 2010; Escuder-Viruete & Perez-Estaun, 2013), and in the rocks from the Shoalwater and Wandilla terranes in the northern New England Belt in

Australia, which record a major increase in temperature with a minor concomitant decrease in pressure of less than ~ 3 kbar (Leitch *et al.*, 1993), the inferred increase in temperature recorded by rocks from the Gaub and Kuiseb Canyons appear to have occurred with no concomitant change in pressure. One of the most probable reasons for the difference in pressure changes is the occurrence or absence of minor burial or minor exhumation of the rocks at the time of the subduction of the heat source that resulted in the temperature increase. Minor burial would facilitate a minor increase in pressure, whereas minor exhumation would cause a minor decrease in pressure. By contrast, stable tectonics, with neither minor, burial nor minor exhumation, would result in a relatively constant pressure during the subduction of the heat source.

In both the Sierra del Convento, La Corea and Rio San Juan mélanges in Cuba and the Shoalwater and Wandilla terranes in the northern New England Belt in Australia, the subduction of a heat source resulted in a ~ 150 °C increase in temperature (Garcia-Casco *et al.*, 2008; Blanco-Quintero *et al.*, 2010; Escuder-Viruete & Perez-Estaun, 2013; Leitch *et al.*, 1993). By contrast, in the rocks from the Gaub and Kuiseb Canyons, the inferred increase in temperature, presumably resulting from the subduction of a spreading ridge, is only ~ 60 °C. This discrepancy can possibly be attributed to the effective warmth of the subducting heat source, whereby certain spreading ridges may provide more heat to the overlying accretionary prism than others. Alternatively, the difference could be ascribed to the ability of the subducting heat source to only heat the rocks within the overlying accretionary prism to a certain temperature. Given this limitation, rocks that are closer to the temperature limit at the onset of the subduction of the heat source would record a smaller increase in temperature compared to those that are further from the temperature limit – i.e. warmer rocks may record less of an increase in temperature than cooler rocks. Moreover, the thickness of the accretionary prism and the location of the rocks within the prism at the time of the subduction of the heat source may affect the magnitude of the increase in temperature recorded by the rocks.

7.5. Implications for the Southern Zone: Record of the collisional event

The apparent lack of recognition of the collision between the Congo and Kalahari Cratons by the rocks of the Gaub and Kuiseb Canyons raises a considerable amount of suspicion as to where the petrographic and thermobarometric changes relating to the collisional event are in fact recorded. As noted in *Chapter 2*, the extent of deformation of accretionary prisms (HP-LT rocks) involved in collision orogens is highly dependent on the mechanism by which the rocks were exhumed prior to or during collision (Platt, 1993). Deformation relating to collision may be distributed across the entire prism (e.g. Beaumont *et al.*, 2001), along the boundaries of accreted material, specifically along thrust faults (e.g. Chemenda *et al.*, 1995),

around small blocks of low density material, such as serpentinites, in which the HP-LT rocks are incorporated (e.g. Guillet *et al.*, 2000), and at the front or rear of the accretionary prism where exhumation by divergence occurs (e.g. Malusa *et al.*, 2011).

The apparent lack of deformation relating to the collision and exhumation event in the rocks of the Gaub and Kuiseb Canyons rules out the possibility of deformation across the entire accretionary prism. Moreover, the lack of serpentinites and the spatial extent of the Southern Zone, or at least the Gaub and Kuiseb Canyons, rules out the incorporation and exhumation of the HP-LT rocks in low density serpentinites. Therefore, assuming that the boundaries of the subduction zone remained relatively stationary during convergence (i.e. no divergence by slab rollback and by migration of the upper plate away from the subduction zone), the most likely mechanism for the exhumation and resulting deformation of the rocks of the Southern Zone may be along discrete reactivated thrust faults, similar to those described by Chemenda *et al.* (2001) for certain areas of the Himalayas, Alps, New Caledonia and Oman and eastern Pamir orogenies.

It is speculated that the rocks of the Southern Zone were exhumed as discrete segments, with deformation relating to the collision of the Congo and Kalahari Cratons being concentrated along discrete zones around these segments. The location of the Gaub and Kuiseb Canyons away from these discrete deformation zones, or exhumation thrust faults, would have barred them from being deformed during collision and hence allowed for their preservation during exhumation. Importantly, the fact that the rocks from the Gaub and Kuiseb Canyons record closely comparable depths of burial even though there is a true tectonostratigraphic depth of ~ 10 km between them, implies that there must be at least one of these exhumation thrust faults between the Gaub and Kuiseb Canyons, along which the rocks from one of the canyons were exhumed to a similar structural level as rocks in the other. The Gomab River Line, which is comprised of mappable, large-scale thrusts along which the rocks of the Southern Zone have been upthrown, and the Frontal Thrust, along which the rocks of the Southern Margin Zone (and Southern Zone) have been upthrown (Kukla, 1992; Miller, 2008), may be representative of these exhumation thrust faults, with the former being ideally located between the Gaub and Kuiseb Canyons. However, the lack of investigation into the kinematics of the Gomab River Line and Frontal Thrust hinders the accurate assessment of this and is beyond the scope of this study.

An alternative explanation for the discrepancy between the recorded depths of burial and true tectonostratigraphic depths of the rocks from the Gaub and Kuiseb Canyons is that the rocks were inclined at the time of metamorphism. In this case, the pressure conditions recorded by the observed mineral assemblages in the rocks would be representative of the exact crustal level at which the rocks

were buried. However, given the suggestion by Kukla & Stanistreet (1991) that the Southern Zone is an accretionary prism and the description of the internal geometry of a prism as described by Moore & Byrne (1987), the existence of a fault, or several faults, seems very likely. It is for this reason that the discrepancy between the recorded depths of burial and true tectonostratigraphic depths of the rocks from the Gaub and Kuiseb Canyons is considered to be most likely due to faulting and that the exhumation of the rocks of the Southern Zone therefore occurred as discrete segments with surrounding zones of deformation.

7.6. Recognition of spreading ridge subduction in other HP-LT terranes

While the subduction of a heat source, namely very young, hot oceanic crust and/or a spreading ridge, has been presented as a likely explanation for the metamorphic evolution of a few other HP-LT metamorphic terranes, such as the northern New England Belt in Australia (Leitch *et al.*, 1993) and the Sierra del Convento, La Corea and Rio San Juan melanges in Cuba (Garcia-Casco *et al.*, 2008; Blanco-Quintero *et al.*, 2010; Escuder-Viruete & Perez-Estaun, 2013), it is proposed that the increase in temperature resulting from the subduction of a spreading ridge is more prevalent in HP-LT terranes than is presently documented.

The subduction of a spreading ridge is most likely in those HP-LT terranes where convergence was followed by collision. This is mainly due to the fact that the entire intervening (oceanic-) slab, including the spreading ridge, has to be completely consumed in order for collision to take place. Unfortunately, in many orogenic belts, the extensive overprinting of the HP-LT rocks during collision, or an equivalent change in tectonics, makes it difficult to recognise the prograde increase in temperature caused by the subduction of a spreading ridge.

One such candidate for a HP-LT terrane were the change in metamorphic evolution has been described, but not recognised as having been due to the subduction of a spreading ridge, is the San Emigdio Schist in the Franciscan Complex in southern California, where subduction was followed by strike-slip tectonics (Ernst, 1981; Wakabayashi, 1992). Chapman *et al.* (2011) noted that the metapsammitic rocks occurring at low structural levels in the San Emigdio Schist contain abundant, non-preferentially orientated, altered garnet and kyanite porphyroblasts, both of which overprint a prominent fabric that is defined by the alignment of muscovite, chlorite, biotite, plagioclase and quartz. The post-tectonic, higher temperature assemblage in these rocks, namely the overprinting porphyroblasts, has been attributed to the effective horizontal movement of underplated, accreted material beneath the then recently active southern Sierra Nevada and southern California magmatic batholiths, with the subsequent alteration of the porphyroblasts, specifically the extensive fracturing of the garnet porphyroblasts and the chloritization of the rims of the kyanite

porphyroblasts, having been ascribed to the rapid exhumation of the accreted material (Chapman *et al.*, 2011).

However, in accordance with the petrography and inferred metamorphic evolution of the rocks from the Gaub and Kuiseb Canyons, it is speculated that the growth of the overprinting porphyroblasts in the metapsammitic rocks may have been due to the subduction of a spreading ridge after the development of the fabric during initial convergence. The later alteration of the porphyroblasts may have been due to a change from subduction to strike-slip tectonics of the Franciscan Complex. This is supported by the metamorphic evolution (P-T) of the metapsammitic rocks from the San Emigdio Schist, which involves a similar increase in temperature to that recorded in the rocks from the La Corea and melanges in Cuba, from the Gaub and Kuiseb Canyons, and from the northern New England Belt in Australia, but with a slightly greater change in pressure – refer to *Figure 39* above.

8. Conclusion

The Southern Zone of the Damara Belt in central Namibia was first recognised as an accretionary prism by Kukla & Stanistreet (1991), who suggested that that the convergence and subsequent collision of the Congo and Kalahari Cratons at ~ 542 Ma resulted in the closing of the Khomas Sea, a small ocean that had formed during a period of spreading between ~ 750 and ~ 600 Ma, and the formation of an accretionary prism. The record of high pressure – low temperature metamorphic conditions and associated low geothermal gradients recorded by the rocks of the Southern Zone, the occurrence of intercalated slices of metapsammopelitic and metamafic rocks with distinct fabrics that formed by deformation to high strain, the location of the Southern Zone structurally adjacent to a HT-LP metamorphic terrane and an age of metamorphism that is inclusive of the early-Palaeozoic, all provide evidence for the evolution of the Southern Zone in an accretionary prism environment (Kukla & Stanistreet, 1991; Kukla, 1992; Miller, 2008). However, despite the recognition of the Southern Zone as an accretionary prism, the details as to how exactly the supposed convergent margin evolved and the geodynamic factor/s responsible for its metamorphic evolution remained largely undetermined.

Insight into the details of the geodynamic factors responsible for variations in the metamorphic evolution of an accretionary prism, as well as observation of the textural relations within the rocks from the Gaub and Kuiseb Canyons and the determination of the P-T conditions at which these rocks were metamorphosed, has facilitated an understanding of the metamorphic evolution of the rocks of the Southern Zone. This has helped to elucidate that the Southern Zone of the Damara Belt represents one of the oldest, largest and best preserved examples of an accretionary prism in the rock record. Moreover, it has allowed an understanding of the record of the collision between the Congo and Kalahari Cratons in the Southern Zone and has enabled deliberation as to the recognition of other HP-LT terranes whose metamorphic evolution is likely to have been governed by the same geodynamic factor as that operational in the Southern Zone.

Thermobarometric mineral stability constraints derived from modelled pseudosections indicate that the inferred peak mineral assemblages in the metapelites and metamafics (*M1b*) are stable at P-T conditions of ~ 9.8 kbar and ~ 600 °C in the Gaub Canyon, and ~ 10.5 kbar and ~ 605 °C in the Kuiseb Canyon. These P-T conditions equate to geothermal gradients of ~ 18.5 °C/km and ~ 17.3 °C/km, respectively. However, it is apparent that the early, syn-tectonic fabric-forming mineral assemblages in these rocks (*M1a*) may have formed at consistent pressures of ~ 8.4 to 11.8 kbar, but at lower temperatures of ~ 535 to 550 °C in the Gaub Canyon, and at similar pressures of ~ 10.5 to 10.8 kbar, but lower temperatures of ~ 540 to 545 °C in the Kuiseb Canyon. These P-T conditions equate to cooler geothermal gradients of ~ 16.6 °C/km and

~ 15.1 °C/km, respectively. The pressure recorded by the rocks from the Gaub Canyon (~ 9.8 kbar) corresponds to the burial of the accreted material to depths of ~ 30 km, whereas that recorded by the rocks of the Kusieb Canyon (~ 10.5 kbar) corresponds to depths of burial of ~ 33 km.

Evidently, the metamorphic evolution of the metapelitic and metamafic rocks from the Gaub and Kuiseb Canyons is most likely to have involved a near-isobaric increase in temperature of ~ 60 °C while the rocks were near peak pressure. The consistency between the pressure range at which fabric formation (*M1a*) occurred and the pressures at which the inferred peak mineral assemblages (*M1b*) are stable, as well as the notable lack of deformation and rotation of the porphyroblasts that overprint the penetrative foliation in the metapelites, indicates that the increase in temperature transpired in a static environment, without attendant deformation or changes in differential strain and was probably in response to a fairly rapid heat pulse.

In addition to the ability of the subduction of a heat source to adequately explain this near-isobaric, rapid heat pulse, the refutation of other geodynamic factors, such as long-lived convergence, a change in the angle of subduction and continental crust collision, that could possibly have been accountable for the increase in temperature, as well as the resemblance of the metamorphic evolution of the Gaub and Kuiseb Canyons to those of other known HP-LT metamorphic terranes in which the increases in temperature have been attributed to the subduction of a heat source, and the existence of the Matchless Amphibolite Member as a conceivable representation of a spreading ridge, all provide evidence to support speculation that the increase in temperature was most probably as a result of the subduction of a heat source, perhaps the spreading ridge that had once formed the Khomas Sea.

Interestingly, the lack of deformation and rotation of the overprinting porphyroblasts in the metapelites suggests that the collision between the Congo and Kalahari Cratons is not recorded by the rocks of Gaub and Kuiseb Canyons, which in turn indicates that the rocks of the Southern Zone were most likely exhumed as discrete portions, with the petrographic and thermobarometric changes pertaining to the collisional event occurring along discrete exhumation thrust faults around these portions.

Despite the metamorphic evolution of a few HP-LT terranes having been attributed to the subduction of a heat source, it is proposed that the change in the metamorphic evolution of HP-LT terranes resulting from the subduction of a spreading ridge is more widespread than is currently recognised. The subduction of a spreading ridge is most likely to have occurred in HP-LT terranes where convergence was followed by collision, as it is in these HP-LT terranes where the complete consumption of the intervening (oceanic-) slab, including the spreading ridge, would have had to have occurred in order to allow

for collision. However, the extensive deformation of the HP-LT rocks during collision or an equivalent change in tectonics, often hinders the recognition of the prograde increase in temperature attributable to the subduction of a spreading ridge.

Acknowledgements

I would like to express my sincere gratitude to the following people who have assisted me in the completion of this research:

Dr J.F.A. Diener, my supervisor, for his willingness to convey his unrivalled knowledge of metamorphic petrology and for his passion towards the subject. Furthermore, for his encouragement, guidance and seemingly tireless patience throughout the duration of this research, especially with the time required for me to gain an understanding of Thermocalc.

Dr A. Fagereng, my co-supervisor, for his input on the structural petrology part of this research and for constantly providing a different, non-metamorphic petrologist's view of the overall research. Moreover, for motivating me by often enquiring as to the progress of the research, especially during the write-up phase.

The National Research Fund (NRF), for providing financial assistance in the form of an NRF Innovation Master's Scholarship towards the completion of this research.

The Post-Graduate Funding Office (PGFO) at the University of Cape Town (UCT), for providing financial assistance in the form of a Master's Research Scholarship and a Harry Crossley Fellowship Scholarship towards the completion of this research. [*Phys. Address:* Post-Graduate Funding Office, Upper Level, Otto Beit Building, University Avenue, Upper Campus, University of Cape Town, Rondebosch, 7701, Cape Town].

Dr Cynthia Sanchez-Garrido and the other laboratory personnel at the Department of Soil Sciences at the University of Stellenbosch, for their assistance with fusion disc preparation and for conducting the X-ray Fluorescence analyses required for this research.

Ms Christel Tinguely at the Department of Geological Sciences at the University of Cape Town, for her unmatched expertise in the operation of the Electron Microprobe (EMP) and for her patience during the period over which EMP analyses required for this research were conducted.

Mr David Wilson at the Department of Geological Sciences at the University of Cape Town, for preparing the normal thin sections required for this research.

The organisers of the 6th Igneous and Metamorphic Study Group (IMSG) Conference, specifically Prof Chris Gauert, Prof Marian Tredoux and Dr Frederick Roelofse, for affording me the opportunity to present my research to other academics and thus gain valuable feedback.

My parents, Mr Alastair Cross and Mrs Belinda Cross, for their constant support, consideration and patience throughout the duration of this research and for taking an interest in the details of the research.

Ms Nikki Pearson, for her selfless understanding throughout the duration of the research, as well as for her patient temperament and unfaltering belief in my ability to complete this research.

References

Agard, P., Searle, M. P., Alsop, G. I. and Dubacq, B. 2010. Crustal stacking and expulsion tectonics during continental seduction: P-T deformation constraints from Oman, *Tectonics*, 29: 1 – 19.

Aoki, K., Kitajima, K., Masago, H., Nishizawa, M. Terabayashi, M., Omori, S., Yokoyama, T., Takahata, N., Sano, Y. and Maruyama, S. 2009. Metamorphic P-T-time history of the Sanbagwa belt in central Shikoku, Japan and implication for retrograde metamorphism during exhumation, *Lithos*, 113: 393 – 407.

Bates, R. L. and Jackson, J. A. 1984. *Dictionary of Geological Terms*, 3rd edn, Anchor Press, Random House Inc., New York, United States of America.

Beaumont, C., Jamieson, R. A., Nguyen, M. H. and Lee, B. 2001. Himalayan tectonics explained by extrusion of a low-viscosity crustal channel coupled to focused surface denudation, *Nature*, 414: 738 – 742.

Blanco-Quintero, I. F., Garcia-Casco, A., Rojas-Agramonte, Y., Rodriguez-Vega, A., Lazro, C. and Iturralde-Vinent, M. A. 2010. Metamorphic evolution of subducted hot oceanic crust (La Corea Melange, Cuba), *American Journal of Science*, 310: 889 – 915.

Brown, M. 2007. Metamorphic conditions in orogenic belts: A record of secular change, *International Geology Review*, 49 (3): 193 – 234.

Carlson, W. D., Denison, C. and Ketcham, R. A. 1995. Controls on the nucleation and growth of porphyroblasts: Kinematics from natural textures and numerical models, *Geological Journal*, 30 (3 – 4): 207 – 225.

Chapman, A. D., Luffi, P. I., Saleeby, J. B. and Petersen, S. 2011. Metamorphic evolution, partial melting and rapid exhumation above an ancient flat slab: insights from the San Emigdio Schist, southern California, *Journal of Metamorphic Geology*, 29: 601 – 626.

Chemenda, A. I., Mattauer, M., Malavieille, J. and Bokun, A. N. 1995. A mechanism for syn-collisional rock exhumation and associated faulting: Results from physical modelling, *Earth and Planetary Science Letters*, 132: 225 – 232.

Coggan, R. and Holland, T. J. B. 2002. Mixing properties of phengitic micas and revised garnet-phengite thermometers, *Journal of Metamorphic Petrology*, 20 (1): 683 – 696.

Deer, W.A., Howie, R.A. and Zussman, J. 1992. *An Introduction to the Rock Forming Minerals*, 2nd edn, Pearson Education Limited, Essex, England.

Diener, J. F. A., Powell, R., White, R. W. and Holland, T. J. B. 2007. A new thermodynamic model for clino- and orthoamphiboles in the system Na_2O-CaO-FeO-MgO-Al_2O_3-SiO_2-H_2O-O, *Journal of Metamorphic Geology*, 25 (6): 631 – 656.

Diener, J. F. A. and Powell, R. 2012. Revised activity-composition models for clinopyroxene and amphibole, *Journal of Metamorphic Geology*, 30 (2): 131 – 142.

Ernst, W. G. 1973. Blueschist Metamorphism and P-T Regimes in Active Subduction Zones, *Tectonophysics*, 17: 255 – 272.

Ernst, W. G. 1981. *The Geotectonic Development of California*, Rubey Colloquium Series, Vol. 1, Prentice Hall Inc., Upper Saddle River, New Jersey, United States of America.

Ernst, W. G. 1988. Tectonic history of subduction zones inferred from retrograde blueschist P-T paths, *Geology*, 16: 1081 – 1084.

Ernst, W. G., Maruyama, S. and Wallis, S. 1997. Buoyancy-driven, rapid exhumation of ultra high pressure metamorphosed continental crust, *Proceedings of the National Academy of Sciences*, 94: 9532 – 9537.

Ernst, W. G. 2010. Subduction zone metamorphism – pioneering contributions from the Alps, *International Geology Review*, 52 (10 – 12): 1021 – 1039.

Escuder-Viruete, J. and Perez-Estaun, A. 2013. Contrasting exhumation P-T paths followed by high-P rocks in the northern Caribbean subduction-accretionary complex: Insights from the structural geology, microtextures and equilibrium assemblage diagrams, *Lithos*, 160 – 161: 117 – 144.

Fagereng, A. and Cooper, A. F. 2010. The metamorphic history of rocks buried, accreted and exhumed in an accretionary prism: an example from the Otago Schist, New Zealand, *Journal of Metamorphic Geology*, 28: 935 – 954.

Garcia-Casco, A., Lazro, C., Rojas-Agramonte, Y., Kroner, A., Torres-Roldan, R. L., Nunez, K., Neubauer, F., Millan, G. and Blanco-Quintero, I. F. 2008. Partial melting and P-T Path of Subducted Oceanic Crust (Sierra del Convento Melange, Cuba), *Journal of Petrology*, 49 (1): 129 – 161.

Gasco, I., Gattiglio, M. and Borghi, A. 2013. Review of metamorphic and kinematic data from Internal Crystalline Massifs (Western Alps): PTt paths and exhumation history, *Journal of Geodynamics*, 63: 1 – 19.

Gebauer, D., Schertl, H. P., Brix, M. and Schreyer, W. 1997. 35 Ma old ultrahigh-pressure metamorphism and evidence for very rapid exhumation in the Dora Maira Massif, Western Alps, *Lithos*, 41: 5 – 24.

Ghent, E. D., Roddick, J. C. and Black, P. M. 1994. $^{40}Ar/^{39}Ar$ dating of white micas from the epidote to the omphacite zones, northern New Caledonia: tectonic implications, *Canadian Journal of Earth Sciences*, 31: 995 – 1001.

Google Earth, 5.0. 2012. The south-western regions of Namibia, 22° 29’ – 24° 00’ S, 14° 50’ – 17° 39’ E, elevation 300 – 2000 m, hybrid data layer, imagery dates: Sep 17 2009 – 23 Oct 2010, *Google Developers Inc.* [accessed: 25 March 2012].

Green, E., Holland, T., and Powell, R. 2007. An order-disorder model for omphacitic pyroxenes in the system jadeite-diopside-hedenbergite-acmite, with applications to eclogite rocks, *American Mineralogist*, 92 (7): 1181 – 1189.

Guillot, S., Hattori, K. H. and de Sigoyer, J. 2000. Mantle wedge serpentinization and exhumation of eclogites, insights from eastern Ladakh, northwest Himalaya, *Geology*, 28: 199 – 202.

Guiraud, M., Powell, R. and Rebay, G. 2001. H_2O in metamorphism and unexpected behaviour in the preservation of metamorphic mineral assemblages, *Journal of Metamorphic Petrology*, 19 (4): 445 – 454.

Holland, T. J. B. and Powell, R. 1998. An internally consistent thermodynamic data set for phases of petrological interest, *Journal of Metamorphic Geology*, 16 (3): 309 – 343.

Holland, T., Baker, J. and Powell, R. 1998. Mixing properties and activity-composition and relationships of chlorites in the system MgO-FeO-Al_2O_3-SiO_2-H_2O, *European Journal of Mineralogy*, 10 (3): 395 – 406.

Holland, T. and Powell, R. 2003. Activity-composition relations for phases in petrological calculations: an asymmetric multicomponent formulation, *Contributions to Mineralogy and Petrology*, 145 (4): 492 – 501.

Iwamori, H. 2000. Thermal effects of ridge subduction and its implications for the origin of granitic batholiths and paired metamorphic belts, *Earth and Planetary Science Letters*, 181: 131 – 144.

Kasch, K. W. 1981. The structural geology, metamorphic petrology and tectonothermal evolution of the southern Damara belt around Omitara, South West Africa/Namibia, *Bulletin of Precambrian Research Unit*, 27: 333 – 342.

Korsch, R. J., Adams, C. J., Black, L. P., Foster, D. A., Fraser, G. L., Murray, C. G., Foudoulis, C. and Griffin, W. L. 2008. Geochronology and provenance of the Mid- to Late- Palaeozoic accretionary wedge and Gympie Terrane, New England Orogen, eastern Australia, *Australian Journal of Earth Sciences*, 28: 33 – 42.

Kukla, P. A. and Stanistreet, I. G. 1991. Record of the Damaran Khomas Hochland accretionary prism in central Namibia: Refutation of an "ensialic" origin of a Late Proterozoic orogenic belt, *Geology*, 19: 473 – 476.

Kukla, P. A. 1992. *Tectonics and Sedimentation of a Late Proterozoic Damaran Convergent Continental Margin, Khomas Hochland, Central Namibia*, Memoir 12, Geological Survey, Ministry of Mines and Energy, Windhoek, Namibia.

Leitch, E. C., Morand, V. J., Fergusson, C. L., Henderson, R. A. and Carr, P. F. 1993. Accretion and post-accretion metamorphism in subduction complex terranes of the New England Fold Belt, eastern Australia, *Journal of Metamorphic Geology*, 11: 309 – 318.

Mackenzie, W.S. and Guilford, C. 1980. *Atlas of rock-forming minerals in thin-section*, Pearson Education Limited, Essex, England.

Malasoma, A. and Marroni, M. 2007. HP/LT metamorphism in the Volparone Breccia (Northern Corsica, France): evidence for involvement of the Europe/Corsica continental margin in the Alpine subduction zone, *Journal of Metamorphic Geology*, 25: 529 – 545.

Malusa, M. G., Faccenna, C., Garzanti, E. and Polino, R. 2011. Divergence in subduction zones and exhumation of high pressure rocks (Eocene Western Alps), *Earth and Planetary Science Letters*, 310: 21 – 32.

Marmo, B. A., Clarke, G. L. and Powell, R. 2002. Fractionation of bulk rock composition due to porphyroblast growth: effects on eclogite facies mineral equilibria, Pam Peninsula, New Caledonia, *Journal of Metamorphic Geology*, 20 (1): 151 – 165.

Marshak, S. 2005. *Earth: Portrait of a Planet*, 2nd edn, W.W. Norton & Company Inc., New York, United States of America.

Maruyama, S., Masago, H., Katayama, I., Iwase, Y., Toriumi, M., Omori, S. and Aoki, K. 2010. A new perspective on metamorphism and metamorphic belts, *Gondwana Research*, 18: 106 – 137.

Massone, H-J., Opitz, J., Theye, T. and Nasir, S. 2013. Evolution of a very deeply subducted metasediment from As Sifah, northeastern coast of Oman, *Lithos*, 156 – 159: 171 – 185.

Miller, R.G. 1983. *Evolution of the Damara Orogen of South West Africa/Namibia*, Special Publication No. 11, The Geological Society of South Africa, Johannesburg, South Africa.

Miller, R.G. 2008. *The Geology of Namibia*, Vol. 2: Neoproterozoic to Lower Palaeozoic, Geological Survey, Ministry of Mines and Energy, Windhoek, Namibia.

Miyashiro, A. 1961. Evolution of Metamorphic Belts, *Journal of Petrology*, 2: 277 – 311.

Moore, J. C. and Byrne, T. 1987. Thickening of fault zones: A mechanism of melange formation in accreting sediments, *Geology*, 15 (11): 1040 – 1043.

Nishimura, Y., Coombs, D. S., Landis, C. A. and Itaya, T. 2000. Continuous metamorphic gradient documented by graphitization and K-Ar age, southeast Otago, New Zealand, *American Mineralogist*, 85: 1625 – 1636.

Oxburgh, E. R. and Turcotte, D. L. 1971. Origin of Paired Metamorphic Belts and Crustal Dilation in Island Arc Regions, *Journal of Geophysical Research*, 76 (5): 1315 – 1327.

Peacock, S. M. 2003. Thermal Structure and Metamorphic Evolution of Subducting Slabs, *American Geophysical Union Monograph*, 28 (3): 1 – 16.

Phillips, G., Hand, M. and Offler, R. 2008. P-T-t deformation framework of an accretionary prism, southern New England Orogen, eastern Australia: Implications for blueschist exhumation and metamorphic switching, *Tectonics*, 27: 1 – 15.

Platt, J. P. 1993. Exhumation of high-pressure rocks: a review of concepts and processes, *Terra Nova*, 5: 119 – 133.

Potel, S., Ferreiro Mahlmann, R. Stern, W. B., Mullis, J. and Frey, M. 2006. Very Low-grade Metamorphic Evolution under High-pressure/Low-temperature Conditions, NW New Caledonia (SW Pacific), *Journal of Petrology*, 47 (5): 991 – 1015.

Powell, R. and Holland, T. J. B. 2008. On Thermobarometry, *Journal of Metamorphic Geology*, 26 (2): 155 – 179.

Ring, U., Brandon, M. T., Willet, S. D. and Lister, G. S. 1999. Exhumation processes, *Geological Society of London Special Publications*, 154: 1 – 27.

Sawyer, E. W. 1981. Damaran structural and metamorphic geology of an area south-east of Walvis Bay, South West Africa/Namibia, *Memoir of Geology Survey of South West Africa*, 7: 83 – 91.

Tinkham, D.K. and Ghent, E. D. 2005. Estimating P-T conditions of garnet growth with isochemical phase diagram sections and the problem of effective bulk-composition, *The Canadian Mineralogist*, 43 (1): 35 – 50.

Wakabayashi, J. 1992. Nappes, Tectonics of Oblique Plate Convergence, and Metamorphic Evolution Related to 140 Million Years of Continuous Subduction, Franciscan Complex, California, *Journal of Geology*, 100 (1): 19 – 40.

White, R. W., Powell, R., Holland, T. J. B. and Worley, B. A. 2000. The effect of TiO2 and Fe2O3 on metapelitic assemblages at greenschist and amphibolite facies conditions: mineral equilibria calculations in the system K_2O-FeO-MgO-Al_2O_3-SiO_2-H_2O-TiO_2-Fe_2O_3, *Journal of Metamorphic Petrology*, 18 (5): 497 – 511.

White, R. W., Powell, R. and Clarke, G. L. 2002. The interpretation of reaction textures in Fe-rich metapelitic granulites of the Musgrave Block, central Australia: constraints from mineral equilibria calculations in the system K_2O-FeO-MgO-Al_2O_3-SiO_2-H_2O-TiO_2-Fe_2O_3, *Journal of Metamorphic Geology*, 20 (1): 41 – 55.

White, R. W., Powell, R. and Holland, T. J. B. 2007. Progress relating to calculation of partial melt equilibria for metapelites, *Journal of Metamorphic Petrology*, 25 (5): 511 – 527.

Willis, J.P. 1999. *Instrumental parameters and data quality for routine major and trace element determinations by WD XFDS*, Department of Geological Sciences, University of Cape Town.

Willner, A. P. 2005. Pressure-Temperature Evolution of a Late Palaeozoic Paired Metamorphic Belt in North-Central Chile (34°-35°30'S), *Journal of Petrology*, 46 (9): 1805 – 1833.

Willner, A. P., Thomson, S. N., Kroner, A., Wartho, J. A. Wijbrans, J. R. and Herve, F. 2005. Time markers for the evolution and exhumation history of a Late Palaeozoic paired metamorphic belt in north-central Chile (34° - 35°30'S), *Journal of Petrology*, 46: 1835 – 1858.

Zhou, G., Liu, Y. J., Eide, E. A., Liou, J. G. and Ernst, W. G. 1993. High-pressure/low-temperature metamorphism in northern Hubei Province, central China, *Journal of Metamorphic Geology*, 11: 561 – 574.

Appendix A

Bulk Rock Geochemistry Data obtained by XRF Analyses

Major element analysis by XRF, Rh Tube, 2.4kW

Specimen:	GB4	GB5	GB8	GB10	GB13	MA29	MA31	MA32NV	MA32V	MA35	MA37	MA38	MA39	MA40	MA43	MA44
Rock Type:	Metamafic	Metamafic	Metapelite	Metapelite	Metapelite	Metapelite	Metapelite	Metamafic	Metamafic	Metapelite	Calc-silicate	Metapelite	Metapelite	Metapelite	Metamafic	Metamafic
Oxide conc. (wt%)																
SiO2	48.03	44.89	56.01	78.85	60.61	44.30	44.60	43.89	48.92	40.29	57.42	56.11	55.04	44.50	43.35	46.26
TiO2	2.21	1.33	1.04	0.50	0.85	1.24	1.21	1.04	1.36	1.40	0.76	1.13	1.03	1.34	1.51	1.65
Al2O3	14.30	9.39	18.83	8.18	16.72	24.98	26.74	12.86	14.25	23.87	15.70	20.51	20.48	25.38	12.60	15.97
Fe2O3	12.60	11.56	10.60	5.02	8.90	11.15	12.29	9.89	11.28	13.21	5.83	9.84	9.31	10.11	11.38	12.16
MnO	0.18	0.18	0.09	0.04	0.16	0.19	0.17	0.15	0.18	0.19	0.45	0.12	0.13	0.15	0.19	0.17
MgO	7.08	17.41	3.81	2.15	3.71	5.22	5.94	7.21	8.55	6.74	2.73	4.76	4.74	4.96	6.68	5.90
CaO	9.97	10.03	1.52	0.80	1.11	1.42	0.72	11.31	10.94	1.49	9.75	0.84	0.85	1.66	9.85	15.31
Na2O	1.36	0.30	0.54	0.02	0.34	1.46	0.35	1.78	2.07	1.52	0.77	0.52	0.92	1.91	2.17	0.72
K2O	0.81	0.07	3.51	1.62	3.73	6.20	4.40	0.09	0.06	7.22	1.51	2.88	4.19	5.63	0.28	0.04
P2O5	0.21	0.13	0.13	0.08	0.16	0.26	0.20	0.04	0.07	0.25	0.35	0.25	0.19	0.06	0.14	0.15
Cr2O3	0.05	0.22	0.03	0.01	0.02	0.02	0.03	0.06	0.08	0.02	0.01	0.02	0.02	0.03	0.04	0.06
H2O	0.00	0.00	0.06	0.05	0.12	0.04	0.08	0.08	0.06	0.14	0.08	0.20	0.14	0.14	0.16	0.36
LOI	1.63	3.78	3.83	1.46	2.54	2.80	2.74	12.06	1.36	2.92	3.90	1.70	2.26	3.04	11.87	1.55
Total	98.43	99.29	100.00	98.78	98.96	99.28	99.47	100.46	99.18	99.26	99.26	98.87	99.30	98.91	100.22	100.29

Note: H2O = H2O loss or gain at 110 °C LOI = Weight loss or gain at 950 °C

Appendix B

Mineral Chemistry Data obtained by EMP Analyses

Amphiboles

Analysis Label (Specimen_mineral_grain/zone:spot number)	gb4_amph_1b	gb4_amph_1a	gb4_amph_2b	gb4_amph_2a	gb4_amph_3b	gb4_amph_3a	gb4_amph_4a	gb4_amph_5b	gb4_amph_5a	gb4_amph_6b	gb4_amph_6a	gb4_amph_7b	gb4_amph_7a	gb4_amph_8a	gb4_amph_10a	ma44_amph_1a	ma44_amph_1c	ma44_amph_1b	ma44_amph_1e	ma44_amph_1d	ma44_amph_2c	ma44_amph_2b
Mineral Probed:	hb	hb	hb	hb	hb	hb	hb	hb	hb	hb	hb	hb	hb	hb	hb	hb	hb	hb	hb	hb	hb	hb
Core/Int/Rim:	Rim	Core	Rim	Core	Rim	Core	Core	Rim	Core	Rim	Core	Rim	Core	Core	Core	Core	Rim	Core	Rim	Core	Rim	Int
EMP Initial Results:																						
Oxide conc. (wt%)																						
SiO2	44.39	43.32	42.48	42.44	42.26	47.65	46.92	42.47	44.94	42.36	43.67	42.76	42.63	42.72	41.14	42.86	43.67	44.13	43.08	43.36	43.01	44.00
TiO2	0.38	0.41	0.48	0.44	0.46	0.26	0.28	0.50	0.37	0.73	0.44	0.46	0.48	0.45	0.46	0.43	0.41	0.34	0.39	0.43	0.36	0.38
Al2O3	11.81	13.88	14.69	15.80	14.85	9.51	10.15	14.14	11.22	14.25	13.19	14.70	15.22	14.37	14.74	12.79	12.90	12.34	13.32	13.20	13.17	12.48
Cr2O3	0.02	0.02	0.05	0.07	0.00	0.04	0.10	0.02	0.04	0.02	0.05	0.03	0.07	0.06	0.01	0.07	0.08	0.04	0.05	0.07	0.07	0.07
FeO	15.35	15.83	16.45	16.75	16.25	14.13	14.24	16.92	14.98	17.11	16.12	16.16	16.43	16.72	16.14	15.72	15.36	15.25	15.47	15.45	15.67	15.31
MnO	0.21	0.28	0.32	0.32	0.31	0.37	0.36	0.24	0.32	0.27	0.36	0.32	0.29	0.29	0.33	0.24	0.25	0.31	0.32	0.28	0.27	0.29
MgO	11.69	10.87	10.15	9.66	9.99	13.12	12.66	9.96	12.07	9.92	10.67	10.08	9.93	9.75	9.86	10.51	10.44	10.76	10.36	10.30	10.06	10.75
CaO	11.46	11.15	11.29	10.85	11.26	11.17	11.09	11.42	11.50	11.41	11.44	11.20	11.47	11.38	10.98	11.60	11.63	11.74	11.68	11.77	11.71	11.80
Na2O	1.48	1.68	1.70	2.02	1.78	1.28	1.26	1.61	1.42	1.69	1.59	1.80	1.66	1.71	1.76	1.35	1.33	1.24	1.33	1.27	1.33	1.29
K2O	0.29	0.37	0.48	0.37	0.40	0.22	0.28	0.44	0.25	0.47	0.33	0.46	0.47	0.44	0.40	0.10	0.13	0.09	0.10	0.15	0.10	0.10
Total	97.09	97.82	98.08	98.72	97.56	97.76	97.34	97.71	97.10	98.23	97.86	97.97	98.65	97.90	95.81	95.67	96.21	96.24	96.10	96.27	95.75	96.47
Cations:																						
Si	6.60	6.41	6.31	6.25	6.30	6.95	6.89	6.34	6.67	6.30	6.48	6.34	6.29	6.36	6.26	6.49	6.55	6.61	6.48	6.51	6.50	6.58
Ti	0.04	0.05	0.05	0.05	0.05	0.03	0.03	0.06	0.04	0.08	0.05	0.05	0.05	0.05	0.05	0.05	0.05	0.04	0.04	0.05	0.04	0.04
Al	2.07	2.42	2.57	2.74	2.61	1.64	1.76	2.49	1.96	2.50	2.31	2.57	2.65	2.52	2.64	2.28	2.28	2.18	2.36	2.34	2.35	2.20
Cr	0.00	0.00	0.01	0.01	0.00	0.00	0.01	0.00	0.00	0.00	0.01	0.00	0.01	0.01	0.00	0.01	0.01	0.00	0.01	0.01	0.01	0.01
Fe	1.91	1.96	2.04	2.06	2.03	1.72	1.75	2.11	1.86	2.13	2.00	2.00	2.03	2.08	2.05	1.99	1.93	1.91	1.95	1.94	1.98	1.92
Mn	0.03	0.04	0.04	0.04	0.04	0.05	0.04	0.03	0.04	0.03	0.05	0.04	0.04	0.04	0.04	0.03	0.03	0.04	0.04	0.04	0.03	0.04
Mg	2.59	2.40	2.25	2.12	2.22	2.85	2.77	2.22	2.67	2.20	2.36	2.23	2.18	2.16	2.24	2.37	2.33	2.40	2.32	2.30	2.27	2.40
Ca	1.83	1.77	1.80	1.71	1.80	1.75	1.74	1.83	1.83	1.82	1.82	1.78	1.81	1.82	1.79	1.88	1.87	1.88	1.88	1.89	1.90	1.89
Na	0.43	0.48	0.49	0.58	0.51	0.36	0.36	0.47	0.41	0.49	0.46	0.52	0.47	0.49	0.52	0.40	0.39	0.36	0.39	0.37	0.39	0.37
K	0.06	0.07	0.09	0.07	0.08	0.04	0.05	0.08	0.05	0.09	0.06	0.09	0.09	0.08	0.08	0.02	0.03	0.02	0.02	0.03	0.02	0.02
Total (All)	15.56	15.60	15.64	15.64	15.64	15.40	15.40	15.63	15.53	15.65	15.58	15.62	15.61	15.61	15.67	15.52	15.46	15.45	15.49	15.47	15.49	15.47
Total (Majors ONLY)	15.56	15.60	15.64	15.64	15.64	15.39	15.39	15.63	15.53	15.65	15.57	15.62	15.61	15.61	15.67	15.51	15.45	15.44	15.49	15.46	15.48	15.46
Al(VI) (= Si + Al - 8)	0.67	0.84	0.88	1.00	0.91	0.59	0.64	0.83	0.63	0.80	0.78	0.91	0.93	0.88	0.90	0.77	0.83	0.79	0.84	0.84	0.85	0.78
Al(IV) (= Al - Al(VI))	1.40	1.59	1.69	1.75	1.70	1.05	1.11	1.66	1.33	1.70	1.52	1.66	1.71	1.64	1.74	1.51	1.45	1.39	1.52	1.49	1.50	1.42

Note: Analyses conducted on the same mineral grain (e.g. 1 core analysis and 2 rim analyses on a specific amphibole grain) are highlighted in the same colour and enclosed in the same thick black box.

Amphiboles cont.

Analysis Label (Specimen_mineral_grain/zone:spot number)	ma44_amph_2a	ma44_amph_2d	ma44_amph_2e	ma44_amph_2h	ma44_amph_2g	ma44_amph_4d	ma44_amph_4c	ma44_amph_4f	ma44_amph_4e	ma44_amph_6c	ma44_amph_6a	ma44_amph_6b	ma44_amph_6d	ma44_amph_7c	ma44_amph_7a	ma44_amph_7b	ma44_amph_7d
Mineral Probed:	act	act	hb	hb	hb	hb	hb	hb	hb	hb	act	act	hb	hb	act	act	hb
Core/Int/Rim:	Core	Core	Rim	Rim	Core	Rim	Core	Rim	Core	Rim	Core	Core	Rim	Rim	Core	Core	Rim
EMP Initial Results:																	
Oxide conc. (wt%)																	
SiO2	52.45	52.25	43.09	43.20	42.88	42.25	42.03	42.37	42.31	44.33	51.45	51.42	43.40	44.56	50.06	51.40	43.39
TiO2	0.06	0.09	0.44	0.47	0.42	0.45	0.46	0.53	0.40	0.38	0.13	0.07	0.37	0.36	0.16	0.15	0.39
Al2O3	2.55	2.76	13.20	12.53	13.29	13.03	13.95	13.69	13.33	11.25	4.23	3.69	12.85	12.14	5.39	4.27	13.34
Cr2O3	0.04	0.09	0.11	0.04	0.04	0.02	0.05	0.10	0.06	0.06	0.02	0.01	0.07	0.03	0.03	0.06	0.07
FeO	11.58	11.38	16.03	15.64	16.07	15.61	16.22	16.11	15.96	15.12	11.76	11.62	15.38	15.47	12.60	12.06	15.86
MnO	0.30	0.27	0.27	0.28	0.29	0.34	0.31	0.25	0.29	0.25	0.27	0.26	0.23	0.29	0.34	0.30	0.31
MgO	16.27	16.03	10.11	10.65	10.20	10.59	9.88	9.83	10.41	11.46	15.59	16.04	10.57	11.20	15.15	15.74	10.72
CaO	12.19	12.17	11.69	11.68	11.51	11.69	11.43	11.57	11.58	11.89	12.19	12.18	11.62	11.78	12.15	12.19	11.61
Na2O	0.24	0.26	1.36	1.33	1.41	1.34	1.50	1.44	1.38	1.20	0.39	0.38	1.24	1.28	0.54	0.42	1.34
K2O	0.03	0.04	0.09	0.10	0.07	0.11	0.09	0.12	0.09	0.08	0.04	0.03	0.10	0.09	0.05	0.03	0.09
Total	95.71	95.34	96.39	95.92	96.18	95.42	95.92	96.01	95.81	96.02	96.07	95.70	95.84	97.19	96.48	96.62	97.12
Cations:																	
Si	7.68	7.68	6.48	6.52	6.46	6.42	6.37	6.41	6.41	6.66	7.52	7.54	6.54	6.61	7.34	7.49	6.47
Ti	0.01	0.01	0.05	0.05	0.05	0.05	0.05	0.06	0.05	0.04	0.01	0.01	0.04	0.04	0.02	0.02	0.04
Al	0.44	0.48	2.34	2.23	2.36	2.34	2.49	2.44	2.38	1.99	0.73	0.64	2.28	2.12	0.93	0.73	2.34
Cr	0.01	0.01	0.01	0.01	0.00	0.00	0.01	0.01	0.01	0.01	0.00	0.00	0.01	0.00	0.00	0.01	0.01
Fe	1.42	1.40	2.02	1.97	2.03	1.99	2.06	2.04	2.02	1.90	1.44	1.43	1.94	1.92	1.54	1.47	1.98
Mn	0.04	0.03	0.03	0.04	0.04	0.04	0.04	0.03	0.04	0.03	0.03	0.03	0.03	0.04	0.04	0.04	0.04
Mg	3.55	3.51	2.27	2.40	2.29	2.40	2.23	2.22	2.35	2.57	3.40	3.51	2.37	2.48	3.31	3.42	2.38
Ca	1.91	1.92	1.88	1.89	1.86	1.90	1.86	1.88	1.88	1.91	1.91	1.91	1.88	1.87	1.91	1.90	1.85
Na	0.07	0.07	0.40	0.39	0.41	0.39	0.44	0.42	0.41	0.35	0.11	0.11	0.36	0.37	0.15	0.12	0.39
K	0.01	0.01	0.02	0.02	0.01	0.02	0.02	0.02	0.02	0.02	0.01	0.01	0.02	0.02	0.01	0.01	0.02
Total (All)	15.13	15.11	15.50	15.51	15.52	15.56	15.56	15.53	15.56	15.48	15.16	15.19	15.47	15.47	15.26	15.19	15.52
Total (Majors ONLY)	15.12	15.10	15.49	15.51	15.51	15.56	15.55	15.52	15.55	15.47	15.16	15.18	15.46	15.47	15.26	15.18	15.51
Al(VI) (= Si + Al - 8)	0.12	0.15	0.82	0.75	0.83	0.76	0.86	0.85	0.79	0.65	0.25	0.18	0.82	0.74	0.27	0.22	0.81
Al(IV) (= Al - Al(VI))	0.32	0.32	1.52	1.48	1.54	1.58	1.63	1.59	1.59	1.34	0.48	0.46	1.46	1.39	0.66	0.51	1.53

Note: Analyses conducted on the same mineral grain (e.g. 1 core analysis and 2 rim analyses on a specific amphibole grain) are highlighted in the same colour and enclosed in the same thick black box.

Biotites

Analysis Label (Specimen_mineral_grain/zone:spot number)	gb8_bi_1c	gb8_bi_1a	gb8_bi_1b	gb8_bi_2b	gb8_bi_2c	gb8_bi_2d	gb8_bi_2e	gb8_bi_3b	gb8_bi_3a	gb8_bi_3c	gb8_bi_4b	gb8_bi_4a	gb8_bi_4c	gb8_bi_5b	gb8_bi_5a	gb8_bi_6c	gb8_bi_6d	gb8_bi_6b	gb8_bi_7a	gb8_bi_8c	gb8_bi_8b
Mineral Probed:	bi	bi	bi	bi	bi	bi	bi	bi	bi	bi	bi	bi	bi	bi	bi	bi	bi	bi	bi	bi	bi
Core/Rim/Int:	Rim	Int	Core	Rim	Rim	Int	Rim	Int	Core	Core	Rim	Int	Rim	Int	Core	Rim	Int	Core	Core	Rim	Int
EMP Initial Results:																					
Oxide conc. (wt%)																					
SiO2	37.11	37.15	36.97	36.66	36.69	37.02	37.17	37.31	37.38	36.85	36.68	36.59	37.08	36.97	37.28	37.03	37.30	36.81	37.75	37.32	36.90
TiO2	1.26	1.55	1.55	1.91	1.83	1.47	1.86	1.69	1.44	1.96	2.04	2.14	1.50	1.96	1.98	2.00	2.01	1.50	1.47	1.86	1.56
Al2O3	20.00	19.30	19.58	18.86	19.43	19.28	19.07	19.43	19.57	18.99	18.53	18.92	18.99	19.23	19.52	19.04	19.05	19.51	19.32	19.24	19.50
Cr2O3	0.06	0.06	0.04	0.03	0.06	0.03	0.04	0.05	0.04	0.03	0.02	0.00	0.06	0.06	0.00	0.03	0.02	0.05	0.03	0.03	0.03
FeO	21.08	21.58	21.01	21.98	21.64	22.05	21.93	21.62	20.88	21.28	21.04	21.07	21.36	20.87	21.08	21.66	20.84	21.17	19.98	20.36	20.38
MnO	0.07	0.03	0.03	0.04	0.09	0.09	0.11	0.05	0.00	0.05	0.04	0.05	0.00	0.04	0.07	0.11	0.03	0.05	0.06	0.00	0.07
MgO	10.55	10.52	10.24	10.67	10.97	11.01	10.50	10.93	11.00	10.67	11.04	10.75	11.41	11.15	11.21	10.84	11.19	11.65	11.99	11.81	11.90
CaO	0.00	0.00	0.00	0.01	0.00	0.00	0.00	0.00	0.01	0.10	0.02	0.00	0.00	0.00	0.00	0.00	0.00	0.01	0.00	0.00	0.00
NaO	0.21	0.17	0.19	0.28	0.20	0.25	0.24	0.19	0.23	0.36	0.15	0.26	0.16	0.16	0.18	0.14	0.16	0.16	0.26	0.23	0.25
K2O	9.48	9.45	9.41	9.20	9.40	9.27	9.48	9.26	9.14	8.86	9.41	9.64	9.50	9.46	9.55	9.53	9.47	9.31	9.59	9.55	9.26
Total	99.82	99.81	99.03	99.65	100.31	100.47	100.40	100.53	99.69	99.15	98.99	99.42	100.06	99.90	100.87	100.39	100.07	100.21	100.46	100.40	99.86
Cations:																					
Si	2.70	2.71	2.71	2.69	2.67	2.69	2.70	2.70	2.71	2.70	2.70	2.68	2.70	2.69	2.69	2.69	2.71	2.67	2.72	2.69	2.68
Ti	0.07	0.08	0.09	0.11	0.10	0.08	0.10	0.09	0.08	0.11	0.11	0.12	0.08	0.11	0.11	0.11	0.11	0.08	0.08	0.10	0.09
Al	1.71	1.66	1.69	1.63	1.67	1.65	1.63	1.66	1.67	1.64	1.61	1.64	1.63	1.65	1.66	1.63	1.63	1.67	1.64	1.64	1.67
Cr	0.00	0.00	0.00	0.00	0.00	0.00	0.00	0.00	0.00	0.00	0.00	0.00	0.00	0.00	0.00	0.00	0.00	0.00	0.00	0.00	0.00
Fe	1.28	1.32	1.29	1.35	1.32	1.34	1.33	1.31	1.27	1.30	1.29	1.29	1.30	1.27	1.27	1.32	1.26	1.28	1.20	1.23	1.24
Mn	0.00	0.00	0.00	0.00	0.01	0.01	0.01	0.00	0.00	0.00	0.00	0.00	0.00	0.00	0.00	0.01	0.00	0.00	0.00	0.00	0.00
Mg	1.14	1.14	1.12	1.17	1.19	1.19	1.14	1.18	1.19	1.17	1.21	1.18	1.24	1.21	1.20	1.17	1.21	1.26	1.29	1.27	1.29
Ca	0.00	0.00	0.00	0.00	0.00	0.00	0.00	0.00	0.00	0.01	0.00	0.00	0.00	0.00	0.00	0.00	0.00	0.00	0.00	0.00	0.00
Na	0.03	0.02	0.03	0.04	0.03	0.03	0.03	0.03	0.03	0.05	0.02	0.04	0.02	0.02	0.03	0.02	0.02	0.02	0.04	0.03	0.03
K	0.88	0.88	0.88	0.86	0.87	0.86	0.88	0.85	0.85	0.83	0.88	0.90	0.88	0.88	0.88	0.88	0.88	0.86	0.88	0.88	0.86
Total (All)	7.83	7.82	7.81	7.84	7.85	7.85	7.83	7.82	7.81	7.81	7.84	7.85	7.86	7.83	7.83	7.83	7.82	7.85	7.84	7.84	7.85
Total (Majors ONLY)	7.82	7.82	7.81	7.84	7.84	7.85	7.83	7.82	7.81	7.81	7.83	7.85	7.85	7.82	7.83	7.83	7.82	7.85	7.84	7.84	7.85
Al(VI) (= (Si + Al) - 4)	0.41	0.37	0.40	0.32	0.33	0.34	0.34	0.35	0.39	0.34	0.31	0.32	0.33	0.34	0.34	0.32	0.33	0.34	0.35	0.33	0.34
Al(IV) (= Al - Al(VI))	1.30	1.29	1.29	1.31	1.33	1.31	1.30	1.30	1.29	1.30	1.30	1.32	1.30	1.31	1.31	1.31	1.29	1.33	1.28	1.31	1.32
Ti (apfu)	0.07	0.08	0.09	0.11	0.10	0.08	0.10	0.09	0.08	0.11	0.11	0.12	0.08	0.11	0.11	0.11	0.11	0.08	0.08	0.10	0.09
XFe (= Fe/(Fe + Mg))	0.53	0.54	0.54	0.54	0.53	0.53	0.54	0.53	0.52	0.53	0.52	0.52	0.51	0.51	0.51	0.53	0.51	0.50	0.48	0.49	0.49

Note: Analyses conducted on the same mineral grain (e.g. 1 core analysis and 2 rim analyses on a specific biotite grain) are highlighted in the same colour and enclosed in the same thick black box.

Biotites cont.

Analysis Label (Specimen_mineral_grain/zone:spot number)	gb8_bi_8a	gb8_bi_9a	gb8_bi_9b	gb8_bi_10b	gb8_bi_10c	gb8_bi_10d	gb8_bi_10e	gb8_bi_12b	gb8_bi_12c	gb8_bi_12a	gb8_bi_12d	gb8_bi_13a	gb8_bi_14a	gb8_bi_14b	gb8_bi_14c	gb8_bi_16a	gb8_bi_16b	gb8_bi_17b	gb8_bi_17a	gb8_bi_17c	gb8_bi_18a
Mineral Probed:	bi	bi	bi	bi	bi	bi	bi	bi	bi	bi	bi	bi	bi	bi	bi	bi	bi	bi	bi	bi	bi
Core/Rim/Int:	Core	Rim	Core	Core	Int	Core	Int	Rim	Int	Core	Int	Core	Rim	Core	Core	Core	Core	Int	Core	Core	Core
EMP Initial Results:																					
Oxide conc. (wt%)																					
SiO2	37.66	37.25	37.16	37.55	37.37	37.08	37.17	37.39	37.56	37.47	36.27	37.39	37.57	37.07	37.33	37.45	37.47	36.79	37.07	36.84	37.19
TiO2	1.34	1.71	1.35	1.48	1.46	1.48	1.30	1.46	1.38	1.48	1.51	1.53	1.60	1.32	1.49	1.51	1.44	1.95	1.49	1.61	1.49
Al2O3	19.67	19.14	19.45	19.35	19.38	19.47	18.87	19.64	19.56	19.40	19.37	19.36	19.76	19.69	19.69	19.52	19.47	18.46	18.94	19.13	19.30
Cr2O3	0.00	0.05	0.00	0.01	0.00	0.04	0.07	0.06	0.05	0.02	0.07	0.04	0.03	0.03	0.05	0.06	0.01	0.03	0.09	0.06	0.03
FeO	20.20	20.56	20.02	19.94	19.08	20.01	19.68	19.95	20.02	20.35	21.23	20.79	19.53	20.06	20.06	20.04	19.72	20.54	20.03	20.11	19.91
MnO	0.07	0.02	0.05	0.03	0.03	0.05	0.09	0.04	0.11	0.09	0.00	0.10	0.04	0.00	0.02	0.00	0.05	0.06	0.02	0.11	0.02
MgO	11.64	11.37	11.86	11.90	11.93	12.26	12.50	11.99	12.07	11.77	12.27	11.95	11.82	12.04	11.79	11.89	11.86	11.99	11.94	12.37	11.93
CaO	0.00	0.00	0.00	0.00	0.00	0.00	0.00	0.00	0.00	0.00	0.00	0.00	0.00	0.00	0.00	0.00	0.00	0.00	0.00	0.00	0.00
NaO	0.27	0.16	0.23	0.22	0.25	0.22	0.29	0.18	0.27	0.18	0.17	0.17	0.19	0.22	0.20	0.23	0.18	0.27	0.25	0.31	0.23
K2O	9.60	9.56	9.48	9.45	9.67	9.59	9.56	9.38	9.52	9.67	8.75	9.17	9.60	9.57	9.62	9.52	9.51	9.32	9.44	9.47	9.30
Total	100.45	99.81	99.60	99.93	99.17	100.20	99.52	100.10	100.53	100.43	99.64	100.51	100.14	100.00	100.24	100.23	99.71	99.42	99.26	100.00	99.40
Cations:																					
Si	2.71	2.71	2.70	2.71	2.72	2.68	2.70	2.70	2.70	2.70	2.64	2.69	2.70	2.68	2.69	2.70	2.71	2.69	2.70	2.67	2.70
Ti	0.07	0.09	0.07	0.08	0.08	0.08	0.07	0.08	0.07	0.08	0.08	0.08	0.09	0.07	0.08	0.08	0.08	0.11	0.08	0.09	0.08
Al	1.67	1.64	1.66	1.65	1.66	1.66	1.62	1.67	1.66	1.65	1.66	1.64	1.68	1.68	1.67	1.66	1.66	1.59	1.63	1.64	1.65
Cr	0.00	0.00	0.00	0.00	0.00	0.00	0.00	0.00	0.00	0.00	0.00	0.00	0.00	0.00	0.00	0.00	0.00	0.00	0.00	0.00	0.00
Fe	1.22	1.25	1.22	1.21	1.16	1.21	1.20	1.20	1.20	1.23	1.29	1.25	1.18	1.21	1.21	1.21	1.19	1.26	1.22	1.22	1.21
Mn	0.00	0.00	0.00	0.00	0.00	0.00	0.01	0.00	0.01	0.01	0.00	0.01	0.00	0.00	0.00	0.00	0.00	0.00	0.00	0.01	0.00
Mg	1.25	1.23	1.28	1.28	1.29	1.32	1.35	1.29	1.29	1.27	1.33	1.28	1.27	1.30	1.27	1.28	1.28	1.31	1.30	1.34	1.29
Ca	0.00	0.00	0.00	0.00	0.00	0.00	0.00	0.00	0.00	0.00	0.00	0.00	0.00	0.00	0.00	0.00	0.00	0.00	0.00	0.00	0.00
Na	0.04	0.02	0.03	0.03	0.03	0.03	0.04	0.03	0.04	0.03	0.02	0.02	0.03	0.03	0.03	0.03	0.03	0.04	0.03	0.04	0.03
K	0.88	0.89	0.88	0.87	0.90	0.88	0.89	0.86	0.87	0.89	0.81	0.84	0.88	0.88	0.89	0.88	0.88	0.87	0.88	0.88	0.86
Total (All)	7.84	7.83	7.85	7.83	7.84	7.87	7.88	7.83	7.85	7.85	7.86	7.83	7.82	7.86	7.84	7.84	7.83	7.86	7.85	7.88	7.84
Total (Majors ONLY)	7.84	7.83	7.85	7.83	7.84	7.87	7.88	7.83	7.85	7.85	7.85	7.83	7.82	7.86	7.84	7.84	7.83	7.86	7.85	7.88	7.83
Al(VI) (= (Si + Al) - 4)	0.38	0.35	0.36	0.36	0.38	0.34	0.32	0.37	0.36	0.35	0.31	0.34	0.38	0.36	0.37	0.36	0.37	0.28	0.33	0.31	0.36
Al(IV) (= Al - Al(VI))	1.29	1.29	1.30	1.29	1.28	1.32	1.30	1.30	1.30	1.30	1.36	1.31	1.30	1.32	1.31	1.30	1.29	1.31	1.30	1.33	1.30
Ti (apfu)	0.07	0.09	0.07	0.08	0.08	0.08	0.07	0.08	0.07	0.08	0.08	0.08	0.09	0.07	0.08	0.08	0.08	0.11	0.08	0.09	0.08
XFe (= Fe/(Fe + Mg))	0.49	0.50	0.49	0.48	0.47	0.48	0.47	0.48	0.48	0.49	0.49	0.49	0.48	0.48	0.49	0.49	0.48	0.49	0.48	0.48	0.48

Note: Analyses conducted on the same mineral grain (e.g. 1 core analysis and 2 rim analyses on a specific biotite grain) are highlighted in the same colour and enclosed in the same thick black box.

Biotites cont.

Analysis Label (Specimen_mineral grain/zone:spot number)	gb8_bi_19a	gb8_bi_19b	gb8_bi_20b	gb8_bi_20c	gb8_bi_20a	gb8_bi_21b	gb8_bi_21c	gb8_bi_21a	gb10_bi_1f	gb10_bi_1i	gb10_bi_1a	gb10_bi_1e	gb10_bi_1b	gb10_bi_1c	gb10_bi_1d	gb10_bi_1g	gb10_bi_1h	gb10_bi_1j	gb10_bi_2b	gb10_bi_2a	gb10_bi_2d
Mineral Probed:	bi	bi	bi	bi	bi	bi	bi	bi	bi	bi	bi	bi	bi	bi	bi	bi	bi	bi	bi	bi	bi
Core/Rim/Int:	Rim	Core	Rim	Int	Core	Rim	Int	Core	Rim	Rim	Int	Int	Core	Core	Core	Int	Int	Rim	Rim	Int	Core
EMP Initial Results:																					
Oxide conc. (wt%)																					
SiO2	36.97	36.98	37.32	37.06	37.03	37.39	37.31	37.52	37.90	37.38	37.86	37.56	37.44	37.73	37.65	37.95	37.82	37.62	37.56	37.56	37.72
TiO2	1.56	1.51	1.51	1.54	1.63	1.64	2.19	1.50	1.54	1.59	1.42	1.45	1.34	1.41	1.31	1.48	1.41	1.74	1.42	1.33	1.42
Al2O3	18.86	19.01	19.48	19.43	19.35	20.07	19.04	19.34	19.66	19.77	20.19	19.83	19.89	19.86	19.72	20.01	19.88	19.44	19.74	19.66	19.93
Cr2O3	0.00	0.04	0.00	0.04	0.00	0.03	0.04	0.04	0.02	0.02	0.01	0.00	0.03	0.02	0.04	0.03	0.04	0.05	0.02	0.00	0.05
FeO	20.35	20.18	20.39	20.36	20.21	19.50	20.41	20.28	18.50	18.28	18.39	18.46	19.21	18.40	18.03	18.60	18.45	18.28	18.86	18.94	18.62
MnO	0.02	0.04	0.00	0.05	0.03	0.06	0.05	0.00	0.02	0.06	0.04	0.04	0.10	0.06	0.00	0.08	0.05	0.09	0.04	0.04	0.02
MgO	11.68	12.00	11.77	11.81	11.63	11.61	10.97	11.85	12.97	12.78	12.61	12.72	12.66	12.66	12.85	12.63	12.94	12.24	12.69	12.56	12.73
CaO	0.00	0.00	0.00	0.00	0.00	0.00	0.00	0.00	0.00	0.00	0.00	0.00	0.02	0.00	0.00	0.00	0.00	0.01	0.00	0.00	0.00
NaO	0.25	0.26	0.16	0.21	0.18	0.18	0.15	0.21	0.43	0.43	0.45	0.39	0.40	0.40	0.43	0.45	0.46	0.38	0.38	0.41	0.43
K2O	9.47	9.60	9.52	9.51	9.58	9.48	9.48	9.45	9.25	9.33	9.12	9.19	8.46	9.12	9.07	9.04	9.22	9.18	9.10	9.17	9.38
Total	99.15	99.62	100.15	100.00	99.63	99.97	99.65	100.19	100.29	99.64	100.09	99.64	99.54	99.66	99.10	100.27	100.27	99.03	99.82	99.68	100.30
Cations:																					
Si	2.70	2.69	2.70	2.69	2.69	2.69	2.71	2.71	2.71	2.69	2.70	2.70	2.69	2.71	2.71	2.71	2.70	2.72	2.70	2.71	2.70
Ti	0.09	0.08	0.08	0.08	0.09	0.09	0.12	0.08	0.08	0.09	0.08	0.08	0.07	0.08	0.07	0.08	0.08	0.09	0.08	0.07	0.08
Al	1.63	1.63	1.66	1.66	1.66	1.70	1.63	1.65	1.65	1.68	1.70	1.68	1.69	1.68	1.68	1.68	1.67	1.66	1.67	1.67	1.68
Cr	0.00	0.00	0.00	0.00	0.00	0.00	0.00	0.00	0.00	0.00	0.00	0.00	0.00	0.00	0.00	0.00	0.00	0.00	0.00	0.00	0.00
Fe	1.25	1.23	1.23	1.23	1.23	1.18	1.24	1.22	1.10	1.10	1.10	1.11	1.16	1.10	1.09	1.11	1.10	1.11	1.13	1.14	1.11
Mn	0.00	0.00	0.00	0.00	0.00	0.00	0.00	0.00	0.00	0.00	0.00	0.00	0.01	0.00	0.00	0.01	0.00	0.01	0.00	0.00	0.00
Mg	1.27	1.30	1.27	1.28	1.26	1.25	1.19	1.27	1.38	1.37	1.34	1.36	1.36	1.35	1.38	1.34	1.38	1.32	1.36	1.35	1.36
Ca	0.00	0.00	0.00	0.00	0.00	0.00	0.00	0.00	0.00	0.00	0.00	0.00	0.00	0.00	0.00	0.00	0.00	0.00	0.00	0.00	0.00
Na	0.04	0.04	0.02	0.03	0.02	0.03	0.02	0.03	0.06	0.06	0.06	0.05	0.06	0.06	0.06	0.06	0.06	0.05	0.05	0.06	0.06
K	0.88	0.89	0.88	0.88	0.89	0.87	0.88	0.87	0.84	0.86	0.83	0.84	0.78	0.84	0.83	0.82	0.84	0.85	0.83	0.84	0.86
Total (All)	7.86	7.87	7.84	7.85	7.85	7.81	7.80	7.84	7.83	7.84	7.82	7.83	7.81	7.82	7.82	7.81	7.84	7.81	7.83	7.84	7.84
Total (Majors ONLY)	7.86	7.87	7.84	7.85	7.85	7.81	7.80	7.83	7.83	7.84	7.82	7.83	7.80	7.82	7.82	7.81	7.84	7.80	7.83	7.84	7.84
Al(VI) (= (Si + Al) - 4)	0.33	0.32	0.36	0.35	0.35	0.40	0.34	0.35	0.36	0.37	0.40	0.38	0.38	0.39	0.39	0.39	0.37	0.38	0.37	0.37	0.38
Al(IV) (= Al - Al(VI))	1.30	1.31	1.30	1.31	1.31	1.31	1.29	1.29	1.29	1.31	1.30	1.30	1.31	1.29	1.29	1.29	1.30	1.28	1.30	1.29	1.30
Ti (apfu)	0.09	0.08	0.08	0.08	0.09	0.09	0.12	0.08	0.08	0.09	0.08	0.08	0.07	0.08	0.07	0.08	0.08	0.09	0.08	0.07	0.08
XFe (= Fe/(Fe + Mg))	0.49	0.49	0.49	0.49	0.49	0.49	0.51	0.49	0.44	0.45	0.45	0.45	0.46	0.45	0.44	0.45	0.44	0.46	0.45	0.46	0.45

Note: Analyses conducted on the same mineral grain (e.g. 1 core analysis and 2 rim analyses on a specific biotite grain) are highlighted in the same colour and enclosed in the same thick black box.

Biotites cont.

Analysis Label (Specimen_mineral grain/zone:spot number)	gb10_bi_2c	gb10_bi_3c	gb10_bi_3d	gb10_bi_3a	gb10_bi_3b	gb10_bi_3f	gb10_bi_3e	gb10_bi_3g	gb10_bi_5b	gb10_bi_5a	gb10_bi_5c	gb10_bi_5d	gb10_bi_5e	gb10_bi_5g	gb10_bi_5f	gb10_bi_4b	gb10_bi_4a	gb10_bi_4c	gb10_bi_4d	gb10_bi_4e	gb10_bi_4f
Mineral Probed:	bi	bi	bi	bi	bi	bi	bi	bi	bi	bi	bi	bi	bi	bi	bi	bi	bi	bi	bi	bi	bi
Core/Rim/Int:	Int	Rim	Rim	Int	Core	Int	Rim	Rim	Rim	Int	Core	Int	Int	Rim	Int	Int	Core	Core	Rim	Int	Core
EMP Initial Results:																					
Oxide conc. (wt%)																					
SiO2	37.51	37.61	37.62	37.75	37.57	37.69	37.39	37.67	37.64	37.80	37.58	37.44	37.61	37.60	37.59	37.47	37.56	37.45	37.65	38.22	37.58
TiO2	1.40	1.47	1.39	1.33	1.33	1.43	1.45	1.64	1.28	1.39	1.40	1.50	1.43	1.41	1.34	1.43	1.38	1.36	1.46	1.46	1.37
Al2O3	19.41	19.26	19.33	19.83	19.81	19.88	20.03	19.58	20.02	20.17	19.97	19.62	19.75	19.64	20.16	19.65	19.90	19.48	19.73	19.91	19.89
Cr2O3	0.04	0.04	0.00	0.04	0.02	0.02	0.00	0.02	0.01	0.08	0.03	0.07	0.04	0.03	0.03	0.05	0.03	0.02	0.02	0.02	0.05
FeO	18.96	19.31	18.90	18.07	18.42	18.73	18.42	18.02	17.63	17.79	18.40	18.38	18.83	18.13	18.39	18.91	18.57	18.63	19.22	18.80	18.56
MnO	0.05	0.04	0.05	0.00	0.04	0.04	0.03	0.05	0.06	0.11	0.07	0.03	0.02	0.09	0.07	0.06	0.03	0.05	0.05	0.00	0.06
MgO	12.51	10.86	12.63	12.69	12.50	12.85	12.85	12.92	12.60	12.77	12.79	12.77	12.87	13.12	12.82	12.70	12.77	12.79	12.83	12.54	12.67
CaO	0.00	0.02	0.03	0.01	0.01	0.00	0.11	0.00	0.02	0.00	0.00	0.00	0.00	0.00	0.00	0.00	0.00	0.00	0.02	0.01	0.00
NaO	0.29	0.25	0.36	0.43	0.48	0.33	0.30	0.35	0.53	0.57	0.55	0.51	0.45	0.39	0.31	0.38	0.44	0.43	0.36	0.46	0.54
K2O	9.33	9.19	9.02	9.16	8.97	9.35	8.55	9.34	9.22	9.30	9.07	9.02	9.19	9.21	8.66	9.12	9.13	9.12	8.98	8.94	8.98
Total	99.50	98.06	99.33	99.31	99.15	100.31	99.13	99.60	99.01	99.98	99.86	99.34	100.20	99.62	99.38	99.77	99.81	99.33	100.32	100.37	99.70
Cations:																					
Si	2.71	2.76	2.72	2.72	2.71	2.69	2.69	2.71	2.71	2.70	2.69	2.70	2.69	2.70	2.70	2.70	2.70	2.70	2.69	2.72	2.70
Ti	0.08	0.08	0.08	0.07	0.07	0.08	0.08	0.09	0.07	0.07	0.08	0.08	0.08	0.08	0.07	0.08	0.07	0.07	0.08	0.08	0.07
Al	1.65	1.66	1.65	1.68	1.68	1.68	1.70	1.66	1.70	1.70	1.69	1.67	1.67	1.66	1.71	1.67	1.68	1.66	1.66	1.67	1.68
Cr	0.00	0.00	0.00	0.00	0.00	0.00	0.00	0.00	0.00	0.00	0.00	0.00	0.00	0.00	0.00	0.00	0.00	0.00	0.00	0.00	0.00
Fe	1.15	1.18	1.14	1.09	1.11	1.12	1.11	1.08	1.06	1.06	1.10	1.11	1.13	1.09	1.10	1.14	1.11	1.13	1.15	1.12	1.11
Mn	0.00	0.00	0.00	0.00	0.00	0.00	0.00	0.00	0.00	0.01	0.00	0.00	0.00	0.01	0.00	0.00	0.00	0.00	0.00	0.00	0.00
Mg	1.35	1.19	1.36	1.36	1.34	1.37	1.38	1.38	1.35	1.36	1.37	1.37	1.37	1.40	1.37	1.36	1.37	1.38	1.37	1.33	1.36
Ca	0.00	0.00	0.00	0.00	0.00	0.00	0.01	0.00	0.00	0.00	0.00	0.00	0.00	0.00	0.00	0.00	0.00	0.00	0.00	0.00	0.00
Na	0.04	0.04	0.05	0.06	0.07	0.05	0.04	0.05	0.07	0.08	0.08	0.07	0.06	0.05	0.04	0.05	0.06	0.06	0.05	0.06	0.08
K	0.86	0.86	0.83	0.84	0.83	0.85	0.79	0.86	0.85	0.85	0.83	0.83	0.84	0.84	0.79	0.84	0.84	0.84	0.82	0.81	0.82
Total (All)	7.84	7.78	7.83	7.82	7.82	7.84	7.79	7.83	7.83	7.84	7.84	7.83	7.85	7.84	7.79	7.84	7.84	7.84	7.83	7.80	7.83
Total (Majors ONLY)	7.84	7.77	7.83	7.82	7.82	7.84	7.79	7.83	7.83	7.83	7.84	7.83	7.84	7.84	7.79	7.83	7.83	7.84	7.83	7.80	7.83
Al(VI) (= (Si + Al) - 4)	0.36	0.42	0.36	0.40	0.40	0.37	0.39	0.36	0.41	0.40	0.38	0.37	0.36	0.36	0.40	0.36	0.38	0.36	0.36	0.39	0.38
Al(IV) (= Al - Al(VI))	1.29	1.24	1.28	1.28	1.29	1.31	1.31	1.29	1.29	1.30	1.31	1.30	1.31	1.30	1.30	1.30	1.30	1.30	1.31	1.28	1.30
Ti (apfu)	0.08	0.08	0.08	0.07	0.07	0.08	0.08	0.09	0.07	0.07	0.08	0.08	0.08	0.08	0.07	0.08	0.07	0.07	0.08	0.08	0.07
XFe (= Fe/(Fe + Mg))	0.46	0.50	0.46	0.44	0.45	0.45	0.45	0.44	0.44	0.44	0.45	0.45	0.45	0.44	0.45	0.46	0.45	0.45	0.46	0.46	0.45

Note: Analyses conducted on the same mineral grain (e.g. 1 core analysis and 2 rim analyses on a specific biotite grain) are highlighted in the same colour and enclosed in the same thick black box.

Biotites cont.

Analysis Label (Specimen_mineral_grain/zone:spot number)	gb10_bi_4g	gb10_bi_4h	gb10_bi_4k	gb10_bi_4i	gb10_bi_4j	gb10_bi_4l	gb10_bi_4m	gb10_bi_4n	gb10_bi_4r	gb10_bi_4o	gb10_bi_4p	gb10_bi_4q	gb10_bi_4s	gb10_bi_4t	gb10_bi_4u	gb10_bi_6b	gb10_bi_6a	gb10_bi_7a	gb10_bi_7b	gb10_bi_8a	gb10_bi_8b
Mineral Probed:	bi	bi	bi	bi	bi	bi	bi	bi	bi	bi	bi	bi	bi	bi	bi	bi	bi	bi	bi	bi	bi
Core/Rim/Int:	Rim	Int	Core	Int	Core	Core	Rim	Core	Rim	Int	Int	Core	Int	Int	Core	Int	Core	Rim	Core	Rim	Core
EMP Initial Results:																					
Oxide conc. (wt%)																					
SiO2	37.85	37.97	37.40	37.79	37.80	36.74	37.89	37.89	37.74	37.34	37.73	38.05	37.40	37.71	37.74	37.47	37.76	36.66	36.44	37.56	37.58
TiO2	1.50	1.39	1.24	1.37	1.37	1.39	1.41	1.35	1.42	1.32	1.36	1.26	1.42	1.38	1.36	1.61	1.31	1.50	1.37	1.30	1.24
Al2O3	19.99	20.15	20.49	20.02	19.60	19.12	19.89	19.86	19.76	19.64	20.09	19.77	19.50	19.85	19.77	19.81	19.82	19.40	19.24	19.70	19.97
Cr2O3	0.04	0.06	0.03	0.06	0.05	0.02	0.04	0.00	0.00	0.04	0.01	0.02	0.03	0.00	0.00	0.01	0.06	0.07	0.02	0.03	0.02
FeO	18.00	18.46	18.03	18.14	18.59	18.25	17.80	18.73	18.29	18.88	18.32	18.54	18.61	18.74	18.96	18.71	18.41	18.46	18.32	18.01	18.25
MnO	0.04	0.07	0.05	0.04	0.05	0.00	0.07	0.02	0.03	0.04	0.07	0.05	0.07	0.02	0.05	0.04	0.11	0.01	0.02	0.06	0.06
MgO	12.75	12.69	12.77	12.51	12.64	12.30	13.07	12.74	13.00	13.13	12.58	12.66	12.76	12.57	12.36	12.77	12.88	13.17	12.64	12.96	12.90
CaO	0.00	0.00	0.00	0.00	0.00	0.00	0.00	0.00	0.00	0.00	0.00	0.00	0.00	0.00	0.00	0.00	0.00	0.03	0.03	0.05	0.05
NaO	0.42	0.41	0.35	0.36	0.43	0.41	0.41	0.42	0.36	0.37	0.39	0.41	0.42	0.44	0.42	0.42	0.43	0.57	0.69	0.52	0.58
K2O	9.08	9.16	9.14	9.22	9.15	9.06	9.41	9.11	9.37	8.83	9.17	9.05	9.26	9.18	9.08	9.29	9.14	9.16	9.13	8.79	9.07
Total	99.66	100.35	99.50	99.50	99.68	97.30	100.00	100.12	99.98	99.60	99.73	99.81	99.46	99.89	99.73	100.14	99.91	99.02	97.90	98.97	99.72
Cations:																					
Si	2.71	2.71	2.68	2.71	2.72	2.71	2.71	2.71	2.70	2.69	2.71	2.73	2.70	2.71	2.71	2.69	2.71	2.66	2.68	2.71	2.70
Ti	0.08	0.07	0.07	0.07	0.07	0.08	0.08	0.07	0.08	0.07	0.07	0.07	0.08	0.07	0.07	0.09	0.07	0.08	0.08	0.07	0.07
Al	1.69	1.69	1.73	1.69	1.66	1.66	1.68	1.67	1.67	1.67	1.70	1.67	1.66	1.68	1.68	1.67	1.67	1.66	1.67	1.67	1.69
Cr	0.00	0.00	0.00	0.00	0.00	0.00	0.00	0.00	0.00	0.00	0.00	0.00	0.00	0.00	0.00	0.00	0.00	0.00	0.00	0.00	0.00
Fe	1.08	1.10	1.08	1.09	1.12	1.13	1.06	1.12	1.10	1.14	1.10	1.11	1.12	1.12	1.14	1.12	1.10	1.12	1.13	1.09	1.10
Mn	0.00	0.00	0.00	0.00	0.00	0.00	0.00	0.00	0.00	0.00	0.00	0.00	0.00	0.00	0.00	0.00	0.01	0.00	0.00	0.00	0.00
Mg	1.36	1.35	1.37	1.34	1.35	1.35	1.39	1.36	1.39	1.41	1.34	1.35	1.37	1.34	1.32	1.36	1.38	1.43	1.38	1.39	1.38
Ca	0.00	0.00	0.00	0.00	0.00	0.00	0.00	0.00	0.00	0.00	0.00	0.00	0.00	0.00	0.00	0.00	0.00	0.00	0.00	0.00	0.00
Na	0.06	0.06	0.05	0.05	0.06	0.06	0.06	0.06	0.05	0.05	0.05	0.06	0.06	0.06	0.06	0.06	0.06	0.08	0.10	0.07	0.08
K	0.83	0.83	0.84	0.84	0.84	0.85	0.86	0.83	0.86	0.81	0.84	0.83	0.85	0.84	0.83	0.85	0.84	0.85	0.86	0.81	0.83
Total (All)	7.81	7.82	7.82	7.81	7.83	7.84	7.84	7.83	7.84	7.84	7.82	7.81	7.85	7.83	7.82	7.84	7.83	7.89	7.89	7.82	7.85
Total (Majors ONLY)	7.81	7.81	7.82	7.81	7.82	7.84	7.83	7.83	7.84	7.84	7.82	7.81	7.85	7.83	7.82	7.84	7.83	7.88	7.89	7.82	7.85
Al(VI) (= (Si + Al) - 4)	0.40	0.40	0.42	0.41	0.38	0.37	0.38	0.38	0.37	0.35	0.40	0.39	0.36	0.38	0.39	0.36	0.38	0.32	0.34	0.38	0.39
Al(IV) (= Al - Al(VI))	1.29	1.29	1.32	1.29	1.28	1.29	1.29	1.29	1.30	1.31	1.29	1.27	1.30	1.29	1.29	1.31	1.29	1.34	1.32	1.29	1.30
Ti (apfu)	0.08	0.07	0.07	0.07	0.07	0.08	0.08	0.07	0.08	0.07	0.07	0.07	0.08	0.07	0.07	0.09	0.07	0.08	0.08	0.07	0.07
XFe (= Fe/(Fe + Mg))	0.44	0.45	0.44	0.45	0.45	0.45	0.43	0.45	0.44	0.45	0.45	0.45	0.45	0.46	0.46	0.45	0.45	0.44	0.45	0.44	0.44

Note: Analyses conducted on the same mineral grain (e.g. 1 core analysis and 2 rim analyses on a specific biotite grain) are highlighted in the same colour and enclosed in the same thick black box.

Biotites cont.

Analysis Label (Specimen_mineral grain/zone:spot number)	gb10_bi_8c	gb10_bi_9c	gb10_bi_9a	gb10_bi_9b	gb10_bi_10a	gb10_bi_10c	gb10_bi_10b	gb10_bi_10d	gb10_chl_3a	gb10_chl_3b	gb10_chl_4a	gb10_chl_4b	gb10_chl_4c	gb10_chl_4d	gb10_chl_5b	gb10_chl_5e	gb10_chl_5a	gb10_chl_5c	gb10_chl_5d	gb10_chl_7b	gb10_chl_7a
Mineral Probed:	bi	bi	bi	bi	bi	bi	bi	bi	bi	bi	bi	bi	bi	bi	bi	bi	bi	bi	bi	bi	bi
Core/Rim/Int:	Rim	Rim	Core	Core	Rim	Int	Core	Int	Rim	Core	Rim	Core	Core	Rim	Rim	Int	Core	Core	Rim	Rim	Core
EMP Initial Results:																					
Oxide conc. (wt%)																					
SiO2	37.46	37.84	37.72	36.94	37.07	37.87	37.44	38.02	36.78	36.85	36.68	36.68	36.74	36.19	36.36	36.68	36.74	36.43	36.49	36.76	36.19
TiO2	1.20	1.37	1.40	1.36	1.59	1.36	1.32	1.45	1.35	1.30	1.40	1.40	1.34	1.45	1.34	1.41	1.37	1.35	1.41	1.42	1.38
Al2O3	20.05	19.85	19.76	19.49	19.35	19.52	19.57	19.53	19.97	19.55	19.47	19.75	19.91	19.38	19.81	19.68	19.83	19.72	19.54	19.59	19.44
Cr2O3	0.05	0.08	0.05	0.05	0.04	0.02	0.00	0.03	0.04	0.05	0.03	0.03	0.04	0.02	0.03	0.03	0.09	0.04	0.01	0.05	0.02
FeO	18.93	18.18	18.25	18.47	18.80	18.65	18.70	18.53	18.32	18.73	18.50	18.79	18.59	18.71	18.83	18.68	18.50	18.64	18.48	19.00	19.07
MnO	0.02	0.06	0.05	0.02	0.05	0.06	0.04	0.01	0.03	0.05	0.06	0.00	0.06	0.04	0.02	0.01	0.03	0.02	0.07	0.01	0.00
MgO	12.58	12.39	12.72	12.65	12.87	12.92	12.99	12.63	12.26	12.33	12.36	12.18	12.36	11.95	12.27	12.33	12.37	12.25	12.05	12.14	12.05
CaO	0.03	0.00	0.00	0.00	0.00	0.00	0.07	0.00	0.00	0.00	0.00	0.00	0.00	0.02	0.00	0.00	0.01	0.02	0.01	0.00	0.00
NaO	0.50	0.37	0.42	0.30	0.37	0.35	0.39	0.37	0.36	0.58	0.43	0.52	0.39	0.40	0.46	0.51	0.52	0.44	0.49	0.44	0.41
K2O	9.07	9.21	9.07	9.01	9.27	9.26	9.12	9.33	9.25	9.07	9.27	9.14	9.25	9.02	8.91	9.09	9.16	9.18	9.15	9.08	9.13
Total	99.89	99.34	99.44	98.29	99.41	100.00	99.64	99.90	98.36	98.51	98.20	98.50	98.68	97.18	98.02	98.41	98.62	98.08	97.69	98.49	97.69
Cations:																					
Si	2.69	2.72	2.71	2.69	2.68	2.71	2.70	2.73	2.68	2.69	2.69	2.68	2.68	2.68	2.67	2.68	2.68	2.67	2.69	2.69	2.67
Ti	0.06	0.07	0.08	0.07	0.09	0.07	0.07	0.08	0.07	0.07	0.08	0.08	0.07	0.08	0.07	0.08	0.07	0.07	0.08	0.08	0.08
Al	1.70	1.68	1.67	1.68	1.65	1.65	1.66	1.65	1.72	1.68	1.68	1.70	1.71	1.69	1.71	1.69	1.70	1.70	1.70	1.69	1.69
Cr	0.00	0.00	0.00	0.00	0.00	0.00	0.00	0.00	0.00	0.00	0.00	0.00	0.00	0.00	0.00	0.00	0.01	0.00	0.00	0.00	0.00
Fe	1.14	1.09	1.10	1.13	1.14	1.12	1.13	1.11	1.12	1.14	1.13	1.15	1.13	1.16	1.16	1.14	1.13	1.14	1.14	1.16	1.18
Mn	0.00	0.00	0.00	0.00	0.00	0.00	0.00	0.00	0.00	0.00	0.00	0.00	0.00	0.00	0.00	0.00	0.00	0.00	0.00	0.00	0.00
Mg	1.35	1.33	1.36	1.38	1.39	1.38	1.39	1.35	1.33	1.34	1.35	1.33	1.34	1.32	1.34	1.34	1.34	1.34	1.32	1.32	1.33
Ca	0.00	0.00	0.00	0.00	0.00	0.00	0.01	0.00	0.00	0.00	0.00	0.00	0.00	0.00	0.00	0.00	0.00	0.00	0.00	0.00	0.00
Na	0.07	0.05	0.06	0.04	0.05	0.05	0.05	0.05	0.05	0.08	0.06	0.07	0.05	0.06	0.07	0.07	0.07	0.06	0.07	0.06	0.06
K	0.83	0.85	0.83	0.84	0.86	0.85	0.84	0.85	0.86	0.84	0.87	0.85	0.86	0.85	0.83	0.85	0.85	0.86	0.86	0.85	0.86
Total (All)	7.84	7.81	7.82	7.83	7.86	7.84	7.85	7.82	7.84	7.86	7.86	7.86	7.85	7.85	7.85	7.86	7.86	7.86	7.85	7.85	7.86
Total (Majors ONLY)	7.84	7.80	7.82	7.83	7.86	7.83	7.85	7.82	7.84	7.86	7.86	7.85	7.85	7.85	7.85	7.85	7.85	7.86	7.85	7.84	7.86
Al(VI) (= (Si + Al) - 4)	0.39	0.41	0.39	0.37	0.33	0.36	0.36	0.38	0.40	0.37	0.37	0.38	0.38	0.37	0.38	0.37	0.38	0.38	0.38	0.37	0.36
Al(IV) (= Al - Al(VI))	1.31	1.28	1.29	1.31	1.32	1.29	1.30	1.27	1.32	1.31	1.31	1.32	1.32	1.32	1.33	1.32	1.32	1.33	1.31	1.31	1.33
Ti (apfu)	0.06	0.07	0.08	0.07	0.09	0.07	0.07	0.08	0.07	0.07	0.08	0.08	0.07	0.08	0.07	0.08	0.07	0.07	0.08	0.08	0.08
XFe (= Fe/(Fe + Mg))	0.46	0.45	0.45	0.45	0.45	0.45	0.45	0.45	0.46	0.46	0.46	0.46	0.46	0.47	0.46	0.46	0.46	0.46	0.46	0.47	0.47

Note: Analyses conducted on the same mineral grain (e.g. 1 core analysis and 2 rim analyses on a specific biotite grain) are highlighted in the same colour and enclosed in the same thick black box.

Biotites cont.

Analysis Label (Specimen_mineral_grain/zone:spot number)	gb10_chl_7c	gb10_chl_10a	gb10_chl_10d	gb10_chl_10b	gb10_chl_10c	gb10_chl_2a	gb10_chl_2c	gb10_chl_2b	gb10_chl_2d	gb10_chl_2e	gb13_bi_1b	gb13_bi_1c	gb13_bi_1a	gb13_bi_1d	gb13_bi_2b	gb13_bi_2c	gb13_bi_2a	gb13_bi_3b	gb13_bi_3c	gb13_bi_3a	gb13_bi_3e
Mineral Probed:	bi	bi	bi	bi	bi	bi	bi	bi	bi	bi	bi	bi	bi	bi	bi	bi	bi	bi	bi	bi	bi
Core/Rim/Int:	Core	Rim	Int	Core	Rim	Rim	Int	Core	Core	Rim	Rim	Int	Core	Int	Rim	Int	Core	Rim	Int	Core	Rim
EMP Initial Results:																					
Oxide conc. (wt%)																					
SiO2	37.06	37.22	36.71	36.84	36.39	37.00	36.57	36.65	36.60	36.45	37.04	36.26	36.93	36.52	36.66	36.74	36.71	36.85	36.97	37.14	37.09
TiO2	1.41	1.43	1.48	1.33	1.42	1.30	1.34	1.44	1.33	1.37	1.52	1.48	1.43	1.50	1.25	1.46	1.46	1.45	1.48	1.45	1.57
Al2O3	19.96	20.22	19.87	20.04	19.77	20.09	19.45	20.00	19.74	19.71	19.86	19.99	19.78	19.66	19.38	20.23	20.25	20.17	20.33	20.20	20.66
Cr2O3	0.01	0.02	0.02	0.01	0.00	0.00	0.01	0.05	0.01	0.02	0.00	0.07	0.06	0.05	0.03	0.02	0.08	0.00	0.01	0.00	0.05
FeO	18.56	17.73	18.73	18.58	18.92	18.09	18.12	18.91	18.24	18.62	18.01	18.37	18.47	19.11	18.79	18.26	18.15	18.08	18.14	18.31	17.70
MnO	0.01	0.03	0.07	0.10	0.04	0.03	0.04	0.11	0.03	0.10	0.02	0.02	0.08	0.05	0.04	0.07	0.07	0.05	0.01	0.03	0.01
MgO	12.32	12.23	12.43	12.15	12.51	12.40	12.69	12.51	12.26	12.12	12.12	12.30	12.29	12.32	12.67	12.14	12.49	12.31	12.22	12.29	12.41
CaO	0.00	0.00	0.00	0.01	0.00	0.00	0.00	0.00	0.03	0.00	0.04	0.00	0.02	0.00	0.00	0.00	0.01	0.00	0.00	0.00	0.00
NaO	0.45	0.38	0.41	0.41	0.23	0.32	0.46	0.40	0.47	0.44	0.28	0.37	0.34	0.35	0.38	0.47	0.54	0.35	0.43	0.33	0.40
K2O	9.11	9.21	9.25	9.21	9.17	9.30	9.35	9.07	9.05	9.10	8.98	8.91	8.96	8.95	8.83	8.98	8.99	9.09	9.04	9.00	9.05
Total	98.89	98.47	98.97	98.68	98.46	98.53	98.03	99.14	97.76	97.93	97.87	97.77	98.35	98.51	98.03	98.37	98.75	98.35	98.63	98.75	98.94
Cations:																					
Si	2.69	2.70	2.67	2.68	2.66	2.69	2.68	2.66	2.69	2.68	2.70	2.66	2.69	2.67	2.69	2.67	2.66	2.68	2.68	2.69	2.67
Ti	0.08	0.08	0.08	0.07	0.08	0.07	0.07	0.08	0.07	0.08	0.08	0.08	0.08	0.08	0.07	0.08	0.08	0.08	0.08	0.08	0.09
Al	1.71	1.73	1.70	1.72	1.70	1.72	1.68	1.71	1.71	1.71	1.71	1.73	1.70	1.69	1.67	1.74	1.73	1.73	1.74	1.72	1.76
Cr	0.00	0.00	0.00	0.00	0.00	0.00	0.00	0.00	0.00	0.00	0.00	0.00	0.00	0.00	0.00	0.00	0.00	0.00	0.00	0.00	0.00
Fe	1.13	1.08	1.14	1.13	1.16	1.10	1.11	1.15	1.12	1.14	1.10	1.13	1.13	1.17	1.15	1.11	1.10	1.10	1.10	1.11	1.07
Mn	0.00	0.00	0.00	0.01	0.00	0.00	0.00	0.01	0.00	0.01	0.00	0.00	0.00	0.00	0.00	0.00	0.00	0.00	0.00	0.00	0.00
Mg	1.33	1.32	1.35	1.32	1.36	1.34	1.39	1.35	1.34	1.33	1.32	1.35	1.34	1.34	1.38	1.32	1.35	1.34	1.32	1.33	1.33
Ca	0.00	0.00	0.00	0.00	0.00	0.00	0.00	0.00	0.00	0.00	0.00	0.00	0.00	0.00	0.00	0.00	0.00	0.00	0.00	0.00	0.00
Na	0.06	0.05	0.06	0.06	0.03	0.04	0.07	0.06	0.07	0.06	0.04	0.05	0.05	0.05	0.05	0.07	0.08	0.05	0.06	0.05	0.06
K	0.84	0.85	0.86	0.86	0.86	0.86	0.87	0.84	0.85	0.85	0.84	0.83	0.83	0.83	0.83	0.83	0.83	0.84	0.84	0.83	0.83
Total (All)	7.84	7.81	7.86	7.84	7.85	7.83	7.88	7.85	7.84	7.85	7.80	7.84	7.82	7.84	7.85	7.83	7.84	7.82	7.82	7.81	7.81
Total (Majors ONLY)	7.83	7.81	7.86	7.84	7.85	7.83	7.87	7.85	7.84	7.85	7.80	7.83	7.82	7.84	7.85	7.83	7.84	7.82	7.82	7.81	7.80
Al(VI) (= (Si + Al) - 4)	0.39	0.43	0.37	0.40	0.36	0.41	0.36	0.37	0.39	0.38	0.41	0.39	0.39	0.36	0.36	0.41	0.39	0.41	0.42	0.41	0.43
Al(IV) (= Al - Al(VI))	1.31	1.30	1.33	1.32	1.34	1.31	1.32	1.34	1.31	1.32	1.30	1.34	1.31	1.33	1.31	1.33	1.34	1.32	1.32	1.31	1.33
Ti (apfu)	0.08	0.08	0.08	0.07	0.08	0.07	0.07	0.08	0.07	0.08	0.08	0.08	0.08	0.08	0.07	0.08	0.08	0.08	0.08	0.08	0.09
XFe (= Fe/(Fe + Mg))	0.46	0.45	0.46	0.46	0.46	0.45	0.44	0.46	0.45	0.46	0.45	0.46	0.46	0.47	0.45	0.46	0.45	0.45	0.45	0.46	0.44

Note: Analyses conducted on the same mineral grain (e.g. 1 core analysis and 2 rim analyses on a specific biotite grain) are highlighted in the same colour and enclosed in the same thick black box.

Biotites cont.

Analysis Label (Specimen_mineral_grain/zone:spot number)	gb13_bi_3d	gb13_bi_4b	gb13_bi_4a	gb13_bi_4c	gb13_bi_5b	gb13_bi_5e	gb13_bi_5a	gb13_bi_5d	gb13_bi_5c	gb13_bi_6c	gb13_bi_6b	gb13_bi_6a	gb13_bi_7a	gb13_bi_7c	gb13_bi_7e	gb13_bi_7b	gb13_bi_7d	gb13_bi_7f	gb13_bi_7g	gb13_bi_8b	gb13_bi_8a
Mineral Probed:	bi	bi	bi	bi	bi	bi	bi	bi	bi	bi	bi	bi	bi	bi	bi	bi	bi	bi	bi	bi	bi
Core/Rim/Int:	Core	Rim	Core	Core	Rim	Int	Core	Rim	Core	Rim	Int	Core	Rim	Rim	Int	Core	Core	Int	Rim	Int	Core
EMP Initial Results:																					
Oxide conc. (wt%)																					
SiO2	36.49	36.25	36.29	36.83	36.59	36.58	36.01	36.92	36.71	36.82	36.90	36.83	36.79	36.91	36.43	36.91	36.97	37.01	36.85	36.91	36.88
TiO2	1.48	1.49	1.44	1.34	1.49	1.39	1.51	1.45	1.40	1.49	1.41	1.47	1.41	1.31	1.58	1.42	1.43	1.60	1.43	1.46	1.46
Al2O3	20.04	19.67	19.72	19.92	20.31	19.85	19.69	19.82	20.24	19.92	20.16	19.91	19.77	20.13	20.37	20.17	20.19	20.41	20.65	20.17	20.42
Cr2O3	0.02	0.01	0.02	0.04	0.03	0.03	0.02	0.06	0.02	0.04	0.03	0.04	0.06	0.01	0.01	0.09	0.02	0.04	0.00	0.04	0.04
FeO	18.07	18.41	18.17	18.41	18.47	18.72	18.20	18.72	18.15	18.25	18.24	18.61	19.05	17.85	17.61	18.42	17.95	17.55	18.10	18.13	17.95
MnO	0.07	0.03	0.04	0.02	0.03	0.03	0.04	0.08	0.03	0.08	0.09	0.10	0.04	0.08	0.03	0.01	0.07	0.04	0.09	0.04	0.04
MgO	12.40	12.55	12.20	12.39	11.87	12.36	12.62	12.05	12.43	12.47	12.17	12.42	12.47	12.82	12.29	12.34	12.50	12.45	12.21	12.06	12.24
CaO	0.00	0.00	0.00	0.01	0.00	0.00	0.00	0.00	0.00	0.00	0.00	0.01	0.00	0.00	0.02	0.02	0.00	0.00	0.04	0.00	0.00
NaO	0.36	0.45	0.49	0.37	0.33	0.28	0.38	0.39	0.42	0.44	0.40	0.55	0.35	0.32	0.38	0.30	0.38	0.41	0.40	0.32	0.34
K2O	9.04	8.71	8.93	9.03	8.88	8.83	9.06	8.81	8.99	8.96	8.75	8.82	9.02	9.28	8.84	8.65	9.24	9.08	8.94	9.05	9.11
Total	97.97	97.56	97.30	98.35	98.00	98.06	97.53	98.31	98.39	98.47	98.15	98.77	98.97	98.72	97.57	98.34	98.75	98.60	98.71	98.18	98.48
Cations:																					
Si	2.67	2.66	2.68	2.68	2.67	2.68	2.65	2.69	2.67	2.68	2.69	2.67	2.67	2.68	2.66	2.68	2.68	2.68	2.67	2.69	2.68
Ti	0.08	0.08	0.08	0.07	0.08	0.08	0.08	0.08	0.08	0.08	0.08	0.08	0.08	0.07	0.09	0.08	0.08	0.09	0.08	0.08	0.08
Al	1.73	1.70	1.71	1.71	1.75	1.71	1.71	1.70	1.74	1.71	1.73	1.70	1.69	1.72	1.76	1.73	1.72	1.74	1.76	1.73	1.75
Cr	0.00	0.00	0.00	0.00	0.00	0.00	0.00	0.00	0.00	0.00	0.00	0.00	0.00	0.00	0.00	0.01	0.00	0.00	0.00	0.00	0.00
Fe	1.11	1.13	1.12	1.12	1.13	1.15	1.12	1.14	1.10	1.11	1.11	1.13	1.16	1.08	1.08	1.12	1.09	1.06	1.10	1.10	1.09
Mn	0.00	0.00	0.00	0.00	0.00	0.00	0.00	0.01	0.00	0.01	0.01	0.01	0.00	0.01	0.00	0.00	0.00	0.00	0.01	0.00	0.00
Mg	1.35	1.38	1.34	1.35	1.29	1.35	1.39	1.31	1.35	1.35	1.32	1.34	1.35	1.39	1.34	1.34	1.35	1.34	1.32	1.31	1.32
Ca	0.00	0.00	0.00	0.00	0.00	0.00	0.00	0.00	0.00	0.00	0.00	0.00	0.00	0.00	0.00	0.00	0.00	0.00	0.00	0.00	0.00
Na	0.05	0.06	0.07	0.05	0.05	0.04	0.05	0.06	0.06	0.06	0.06	0.08	0.05	0.05	0.05	0.04	0.05	0.06	0.06	0.05	0.05
K	0.84	0.82	0.84	0.84	0.83	0.82	0.85	0.82	0.83	0.83	0.81	0.82	0.84	0.86	0.82	0.80	0.85	0.84	0.83	0.84	0.84
Total (All)	7.83	7.84	7.84	7.83	7.81	7.82	7.86	7.81	7.83	7.83	7.80	7.84	7.84	7.84	7.81	7.80	7.83	7.81	7.81	7.81	7.81
Total (Majors ONLY)	7.83	7.84	7.84	7.83	7.80	7.82	7.86	7.81	7.83	7.83	7.80	7.84	7.84	7.84	7.81	7.79	7.83	7.81	7.81	7.80	7.81
Al(VI) (= (Si + Al) - 4)	0.40	0.37	0.39	0.39	0.42	0.39	0.36	0.40	0.41	0.39	0.42	0.38	0.37	0.40	0.42	0.41	0.40	0.42	0.43	0.42	0.42
Al(IV) (= Al - Al(VI))	1.33	1.34	1.32	1.32	1.33	1.32	1.35	1.31	1.33	1.32	1.31	1.33	1.33	1.32	1.34	1.32	1.32	1.32	1.33	1.31	1.32
Ti (apfu)	0.08	0.08	0.08	0.07	0.08	0.08	0.08	0.08	0.08	0.08	0.08	0.08	0.08	0.07	0.09	0.08	0.08	0.09	0.08	0.08	0.08
XFe (= Fe/(Fe + Mg))	0.45	0.45	0.46	0.45	0.47	0.46	0.45	0.47	0.45	0.45	0.46	0.46	0.46	0.44	0.45	0.46	0.45	0.44	0.45	0.46	0.45

Note: Analyses conducted on the same mineral grain (e.g. 1 core analysis and 2 rim analyses on a specific biotite grain) are highlighted in the same colour and enclosed in the same thick black box.

Biotites cont.

Analysis Label (Specimen_mineral_grain/zone:spot number)	gb13_bi_9b	gb13_bi_9d	gb13_bi_9c	gb13_bi_9e	gb13_chl_1d	gb13_chl_1c	gb13_chl_1a	gb13_chl_1b	gb13_chl_1f	gb13_chl_1e	gb13_chl_2b	gb13_chl_2c	gb13_chl_3a	gb13_chl_5c	gb13_chl_5e	gb13_chl_5g	gb13_chl_5f	gb13_chl_6b	gb13_chl_6c	gb13_chl_7d	gb13_chl_7c
Mineral Probed:	bi	bi	bi	bi	bi	bi	bi	bi	bi	bi	bi	bi	bi	bi	bi	bi	bi	bi	bi	bi	bi
Core/Rim/Int:	Rim	Int	Core	Rim	Rim	Int	Core	Core	Rim	Core	Int	Core	Core	Core	Int	Rim	Core	Int	Int	Rim	Rim
EMP Initial Results:																					
Oxide conc. (wt%)																					
SiO2	36.49	37.21	37.21	36.99	37.08	37.26	37.21	36.91	36.89	36.55	36.88	36.74	36.92	37.02	37.07	36.86	37.08	36.55	36.73	36.62	37.17
TiO2	1.54	1.46	1.53	1.52	1.48	1.29	1.46	1.51	1.52	1.46	1.48	1.48	1.46	1.48	1.46	1.46	1.51	1.51	1.54	1.38	1.35
Al2O3	20.30	20.72	20.66	20.23	20.30	21.17	20.33	20.42	20.31	20.22	20.24	20.18	20.08	20.20	19.82	20.12	20.47	19.76	19.87	21.67	20.40
Cr2O3	0.06	0.05	0.04	0.01	0.02	0.00	0.04	0.03	0.03	0.00	0.01	0.03	0.00	0.06	0.00	0.01	0.04	0.00	0.00	0.03	0.01
FeO	17.44	17.95	17.39	17.98	18.70	16.97	18.40	18.36	18.41	18.66	18.65	18.41	18.87	18.61	17.76	18.31	18.09	18.91	18.17	17.55	18.51
MnO	0.03	0.00	0.03	0.11	0.03	0.01	0.06	0.07	0.06	0.09	0.02	0.07	0.05	0.06	0.03	0.01	0.05	0.06	0.04	0.06	0.09
MgO	12.54	12.28	12.47	12.46	12.28	12.10	12.32	12.19	12.10	12.25	12.41	12.48	12.15	12.17	12.60	12.30	12.54	12.34	12.30	12.04	12.32
CaO	0.00	0.00	0.00	0.02	0.00	0.00	0.00	0.00	0.00	0.00	0.00	0.00	0.00	0.00	0.00	0.00	0.00	0.00	0.00	0.00	0.00
NaO	0.35	0.41	0.34	0.36	0.30	0.39	0.30	0.27	0.27	0.35	0.36	0.38	0.30	0.30	0.32	0.29	0.28	0.24	0.34	0.29	0.30
K2O	9.02	9.05	9.03	8.84	9.16	9.16	9.15	9.08	9.26	8.64	8.93	8.09	8.15	8.82	8.53	8.05	8.25	9.12	9.15	8.20	8.50
Total	97.77	99.13	98.70	98.52	99.35	98.35	99.28	98.83	98.85	98.22	98.98	97.86	97.99	98.72	97.60	97.40	98.32	98.49	98.13	97.83	98.66
Cations:																					
Si	2.66	2.68	2.68	2.68	2.68	2.69	2.68	2.67	2.68	2.67	2.67	2.68	2.69	2.68	2.70	2.69	2.68	2.67	2.68	2.65	2.69
Ti	0.08	0.08	0.08	0.08	0.08	0.07	0.08	0.08	0.08	0.08	0.08	0.08	0.08	0.08	0.08	0.08	0.08	0.08	0.08	0.08	0.07
Al	1.75	1.76	1.76	1.73	1.73	1.80	1.73	1.74	1.74	1.74	1.73	1.73	1.72	1.73	1.70	1.73	1.75	1.70	1.71	1.85	1.74
Cr	0.00	0.00	0.00	0.00	0.00	0.00	0.00	0.00	0.00	0.00	0.00	0.00	0.00	0.00	0.00	0.00	0.00	0.00	0.00	0.00	0.00
Fe	1.06	1.08	1.05	1.09	1.13	1.02	1.11	1.11	1.12	1.14	1.13	1.12	1.15	1.13	1.08	1.12	1.09	1.15	1.11	1.06	1.12
Mn	0.00	0.00	0.00	0.01	0.00	0.00	0.00	0.00	0.00	0.01	0.00	0.00	0.00	0.00	0.00	0.00	0.00	0.00	0.00	0.00	0.01
Mg	1.36	1.32	1.34	1.35	1.32	1.30	1.32	1.32	1.31	1.33	1.34	1.36	1.32	1.32	1.37	1.34	1.35	1.34	1.34	1.30	1.33
Ca	0.00	0.00	0.00	0.00	0.00	0.00	0.00	0.00	0.00	0.00	0.00	0.00	0.00	0.00	0.00	0.00	0.00	0.00	0.00	0.00	0.00
Na	0.05	0.06	0.05	0.05	0.04	0.05	0.04	0.04	0.04	0.05	0.05	0.05	0.04	0.04	0.05	0.04	0.04	0.03	0.05	0.04	0.04
K	0.84	0.83	0.83	0.82	0.84	0.84	0.84	0.84	0.86	0.80	0.82	0.75	0.76	0.82	0.79	0.75	0.76	0.85	0.85	0.76	0.78
Total (All)	7.82	7.81	7.79	7.81	7.82	7.79	7.81	7.81	7.82	7.81	7.82	7.78	7.77	7.80	7.78	7.76	7.76	7.84	7.83	7.75	7.78
Total (Majors ONLY)	7.82	7.80	7.79	7.80	7.82	7.79	7.81	7.81	7.82	7.81	7.82	7.78	7.77	7.80	7.78	7.76	7.76	7.84	7.83	7.74	7.78
Al(VI) (= (Si + Al) - 4)	0.41	0.44	0.44	0.41	0.40	0.49	0.41	0.42	0.41	0.40	0.40	0.41	0.41	0.41	0.41	0.43	0.43	0.37	0.39	0.50	0.43
Al(IV) (= Al - Al(VI))	1.34	1.32	1.32	1.32	1.32	1.31	1.32	1.33	1.32	1.33	1.33	1.32	1.31	1.32	1.30	1.31	1.32	1.33	1.32	1.35	1.31
Ti (apfu)	0.08	0.08	0.08	0.08	0.08	0.07	0.08	0.08	0.08	0.08	0.08	0.08	0.08	0.08	0.08	0.08	0.08	0.08	0.08	0.08	0.07
XFe (= Fe/(Fe + Mg))	0.44	0.45	0.44	0.45	0.46	0.44	0.46	0.46	0.46	0.46	0.46	0.45	0.47	0.46	0.44	0.46	0.45	0.46	0.45	0.45	0.46

Note: Analyses conducted on the same mineral grain (e.g. 1 core analysis and 2 rim analyses on a specific biotite grain) are highlighted in the same colour and enclosed in the same thick black box.

Biotites cont.

Analysis Label (Specimen_mineral_grain/zone:spot number)	gb13_chl_7b	gb13_chl_8b	gb13_chl_8d	gb13_chl_8f	gb13_chl_8a	gb13_chl_9b	gb13_chl_9a	ma29_bi_1c	ma29_bi_1b	ma29_bi_1a	ma29_bi_1d	ma29_bi_1e	ma29_bi_2a	ma29_bi_2c	ma29_bi_2b	ma29_bi_2e	ma29_bi_2f	ma29_bi_3a	ma29_bi_3e	ma29_bi_3b	ma29_bi_3d
Mineral Probed:	bi	bi	bi	bi	bi	bi	bi	bi	bi	bi	bi	bi	bi	bi	bi	bi	bi	bi	bi	bi	bi
Core/Rim/Int:	Int	Rim	Int	Core	Core	Int	Core	Rim	Int	Core	Core	Rim	Core	Rim	Core	Rim	Core	Rim	Int	Core	Rim
EMP Initial Results:																					
Oxide conc. (wt%)																					
SiO2	36.95	36.28	36.90	36.74	36.68	36.93	36.52	36.35	36.86	37.11	36.60	36.91	36.55	37.45	36.78	36.73	37.19	37.03	36.80	37.14	36.58
TiO2	1.47	1.43	1.41	1.55	1.40	1.40	1.44	1.46	1.60	1.50	1.47	1.57	1.46	1.23	1.48	1.46	1.42	1.77	1.84	1.46	1.60
Al2O3	20.20	20.31	19.95	20.33	20.18	20.43	20.09	19.74	20.15	20.18	19.85	20.41	20.12	20.37	20.20	20.40	20.29	20.37	20.59	20.41	20.04
Cr2O3	0.04	0.00	0.02	0.03	0.01	0.00	0.01	0.00	0.03	0.01	0.02	0.05	0.04	0.06	0.06	0.02	0.01	0.07	0.02	0.03	0.00
FeO	18.07	18.35	18.76	18.24	18.12	18.48	18.59	19.18	19.11	18.64	18.62	17.87	18.58	18.22	18.65	18.09	18.67	18.38	18.44	18.20	18.92
MnO	0.11	0.09	0.06	0.06	0.02	0.05	0.07	0.07	0.00	0.04	0.03	0.05	0.05	0.09	0.01	0.05	0.04	0.04	0.04	0.06	0.04
MgO	12.24	12.27	12.04	12.17	12.38	11.99	12.19	11.70	11.79	11.84	11.81	11.49	11.49	11.88	11.66	11.74	11.78	11.75	11.65	11.83	11.71
CaO	0.00	0.00	0.02	0.00	0.00	0.00	0.00	0.01	0.00	0.00	0.00	0.00	0.00	0.00	0.00	0.00	0.01	0.00	0.00	0.00	0.01
NaO	0.33	0.25	0.34	0.32	0.35	0.40	0.35	0.26	0.27	0.34	0.28	0.34	0.30	0.35	0.31	0.29	0.31	0.28	0.29	0.33	0.24
K2O	8.36	8.55	8.27	8.10	8.99	9.12	8.96	8.77	8.93	9.01	8.81	8.92	8.85	8.88	8.90	8.96	8.95	9.04	8.83	8.97	8.82
Total	97.77	97.53	97.76	97.54	98.13	98.80	98.23	97.54	98.75	98.67	97.49	97.61	97.45	98.53	98.05	97.74	98.67	98.72	98.49	98.42	97.96
Cations:																					
Si	2.69	2.66	2.70	2.68	2.67	2.68	2.67	2.68	2.68	2.69	2.69	2.70	2.69	2.71	2.69	2.69	2.70	2.68	2.67	2.70	2.68
Ti	0.08	0.08	0.08	0.08	0.08	0.08	0.08	0.08	0.09	0.08	0.08	0.09	0.08	0.07	0.08	0.08	0.08	0.10	0.10	0.08	0.09
Al	1.73	1.76	1.72	1.75	1.73	1.75	1.73	1.72	1.73	1.73	1.72	1.76	1.74	1.74	1.74	1.76	1.73	1.74	1.76	1.75	1.73
Cr	0.00	0.00	0.00	0.00	0.00	0.00	0.00	0.00	0.00	0.00	0.00	0.00	0.00	0.00	0.00	0.00	0.00	0.00	0.00	0.00	0.00
Fe	1.10	1.13	1.15	1.11	1.10	1.12	1.14	1.18	1.16	1.13	1.14	1.09	1.14	1.10	1.14	1.11	1.13	1.11	1.12	1.10	1.16
Mn	0.01	0.01	0.00	0.00	0.00	0.00	0.00	0.00	0.00	0.00	0.00	0.00	0.00	0.01	0.00	0.00	0.00	0.00	0.00	0.00	0.00
Mg	1.33	1.34	1.31	1.32	1.35	1.30	1.33	1.29	1.28	1.28	1.29	1.25	1.26	1.28	1.27	1.28	1.27	1.27	1.26	1.28	1.28
Ca	0.00	0.00	0.00	0.00	0.00	0.00	0.00	0.00	0.00	0.00	0.00	0.00	0.00	0.00	0.00	0.00	0.00	0.00	0.00	0.00	0.00
Na	0.05	0.04	0.05	0.05	0.05	0.06	0.05	0.04	0.04	0.05	0.04	0.05	0.04	0.05	0.04	0.04	0.04	0.04	0.04	0.05	0.03
K	0.78	0.80	0.77	0.75	0.84	0.84	0.84	0.82	0.83	0.83	0.83	0.83	0.83	0.82	0.83	0.84	0.83	0.84	0.82	0.83	0.82
Total (All)	7.77	7.80	7.78	7.76	7.82	7.82	7.83	7.81	7.80	7.80	7.80	7.77	7.79	7.78	7.80	7.79	7.79	7.79	7.78	7.79	7.80
Total (Majors ONLY)	7.77	7.80	7.77	7.76	7.82	7.82	7.83	7.81	7.80	7.80	7.80	7.77	7.79	7.78	7.79	7.79	7.79	7.78	7.77	7.79	7.80
Al(VI) (= (Si + Al) - 4)	0.43	0.42	0.41	0.43	0.41	0.42	0.40	0.40	0.41	0.42	0.41	0.46	0.43	0.45	0.43	0.44	0.43	0.42	0.43	0.44	0.41
Al(IV) (= Al - Al(VI))	1.31	1.34	1.30	1.32	1.33	1.32	1.33	1.32	1.32	1.31	1.31	1.30	1.31	1.29	1.31	1.31	1.30	1.32	1.33	1.30	1.32
Ti (apfu)	0.08	0.08	0.08	0.08	0.08	0.08	0.08	0.08	0.09	0.08	0.08	0.09	0.08	0.07	0.08	0.08	0.08	0.10	0.10	0.08	0.09
XFe (= Fe/(Fe + Mg))	0.45	0.46	0.47	0.46	0.45	0.46	0.46	0.48	0.48	0.47	0.47	0.47	0.48	0.46	0.47	0.46	0.47	0.47	0.47	0.46	0.48

Note: Analyses conducted on the same mineral grain (e.g. 1 core analysis and 2 rim analyses on a specific biotite grain) are highlighted in the same colour and enclosed in the same thick black box.

Biotites cont.

Analysis Label (Specimen_mineral_grain/zone:spot number)	ma29_bi_3c	ma29_bi_3g	ma29_bi_3f	ma29_bi_4b	ma29_bi_4a	ma29_bi_5c	ma29_bi_5a	ma29_bi_6a	ma29_bi_6b	ma29_bi_7c	ma29_bi_7d	ma29_bi_7a	ma29_bi_7e	ma29_bi_8b	ma29_bi_8c	ma29_bi_8a	ma29_bi_10a	ma29_bi_10b	ma29_bi_10c	ma29_mu_6x	ma29_chl_1e	ma29_chl_3c
Mineral Probed:	bi	bi	bi	bi	bi	bi	bi	bi	bi	bi	bi	bi	bi	bi	bi	bi	bi	bi	bi	bi	bi	bi
Core/Int/Rim:	Core	Rim	Core	Rim	Core	Int	Core	Core	Core	Rim	Int	Core	Rim	Rim	Int	Core	Core	Core	Core	Core	Int	Rim
EMP Initial Results:																						
Oxide conc. (wt%)																						
SiO2	37.09	36.81	36.26	36.96	36.95	36.95	36.59	37.34	36.60	35.41	36.55	36.46	36.46	36.72	36.47	37.01	36.18	36.08	36.65	36.20	36.92	36.75
TiO2	1.45	1.70	1.59	1.52	1.45	1.46	1.43	1.50	1.43	1.29	1.43	1.47	1.52	1.50	1.46	1.44	1.34	1.47	1.56	1.62	1.53	1.68
Al2O3	20.20	20.12	20.21	20.43	20.45	20.25	20.15	20.39	20.22	20.14	20.48	19.98	20.43	20.52	20.24	20.28	19.98	20.13	20.48	20.04	20.36	20.20
Cr2O3	0.03	0.04	0.03	0.00	0.03	0.01	0.02	0.04	0.02	0.03	0.03	0.00	0.04	0.01	0.01	0.02	0.02	0.05	0.02	0.03	0.03	0.05
FeO	18.08	18.42	18.50	18.05	18.29	18.26	18.76	18.56	18.06	19.42	18.69	18.62	18.33	18.17	18.05	18.75	18.89	19.38	18.44	18.11	18.55	18.12
MnO	0.05	0.03	0.09	0.06	0.05	0.09	0.05	0.01	0.04	0.06	0.00	0.06	0.01	0.05	0.04	0.02	0.06	0.00	0.11	0.03	0.09	0.01
MgO	11.89	12.01	11.75	11.72	11.54	11.73	11.82	11.91	12.11	12.28	11.61	11.99	11.78	11.76	11.85	11.98	12.42	12.70	11.83	12.12	11.89	11.86
CaO	0.00	0.01	0.00	0.00	0.00	0.00	0.00	0.00	0.00	0.00	0.00	0.00	0.00	0.00	0.02	0.00	0.00	0.00	0.00	0.00	0.00	0.00
NaO	0.32	0.32	0.31	0.27	0.28	0.30	0.31	0.30	0.31	0.27	0.32	0.33	0.32	0.25	0.33	0.33	0.27	0.32	0.31	0.33	0.33	0.30
K2O	9.04	8.88	8.68	8.85	8.91	8.95	8.86	8.90	8.99	8.20	8.98	8.87	8.81	9.01	8.69	8.62	8.46	8.34	9.03	8.56	8.78	9.04
Total	98.14	98.34	97.41	97.86	97.95	97.99	97.99	98.95	97.78	97.09	98.09	97.78	97.70	97.99	97.16	98.44	97.63	98.48	98.42	97.04	98.48	98.01
Cations:																						
Si	2.70	2.68	2.67	2.70	2.70	2.70	2.68	2.70	2.68	2.62	2.67	2.67	2.67	2.68	2.68	2.69	2.66	2.63	2.67	2.67	2.68	2.68
Ti	0.08	0.09	0.09	0.08	0.08	0.08	0.08	0.08	0.08	0.07	0.08	0.08	0.08	0.08	0.08	0.08	0.07	0.08	0.09	0.09	0.08	0.09
Al	1.73	1.73	1.75	1.76	1.76	1.74	1.74	1.74	1.74	1.76	1.76	1.73	1.76	1.76	1.75	1.74	1.73	1.73	1.76	1.74	1.74	1.74
Cr	0.00	0.00	0.00	0.00	0.00	0.00	0.00	0.00	0.00	0.00	0.00	0.00	0.00	0.00	0.00	0.00	0.00	0.00	0.00	0.00	0.00	0.00
Fe	1.10	1.12	1.14	1.10	1.12	1.11	1.15	1.12	1.11	1.20	1.14	1.14	1.12	1.11	1.11	1.14	1.16	1.18	1.12	1.12	1.13	1.11
Mn	0.00	0.00	0.01	0.00	0.00	0.01	0.00	0.00	0.00	0.00	0.00	0.00	0.00	0.00	0.00	0.00	0.00	0.00	0.01	0.00	0.01	0.00
Mg	1.29	1.30	1.29	1.27	1.26	1.28	1.29	1.28	1.32	1.36	1.27	1.31	1.29	1.28	1.30	1.30	1.36	1.38	1.28	1.33	1.29	1.29
Ca	0.00	0.00	0.00	0.00	0.00	0.00	0.00	0.00	0.00	0.00	0.00	0.00	0.00	0.00	0.00	0.00	0.00	0.00	0.00	0.00	0.00	0.00
Na	0.04	0.04	0.04	0.04	0.04	0.04	0.04	0.04	0.04	0.04	0.05	0.05	0.05	0.04	0.05	0.05	0.04	0.05	0.04	0.05	0.05	0.04
K	0.84	0.82	0.81	0.82	0.83	0.83	0.83	0.82	0.84	0.78	0.84	0.83	0.82	0.84	0.82	0.80	0.79	0.78	0.84	0.80	0.81	0.84
Total (All)	7.79	7.80	7.80	7.77	7.78	7.79	7.81	7.78	7.81	7.83	7.81	7.82	7.80	7.79	7.79	7.79	7.82	7.83	7.81	7.80	7.79	7.80
Total (Majors ONLY)	7.79	7.80	7.80	7.77	7.78	7.79	7.81	7.78	7.81	7.83	7.81	7.82	7.80	7.79	7.79	7.79	7.82	7.83	7.81	7.80	7.79	7.79
Al(VI) (= (Si + Al) - 4)	0.43	0.41	0.42	0.45	0.45	0.44	0.42	0.43	0.42	0.38	0.44	0.40	0.43	0.44	0.44	0.42	0.39	0.36	0.43	0.41	0.43	0.42
Al(IV) (= Al - Al(VI))	1.30	1.32	1.33	1.30	1.30	1.30	1.32	1.30	1.32	1.38	1.33	1.33	1.33	1.32	1.32	1.31	1.34	1.37	1.33	1.33	1.32	1.32
Ti (apfu)	0.08	0.09	0.09	0.08	0.08	0.08	0.08	0.08	0.08	0.07	0.08	0.08	0.08	0.08	0.08	0.08	0.07	0.08	0.09	0.09	0.08	0.09
XFe (= Fe/(Fe + Mg))	0.46	0.46	0.47	0.46	0.47	0.47	0.47	0.47	0.46	0.47	0.47	0.47	0.47	0.46	0.46	0.47	0.46	0.46	0.47	0.46	0.47	0.46

Note: Analyses conducted on the same mineral grain (e.g. 1 core analysis and 2 rim analyses on a specific biotite grain) are highlighted in the same colour and enclosed in the same thick black box.

Biotites cont.

Analysis Label (Specimen_mineral_grain/zone:spot number)	ma31_bi_1c	ma31_bi_4b	ma31_bi_4e	ma31_bi_4c	ma31_bi_4a	ma31_bi_5c	ma31_bi_5a	ma31_bi_5b	ma38_bi_2a	ma38_bi_2g	ma38_bi_2b	ma38_bi_2h	ma40_bi_1b	ma40_bi_1a	ma40_bi_1d	ma40_bi_1c	ma40_bi_2a	ma40_bi_2b	ma40_bi_2c	ma40_bi_2e	ma40_bi_2d	ma40_bi_2f
Mineral Probed:	bi	bi	bi	bi	bi	bi	bi	bi	bi	bi	bi	bi	bi	bi	bi	bi	bi	bi	bi	bi	bi	bi
Core/Int/Rim:	Rim	Rim	Int	Core	Int	Rim	Core	Core	Rim	Rim	Core	Rim	Rim	Core	Rim	Core	Rim	Core	Core	Rim	Core	Int
EMP Initial Results:																						
Oxide conc. (wt%)																						
SiO2	36.84	37.23	36.95	36.95	36.91	36.77	36.84	37.08	37.99	37.32	37.71	37.81	36.65	37.06	36.79	37.30	36.30	36.65	36.97	36.88	37.10	36.69
TiO2	1.51	1.48	1.50	1.39	1.46	1.62	1.49	1.48	1.45	1.47	1.47	1.52	1.41	1.47	1.43	1.49	1.38	1.46	1.62	1.46	1.45	1.47
Al2O3	20.19	20.38	20.61	20.69	20.00	20.54	20.64	20.45	20.62	20.74	20.72	20.78	20.48	20.43	20.33	20.15	20.21	20.29	20.20	20.18	20.58	20.54
Cr2O3	0.03	0.00	0.01	0.04	0.04	0.05	0.04	0.01	0.04	0.05	0.04	0.06	0.05	0.02	0.04	0.04	0.04	0.07	0.03	0.04	0.06	0.04
FeO	18.08	16.91	16.86	16.67	17.06	17.91	17.87	17.56	16.19	16.19	15.76	15.68	17.81	17.52	17.85	17.66	18.35	17.69	17.70	17.48	17.54	17.74
MnO	0.05	0.06	0.10	0.10	0.08	0.08	0.09	0.10	0.06	0.07	0.07	0.07	0.07	0.08	0.14	0.02	0.08	0.07	0.07	0.07	0.06	0.00
MgO	11.82	12.28	12.34	12.31	12.40	12.11	11.92	11.84	12.84	12.72	12.94	12.62	11.96	11.74	11.85	12.00	12.12	12.23	11.77	11.94	11.82	12.15
CaO	0.00	0.00	0.00	0.00	0.00	0.00	0.00	0.00	0.00	0.00	0.00	0.04	0.00	0.02	0.00	0.01	0.00	0.00	0.00	0.01	0.01	0.01
NaO	0.24	0.23	0.30	0.31	0.24	0.36	0.33	0.32	0.35	0.37	0.36	0.41	0.17	0.28	0.17	0.25	0.17	0.16	0.27	0.25	0.28	0.22
K2O	8.36	9.35	9.07	8.95	9.25	8.69	9.03	8.96	8.38	8.55	8.73	8.60	8.95	8.79	9.06	8.83	8.53	9.11	8.87	9.10	8.82	8.63
Total	97.10	97.93	97.74	97.41	97.45	98.12	98.25	97.80	97.92	97.48	97.80	97.60	97.55	97.41	97.67	97.74	97.18	97.74	97.50	97.40	97.71	97.48
Cations:																						
Si	2.70	2.70	2.69	2.69	2.70	2.67	2.68	2.70	2.73	2.70	2.72	2.72	2.68	2.71	2.69	2.72	2.67	2.68	2.70	2.70	2.70	2.68
Ti	0.08	0.08	0.08	0.08	0.08	0.09	0.08	0.08	0.08	0.08	0.08	0.08	0.08	0.08	0.08	0.08	0.08	0.08	0.09	0.08	0.08	0.08
Al	1.75	1.75	1.77	1.78	1.72	1.76	1.77	1.76	1.75	1.77	1.76	1.77	1.77	1.76	1.75	1.73	1.75	1.75	1.74	1.74	1.77	1.77
Cr	0.00	0.00	0.00	0.00	0.00	0.00	0.00	0.00	0.00	0.00	0.00	0.00	0.00	0.00	0.00	0.00	0.00	0.00	0.00	0.00	0.00	0.00
Fe	1.11	1.03	1.03	1.02	1.04	1.09	1.09	1.07	0.97	0.98	0.95	0.95	1.09	1.07	1.09	1.08	1.13	1.08	1.08	1.07	1.07	1.08
Mn	0.00	0.00	0.01	0.01	0.01	0.01	0.01	0.01	0.00	0.00	0.00	0.00	0.00	0.00	0.01	0.00	0.00	0.00	0.00	0.00	0.00	0.00
Mg	1.29	1.33	1.34	1.34	1.35	1.31	1.29	1.29	1.38	1.37	1.39	1.36	1.30	1.28	1.29	1.30	1.33	1.33	1.28	1.30	1.28	1.32
Ca	0.00	0.00	0.00	0.00	0.00	0.00	0.00	0.00	0.00	0.00	0.00	0.00	0.00	0.00	0.00	0.00	0.00	0.00	0.00	0.00	0.00	0.00
Na	0.03	0.03	0.04	0.04	0.03	0.05	0.05	0.04	0.05	0.05	0.05	0.06	0.02	0.04	0.02	0.04	0.02	0.02	0.04	0.04	0.04	0.03
K	0.78	0.87	0.84	0.83	0.86	0.81	0.84	0.83	0.77	0.79	0.80	0.79	0.84	0.82	0.85	0.82	0.80	0.85	0.83	0.85	0.82	0.80
Total (All)	7.75	7.79	7.79	7.78	7.81	7.79	7.80	7.78	7.73	7.75	7.75	7.73	7.79	7.76	7.79	7.76	7.79	7.80	7.77	7.79	7.76	7.77
Total (Majors ONLY)	7.75	7.79	7.79	7.78	7.80	7.78	7.79	7.78	7.72	7.75	7.75	7.73	7.78	7.76	7.79	7.76	7.79	7.80	7.77	7.79	7.76	7.77
Al(VI) (= (Si + Al) - 4)	0.45	0.45	0.45	0.47	0.42	0.43	0.45	0.46	0.48	0.47	0.47	0.49	0.45	0.47	0.44	0.45	0.42	0.43	0.44	0.44	0.47	0.45
Al(IV) (= Al - Al(VI))	1.30	1.30	1.31	1.31	1.30	1.33	1.32	1.30	1.27	1.30	1.28	1.28	1.32	1.29	1.31	1.28	1.33	1.32	1.30	1.30	1.30	1.32
Ti (apfu)	0.08	0.08	0.08	0.08	0.08	0.09	0.08	0.08	0.08	0.08	0.08	0.08	0.08	0.08	0.08	0.08	0.08	0.08	0.09	0.08	0.08	0.08
XFe (= Fe/(Fe + Mg))	0.46	0.44	0.43	0.43	0.44	0.45	0.46	0.45	0.41	0.42	0.41	0.41	0.46	0.46	0.46	0.45	0.46	0.45	0.46	0.45	0.45	0.45

Note: Analyses conducted on the same mineral grain (e.g. 1 core analysis and 2 rim analyses on a specific biotite grain) are highlighted in the same colour and enclosed in the same thick black box.

Biotites cont.

Analysis Label (Specimen_mineral_grain/zone:spot number)	ma40_bi_3f	ma40_bi_3b	ma40_bi_3a	ma40_bi_3c	ma40_bi_3e	ma40_bi_3d	ma40_bi_4f	ma40_bi_4e	ma40_bi_4d	ma40_bi_4a	ma40_bi_4c	ma40_bi_4b	ma40_bi_4g	ma40_bi_5b2	ma40_bi_5e	ma40_bi_5d	ma40_bi_5a	ma40_bi_5c	ma40_bi_5g	ma40_bi_6b	ma40_bi_6a	ma40_mu_4u
Mineral Probed:	bi	bi	bi	bi	bi	bi	bi	bi	bi	bi	bi	bi	bi	bi	bi	bi	bi	bi	bi	bi	bi	bi
Core/Int/Rim:	Rim	Int	Core	Core	Core	Rim	Rim	Int	Int	Core	Int	Int	Rim	Rim	Rim	Core	Rim	Core	Int	Rim	Core	Core
EMP Initial Results:																						
Oxide conc. (wt%)																						
SiO2	36.94	36.93	37.48	37.22	36.97	37.08	36.46	37.20	37.12	36.79	37.16	37.11	36.14	36.92	37.04	37.28	37.27	37.10	36.97	36.68	36.74	37.20
TiO2	1.50	1.66	1.61	1.53	1.45	1.69	1.52	1.55	1.54	1.54	1.63	1.57	1.54	1.51	1.54	1.55	1.57	1.53	1.43	1.45	1.46	1.44
Al2O3	20.34	20.42	20.31	20.65	20.64	20.38	20.12	20.31	20.29	19.90	20.60	20.46	20.32	20.44	20.56	20.35	20.51	20.40	20.63	20.72	20.53	20.45
Cr2O3	0.01	0.02	0.03	0.04	0.03	0.05	0.04	0.04	0.04	0.01	0.01	0.06	0.05	0.02	0.01	0.04	0.01	0.05	0.06	0.02	0.04	0.02
FeO	17.45	17.02	17.57	18.07	17.58	17.90	17.64	17.75	17.43	18.28	17.47	17.83	18.40	18.13	17.85	17.23	17.25	17.72	17.54	17.62	17.67	17.52
MnO	0.03	0.10	0.08	0.03	0.07	0.01	0.05	0.06	0.01	0.10	0.05	0.04	0.08	0.08	0.05	0.09	0.08	0.06	0.00	0.06	0.08	0.05
MgO	11.96	11.85	11.90	12.17	12.15	11.73	11.83	11.78	12.04	11.83	11.87	11.85	12.29	12.13	11.94	11.92	12.03	11.92	12.21	11.85	11.95	12.28
CaO	0.00	0.01	0.00	0.00	0.00	0.02	0.00	0.00	0.00	0.00	0.01	0.00	0.00	0.01	0.00	0.03	0.02	0.00	0.00	0.00	0.00	0.00
NaO	0.26	0.28	0.32	0.28	0.21	0.28	0.33	0.26	0.24	0.23	0.20	0.23	0.19	0.32	0.27	0.30	0.31	0.26	0.25	0.26	0.22	0.23
K2O	9.04	8.87	8.84	8.67	8.91	9.02	9.00	9.07	8.94	8.86	9.03	8.80	8.57	8.84	8.89	8.77	8.88	8.95	9.05	9.06	9.05	9.07
Total	97.54	97.16	98.14	98.67	98.01	98.16	97.00	98.02	97.66	97.54	98.02	97.96	97.58	98.39	98.16	97.55	97.93	97.99	98.14	97.73	97.73	98.25
Cations:																						
Si	2.70	2.70	2.72	2.69	2.69	2.70	2.69	2.71	2.70	2.70	2.70	2.70	2.65	2.68	2.69	2.71	2.70	2.70	2.68	2.68	2.68	2.70
Ti	0.08	0.09	0.09	0.08	0.08	0.09	0.08	0.08	0.08	0.09	0.09	0.09	0.09	0.08	0.08	0.08	0.09	0.08	0.08	0.08	0.08	0.08
Al	1.75	1.76	1.74	1.76	1.77	1.75	1.75	1.74	1.74	1.72	1.76	1.75	1.76	1.75	1.76	1.75	1.75	1.75	1.77	1.78	1.77	1.75
Cr	0.00	0.00	0.00	0.00	0.00	0.00	0.00	0.00	0.00	0.00	0.00	0.00	0.00	0.00	0.00	0.00	0.00	0.00	0.00	0.00	0.00	0.00
Fe	1.07	1.04	1.06	1.09	1.07	1.09	1.09	1.08	1.06	1.12	1.06	1.08	1.13	1.10	1.08	1.05	1.05	1.08	1.06	1.08	1.08	1.06
Mn	0.00	0.01	0.01	0.00	0.00	0.00	0.00	0.00	0.00	0.01	0.00	0.00	0.01	0.00	0.00	0.01	0.00	0.00	0.00	0.00	0.00	0.00
Mg	1.30	1.29	1.29	1.31	1.32	1.27	1.30	1.28	1.31	1.29	1.28	1.28	1.34	1.31	1.29	1.29	1.30	1.29	1.32	1.29	1.30	1.33
Ca	0.00	0.00	0.00	0.00	0.00	0.00	0.00	0.00	0.00	0.00	0.00	0.00	0.00	0.00	0.00	0.00	0.00	0.00	0.00	0.00	0.00	0.00
Na	0.04	0.04	0.04	0.04	0.03	0.04	0.05	0.04	0.03	0.03	0.03	0.03	0.03	0.04	0.04	0.04	0.04	0.04	0.04	0.04	0.03	0.03
K	0.84	0.83	0.82	0.80	0.83	0.84	0.85	0.84	0.83	0.83	0.84	0.82	0.80	0.82	0.82	0.81	0.82	0.83	0.84	0.84	0.84	0.84
Total (All)	7.78	7.76	7.76	7.77	7.78	7.78	7.80	7.78	7.77	7.79	7.76	7.76	7.80	7.79	7.78	7.75	7.77	7.78	7.79	7.79	7.79	7.79
Total (Majors ONLY)	7.78	7.76	7.76	7.77	7.78	7.77	7.80	7.77	7.77	7.79	7.76	7.76	7.80	7.79	7.78	7.75	7.76	7.77	7.79	7.79	7.79	7.78
Al(VI) (= (Si + Al) - 4)	0.45	0.46	0.45	0.44	0.45	0.44	0.43	0.45	0.45	0.42	0.46	0.45	0.41	0.43	0.45	0.46	0.46	0.45	0.45	0.46	0.45	0.44
Al(IV) (= Al - Al(VI))	1.30	1.30	1.28	1.31	1.31	1.30	1.31	1.29	1.30	1.30	1.30	1.30	1.35	1.32	1.31	1.29	1.30	1.30	1.32	1.32	1.32	1.30
Ti (apfu)	0.08	0.09	0.09	0.08	0.08	0.09	0.08	0.08	0.08	0.09	0.09	0.09	0.09	0.08	0.08	0.08	0.09	0.08	0.08	0.08	0.08	0.08
XFe (= Fe/(Fe + Mg))	0.45	0.45	0.45	0.45	0.45	0.46	0.46	0.46	0.45	0.46	0.45	0.46	0.46	0.46	0.46	0.45	0.45	0.45	0.45	0.45	0.45	0.44

Note: Analyses conducted on the same mineral grain (e.g. 1 core analysis and 2 rim analyses on a specific biotite grain) are highlighted in the same colour and enclosed in the same thick black box.

Chlorites

Analysis Label (Specimen_mineral grain/zone:spot number)	gb8_chl_2a	gb8_chl_2b	gb8_chl_2c	gb8_chl_2d	gb8_chl_2e	gb8_chl_3a	gb8_chl_3c	gb8_chl_3e	gb8_chl_3b	gb8_chl_3d	gb8_chl_4b	gb8_chl_4c	gb8_chl_4d	gb8_chl_4f	gb8_chl_5a	gb8_chl_5e	gb8_chl_5b	gb8_chl_5c	gb8_chl_5d	gb8_chl_5f	gb8_chl_6b
Mineral Probed:	chl	chl	chl	chl	chl	chl	chl	chl	chl	chl	chl	chl	chl	chl	chl	chl	chl	chl	chl	chl	chl
Core/Int/Rim:	Rim	Int	Int	Core	Int	Rim	Rim	Int	Core	Rim	Rim	Int	Core	Core	Rim	Rim	Int	Core	Int	Rim	Rim
EMP Initial Results:																					
Oxide conc. (wt%)																					
SiO2	25.36	26.08	25.45	26.01	25.86	25.76	25.98	25.88	25.64	25.37	25.64	25.49	25.65	25.45	25.71	25.57	26.05	25.94	26.07	25.82	26.39
TiO2	0.10	0.08	0.10	0.07	0.07	0.09	0.07	0.10	0.07	0.06	0.01	0.09	0.06	0.08	0.06	0.11	0.08	0.09	0.09	0.07	0.06
Al2O3	24.21	23.80	24.40	24.26	23.93	23.88	24.52	24.47	24.19	24.22	24.68	24.66	24.65	25.08	24.76	23.84	23.99	23.85	24.13	24.72	24.07
Cr2O3	0.00	0.01	0.00	0.01	0.03	0.03	0.01	0.00	0.01	0.00	0.04	0.02	0.04	0.00	0.01	0.01	0.02	0.02	0.05	0.03	0.00
FeO	25.83	25.28	25.90	24.26	24.76	25.95	25.39	25.23	25.31	25.06	25.50	26.34	26.10	26.04	23.42	26.10	24.31	25.30	25.25	23.99	24.29
MnO	0.05	0.09	0.14	0.04	0.06	0.07	0.11	0.04	0.06	0.00	0.03	0.09	0.04	0.03	0.03	0.05	0.06	0.04	0.05	0.04	0.10
MgO	16.33	16.89	16.24	17.45	17.49	15.97	16.64	16.94	17.51	16.49	16.59	16.13	16.16	16.02	17.90	16.25	17.55	17.25	17.20	18.01	18.20
CaO	0.03	0.03	0.01	0.00	0.01	0.06	0.02	0.03	0.00	0.04	0.03	0.04	0.03	0.02	0.01	0.02	0.03	0.02	0.01	0.03	0.03
NaO	0.15	0.01	0.06	0.03	0.10	0.03	0.03	0.04	0.00	0.04	0.01	0.01	0.00	0.01	0.10	0.05	0.15	0.04	0.02	0.06	0.06
K2O	0.11	0.02	0.02	0.00	0.02	0.00	0.03	0.08	0.00	0.05	0.05	0.02	0.01	0.01	0.03	0.06	0.07	0.00	0.01	0.02	0.00
Total	92.17	92.29	92.33	92.14	92.33	91.84	92.81	92.81	92.80	91.34	92.58	92.90	92.74	92.74	92.03	92.06	92.31	92.55	92.88	92.79	93.20
Cations:																					
Si	2.54	2.59	2.54	2.58	2.57	2.58	2.57	2.56	2.54	2.55	2.54	2.53	2.55	2.53	2.54	2.56	2.58	2.57	2.57	2.54	2.58
Ti	0.01	0.01	0.01	0.00	0.01	0.01	0.01	0.01	0.01	0.00	0.00	0.01	0.00	0.01	0.00	0.01	0.01	0.01	0.01	0.01	0.00
Al	2.86	2.79	2.87	2.83	2.80	2.82	2.86	2.85	2.82	2.87	2.89	2.89	2.88	2.93	2.88	2.82	2.80	2.79	2.81	2.86	2.78
Cr	0.00	0.00	0.00	0.00	0.00	0.00	0.00	0.00	0.00	0.00	0.00	0.00	0.00	0.00	0.00	0.00	0.00	0.00	0.00	0.00	0.00
Fe	2.16	2.10	2.16	2.01	2.05	2.18	2.10	2.09	2.09	2.11	2.12	2.19	2.17	2.16	1.93	2.19	2.01	2.10	2.08	1.97	1.99
Mn	0.00	0.01	0.01	0.00	0.01	0.01	0.01	0.00	0.01	0.00	0.00	0.01	0.00	0.00	0.00	0.00	0.01	0.00	0.00	0.00	0.01
Mg	2.44	2.50	2.42	2.58	2.59	2.39	2.45	2.50	2.58	2.47	2.45	2.39	2.39	2.37	2.64	2.43	2.59	2.55	2.53	2.64	2.66
Ca	0.00	0.00	0.00	0.00	0.00	0.01	0.00	0.00	0.00	0.00	0.00	0.00	0.00	0.00	0.00	0.00	0.00	0.00	0.00	0.00	0.00
Na	0.03	0.00	0.01	0.01	0.02	0.01	0.01	0.01	0.00	0.01	0.00	0.00	0.00	0.00	0.02	0.01	0.03	0.01	0.00	0.01	0.01
K	0.01	0.00	0.00	0.00	0.00	0.00	0.00	0.01	0.00	0.01	0.01	0.00	0.00	0.00	0.00	0.01	0.01	0.00	0.00	0.00	0.00
Total (All)	10.05	10.01	10.02	10.01	10.04	10.00	10.00	10.02	10.05	10.02	10.02	10.02	10.01	10.00	10.02	10.03	10.03	10.03	10.02	10.03	10.03
Total (Majors ONLY)	10.05	10.01	10.02	10.01	10.04	10.00	10.00	10.02	10.05	10.02	10.01	10.02	10.00	10.00	10.02	10.03	10.03	10.03	10.01	10.03	10.03
Al(VI) (= (Si + Al) - 4)	1.39	1.38	1.41	1.41	1.36	1.41	1.42	1.41	1.36	1.42	1.43	1.42	1.43	1.46	1.42	1.38	1.38	1.36	1.38	1.40	1.36
Al(IV) (= Al - Al(VI))	1.46	1.41	1.46	1.42	1.43	1.42	1.43	1.44	1.46	1.45	1.46	1.47	1.45	1.47	1.46	1.44	1.42	1.43	1.43	1.46	1.42
XFe (= Fe/(Fe + Mg))	0.47	0.46	0.47	0.44	0.44	0.48	0.46	0.46	0.45	0.46	0.46	0.48	0.48	0.48	0.42	0.47	0.44	0.45	0.45	0.43	0.43

Note: Analyses conducted on the same mineral grain (e.g. 1 core analysis and 2 rim analyses on a specific chlorite grain) are highlighted in the same colour and enclosed in the same thick black box.

Chlorites cont.

Analysis Label (Specimen_mineral grain/zone:spot number)	gb8_chl_6e	gb8_chl_6a	gb8_chl_6c	gb8_chl_6d	gb8_chl_6f	gb8_chl_6g	gb8_chl_6h	gb8_chl_7a	gb8_chl_7e	gb8_chl_7c	gb8_chl_7b	gb8_chl_7d	gb8_chl_7f	gb8_chl_8a	gb8_chl_8d	gb8_chl_8b	gb8_chl_8c	gb8_chl_8e	gb8_bi_1a	gb8_bi_1b	gb8_bi_1c
Mineral Probed:	chl	chl	chl	chl	chl	chl	chl	chl	chl	chl	chl	chl	chl	chl	chl	chl	chl	chl	chl	chl	chl
Core/Int/Rim:	Rim	Int	Core	Core	Int	Rim	Rim	Rim	Rim	Int	Core	Int	Rim	Rim	Rim	Core	Core	Rim	Rim	Rim	Int
EMP Initial Results:																					
Oxide conc. (wt%)																					
SiO2	25.94	25.68	26.21	25.83	25.92	26.44	26.40	25.51	25.78	25.50	25.55	25.82	25.45	25.49	25.48	25.70	25.75	25.98	25.36	25.62	25.61
TiO2	0.09	0.05	0.08	0.08	0.06	0.12	0.07	0.10	0.08	0.07	0.13	0.06	0.09	0.10	0.04	0.09	0.07	0.09	0.05	0.10	0.09
Al2O3	24.57	24.60	24.23	25.15	24.35	23.81	23.90	24.53	24.53	24.32	24.77	23.83	24.45	24.78	24.52	24.59	24.45	24.14	24.46	23.93	24.80
Cr2O3	0.03	0.06	0.03	0.03	0.02	0.04	0.09	0.01	0.00	0.06	0.00	0.02	0.01	0.00	0.05	0.04	0.05	0.11	0.02	0.03	0.01
FeO	24.55	25.72	23.85	24.80	25.31	23.07	23.94	24.26	25.26	26.18	24.28	24.98	24.99	25.57	25.85	26.00	25.63	25.26	25.78	24.12	23.84
MnO	0.06	0.05	0.14	0.01	0.06	0.10	0.09	0.03	0.06	0.05	0.02	0.07	0.02	0.04	0.12	0.01	0.02	0.12	0.07	0.06	0.08
MgO	16.69	16.92	18.19	17.32	17.31	17.97	17.72	17.30	17.10	16.21	17.14	17.86	17.30	16.89	16.85	16.83	17.25	17.68	16.45	17.88	17.75
CaO	0.06	0.03	0.01	0.02	0.02	0.02	0.02	0.03	0.02	0.04	0.02	0.03	0.03	0.03	0.03	0.01	0.02	0.02	0.01	0.01	0.03
NaO	0.02	0.03	0.00	0.00	0.00	0.05	0.06	0.00	0.01	0.02	0.05	0.00	0.05	0.12	0.08	0.05	0.07	0.04	0.14	0.04	0.07
K2O	0.00	0.00	0.01	0.01	0.01	0.01	0.02	0.00	0.02	0.01	0.01	0.00	0.03	0.05	0.05	0.02	0.02	0.03	0.03	0.01	0.01
Total	92.01	93.15	92.74	93.25	93.07	91.64	92.32	91.77	92.86	92.45	91.97	92.67	92.42	93.06	93.06	93.34	93.33	93.48	92.38	91.80	92.29
Cations:																					
Si	2.57	2.53	2.57	2.53	2.55	2.62	2.60	2.54	2.55	2.54	2.54	2.55	2.53	2.52	2.52	2.53	2.54	2.55	2.53	2.55	2.53
Ti	0.01	0.00	0.01	0.01	0.00	0.01	0.01	0.01	0.01	0.01	0.01	0.00	0.01	0.01	0.00	0.01	0.01	0.01	0.00	0.01	0.01
Al	2.87	2.86	2.80	2.90	2.83	2.78	2.78	2.88	2.86	2.86	2.90	2.78	2.86	2.89	2.86	2.86	2.84	2.79	2.88	2.81	2.89
Cr	0.00	0.01	0.00	0.00	0.00	0.00	0.01	0.00	0.00	0.00	0.00	0.00	0.00	0.00	0.00	0.00	0.00	0.01	0.00	0.00	0.00
Fe	2.04	2.12	1.96	2.03	2.09	1.91	1.98	2.02	2.09	2.18	2.02	2.07	2.07	2.11	2.14	2.14	2.11	2.07	2.15	2.01	1.97
Mn	0.01	0.00	0.01	0.00	0.01	0.01	0.01	0.00	0.00	0.00	0.00	0.01	0.00	0.00	0.01	0.00	0.00	0.01	0.01	0.00	0.01
Mg	2.47	2.49	2.66	2.53	2.54	2.65	2.61	2.57	2.52	2.41	2.54	2.63	2.56	2.49	2.49	2.47	2.53	2.59	2.45	2.65	2.61
Ca	0.01	0.00	0.00	0.00	0.00	0.00	0.00	0.00	0.00	0.00	0.00	0.00	0.00	0.00	0.00	0.00	0.00	0.00	0.00	0.00	0.00
Na	0.00	0.00	0.00	0.00	0.00	0.01	0.01	0.00	0.00	0.00	0.01	0.00	0.01	0.02	0.01	0.01	0.01	0.01	0.03	0.01	0.01
K	0.00	0.00	0.00	0.00	0.00	0.00	0.00	0.00	0.00	0.00	0.00	0.00	0.00	0.01	0.01	0.00	0.00	0.00	0.00	0.00	0.00
Total (All)	9.98	10.03	10.02	10.01	10.03	9.99	10.00	10.02	10.02	10.02	10.01	10.05	10.04	10.05	10.05	10.03	10.05	10.05	10.04	10.04	10.03
Total (Majors ONLY)	9.98	10.03	10.02	10.01	10.02	9.99	10.00	10.01	10.02	10.02	10.01	10.05	10.04	10.05	10.05	10.03	10.04	10.04	10.04	10.04	10.03
Al(VI) (= (Si + Al) - 4)	1.45	1.40	1.38	1.44	1.38	1.39	1.38	1.42	1.40	1.40	1.43	1.33	1.39	1.40	1.38	1.39	1.37	1.34	1.40	1.36	1.42
Al(IV) (= Al - Al(VI))	1.43	1.47	1.43	1.47	1.45	1.38	1.40	1.46	1.45	1.46	1.46	1.45	1.47	1.48	1.48	1.47	1.46	1.45	1.47	1.45	1.47
XFe (= Fe/(Fe + Mg))	0.45	0.46	0.42	0.45	0.45	0.42	0.43	0.44	0.45	0.48	0.44	0.44	0.45	0.46	0.46	0.46	0.45	0.44	0.47	0.43	0.43

Note: Analyses conducted on the same mineral grain (e.g. 1 core analysis and 2 rim analyses on a specific chlorite grain) are highlighted in the same colour and enclosed in the same thick black box.

Chlorites cont.

Analysis Label (Specimen_mineral_grain/zone:spot number)	gb8_bi_1d	gb8_bi_1e	gb8_bi_1f	gb8_bi_1g	gb8_bi_1h	gb8_bi_1i	gb8_bi_1j	gb8_bi_13b	gb10_chl_11b	gb10_chl_11a	gb10_chl_8a	gb10_chl_8c	gb10_chl_8d	gb10_chl_8e	gb10_chl_8l	gb10_chl_8b	gb10_chl_8i	gb10_chl_8g	gb10_chl_8m	gb10_chl_9b	gb10_chl_9d
Mineral Probed:	chl	chl	chl	chl	chl	chl	chl	chl	chl	chl	chl	chl	chl	chl	chl	chl	chl	chl	chl	chl	chl
Core/Int/Rim:	Int	Core	Core	Core	Int	Rim	Rim	Int	Int	Core	Rim	Rim	Rim	Int	Int	Core	Int	Rim	Rim	Int	Int
EMP Initial Results:																					
Oxide conc. (wt%)																					
SiO2	25.62	25.42	25.79	25.83	25.51	25.64	25.72	25.71	25.49	25.37	25.15	25.21	25.20	25.33	24.83	25.12	25.58	25.44	25.24	25.58	25.19
TiO2	0.05	0.07	0.07	0.07	0.09	0.09	0.08	0.08	0.07	0.04	0.08	0.09	0.07	0.07	0.05	0.09	0.10	0.09	0.08	0.06	0.05
Al2O3	24.42	24.63	24.06	24.30	24.26	24.11	23.91	24.84	24.00	24.16	24.22	24.60	24.97	24.52	24.49	24.85	23.92	24.00	24.70	24.05	24.92
Cr2O3	0.00	0.03	0.00	0.00	0.03	0.04	0.00	0.03	0.04	0.04	0.03	0.00	0.01	0.04	0.03	0.02	0.03	0.03	0.00	0.01	0.02
FeO	23.94	26.39	26.62	25.92	26.05	25.85	26.12	25.11	22.22	22.53	23.76	23.17	23.09	23.59	22.53	23.14	22.88	24.34	22.78	22.29	22.61
MnO	0.02	0.08	0.04	0.07	0.05	0.09	0.06	0.01	0.07	0.07	0.06	0.07	0.06	0.06	0.06	0.07	0.07	0.04	0.03	0.04	0.06
MgO	17.49	16.13	16.05	16.59	16.28	16.58	16.46	17.32	18.00	18.59	17.44	17.89	18.05	18.01	17.77	17.93	18.67	17.53	17.63	18.52	18.32
CaO	0.03	0.02	0.02	0.01	0.07	0.04	0.02	0.01	0.02	0.02	0.02	0.03	0.02	0.01	0.03	0.03	0.03	0.03	0.05	0.04	0.01
NaO	0.00	0.01	0.03	0.00	0.32	0.18	0.00	0.05	0.04	0.06	0.09	0.08	0.02	0.03	0.01	0.07	0.11	0.06	0.07	0.11	0.01
K2O	0.00	0.00	0.02	0.01	0.11	0.06	0.00	0.01	0.02	0.05	0.03	0.00	0.01	0.02	0.02	0.04	0.04	0.02	0.05	0.04	0.03
Total	91.58	92.77	92.70	92.80	92.77	92.69	92.38	93.18	89.96	90.93	90.88	91.14	91.51	91.69	89.81	91.36	91.44	91.59	90.63	90.75	91.21
Cations:																					
Si	2.55	2.53	2.57	2.56	2.54	2.55	2.57	2.53	2.57	2.53	2.53	2.52	2.50	2.52	2.51	2.50	2.54	2.54	2.53	2.55	2.50
Ti	0.00	0.01	0.01	0.01	0.01	0.01	0.01	0.01	0.01	0.00	0.01	0.01	0.01	0.01	0.00	0.01	0.01	0.01	0.01	0.00	0.00
Al	2.87	2.89	2.83	2.84	2.85	2.83	2.81	2.88	2.85	2.84	2.87	2.89	2.92	2.87	2.92	2.92	2.80	2.83	2.92	2.83	2.92
Cr	0.00	0.00	0.00	0.00	0.00	0.00	0.00	0.00	0.00	0.00	0.00	0.00	0.00	0.00	0.00	0.00	0.00	0.00	0.00	0.00	0.00
Fe	1.99	2.20	2.22	2.15	2.17	2.15	2.18	2.06	1.87	1.88	2.00	1.93	1.92	1.96	1.90	1.93	1.90	2.03	1.91	1.86	1.88
Mn	0.00	0.01	0.00	0.01	0.00	0.01	0.01	0.00	0.01	0.01	0.00	0.01	0.00	0.01	0.01	0.01	0.01	0.00	0.00	0.00	0.01
Mg	2.60	2.39	2.38	2.45	2.42	2.46	2.45	2.54	2.70	2.77	2.61	2.66	2.67	2.67	2.68	2.66	2.77	2.61	2.63	2.76	2.71
Ca	0.00	0.00	0.00	0.00	0.01	0.00	0.00	0.00	0.00	0.00	0.00	0.00	0.00	0.00	0.00	0.00	0.00	0.00	0.01	0.00	0.00
Na	0.00	0.00	0.01	0.00	0.06	0.04	0.00	0.01	0.01	0.01	0.02	0.01	0.00	0.01	0.00	0.01	0.02	0.01	0.01	0.02	0.00
K	0.00	0.00	0.00	0.00	0.01	0.01	0.00	0.00	0.00	0.01	0.00	0.00	0.00	0.00	0.00	0.01	0.00	0.00	0.01	0.01	0.00
Total (All)	10.01	10.02	10.02	10.02	10.07	10.05	10.02	10.03	10.01	10.05	10.04	10.04	10.03	10.04	10.03	10.04	10.06	10.04	10.02	10.04	10.03
Total (Majors ONLY)	10.01	10.02	10.02	10.02	10.06	10.05	10.02	10.03	10.01	10.05	10.04	10.04	10.03	10.04	10.03	10.04	10.06	10.04	10.02	10.04	10.03
Al(VI) (= (Si + Al) - 4)	1.42	1.42	1.40	1.40	1.39	1.38	1.38	1.41	1.41	1.37	1.40	1.41	1.42	1.39	1.43	1.42	1.35	1.37	1.44	1.38	1.42
Al(IV) (= Al - Al(VI))	1.45	1.47	1.43	1.44	1.46	1.45	1.43	1.47	1.43	1.47	1.47	1.48	1.50	1.48	1.49	1.50	1.46	1.46	1.47	1.45	1.50
XFe (= Fe/(Fe + Mg))	0.43	0.48	0.48	0.47	0.47	0.47	0.47	0.45	0.41	0.40	0.43	0.42	0.42	0.42	0.42	0.42	0.41	0.44	0.42	0.40	0.41

Note: Analyses conducted on the same mineral grain (e.g. 1 core analysis and 2 rim analyses on a specific chlorite grain) are highlighted in the same colour and enclosed in the same thick black box.

Chlorites cont.

Analysis Label (Specimen_mineral grain/zone:spot number)	gb10_chl_9a	gb10_chl_9c	gb10_chl_9e	gb10_chl_9f	gb10_chl_9g	gb10_mu_2a*	gb10_mu_2b*	gb10_mu_2c*	gb13_chl_2f	ma29_chl_1f	ma29_chl_1b	ma29_chl_1a	ma29_chl_1c	ma29_chl_1d	ma29_chl_1l	ma29_chl_1j	ma29_chl_1i	ma29_chl_1n	ma29_chl_1m	ma29_chl_2b	ma29_chl_2a
Mineral Probed:	chl	chl	chl	chl	chl	chl	chl	chl	chl	chl	chl	chl	chl	chl	chl	chl	chl	chl	chl	chl	chl
Core/Int/Rim:	Core	Core	Core	Int	Int	Core	Core	Core	Rim	Rim	Int	Core	Core	Int	Rim	Int	Core	Rim	Core	Rim	Core
EMP Initial Results:																					
Oxide conc. (wt%)																					
SiO2	24.96	25.28	25.19	24.98	25.60	25.35	25.53	25.15	25.60	25.80	25.61	25.71	25.55	25.87	25.80	25.52	25.32	25.48	25.49	25.45	25.31
TiO2	0.05	0.07	0.08	0.06	0.07	0.10	0.06	0.09	0.09	0.11	0.05	0.08	0.05	0.09	0.08	0.21	0.07	0.09	0.08	0.07	0.09
Al2O3	24.38	24.67	24.65	24.82	24.89	24.64	24.34	24.89	25.13	24.21	25.03	24.59	24.72	24.72	24.89	24.54	24.91	24.18	24.94	24.62	24.88
Cr2O3	0.03	0.05	0.00	0.06	0.00	0.02	0.02	0.05	0.00	0.01	0.07	0.04	0.00	0.00	0.00	0.00	0.00	0.01	0.00	0.04	0.02
FeO	22.82	23.08	22.77	23.30	23.14	23.13	22.96	22.70	22.95	22.84	23.27	23.65	23.60	23.35	23.45	23.57	23.72	23.56	23.16	23.19	23.80
MnO	0.09	0.06	0.07	0.08	0.07	0.02	0.05	0.06	0.07	0.06	0.09	0.06	0.05	0.10	0.07	0.06	0.06	0.05	0.07	0.09	0.06
MgO	18.28	18.37	17.80	18.05	18.17	17.88	17.78	17.95	18.07	17.88	17.44	17.55	17.53	17.56	17.79	17.48	17.42	17.22	17.40	17.88	17.60
CaO	0.04	0.02	0.06	0.03	0.00	0.03	0.02	0.00	0.03	0.01	0.02	0.03	0.02	0.01	0.02	0.01	0.03	0.03	0.03	0.02	0.02
NaO	0.07	0.05	0.11	0.03	0.01	0.05	0.05	0.10	0.04	0.04	0.02	0.04	0.05	0.00	0.03	0.02	0.07	0.03	0.04	0.03	0.02
K2O	0.04	0.01	0.06	0.02	0.05	0.08	0.11	0.05	0.03	0.01	0.01	0.01	0.02	0.00	0.01	0.02	0.02	0.09	0.02	0.03	0.03
Total	90.76	91.66	90.79	91.42	92.01	91.30	90.91	91.04	92.01	90.96	91.61	91.75	91.57	91.71	92.14	91.44	91.62	90.75	91.22	91.43	91.83
Cations:																					
Si	2.50	2.51	2.52	2.49	2.53	2.52	2.55	2.51	2.52	2.57	2.54	2.55	2.54	2.56	2.54	2.54	2.52	2.56	2.54	2.53	2.51
Ti	0.00	0.01	0.01	0.00	0.01	0.01	0.00	0.01	0.01	0.01	0.00	0.01	0.00	0.01	0.01	0.02	0.01	0.01	0.01	0.01	0.01
Al	2.88	2.88	2.91	2.91	2.90	2.89	2.87	2.92	2.92	2.84	2.93	2.88	2.90	2.89	2.89	2.88	2.92	2.86	2.93	2.89	2.91
Cr	0.00	0.00	0.00	0.00	0.00	0.00	0.00	0.00	0.00	0.00	0.01	0.00	0.00	0.00	0.00	0.00	0.00	0.00	0.00	0.00	0.00
Fe	1.91	1.91	1.91	1.94	1.91	1.93	1.92	1.89	1.89	1.90	1.93	1.96	1.96	1.93	1.93	1.96	1.97	1.98	1.93	1.93	1.98
Mn	0.01	0.00	0.01	0.01	0.01	0.00	0.00	0.01	0.01	0.00	0.01	0.01	0.00	0.01	0.01	0.01	0.01	0.00	0.01	0.01	0.01
Mg	2.73	2.72	2.65	2.68	2.67	2.65	2.65	2.67	2.65	2.66	2.58	2.60	2.60	2.59	2.62	2.59	2.58	2.58	2.58	2.65	2.60
Ca	0.00	0.00	0.01	0.00	0.00	0.00	0.00	0.00	0.00	0.00	0.00	0.00	0.00	0.00	0.00	0.00	0.00	0.00	0.00	0.00	0.00
Na	0.01	0.01	0.02	0.01	0.00	0.01	0.01	0.02	0.01	0.01	0.00	0.01	0.01	0.00	0.01	0.00	0.01	0.01	0.01	0.01	0.00
K	0.00	0.00	0.01	0.00	0.01	0.01	0.01	0.01	0.00	0.00	0.00	0.00	0.00	0.00	0.00	0.00	0.00	0.01	0.00	0.00	0.00
Total (All)	10.06	10.05	10.03	10.05	10.02	10.03	10.02	10.03	10.02	10.00	10.00	10.01	10.01	9.99	10.01	10.01	10.02	10.01	10.00	10.02	10.03
Total (Majors ONLY)	10.06	10.05	10.03	10.05	10.02	10.03	10.02	10.03	10.02	10.00	9.99	10.01	10.01	9.99	10.01	10.01	10.02	10.01	10.00	10.02	10.03
Al(VI) (= (Si + Al) - 4)	1.38	1.39	1.43	1.40	1.42	1.42	1.42	1.43	1.44	1.42	1.46	1.43	1.44	1.45	1.44	1.42	1.44	1.42	1.46	1.42	1.42
Al(IV) (= Al - Al(VI))	1.50	1.49	1.48	1.51	1.47	1.48	1.45	1.49	1.48	1.43	1.46	1.45	1.46	1.44	1.46	1.46	1.48	1.44	1.46	1.47	1.49
XFe (= Fe/(Fe + Mg))	0.41	0.41	0.42	0.42	0.42	0.42	0.42	0.42	0.42	0.42	0.43	0.43	0.43	0.43	0.43	0.43	0.43	0.43	0.43	0.42	0.43

Note: Analyses conducted on the same mineral grain (e.g. 1 core analysis and 2 rim analyses on a specific chlorite grain) are highlighted in the same colour and enclosed in the same thick black box.

Chlorites cont.

Analysis Label (Specimen_mineral grain/zone:spot number)	ma29_chl_3b	ma29_chl_3a	ma29_chl_6c	ma29_chl_6a	ma29_chl_6e	ma29_chl_6d	ma29_chl_4b	ma29_chl_4a	ma29_chl_4d	ma29_chl_4e	ma29_chl_4c	ma29_chl_5b	ma29_chl_5c	ma29_chl_5a	ma29_chl_7b	ma29_chl_7a	ma31_chl_1d	ma31_chl_1c	ma31_chl_1a	ma31_chl_1b	ma31_chl_2c
Mineral Probed:	chl	chl	chl	chl	chl	chl	chl	chl	chl	chl	chl	chl	chl	chl	chl	chl	chl	chl	chl	chl	chl
Core/Int/Rim:	Int	Core	Int	Core	Rim	Core	Rim	Core	Rim	Int	Core	Rim	Int	Core	Rim	Core	Rim	Int	Core	Core	Rim
EMP Initial Results:																					
Oxide conc. (wt%)																					
SiO2	25.53	25.39	25.37	25.80	25.69	25.27	25.52	25.72	25.54	25.24	25.31	25.62	25.70	25.24	25.84	25.51	25.91	25.88	25.97	25.52	25.93
TiO2	0.07	0.08	0.04	0.10	0.08	0.08	0.09	0.06	0.07	0.14	0.07	0.11	0.07	0.09	0.11	0.05	0.09	0.11	0.09	0.11	0.11
Al2O3	25.21	25.09	24.73	25.14	24.54	24.81	24.57	24.58	24.68	24.57	24.89	24.31	24.88	25.17	24.16	24.48	24.52	24.85	24.29	24.72	24.48
Cr2O3	0.03	0.04	0.00	0.02	0.04	0.00	0.05	0.03	0.03	0.01	0.02	0.05	0.04	0.02	0.01	0.02	0.02	0.03	0.05	0.03	0.00
FeO	23.26	22.89	22.87	22.05	23.15	23.59	23.49	23.18	23.51	23.52	22.82	22.81	23.31	23.61	23.52	23.12	22.19	22.01	21.96	21.81	22.47
MnO	0.05	0.09	0.04	0.08	0.09	0.03	0.05	0.04	0.09	0.07	0.08	0.13	0.07	0.08	0.07	0.06	0.08	0.12	0.05	0.12	0.13
MgO	17.59	17.85	17.65	17.83	17.55	17.42	17.59	17.93	17.53	17.17	17.52	17.83	17.89	17.48	17.46	17.76	18.04	17.97	18.15	17.95	17.67
CaO	0.05	0.02	0.08	0.02	0.03	0.03	0.01	0.00	0.03	0.06	0.03	0.02	0.01	0.05	0.03	0.02	0.02	0.03	0.00	0.04	0.01
NaO	0.04	0.00	0.05	0.04	0.05	0.05	0.00	0.04	0.07	0.13	0.11	0.04	0.05	0.06	0.03	0.00	0.01	0.04	0.05	0.06	0.01
K2O	0.01	0.01	0.02	0.02	0.02	0.02	0.01	0.01	0.05	0.03	0.02	0.03	0.00	0.02	0.24	0.01	0.03	0.01	0.01	0.03	0.04
Total	91.83	91.45	90.85	91.09	91.25	91.30	91.38	91.60	91.60	90.94	90.87	90.94	92.02	91.82	91.48	91.02	90.91	91.06	90.62	90.39	90.85
Cations:																					
Si	2.52	2.52	2.53	2.55	2.56	2.52	2.54	2.55	2.54	2.53	2.53	2.56	2.54	2.50	2.57	2.55	2.57	2.56	2.59	2.55	2.58
Ti	0.00	0.01	0.00	0.01	0.01	0.01	0.01	0.00	0.00	0.01	0.01	0.01	0.01	0.01	0.01	0.00	0.01	0.01	0.01	0.01	0.01
Al	2.94	2.93	2.91	2.93	2.88	2.92	2.88	2.87	2.89	2.90	2.93	2.86	2.89	2.94	2.84	2.88	2.87	2.90	2.85	2.91	2.87
Cr	0.00	0.00	0.00	0.00	0.00	0.00	0.00	0.00	0.00	0.00	0.00	0.00	0.00	0.00	0.00	0.00	0.00	0.00	0.00	0.00	0.00
Fe	1.92	1.90	1.91	1.83	1.93	1.97	1.96	1.92	1.95	1.97	1.91	1.90	1.92	1.96	1.96	1.93	1.84	1.82	1.83	1.82	1.87
Mn	0.00	0.01	0.00	0.01	0.01	0.00	0.00	0.00	0.01	0.01	0.01	0.01	0.01	0.01	0.01	0.00	0.01	0.01	0.00	0.01	0.01
Mg	2.59	2.64	2.63	2.63	2.60	2.59	2.61	2.65	2.60	2.57	2.61	2.65	2.63	2.58	2.59	2.64	2.67	2.65	2.69	2.67	2.62
Ca	0.01	0.00	0.01	0.00	0.00	0.00	0.00	0.00	0.00	0.01	0.00	0.00	0.00	0.00	0.00	0.00	0.00	0.00	0.00	0.00	0.00
Na	0.01	0.00	0.01	0.01	0.01	0.01	0.00	0.01	0.01	0.03	0.02	0.01	0.01	0.01	0.01	0.00	0.00	0.01	0.01	0.01	0.00
K	0.00	0.00	0.00	0.00	0.00	0.00	0.00	0.00	0.01	0.00	0.00	0.00	0.00	0.00	0.03	0.00	0.00	0.00	0.00	0.00	0.01
Total (All)	10.00	10.01	10.01	9.98	10.00	10.02	10.01	10.01	10.02	10.02	10.01	10.01	10.01	10.02	10.02	10.01	9.99	9.98	9.99	9.99	9.98
Total (Majors ONLY)	10.00	10.01	10.01	9.97	10.00	10.02	10.01	10.01	10.02	10.02	10.01	10.00	10.01	10.02	10.02	10.01	9.98	9.98	9.98	9.99	9.98
Al(VI) (= (Si + Al) - 4)	1.46	1.45	1.45	1.49	1.44	1.44	1.42	1.42	1.43	1.43	1.46	1.42	1.43	1.45	1.41	1.43	1.45	1.47	1.44	1.46	1.46
Al(IV) (= Al - Al(VI))	1.48	1.48	1.47	1.45	1.44	1.48	1.46	1.45	1.46	1.47	1.47	1.44	1.46	1.50	1.43	1.45	1.43	1.44	1.41	1.45	1.42
XFe (= Fe/(Fe + Mg))	0.43	0.42	0.42	0.41	0.43	0.43	0.43	0.42	0.43	0.43	0.42	0.42	0.42	0.43	0.43	0.42	0.41	0.41	0.40	0.41	0.42

Note: Analyses conducted on the same mineral grain (e.g. 1 core analysis and 2 rim analyses on a specific chlorite grain) are highlighted in the same colour and enclosed in the same thick black box.

Chlorites cont.

Analysis Label (Specimen_mineral grain/zone:spot number)	ma31_chl_2d	ma31_chl_2b	ma31_chl_2a	ma31_chl_2e	ma31_chl_3c	ma31_chl_3a	ma31_chl_3b	ma31_chl_3d	ma31_chl_4b	ma31_chl_4c	ma31_chl_4g	ma31_chl_4a	ma31_chl_4d	ma31_chl_4f	ma31_chl_4e	ma31_mu_2e	ma38_chl_1c	ma38_chl_1d	ma38_chl_1a	ma38_chl_1e	ma38_chl_1b
Mineral Probed:	chl	chl	chl	chl	chl	chl	chl	chl	chl	chl	chl	chl	chl	chl	chl	chl	chl	chl	chl	chl	chl
Core/Int/Rim:	Rim	Int	Core	Rim	Rim	Int	Core	Rim	Rim	Int	Int	Core	Int	Core	Core	Core	Rim	Int	Core	Core	Rim
EMP Initial Results:																					
Oxide conc. (wt%)																					
SiO2	25.63	25.58	25.70	25.92	25.80	26.10	25.99	26.18	25.96	25.65	25.43	25.60	25.53	25.89	25.55	26.01	25.66	26.29	26.14	25.93	25.73
TiO2	0.09	0.09	0.09	0.07	0.08	0.07	0.12	0.07	0.07	0.09	0.05	0.07	0.15	0.12	0.09	0.07	0.10	0.19	0.10	0.09	0.07
Al2O3	24.18	24.60	25.09	24.99	24.72	24.97	24.73	24.24	24.50	24.88	24.66	24.52	25.00	24.95	24.69	24.21	25.03	25.34	24.73	25.09	25.22
Cr2O3	0.04	0.00	0.03	0.04	0.02	0.05	0.01	0.01	0.01	0.03	0.03	0.01	0.00	0.00	0.02	0.06	0.00	0.05	0.04	0.05	0.05
FeO	23.47	22.26	22.16	21.86	21.64	21.92	21.85	21.85	21.67	21.36	21.85	20.97	21.34	21.72	21.65	21.08	20.19	20.29	20.50	20.50	20.13
MnO	0.08	0.06	0.09	0.11	0.08	0.14	0.08	0.05	0.06	0.11	0.07	0.13	0.12	0.08	0.12	0.11	0.12	0.07	0.09	0.13	0.09
MgO	17.13	17.32	18.58	17.82	18.26	17.66	18.43	18.25	18.32	18.48	18.19	18.34	18.12	18.20	18.08	18.99	18.68	18.23	18.36	18.48	18.49
CaO	0.01	0.02	0.02	0.02	0.02	0.01	0.00	0.03	0.01	0.01	0.07	0.03	0.04	0.01	0.03	0.04	0.03	0.04	0.01	0.00	0.03
NaO	0.01	0.00	0.02	0.02	0.02	0.04	0.03	0.02	0.00	0.04	0.05	0.04	0.06	0.01	0.06	0.09	0.12	0.08	0.08	0.08	0.05
K2O	0.07	0.01	0.02	0.09	0.01	0.01	0.00	0.05	0.02	0.02	0.03	0.00	0.02	0.01	0.02	0.03	0.02	0.04	0.02	0.02	0.03
Total	90.71	89.95	91.79	90.94	90.64	90.97	91.24	90.75	90.62	90.67	90.42	89.71	90.37	90.98	90.32	90.69	89.95	90.63	90.08	90.38	89.89
Cations:																					
Si	2.57	2.57	2.53	2.57	2.56	2.59	2.57	2.60	2.58	2.55	2.54	2.57	2.54	2.56	2.55	2.58	2.55	2.59	2.60	2.57	2.56
Ti	0.01	0.01	0.01	0.01	0.01	0.01	0.01	0.00	0.01	0.01	0.00	0.01	0.01	0.01	0.01	0.01	0.01	0.01	0.01	0.01	0.01
Al	2.86	2.91	2.91	2.92	2.90	2.92	2.88	2.84	2.87	2.91	2.90	2.90	2.94	2.91	2.91	2.83	2.94	2.94	2.90	2.93	2.96
Cr	0.00	0.00	0.00	0.00	0.00	0.00	0.00	0.00	0.00	0.00	0.00	0.00	0.00	0.00	0.00	0.00	0.00	0.00	0.00	0.00	0.00
Fe	1.97	1.87	1.82	1.81	1.80	1.82	1.80	1.82	1.80	1.77	1.83	1.76	1.78	1.80	1.81	1.75	1.68	1.67	1.70	1.70	1.67
Mn	0.01	0.01	0.01	0.01	0.01	0.01	0.01	0.00	0.00	0.01	0.01	0.01	0.01	0.01	0.01	0.01	0.01	0.01	0.01	0.01	0.01
Mg	2.56	2.59	2.73	2.63	2.71	2.61	2.71	2.70	2.71	2.73	2.71	2.74	2.69	2.69	2.69	2.81	2.77	2.68	2.72	2.73	2.74
Ca	0.00	0.00	0.00	0.00	0.00	0.00	0.00	0.00	0.00	0.00	0.01	0.00	0.00	0.00	0.00	0.00	0.00	0.00	0.00	0.00	0.00
Na	0.00	0.00	0.00	0.00	0.00	0.01	0.01	0.00	0.00	0.01	0.01	0.01	0.01	0.00	0.01	0.02	0.02	0.01	0.02	0.02	0.01
K	0.01	0.00	0.00	0.01	0.00	0.00	0.00	0.01	0.00	0.00	0.00	0.00	0.00	0.00	0.00	0.00	0.00	0.01	0.00	0.00	0.00
Total (All)	10.00	9.97	10.01	9.97	9.98	9.95	9.99	9.98	9.98	10.00	10.01	9.98	9.98	9.98	9.99	10.01	9.99	9.93	9.95	9.97	9.96
Total (Majors ONLY)	9.99	9.97	10.01	9.97	9.98	9.95	9.99	9.98	9.98	9.99	10.01	9.98	9.98	9.98	9.99	10.00	9.99	9.93	9.95	9.96	9.96
Al(VI) (= (Si + Al) - 4)	1.43	1.48	1.44	1.49	1.46	1.50	1.45	1.44	1.45	1.46	1.44	1.46	1.48	1.47	1.46	1.41	1.49	1.53	1.49	1.50	1.51
Al(IV) (= Al - Al(VI))	1.43	1.43	1.47	1.43	1.44	1.41	1.43	1.40	1.42	1.45	1.46	1.43	1.46	1.44	1.45	1.42	1.45	1.41	1.40	1.43	1.44
XFe (= Fe/(Fe + Mg))	0.43	0.42	0.40	0.41	0.40	0.41	0.40	0.40	0.40	0.39	0.40	0.39	0.40	0.40	0.40	0.38	0.38	0.38	0.39	0.38	0.38

Note: Analyses conducted on the same mineral grain (e.g. 1 core analysis and 2 rim analyses on a specific chlorite grain) are highlighted in the same colour and enclosed in the same thick black box.

Chlorites cont.

Analysis Label (Specimen_mineral grain/zone:spot number)	ma38_chl_1g	ma38_chl_1h	ma38_chl_1f	ma38_chl_1i	ma38_chl_1j	ma38_chl_1m	ma38_chl_2c	ma38_chl_2d	ma38_chl_2e	ma38_chl_2g	ma38_chl_2f	ma38_chl_3b	ma38_chl_3a	ma38_chl_3e	ma38_chl_3d	ma38_chl_3h	ma38_chl_3g	ma38_mu_m6	ma38_mu_m4	ma40_chl_1a	ma40_chl_1h
Mineral Probed:	chl	chl	chl	chl	chl	chl	chl	chl	chl	chl	chl	chl	chl	chl	chl	chl	chl	chl	chl	chl	chl
Core/Int/Rim:	Rim	Int	Core	Int	Core	Int	Core	Rim	Int	Core	Rim	Rim	Core	Core	Rim	Rim	Core	Core	Core	Rim	Rim
EMP Initial Results:																					
Oxide conc. (wt%)																					
SiO2	25.16	26.05	25.44	25.73	26.32	26.12	26.11	25.82	26.29	25.97	25.53	25.44	26.21	25.39	25.56	25.33	25.32	26.07	26.04	25.76	25.57
TiO2	0.08	0.06	0.11	0.25	0.07	0.10	0.09	0.18	0.08	0.05	0.08	0.08	0.05	0.12	0.17	0.09	0.08	0.08	0.11	0.09	0.26
Al2O3	25.20	24.93	24.86	24.47	24.34	24.57	24.56	24.90	25.35	24.81	25.06	24.24	25.20	24.65	24.72	25.74	25.20	24.88	25.01	24.76	24.78
Cr2O3	0.06	0.02	0.00	0.04	0.05	0.00	0.00	0.00	0.03	0.06	0.07	0.10	0.08	0.05	0.06	0.06	0.06	0.03	0.01	0.07	0.06
FeO	20.62	19.97	20.53	20.39	20.60	20.42	20.27	20.16	20.11	20.84	20.31	20.97	21.25	20.73	20.53	21.67	21.36	19.98	20.41	22.47	22.38
MnO	0.13	0.06	0.14	0.11	0.11	0.08	0.07	0.11	0.04	0.10	0.03	0.10	0.08	0.08	0.09	0.04	0.09	0.09	0.09	0.13	0.10
MgO	18.31	18.67	18.44	18.49	18.45	18.57	18.15	18.08	17.32	18.17	17.97	18.08	17.83	18.06	18.13	17.49	17.99	18.66	18.14	17.47	17.63
CaO	0.02	0.00	0.02	0.03	0.02	0.02	0.02	0.03	0.03	0.02	0.02	0.02	0.00	0.02	0.03	0.00	0.01	0.01	0.01	0.02	0.02
NaO	0.09	0.06	0.20	0.07	0.04	0.07	0.07	0.05	0.05	0.03	0.05	0.06	0.04	0.04	0.00	0.01	0.02	0.04	0.06	0.03	0.04
K2O	0.05	0.01	0.09	0.01	0.02	0.01	0.01	0.01	0.15	0.01	0.01	0.02	0.01	0.02	0.01	0.02	0.01	0.02	0.02	0.02	0.01
Total	89.72	89.82	89.83	89.60	90.02	89.96	89.34	89.34	89.45	90.07	89.13	89.10	90.76	89.17	89.29	90.46	90.14	89.86	89.89	90.82	90.83
Cations:																					
Si	2.52	2.59	2.54	2.57	2.62	2.60	2.61	2.58	2.62	2.59	2.56	2.57	2.59	2.56	2.57	2.52	2.53	2.59	2.59	2.57	2.55
Ti	0.01	0.00	0.01	0.02	0.01	0.01	0.01	0.01	0.01	0.00	0.01	0.01	0.00	0.01	0.01	0.01	0.01	0.01	0.01	0.01	0.02
Al	2.97	2.92	2.93	2.88	2.85	2.88	2.90	2.94	2.98	2.91	2.97	2.89	2.94	2.93	2.93	3.02	2.97	2.91	2.93	2.91	2.91
Cr	0.01	0.00	0.00	0.00	0.00	0.00	0.00	0.00	0.00	0.01	0.01	0.01	0.01	0.00	0.00	0.00	0.00	0.00	0.00	0.01	0.00
Fe	1.73	1.66	1.72	1.71	1.71	1.70	1.70	1.69	1.68	1.74	1.71	1.77	1.76	1.75	1.72	1.80	1.78	1.66	1.70	1.87	1.86
Mn	0.01	0.01	0.01	0.01	0.01	0.01	0.01	0.01	0.00	0.01	0.00	0.01	0.01	0.01	0.01	0.00	0.01	0.01	0.01	0.01	0.01
Mg	2.73	2.76	2.75	2.76	2.74	2.75	2.71	2.70	2.57	2.70	2.69	2.72	2.63	2.71	2.71	2.60	2.68	2.76	2.69	2.59	2.62
Ca	0.00	0.00	0.00	0.00	0.00	0.00	0.00	0.00	0.00	0.00	0.00	0.00	0.00	0.00	0.00	0.00	0.00	0.00	0.00	0.00	0.00
Na	0.02	0.01	0.04	0.01	0.01	0.01	0.01	0.01	0.01	0.01	0.01	0.01	0.01	0.01	0.00	0.00	0.00	0.01	0.01	0.01	0.01
K	0.01	0.00	0.01	0.00	0.00	0.00	0.00	0.00	0.02	0.00	0.00	0.00	0.00	0.00	0.00	0.00	0.00	0.00	0.00	0.00	0.00
Total (All)	10.00	9.95	10.01	9.97	9.95	9.96	9.94	9.94	9.90	9.96	9.95	9.98	9.94	9.97	9.96	9.96	9.98	9.95	9.94	9.97	9.98
Total (Majors ONLY)	9.99	9.95	10.01	9.97	9.95	9.96	9.94	9.94	9.89	9.95	9.94	9.98	9.93	9.97	9.95	9.96	9.98	9.95	9.94	9.97	9.98
Al(VI) (= (Si + Al) - 4)	1.49	1.51	1.47	1.46	1.47	1.48	1.51	1.52	1.60	1.50	1.53	1.45	1.53	1.48	1.49	1.54	1.49	1.50	1.52	1.47	1.46
Al(IV) (= Al - Al(VI))	1.48	1.41	1.46	1.43	1.38	1.40	1.39	1.42	1.38	1.41	1.44	1.43	1.41	1.44	1.43	1.48	1.47	1.41	1.41	1.43	1.45
XFe (= Fe/(Fe + Mg))	0.39	0.38	0.38	0.38	0.39	0.38	0.39	0.38	0.39	0.39	0.39	0.39	0.40	0.39	0.39	0.41	0.40	0.38	0.39	0.42	0.42

Note: Analyses conducted on the same mineral grain (e.g. 1 core analysis and 2 rim analyses on a specific chlorite grain) are highlighted in the same colour and enclosed in the same thick black box.

Chlorites cont.

Analysis Label (Specimen_mineral_grain/zone:spot number)	ma40_chl_1i	ma40_chl_1c	ma40_chl_1e	ma40_chl_1g	ma40_chl_1b	ma40_chl_1k	ma40_chl_1f	ma40_chl_1j	ma40_chl_1l	ma40_chl_1m	ma40_chl_1n
Mineral Probed:	chl	chl	chl	chl	chl	chl	chl	chl	chl	chl	chl
Core/Int/Rim:	Rim	Int	Int	Core	Core	Core	Int	Rim	Rim	Rim	Int
EMP Initial Results:											
Oxide conc. (wt%)											
SiO2	25.75	25.08	25.38	25.39	25.34	25.42	25.75	25.77	25.78	25.73	25.12
TiO2	0.07	0.07	0.07	0.06	0.04	0.12	0.28	0.07	0.07	0.08	0.08
Al2O3	24.61	24.89	25.30	24.56	25.29	24.87	25.04	24.78	24.76	23.43	24.57
Cr2O3	0.04	0.04	0.05	0.00	0.03	0.06	0.04	0.08	0.03	0.02	0.02
FeO	22.45	22.69	22.79	22.63	22.80	22.01	22.54	22.33	22.20	23.15	22.51
MnO	0.11	0.13	0.03	0.09	0.10	0.09	0.11	0.04	0.07	0.09	0.10
MgO	17.87	17.39	17.64	17.61	17.37	17.57	17.58	17.45	17.65	17.31	17.41
CaO	0.01	0.02	0.02	0.04	0.01	0.00	0.01	0.04	0.02	0.09	0.06
NaO	0.05	0.04	0.03	0.03	0.01	0.03	0.03	0.01	0.01	0.05	0.14
K2O	0.02	0.03	0.01	0.02	0.01	0.00	0.01	0.00	0.01	0.04	0.01
Total	90.98	90.38	91.32	90.42	91.01	90.17	91.39	90.58	90.61	89.99	90.02
Cations:											
Si	2.56	2.52	2.52	2.55	2.52	2.55	2.55	2.57	2.57	2.60	2.53
Ti	0.01	0.01	0.01	0.00	0.00	0.01	0.02	0.01	0.01	0.01	0.01
Al	2.89	2.95	2.96	2.90	2.97	2.94	2.92	2.91	2.91	2.79	2.92
Cr	0.00	0.00	0.00	0.00	0.00	0.00	0.00	0.01	0.00	0.00	0.00
Fe	1.87	1.91	1.89	1.90	1.90	1.84	1.87	1.86	1.85	1.96	1.90
Mn	0.01	0.01	0.00	0.01	0.01	0.01	0.01	0.00	0.01	0.01	0.01
Mg	2.65	2.60	2.61	2.63	2.58	2.62	2.59	2.60	2.62	2.61	2.62
Ca	0.00	0.00	0.00	0.00	0.00	0.00	0.00	0.00	0.00	0.01	0.01
Na	0.01	0.01	0.01	0.01	0.00	0.01	0.01	0.00	0.00	0.01	0.03
K	0.00	0.00	0.00	0.00	0.00	0.00	0.00	0.00	0.00	0.01	0.00
Total (All)	9.99	10.01	10.00	10.00	9.99	9.98	9.97	9.97	9.97	10.00	10.02
Total (Majors ONLY)	9.99	10.00	10.00	10.00	9.99	9.97	9.97	9.96	9.97	10.00	10.01
Al(VI) (= (Si + Al) - 4)	1.45	1.46	1.48	1.45	1.49	1.48	1.47	1.48	1.48	1.39	1.45
Al(IV) (= Al - Al(VI))	1.44	1.48	1.48	1.45	1.48	1.45	1.45	1.43	1.43	1.40	1.47
XFe (= Fe/(Fe + Mg))	0.41	0.42	0.42	0.42	0.42	0.41	0.42	0.42	0.41	0.43	0.42

Note: Analyses conducted on the same mineral grain (e.g. 1 core analysis and 2 rim analyses on a specific chlorite grain) are highlighted in the same colour and enclosed in the same thick black box.

Epidotes

Analysis Label (Specimen_mineral_grain/zone:spot number)	gb4_ep_1b	gb4_ep_1a	gb4_ep_2a	gb4_ep_2b	gb4_ep_3b	gb4_ep_3c	gb4_ep_3a	gb4_ep_3e	gb4_ep_3d	gb4_ep_3f	gb4_ep_3g	gb4_ep_3h	gb4_amph_9a	gb4_sph_test	ma44_amph_2f	ma44_amph_3b	ma44_amph_3a	ma44_amph_3d	ma44_amph_3c	ma44_amph_3f	ma44_amph_3e	ma44_amph_4b	ma44_amph_4a
Mineral Probed:	ep	ep	ep	ep	ep	ep	ep	ep	ep	ep	ep	ep	ep	ep	ep	ep	ep	ep	ep	ep	ep	ep	ep
Core/Int/Rim:	Rim	Core	Core	Core	Rim	Int	Core	Rim	Core	Rim	Core	Core	Core	Core	Core	Rim	Core	Rim	Core	Rim	Core	Rim	Core
EMP Initial Results:																							
Oxide conc. (wt%)																							
SiO2	37.11	37.59	37.72	37.93	36.70	36.92	37.62	37.01	37.32	37.39	37.42	37.57	37.21	37.31	37.09	36.72	37.00	36.92	36.77	36.96	36.96	36.66	37.11
TiO2	0.10	0.08	0.03	0.11	0.12	0.13	0.06	0.12	0.02	0.05	0.11	0.12	0.09	0.08	0.24	0.13	0.07	0.13	0.12	0.15	0.28	0.06	0.11
Al2O3	24.79	24.73	25.36	24.16	24.74	24.30	25.08	25.65	24.55	25.30	25.50	25.35	25.45	24.88	28.33	27.06	26.41	27.11	26.91	27.09	26.35	25.67	27.54
Cr2O3	0.05	0.00	0.07	0.01	0.03	0.00	0.00	0.00	0.04	0.04	0.00	0.04	0.01	0.00	0.05	0.00	0.00	0.05	0.00	0.04	0.04	0.04	0.09
FeO	9.68	10.27	9.16	9.58	9.88	10.30	9.72	8.73	9.90	9.22	9.32	9.69	11.42	12.05	7.18	8.84	9.62	8.27	8.56	8.73	9.52	10.35	8.15
MnO	0.26	0.32	0.11	0.12	0.25	0.34	0.13	0.18	0.18	0.20	0.16	0.29	0.29	0.21	0.12	0.24	0.09	0.15	0.10	0.15	0.14	0.13	0.09
MgO	0.08	0.04	0.00	0.69	0.03	0.02	0.03	0.03	0.02	0.06	0.02	0.04	0.01	0.03	0.03	0.04	0.02	0.04	0.01	0.06	0.04	0.01	0.04
CaO	22.88	23.06	23.30	22.42	23.04	22.61	23.39	22.93	22.94	23.07	23.10	22.90	23.34	22.98	23.56	23.32	23.38	23.58	23.60	23.54	23.41	23.39	23.62
Na2O	0.00	0.00	0.00	0.08	0.02	0.04	0.02	0.00	0.05	0.00	0.07	0.03	0.00	0.00	0.01	0.03	0.02	0.01	0.01	0.00	0.00	0.03	0.03
K2O	0.00	0.00	0.00	0.00	0.00	0.00	0.00	0.00	0.00	0.00	0.00	0.00	0.00	0.00	0.01	0.00	0.01	0.00	0.00	0.02	0.01	0.01	0.00
Total	94.94	96.09	95.75	95.11	94.81	94.66	96.05	94.64	95.02	95.34	95.69	96.03	97.82	97.54	96.63	96.38	96.63	96.26	96.08	96.74	96.74	96.35	96.78
Cations:																							
Si	5.98	5.99	6.01	6.08	5.93	5.97	5.99	5.96	6.01	5.98	5.97	5.97	5.84	5.88	5.83	5.82	5.85	5.85	5.84	5.83	5.84	5.84	5.84
Ti	0.01	0.01	0.00	0.01	0.01	0.02	0.01	0.01	0.00	0.01	0.01	0.01	0.01	0.01	0.03	0.02	0.01	0.02	0.01	0.02	0.03	0.01	0.01
Al	4.71	4.64	4.76	4.56	4.71	4.63	4.70	4.87	4.66	4.77	4.79	4.75	4.71	4.62	5.25	5.05	4.92	5.06	5.04	5.04	4.91	4.82	5.11
Cr	0.01	0.00	0.01	0.00	0.00	0.00	0.00	0.00	0.00	0.01	0.00	0.00	0.00	0.00	0.01	0.00	0.00	0.01	0.00	0.00	0.01	0.00	0.01
Fe3+	1.30	1.37	1.22	1.28	1.34	1.39	1.29	1.18	1.33	1.23	1.24	1.29	1.50	1.59	0.94	1.17	1.27	1.10	1.14	1.15	1.26	1.38	1.07
Mn	0.04	0.04	0.02	0.02	0.03	0.05	0.02	0.02	0.03	0.03	0.02	0.04	0.04	0.03	0.02	0.03	0.01	0.02	0.01	0.02	0.02	0.02	0.01
Mg	0.02	0.01	0.00	0.17	0.01	0.01	0.01	0.01	0.00	0.01	0.00	0.01	0.00	0.01	0.01	0.01	0.00	0.01	0.00	0.01	0.01	0.00	0.01
Ca	3.95	3.94	3.98	3.85	3.99	3.92	3.99	3.96	3.96	3.96	3.95	3.90	3.93	3.88	3.97	3.96	3.96	4.00	4.02	3.98	3.96	3.99	3.98
Na	0.00	0.00	0.00	0.03	0.01	0.01	0.01	0.00	0.01	0.00	0.02	0.01	0.00	0.00	0.00	0.01	0.01	0.00	0.00	0.00	0.00	0.01	0.01
K	0.00	0.00	0.00	0.00	0.00	0.00	0.00	0.00	0.00	0.00	0.00	0.00	0.00	0.00	0.00	0.00	0.00	0.00	0.00	0.00	0.00	0.00	0.00
Total (All)	16.00	16.00	15.99	16.00	16.03	16.00	16.01	16.00	16.00	16.00	16.01	15.99	16.04	16.01	16.05	16.06	16.05	16.06	16.06	16.06	16.04	16.06	16.06
Total (Majors ONLY)	16.00	16.00	15.98	16.00	16.03	16.00	16.01	16.00	16.00	16.00	16.01	15.99	16.04	16.01	16.04	16.06	16.05	16.05	16.06	16.05	16.03	16.06	16.04
XPs (= Fe3+ / (Al + Fe	0.22	0.23	0.20	0.22	0.22	0.23	0.22	0.19	0.22	0.21	0.21	0.21	0.24	0.26	0.15	0.19	0.21	0.18	0.18	0.19	0.20	0.22	0.17

Note: Analyses conducted on the same mineral grain (e.g. 1 core analysis and 2 rim analyses on a specific epidote grain) are highlighted in the same colour and enclosed in the same thick black box.

Garnets

Analysis Label (Specimen_mineral_grain/zone:spot number)	gb8_gt_1d	gb8_gt_1g	gb8_gt_1h	gb8_gt_1f	gb8_gt_1i	gb8_gt_1j	gb8_gt_1k	gb8_gt_1l	gb8_gt_1m	gb8_gt_1e	gb8_gt_1a	gb8_gt_1b	gb8_gt_1c	gb10_gt_1a	gb10_gt_1b	gb10_gt_1c	gb10_gt_1f	gb10_gt_1i	gb10_gt_1d	gb10_gt_1g	gb10_gt_1j	gb10_gt_1m
Mineral Probed:	gt	gt	gt	gt	gt	gt	gt	gt	gt	gt	gt	gt	gt	gt	gt	gt	gt	gt	gt	gt	gt	gt
Core/Int/Rim:	Rim	Int	Int	Core	Core	Core	Core	Int	Int	Rim	Rim	Rim	Rim	Rim	Rim	Rim	Rim	Rim	Int	Int	Int	Int
EMP Initial Results:																						
Oxide conc. (wt%)																						
SiO2	37.75	37.95	38.16	37.81	37.29	37.64	37.62	37.78	37.75	37.57	37.53	37.80	37.66	37.53	37.27	37.58	37.52	37.49	37.64	37.26	37.68	37.46
TiO2	0.00	0.07	0.07	0.06	0.04	0.07	0.07	0.05	0.12	0.05	0.03	0.12	0.08	0.04	0.11	0.03	0.00	0.02	0.11	0.06	0.05	0.06
Al2O3	21.88	21.82	21.69	21.78	21.51	21.70	21.57	21.85	21.72	21.83	21.80	21.67	21.57	21.82	21.74	21.38	21.82	21.72	21.33	21.68	21.63	21.30
Cr2O3	0.06	0.04	0.02	0.02	0.03	0.03	0.01	0.00	0.04	0.03	0.02	0.03	0.00	0.01	0.01	0.00	0.02	0.04	0.00	0.00	0.01	0.00
FeO	33.52	31.75	32.04	32.17	32.29	31.81	32.00	31.59	32.14	32.71	32.48	31.32	31.60	32.01	32.74	31.95	32.55	32.32	30.22	30.30	30.97	30.62
MnO	1.00	1.38	1.43	1.51	1.64	1.98	1.87	2.25	2.10	0.97	1.97	2.84	1.70	1.34	1.60	1.49	1.33	1.26	3.35	3.26	2.71	2.56
MgO	2.94	2.78	2.67	2.75	2.65	2.60	2.48	2.60	2.55	3.10	2.61	2.42	2.70	3.29	2.65	3.16	3.15	3.34	2.65	3.02	2.82	2.77
CaO	3.79	4.59	4.80	4.23	4.31	4.33	4.16	4.47	4.30	3.81	3.86	4.71	5.17	3.75	3.71	4.56	3.73	3.81	5.00	4.40	4.53	4.87
Na2O	0.02	0.01	0.02	0.02	0.03	0.00	0.02	0.06	0.00	0.02	0.01	0.03	0.03	0.00	0.05	0.01	0.04	0.01	0.04	0.01	0.01	0.00
K2O	0.00	0.00	0.00	0.00	0.00	0.00	0.00	0.00	0.00	0.00	0.00	0.00	0.00	0.00	0.00	0.00	0.00	0.00	0.00	0.00	0.00	0.00
Total	100.97	100.40	100.90	100.35	99.79	100.15	99.80	100.65	100.72	100.09	100.31	100.95	100.51	99.79	99.87	100.16	100.16	100.00	100.34	99.98	100.41	99.64
Cations:																						
Si	2.99	3.01	3.01	3.00	2.99	3.00	3.01	3.00	3.00	2.99	2.99	3.00	2.99	2.99	2.98	2.99	2.99	2.99	3.00	2.98	3.00	3.00
Ti	0.00	0.00	0.00	0.00	0.00	0.00	0.00	0.00	0.01	0.00	0.00	0.01	0.00	0.00	0.01	0.00	0.00	0.00	0.01	0.00	0.00	0.00
Al	2.04	2.04	2.02	2.04	2.03	2.04	2.03	2.04	2.03	2.05	2.05	2.02	2.02	2.05	2.05	2.01	2.05	2.04	2.00	2.04	2.03	2.01
Cr	0.00	0.00	0.00	0.00	0.00	0.00	0.00	0.00	0.00	0.00	0.00	0.00	0.00	0.00	0.00	0.00	0.00	0.00	0.00	0.00	0.00	0.00
Fe	2.22	2.10	2.12	2.14	2.16	2.12	2.14	2.10	2.13	2.18	2.17	2.08	2.10	2.13	2.19	2.13	2.17	2.15	2.01	2.02	2.06	2.05
Mn	0.07	0.09	0.10	0.10	0.11	0.13	0.13	0.15	0.14	0.07	0.13	0.19	0.11	0.09	0.11	0.10	0.09	0.08	0.23	0.22	0.18	0.17
Mg	0.35	0.33	0.31	0.33	0.32	0.31	0.30	0.31	0.30	0.37	0.31	0.29	0.32	0.39	0.32	0.38	0.37	0.40	0.31	0.36	0.33	0.33
Ca	0.32	0.39	0.41	0.36	0.37	0.37	0.36	0.38	0.37	0.32	0.33	0.40	0.44	0.32	0.32	0.39	0.32	0.33	0.43	0.38	0.39	0.42
Na	0.00	0.00	0.00	0.00	0.00	0.00	0.00	0.01	0.00	0.00	0.00	0.00	0.00	0.00	0.01	0.00	0.01	0.00	0.01	0.00	0.00	0.00
K	0.00	0.00	0.00	0.00	0.00	0.00	0.00	0.00	0.00	0.00	0.00	0.00	0.00	0.00	0.00	0.00	0.00	0.00	0.00	0.00	0.00	0.00
Total (All)	7.99	7.97	7.97	7.97	7.99	7.98	7.97	7.98	7.98	7.98	7.98	7.99	8.00	7.98	7.99	8.00	7.99	7.99	8.00	8.00	7.99	7.99
Total (Majors ONLY)	7.99	7.97	7.97	7.97	7.99	7.97	7.97	7.98	7.98	7.98	7.98	7.98	8.00	7.98	7.99	8.00	7.99	7.99	8.00	8.00	7.99	7.99
XGrss (= Ca/(Ca+Fe+M	0.11	0.13	0.14	0.12	0.12	0.13	0.12	0.13	0.12	0.11	0.11	0.14	0.15	0.11	0.11	0.13	0.11	0.11	0.14	0.13	0.13	0.14
XSpss (= Mn/(Mn+Fe+	0.02	0.03	0.03	0.03	0.04	0.05	0.04	0.05	0.05	0.02	0.05	0.06	0.04	0.03	0.04	0.03	0.03	0.03	0.08	0.07	0.06	0.06
XAlm (= Fe/(Fe+Mg+M	0.75	0.72	0.72	0.73	0.73	0.72	0.73	0.71	0.73	0.74	0.74	0.70	0.71	0.73	0.75	0.71	0.73	0.73	0.68	0.68	0.70	0.69
XPy (= Mg/(Mg+Mn+C	0.12	0.11	0.11	0.11	0.11	0.11	0.10	0.10	0.10	0.13	0.11	0.10	0.11	0.13	0.11	0.13	0.13	0.13	0.11	0.12	0.11	0.11

Note: Analyses conducted on the same mineral grain (e.g. 1 core analysis and 2 rim analyses on a specific garnet grain) are highlighted in the same colour and enclosed in the same thick black box.

Garnets cont.

Analysis Label (Specimen_mineral_grain/zone:spot number)	gb10_gt_1e	gb10_gt_1h	gb10_gt_1k	gb10_gt_1u	gb10_gt_1w	gb10_gt_1x	gb10_gt_1o	gb10_gt_1p	gb10_gt_1r	gb10_gt_1t	gb10_gt_1l	gb10_gt_1n	gb10_gt_1q	gb10_gt_1s	gb10_gt_1v	gb10_gt_2a	gb10_gt_2e	gb10_gt_2f	gb10_gt_2b	gb10_gt_2d	gb10_gt_2c	gb10_gt_2h
Mineral Probed:	gt	gt	gt	gt	gt	gt	gt	gt	gt	gt	gt	gt	gt	gt	gt	gt	gt	gt	gt	gt	gt	gt
Core/Int/Rim:	Core	Core	Core	Core	Core	Core	Int	Int	Int	Int	Rim	Rim	Rim	Rim	Rim	Rim	Rim	Rim	Int	Int	Core	Int
EMP Initial Results:																						
Oxide conc. (wt%)																						
SiO2	37.45	37.46	37.54	37.33	37.64	37.56	37.61	37.79	37.41	37.51	37.64	37.51	37.36	37.70	37.60	38.02	37.35	37.37	37.55	37.50	37.50	37.75
TiO2	0.13	0.18	0.10	0.10	0.05	0.08	0.08	0.11	0.07	0.11	0.00	0.00	0.05	0.03	0.00	0.02	0.00	0.01	0.05	0.06	0.03	0.01
Al2O3	21.55	21.26	21.39	21.46	21.69	21.43	21.78	21.65	21.39	21.67	21.72	21.57	22.02	21.73	21.65	21.56	21.59	21.43	21.58	21.63	21.66	21.67
Cr2O3	0.02	0.04	0.00	0.02	0.05	0.06	0.04	0.02	0.03	0.04	0.02	0.00	0.01	0.05	0.00	0.03	0.02	0.04	0.00	0.04	0.00	0.05
FeO	29.13	29.15	29.73	29.41	28.73	29.72	31.93	29.98	28.80	28.93	32.23	32.31	31.01	30.34	32.10	30.61	32.24	32.38	30.83	31.58	31.41	32.07
MnO	4.80	4.58	3.72	3.69	5.33	4.71	1.91	3.63	5.10	4.99	1.35	1.26	2.13	2.52	1.38	2.57	1.44	1.35	2.67	2.03	2.69	1.64
MgO	2.45	2.41	2.55	2.53	2.28	2.44	3.10	2.58	2.30	2.37	3.37	3.23	3.35	3.13	2.99	3.23	2.92	3.32	2.92	3.03	3.00	3.26
CaO	4.98	4.91	5.26	5.40	4.64	4.83	4.20	5.13	5.17	5.13	3.80	3.88	4.06	4.53	3.77	4.44	3.86	3.99	4.60	4.09	3.74	4.03
Na2O	0.00	0.00	0.00	0.00	0.00	0.00	0.01	0.05	0.00	0.00	0.04	0.03	0.01	0.00	0.00	0.00	0.02	0.02	0.03	0.03	0.05	0.05
K2O	0.00	0.00	0.00	0.00	0.00	0.00	0.00	0.00	0.00	0.00	0.00	0.00	0.00	0.00	0.00	0.00	0.00	0.00	0.00	0.00	0.00	0.00
Total	100.51	99.99	100.29	99.94	100.42	100.83	100.65	100.94	100.27	100.75	100.17	99.78	100.00	100.03	99.49	100.48	99.44	99.91	100.23	99.99	100.08	100.53
Cations:																						
Si	2.98	3.00	2.99	2.99	3.00	2.99	2.98	2.99	2.99	2.98	2.99	3.00	2.97	3.00	3.01	3.01	3.00	2.99	2.99	2.99	2.99	2.99
Ti	0.01	0.01	0.01	0.01	0.00	0.00	0.00	0.01	0.00	0.01	0.00	0.00	0.00	0.00	0.00	0.00	0.00	0.00	0.00	0.00	0.00	0.00
Al	2.02	2.01	2.01	2.02	2.04	2.01	2.04	2.02	2.01	2.03	2.04	2.03	2.06	2.04	2.04	2.01	2.04	2.02	2.03	2.03	2.04	2.03
Cr	0.00	0.00	0.00	0.00	0.00	0.00	0.00	0.00	0.00	0.00	0.00	0.00	0.00	0.00	0.00	0.00	0.00	0.00	0.00	0.00	0.00	0.00
Fe	1.94	1.95	1.98	1.97	1.91	1.98	2.12	1.98	1.92	1.92	2.14	2.16	2.06	2.02	2.15	2.03	2.16	2.16	2.05	2.11	2.10	2.13
Mn	0.32	0.31	0.25	0.25	0.36	0.32	0.13	0.24	0.35	0.34	0.09	0.09	0.14	0.17	0.09	0.17	0.10	0.09	0.18	0.14	0.18	0.11
Mg	0.29	0.29	0.30	0.30	0.27	0.29	0.37	0.30	0.27	0.28	0.40	0.38	0.40	0.37	0.36	0.38	0.35	0.40	0.35	0.36	0.36	0.39
Ca	0.43	0.42	0.45	0.46	0.40	0.41	0.36	0.44	0.44	0.44	0.32	0.33	0.35	0.39	0.32	0.38	0.33	0.34	0.39	0.35	0.32	0.34
Na	0.00	0.00	0.00	0.00	0.00	0.00	0.00	0.01	0.00	0.00	0.01	0.00	0.00	0.00	0.00	0.00	0.00	0.00	0.00	0.00	0.01	0.01
K	0.00	0.00	0.00	0.00	0.00	0.00	0.00	0.00	0.00	0.00	0.00	0.00	0.00	0.00	0.00	0.00	0.00	0.00	0.00	0.00	0.00	0.00
Total (All)	8.00	7.99	8.00	8.00	7.98	8.00	8.00	8.00	8.00	8.00	7.99	7.99	7.99	7.98	7.97	7.98	7.98	8.00	8.00	7.99	7.99	8.00
Total (Majors ONLY)	8.00	7.98	8.00	8.00	7.98	8.00	7.99	7.99	8.00	7.99	7.99	7.99	7.99	7.98	7.97	7.98	7.98	8.00	8.00	7.99	7.99	7.99
XGrss (= Ca/(Ca+Fe+M	0.14	0.14	0.15	0.16	0.13	0.14	0.12	0.15	0.15	0.15	0.11	0.11	0.12	0.13	0.11	0.13	0.11	0.11	0.13	0.12	0.11	0.12
XSpss (= Mn/(Mn+Fe+	0.11	0.10	0.08	0.08	0.12	0.11	0.04	0.08	0.12	0.11	0.03	0.03	0.05	0.06	0.03	0.06	0.03	0.03	0.06	0.05	0.06	0.04
XAlm (= Fe/(Fe+Mg+M	0.65	0.66	0.66	0.66	0.65	0.66	0.71	0.67	0.64	0.65	0.72	0.73	0.70	0.69	0.74	0.69	0.74	0.72	0.69	0.71	0.71	0.72
XPy (= Mg/(Mg+Mn+C	0.10	0.10	0.10	0.10	0.09	0.10	0.12	0.10	0.09	0.09	0.14	0.13	0.13	0.13	0.12	0.13	0.12	0.13	0.12	0.12	0.12	0.13

Note: Analyses conducted on the same mineral grain (e.g. 1 core analysis and 2 rim analyses on a specific garnet grain) are highlighted in the same colour and enclosed in the same thick black box.

Garnets cont.

Analysis Label (Specimen_mineral_grain/zone:spot number)	gb10_gt_2g	gb10_gt_2i	gb10_gt_2j	gb10_gt_2k	gb10_gt_2l	gb10_gt_2m	gb10_gt_2n	gb10_gt_2o	gb10_gt_2r	gb10_gt_2p	gb10_gt_2q	gb10_gt_2s	gb10_gt_3n	gb10_gt_3l	gb10_gt_3m	gb10_gt_3o	gb10_gt_3p	gb13_gt_1a	gb13_gt_1c	gb13_gt_1d	gb13_gt_1e	gb13_gt_1b
Mineral Probed:	gt	gt	gt	gt	gt	gt	gt	gt	gt	gt	gt	gt	gt	gt	gt	gt	gt	gt	gt	gt	gt	gt
Core/Int/Rim:	Rim	Rim	Rim	Int	Core	Core	Rim	Rim	Rim	Core	Core	Rim	Rim	Int	Core	Core	Rim	Rim	Int	Core	Core	Rim
EMP Initial Results:																						
Oxide conc. (wt%)																						
SiO2	37.62	37.56	37.50	37.38	37.69	37.57	37.70	37.25	37.69	37.34	37.52	37.69	37.32	37.61	37.67	37.61	37.45	38.03	37.48	37.56	37.26	37.85
TiO2	0.07	0.01	0.02	0.05	0.10	0.06	0.07	0.02	0.02	0.05	0.06	0.05	0.01	0.05	0.15	0.05	0.00	0.00	0.07	0.06	0.14	0.02
Al2O3	21.58	21.73	21.62	21.51	21.58	21.58	21.66	21.74	21.68	21.47	21.56	21.63	21.40	21.68	21.54	21.62	21.59	21.78	21.52	21.42	21.02	21.92
Cr2O3	0.03	0.05	0.04	0.00	0.02	0.04	0.01	0.00	0.04	0.03	0.01	0.00	0.02	0.01	0.03	0.05	0.00	0.02	0.03	0.00	0.00	0.03
FeO	31.42	32.47	32.69	31.68	31.54	31.49	31.06	32.69	32.49	31.39	30.59	32.14	32.29	31.21	31.44	31.57	32.06	32.62	31.44	30.64	28.03	33.38
MnO	1.70	1.49	1.33	1.88	2.52	2.25	2.16	1.44	1.40	2.47	2.83	1.51	1.39	2.29	2.50	1.72	1.33	1.02	1.52	3.23	5.22	1.03
MgO	2.77	2.72	3.30	3.16	3.05	3.02	3.12	2.97	3.14	2.92	2.87	2.95	3.24	3.19	2.87	3.04	3.10	3.10	2.92	2.17	1.97	2.93
CaO	4.83	3.81	3.71	4.03	4.32	4.15	4.20	3.91	3.84	4.11	4.83	3.81	3.76	4.13	4.37	4.44	3.88	3.75	5.09	5.17	5.84	3.75
Na2O	0.01	0.02	0.07	0.02	0.00	0.01	0.01	0.01	0.01	0.00	0.01	0.01	0.04	0.04	0.02	0.09	0.04	0.06	0.03	0.09	0.04	0.02
K2O	0.00	0.00	0.00	0.00	0.00	0.00	0.00	0.00	0.00	0.00	0.00	0.00	0.00	0.00	0.00	0.00	0.00	0.00	0.00	0.00	0.00	0.00
Total	100.03	99.87	100.27	99.71	100.82	100.16	99.99	100.03	100.31	99.78	100.29	99.78	99.47	100.21	100.59	100.18	99.45	100.38	100.09	100.35	99.52	100.92
Cations:																						
Si	3.00	3.00	2.99	2.99	2.99	2.99	3.00	2.98	3.00	2.99	2.99	3.01	2.99	2.99	2.99	2.99	3.00	3.01	2.99	3.00	3.00	2.99
Ti	0.00	0.00	0.00	0.00	0.01	0.00	0.00	0.00	0.00	0.00	0.00	0.00	0.00	0.00	0.01	0.00	0.00	0.00	0.00	0.00	0.01	0.00
Al	2.03	2.05	2.03	2.03	2.02	2.03	2.03	2.05	2.03	2.03	2.02	2.04	2.02	2.03	2.02	2.03	2.04	2.03	2.02	2.02	2.00	2.04
Cr	0.00	0.00	0.00	0.00	0.00	0.00	0.00	0.00	0.00	0.00	0.00	0.00	0.00	0.00	0.00	0.00	0.00	0.00	0.00	0.00	0.00	0.00
Fe	2.09	2.17	2.18	2.12	2.09	2.10	2.07	2.18	2.16	2.10	2.04	2.15	2.17	2.08	2.09	2.10	2.15	2.16	2.10	2.05	1.89	2.21
Mn	0.11	0.10	0.09	0.13	0.17	0.15	0.15	0.10	0.09	0.17	0.19	0.10	0.09	0.15	0.17	0.12	0.09	0.07	0.10	0.22	0.36	0.07
Mg	0.33	0.32	0.39	0.38	0.36	0.36	0.37	0.35	0.37	0.35	0.34	0.35	0.39	0.38	0.34	0.36	0.37	0.37	0.35	0.26	0.24	0.35
Ca	0.41	0.33	0.32	0.35	0.37	0.35	0.36	0.33	0.33	0.35	0.41	0.33	0.32	0.35	0.37	0.38	0.33	0.32	0.43	0.44	0.50	0.32
Na	0.00	0.00	0.01	0.00	0.00	0.00	0.00	0.00	0.00	0.00	0.00	0.00	0.01	0.01	0.00	0.01	0.01	0.01	0.00	0.01	0.01	0.00
K	0.00	0.00	0.00	0.00	0.00	0.00	0.00	0.00	0.00	0.00	0.00	0.00	0.00	0.00	0.00	0.00	0.00	0.00	0.00	0.00	0.00	0.00
Total (All)	7.98	7.98	8.00	7.99	8.00	7.99	7.98	8.00	7.99	7.99	8.00	7.97	8.00	7.99	7.99	8.00	7.98	7.97	8.00	8.00	8.00	7.98
Total (Majors ONLY)	7.98	7.97	8.00	7.99	8.00	7.99	7.98	8.00	7.98	7.99	8.00	7.97	7.99	7.99	7.99	7.99	7.98	7.97	8.00	8.00	8.00	7.98
XGrss (= Ca/(Ca+Fe+M	0.14	0.11	0.11	0.12	0.12	0.12	0.12	0.11	0.11	0.12	0.14	0.11	0.11	0.12	0.13	0.13	0.11	0.11	0.15	0.15	0.17	0.11
XSpss (= Mn/(Mn+Fe+	0.04	0.03	0.03	0.04	0.06	0.05	0.05	0.03	0.03	0.06	0.06	0.03	0.03	0.05	0.06	0.04	0.03	0.02	0.03	0.07	0.12	0.02
XAlm (= Fe/(Fe+Mg+M	0.71	0.74	0.73	0.71	0.70	0.71	0.70	0.74	0.73	0.71	0.68	0.73	0.73	0.70	0.70	0.71	0.73	0.74	0.70	0.69	0.63	0.75
XPy (= Mg/(Mg+Mn+C	0.11	0.11	0.13	0.13	0.12	0.12	0.13	0.12	0.13	0.12	0.11	0.12	0.13	0.13	0.11	0.12	0.13	0.13	0.12	0.09	0.08	0.12

Note: Analyses conducted on the same mineral grain (e.g. 1 core analysis and 2 rim analyses on a specific garnet grain) are highlighted in the same colour and enclosed in the same thick black box.

Garnets cont.

Analysis Label (Specimen_mineral_grain/zone:spot number)	gb13_gt_2c	gb13_gt_2e	gb13_gt_2a	gb13_gt_2d	gb13_gt_3c	gb13_gt_3b	gb13_gt_3a	gb13_gt_4b	gb13_gt_4a	gb13_gt_5c	gb13_gt_5d	gb13_gt_5a	gb13_gt_5e	gb13_gt_6e	gb13_gt_6c	gb13_gt_6b	gb13_gt_7b	gb13_gt_7a	gb13_gt_7c	gb13_gt_7d	gb13_gt_7e	gb13_gt_8c
Mineral Probed:	gt	gt	gt	gt	gt	gt	gt	gt	gt	gt	gt	gt	gt	gt	gt	gt	gt	gt	gt	gt	gt	gt
Core/Int/Rim:	Rim	Int	Core	Rim	Rim	Int	Core	Int	Core	Rim	Int	Core	Rim	Rim	Int	Core	Rim	Int	Core	Int	Rim	Rim
EMP Initial Results:																						
Oxide conc. (wt%)																						
SiO2	37.69	37.72	37.73	37.65	37.70	37.87	37.78	37.66	37.59	37.73	37.72	37.35	38.01	37.77	37.89	37.73	38.02	37.88	37.31	37.39	37.59	37.87
TiO2	0.04	0.09	0.11	0.07	0.00	0.01	0.04	0.05	0.08	0.00	0.07	0.14	0.00	0.03	0.06	0.09	0.05	0.08	0.10	0.14	0.06	0.03
Al2O3	22.02	21.82	21.61	21.68	21.73	21.84	21.67	21.77	21.65	21.79	21.61	21.42	21.89	21.90	21.64	21.68	21.71	21.62	21.17	21.39	21.83	22.11
Cr2O3	0.03	0.00	0.04	0.01	0.04	0.00	0.06	0.01	0.06	0.02	0.00	0.02	0.03	0.03	0.04	0.00	0.01	0.03	0.07	0.00	0.01	0.00
FeO	32.36	31.78	31.86	32.42	32.76	32.49	33.38	32.13	32.53	32.15	33.14	31.76	32.72	32.10	32.68	32.72	32.30	31.91	24.86	27.61	31.58	32.79
MnO	0.91	1.63	1.44	0.52	1.14	0.47	0.45	0.47	0.59	1.38	0.56	1.78	1.09	1.35	0.67	0.53	1.04	1.33	9.56	6.75	1.51	1.04
MgO	3.27	2.43	2.46	3.28	3.01	3.47	3.37	3.06	3.26	3.04	2.76	2.31	3.26	3.21	2.94	2.97	3.12	2.54	1.31	1.65	3.42	3.26
CaO	3.83	5.55	5.41	4.59	3.85	4.20	4.14	4.97	4.66	4.00	4.60	5.31	3.84	3.86	4.87	4.59	4.69	5.50	6.13	6.02	3.87	3.86
Na2O	0.00	0.01	0.04	0.03	0.03	0.04	0.03	0.06	0.05	0.04	0.00	0.01	0.03	0.02	0.02	0.04	0.08	0.00	0.05	0.02	0.05	0.05
K2O	0.00	0.00	0.00	0.00	0.00	0.00	0.00	0.00	0.00	0.00	0.00	0.00	0.00	0.00	0.00	0.00	0.00	0.00	0.00	0.00	0.00	0.00
Total	100.15	101.03	100.70	100.25	100.25	100.39	100.93	100.17	100.47	100.16	100.46	100.10	100.87	100.27	100.81	100.34	101.02	100.89	100.57	100.96	99.92	101.00
Cations:																						
Si	2.99	2.98	2.99	2.99	3.00	3.00	2.99	2.99	2.98	3.00	3.00	2.99	3.00	3.00	3.00	3.00	3.00	3.00	2.99	2.98	2.99	2.99
Ti	0.00	0.01	0.01	0.00	0.00	0.00	0.00	0.00	0.00	0.00	0.00	0.01	0.00	0.00	0.00	0.01	0.00	0.00	0.01	0.01	0.00	0.00
Al	2.06	2.03	2.02	2.03	2.04	2.04	2.02	2.04	2.02	2.04	2.02	2.02	2.04	2.05	2.02	2.03	2.02	2.02	2.00	2.01	2.05	2.05
Cr	0.00	0.00	0.00	0.00	0.00	0.00	0.00	0.00	0.00	0.00	0.00	0.00	0.00	0.00	0.00	0.00	0.00	0.00	0.00	0.00	0.00	0.00
Fe	2.15	2.10	2.11	2.15	2.18	2.15	2.21	2.13	2.16	2.14	2.20	2.12	2.16	2.13	2.16	2.17	2.13	2.11	1.67	1.84	2.10	2.16
Mn	0.06	0.11	0.10	0.03	0.08	0.03	0.03	0.03	0.04	0.09	0.04	0.12	0.07	0.09	0.04	0.04	0.07	0.09	0.65	0.46	0.10	0.07
Mg	0.39	0.29	0.29	0.39	0.36	0.41	0.40	0.36	0.39	0.36	0.33	0.28	0.38	0.38	0.35	0.35	0.37	0.30	0.16	0.20	0.41	0.38
Ca	0.33	0.47	0.46	0.39	0.33	0.36	0.35	0.42	0.40	0.34	0.39	0.46	0.32	0.33	0.41	0.39	0.40	0.47	0.53	0.51	0.33	0.33
Na	0.00	0.00	0.01	0.00	0.00	0.01	0.00	0.01	0.01	0.01	0.00	0.00	0.00	0.00	0.00	0.01	0.01	0.00	0.01	0.00	0.01	0.01
K	0.00	0.00	0.00	0.00	0.00	0.00	0.00	0.00	0.00	0.00	0.00	0.00	0.00	0.00	0.00	0.00	0.00	0.00	0.00	0.00	0.00	0.00
Total (All)	7.98	7.99	7.99	7.99	7.98	7.99	8.00	7.99	8.00	7.98	7.99	7.99	7.98	7.98	7.99	7.99	7.99	7.99	8.01	8.01	7.99	7.99
Total (Majors ONLY)	7.97	7.99	7.99	7.99	7.98	7.99	8.00	7.99	8.00	7.98	7.99	7.99	7.98	7.98	7.99	7.99	7.99	7.99	8.00	8.01	7.99	7.99
XGrss (= Ca/(Ca+Fe+M	0.11	0.16	0.16	0.13	0.11	0.12	0.12	0.14	0.13	0.12	0.13	0.15	0.11	0.11	0.14	0.13	0.13	0.16	0.18	0.17	0.11	0.11
XSpss (= Mn/(Mn+Fe+	0.02	0.04	0.03	0.01	0.03	0.01	0.01	0.01	0.01	0.03	0.01	0.04	0.02	0.03	0.02	0.01	0.02	0.03	0.22	0.15	0.03	0.02
XAlm (= Fe/(Fe+Mg+M	0.74	0.71	0.71	0.73	0.74	0.73	0.74	0.72	0.72	0.73	0.74	0.71	0.73	0.73	0.73	0.74	0.72	0.71	0.56	0.61	0.72	0.74
XPy (= Mg/(Mg+Mn+C	0.13	0.10	0.10	0.13	0.12	0.14	0.13	0.12	0.13	0.12	0.11	0.09	0.13	0.13	0.12	0.12	0.12	0.10	0.05	0.07	0.14	0.13

Note: Analyses conducted on the same mineral grain (e.g. 1 core analysis and 2 rim analyses on a specific garnet grain) are highlighted in the same colour and enclosed in the same thick black box.

Garnets cont.

Analysis Label (Specimen_mineral_grain/zone:spot number)	gb13_gt_8e	gb13_gt_8b	gb13_gt_8a	gb13_gt_8f	gb13_gt_9c	gb13_gt_9e	gb13_gt_9b	gb13_gt_10e	gb13_gt_10b	gb13_gt_10a	gb13_gt_10d	gb13_gt_10f	gb13_gt_10g	gb13_gt_11a	gb13_gt_11b	gb13_gt_11f	gb13_gt_11c	gb13_gt_11g	gb13_gt_11d	gb13_gt_11e	gb13_gt_11h	gb13_gt_11i
Mineral Probed: Core/Int/Rim:	gt Rim	gt Int	gt Core	gt Rim	gt Rim	gt Rim	gt Int	gt Rim	gt Int	gt Core	gt Core	gt Int	gt Rim	gt Rim	gt Rim	gt Rim	gt Int	gt Int	gt Core	gt Core	gt Core	gt Int
EMP Initial Results:																						
Oxide conc. (wt%)																						
SiO2	37.60	37.84	37.11	38.26	37.67	37.55	37.80	38.10	37.85	37.75	37.45	37.70	37.64	37.88	37.92	37.68	37.54	37.55	37.37	37.22	37.42	37.52
TiO2	0.04	0.10	0.12	0.01	0.02	0.01	0.08	0.00	0.11	0.05	0.12	0.05	0.05	0.03	0.07	0.06	0.10	0.10	0.12	0.13	0.09	0.03
Al2O3	21.73	21.52	21.14	21.83	21.83	21.66	21.54	21.95	21.41	21.72	21.41	21.48	21.89	21.92	21.78	21.60	21.20	21.60	21.26	21.06	21.31	21.45
Cr2O3	0.04	0.03	0.03	0.03	0.01	0.00	0.04	0.02	0.00	0.00	0.03	0.05	0.03	0.02	0.03	0.12	0.00	0.00	0.00	0.01	0.00	0.00
FeO	32.61	31.67	28.99	33.01	32.78	32.62	32.88	32.08	32.80	32.88	29.97	31.24	32.80	32.82	32.92	33.08	29.49	31.99	26.36	25.77	29.12	31.69
MnO	1.05	0.73	5.46	0.67	1.01	0.93	0.51	1.01	0.25	0.86	4.18	2.30	0.98	0.95	0.90	0.42	3.96	0.99	6.92	7.85	5.48	1.51
MgO	3.10	2.71	1.90	3.47	3.18	3.17	2.81	3.21	3.09	2.74	1.99	2.39	3.33	3.22	3.32	3.45	2.01	2.66	1.54	1.45	1.88	2.49
CaO	4.04	5.97	5.26	3.51	3.72	3.76	4.77	4.05	4.77	4.99	5.36	5.28	3.97	3.86	3.73	3.88	5.41	5.39	6.53	6.41	5.29	5.15
Na2O	0.04	0.00	0.03	0.04	0.00	0.04	0.00	0.01	0.04	0.02	0.03	0.01	0.01	0.03	0.04	0.03	0.01	0.04	0.03	0.01	0.02	0.04
K2O	0.00	0.00	0.00	0.00	0.00	0.00	0.00	0.00	0.00	0.00	0.00	0.00	0.00	0.00	0.00	0.00	0.00	0.00	0.00	0.00	0.00	0.00
Total	100.24	100.57	100.04	100.83	100.22	99.74	100.44	100.43	100.32	101.01	100.53	100.51	100.70	100.73	100.71	100.32	99.71	100.32	100.13	99.93	100.61	99.87
Cations:																						
Si	2.99	3.00	2.99	3.01	2.99	3.00	3.00	3.01	3.01	2.99	2.99	3.00	2.98	2.99	3.00	2.99	3.01	2.99	2.99	2.99	2.99	3.00
Ti	0.00	0.01	0.01	0.00	0.00	0.00	0.00	0.00	0.01	0.00	0.01	0.00	0.00	0.00	0.00	0.00	0.01	0.01	0.01	0.01	0.01	0.00
Al	2.04	2.01	2.00	2.03	2.05	2.04	2.02	2.04	2.00	2.03	2.01	2.01	2.04	2.04	2.03	2.02	2.01	2.03	2.01	2.00	2.01	2.02
Cr	0.00	0.00	0.00	0.00	0.00	0.00	0.00	0.00	0.00	0.00	0.00	0.00	0.00	0.00	0.00	0.01	0.00	0.00	0.00	0.00	0.00	0.00
Fe	2.17	2.10	1.95	2.17	2.18	2.18	2.18	2.12	2.18	2.18	2.00	2.08	2.17	2.17	2.18	2.20	1.98	2.13	1.77	1.73	1.95	2.12
Mn	0.07	0.05	0.37	0.04	0.07	0.06	0.03	0.07	0.02	0.06	0.28	0.16	0.07	0.06	0.06	0.03	0.27	0.07	0.47	0.54	0.37	0.10
Mg	0.37	0.32	0.23	0.41	0.38	0.38	0.33	0.38	0.37	0.32	0.24	0.28	0.39	0.38	0.39	0.41	0.24	0.32	0.18	0.17	0.22	0.30
Ca	0.34	0.51	0.45	0.30	0.32	0.32	0.41	0.34	0.41	0.42	0.46	0.45	0.34	0.33	0.32	0.33	0.47	0.46	0.56	0.55	0.45	0.44
Na	0.01	0.00	0.00	0.01	0.00	0.01	0.00	0.00	0.01	0.00	0.00	0.00	0.00	0.00	0.01	0.00	0.00	0.01	0.00	0.00	0.00	0.01
K	0.00	0.00	0.00	0.00	0.00	0.00	0.00	0.00	0.00	0.00	0.00	0.00	0.00	0.00	0.00	0.00	0.00	0.00	0.00	0.00	0.00	0.00
Total (All)	7.99	7.99	8.01	7.97	7.98	7.98	7.98	7.97	7.99	8.00	8.00	7.99	8.00	7.98	7.98	7.99	7.98	8.00	8.00	8.00	8.00	7.99
Total (Majors ONLY)	7.99	7.99	8.00	7.97	7.98	7.98	7.98	7.97	7.99	8.00	8.00	7.99	7.99	7.98	7.98	7.98	7.98	8.00	8.00	8.00	8.00	7.99
XGrss (= Ca/(Ca+Fe+M	0.12	0.17	0.15	0.10	0.11	0.11	0.14	0.12	0.14	0.14	0.15	0.15	0.11	0.11	0.11	0.11	0.16	0.15	0.19	0.18	0.15	0.15
XSpss (= Mn/(Mn+Fe+	0.02	0.02	0.12	0.02	0.02	0.02	0.01	0.02	0.01	0.02	0.09	0.05	0.02	0.02	0.02	0.01	0.09	0.02	0.16	0.18	0.12	0.03
XAlm (= Fe/(Fe+Mg+M	0.73	0.71	0.65	0.74	0.74	0.74	0.74	0.73	0.73	0.73	0.67	0.70	0.73	0.74	0.74	0.74	0.67	0.72	0.59	0.58	0.65	0.72
XPy (= Mg/(Mg+Mn+C	0.12	0.11	0.08	0.14	0.13	0.13	0.11	0.13	0.12	0.11	0.08	0.10	0.13	0.13	0.13	0.14	0.08	0.11	0.06	0.06	0.07	0.10

Note: Analyses conducted on the same mineral grain (e.g. 1 core analysis and 2 rim analyses on a specific garnet grain) are highlighted in the same colour and enclosed in the same thick black box.

Garnets cont.

Analysis Label (Specimen_mineral_grain/zone:spot number)	gb13_gt_11k	gb13_gt_11j	gb13_gt_11l	gb13_gt_12a	gb13_gt_12b	gb13_gt_12c	gb13_gt_12d	gb13_gt_12e	ma29_gt_1c	ma29_gt_1d	ma29_gt_1b	ma29_gt_1a	ma29_gt_1e	ma29_gt_1h	ma29_gt_1g	ma29_gt_1f	ma29_gt_1i	ma29_gt_1j	ma29_gt_1l	ma29_gt_1k	ma29_gt_1m	ma29_gt_1p
Mineral Probed: Core/Int/Rim:	gt Int	gt Rim	gt Rim	gt Rim	gt Int	gt Core	gt Int	gt Rim	gt Rim	gt Rim	gt Int	gt Core	gt Rim	gt Rim	gt Int	gt Core	gt Rim	gt Rim	gt Int	gt Core	gt Rim	gt Rim
EMP Initial Results:																						
Oxide conc. (wt%)																						
SiO2	37.71	37.83	37.78	37.67	37.79	37.73	37.66	38.02	37.68	37.72	37.62	37.31	37.14	37.72	37.79	37.53	37.74	37.76	37.70	37.44	37.50	37.64
TiO2	0.09	0.01	0.03	0.01	0.04	0.07	0.01	0.00	0.00	0.03	0.04	0.07	0.72	0.04	0.04	0.06	0.02	0.00	0.05	0.07	0.01	0.03
Al2O3	21.60	21.75	21.80	21.99	21.83	21.67	22.05	21.72	21.76	22.01	21.68	21.58	21.31	21.84	21.74	21.66	21.74	21.84	21.77	21.34	21.69	21.75
Cr2O3	0.01	0.01	0.00	0.02	0.02	0.00	0.02	0.02	0.05	0.00	0.03	0.04	0.00	0.01	0.00	0.02	0.02	0.00	0.04	0.05	0.00	0.01
FeO	31.54	32.90	32.51	32.86	32.79	32.81	32.60	32.21	34.34	34.28	32.10	27.70	33.17	34.18	31.69	29.00	34.98	33.59	31.76	28.82	33.51	34.83
MnO	1.62	0.86	0.57	1.62	0.58	0.43	1.20	1.46	0.74	0.92	2.03	6.26	1.72	0.73	2.71	5.43	1.09	0.80	2.75	5.43	0.72	1.00
MgO	2.45	3.25	3.38	2.97	3.44	3.34	3.33	3.03	3.24	3.23	2.85	1.94	2.62	3.22	2.53	2.02	2.83	3.25	2.66	1.96	3.43	2.91
CaO	5.89	3.84	3.98	3.81	4.19	4.28	3.89	3.88	2.45	2.67	4.02	5.08	3.02	2.64	4.12	4.96	2.40	3.05	4.01	4.82	2.90	2.37
Na2O	0.06	0.03	0.02	0.01	0.00	0.02	0.01	0.03	0.04	0.05	0.03	0.07	0.05	0.01	0.03	0.04	0.04	0.02	0.00	0.06	0.02	0.05
K2O	0.00	0.00	0.00	0.00	0.00	0.00	0.00	0.00	0.00	0.00	0.00	0.00	0.00	0.00	0.00	0.00	0.00	0.00	0.00	0.00	0.00	0.00
Total	100.97	100.49	100.08	100.96	100.68	100.36	100.77	100.38	100.30	100.91	100.40	100.05	99.75	100.39	100.65	100.72	100.87	100.31	100.74	100.00	99.78	100.59
Cations:																						
Si	2.99	3.00	3.00	2.98	2.99	2.99	2.98	3.01	3.00	2.99	2.99	2.99	2.98	3.00	3.00	2.99	3.00	3.00	2.99	3.00	3.00	3.00
Ti	0.01	0.00	0.00	0.00	0.00	0.00	0.00	0.00	0.00	0.00	0.00	0.00	0.04	0.00	0.00	0.00	0.00	0.00	0.00	0.00	0.00	0.00
Al	2.02	2.03	2.04	2.05	2.03	2.03	2.06	2.03	2.04	2.05	2.03	2.04	2.02	2.05	2.04	2.03	2.04	2.05	2.04	2.02	2.04	2.04
Cr	0.00	0.00	0.00	0.00	0.00	0.00	0.00	0.00	0.00	0.00	0.00	0.00	0.00	0.00	0.00	0.00	0.00	0.00	0.00	0.00	0.00	0.00
Fe	2.09	2.18	2.16	2.17	2.17	2.18	2.16	2.14	2.29	2.27	2.14	1.86	2.23	2.27	2.10	1.93	2.33	2.23	2.11	1.93	2.24	2.32
Mn	0.11	0.06	0.04	0.11	0.04	0.03	0.08	0.10	0.05	0.06	0.14	0.42	0.12	0.05	0.18	0.37	0.07	0.05	0.18	0.37	0.05	0.07
Mg	0.29	0.38	0.40	0.35	0.41	0.39	0.39	0.36	0.38	0.38	0.34	0.23	0.31	0.38	0.30	0.24	0.34	0.38	0.31	0.23	0.41	0.35
Ca	0.50	0.33	0.34	0.32	0.35	0.36	0.33	0.33	0.21	0.23	0.34	0.44	0.26	0.22	0.35	0.42	0.20	0.26	0.34	0.41	0.25	0.20
Na	0.01	0.00	0.00	0.00	0.00	0.00	0.00	0.01	0.01	0.01	0.00	0.01	0.01	0.00	0.00	0.01	0.01	0.00	0.00	0.01	0.00	0.01
K	0.00	0.00	0.00	0.00	0.00	0.00	0.00	0.00	0.00	0.00	0.00	0.00	0.00	0.00	0.00	0.00	0.00	0.00	0.00	0.00	0.00	0.00
Total (All)	8.00	7.99	7.98	7.99	7.99	7.99	7.99	7.97	7.98	7.99	7.99	7.99	7.97	7.98	7.98	7.99	7.98	7.98	7.98	7.99	7.99	7.98
Total (Majors ONLY)	8.00	7.99	7.98	7.99	7.99	7.99	7.99	7.97	7.98	7.99	7.99	7.99	7.97	7.98	7.98	7.99	7.98	7.98	7.98	7.98	7.99	7.98
XGrss (= Ca/(Ca+Fe+M	0.17	0.11	0.12	0.11	0.12	0.12	0.11	0.11	0.07	0.08	0.12	0.15	0.09	0.08	0.12	0.14	0.07	0.09	0.12	0.14	0.08	0.07
XSpss (= Mn/(Mn+Fe+	0.04	0.02	0.01	0.04	0.01	0.01	0.03	0.03	0.02	0.02	0.05	0.14	0.04	0.02	0.06	0.12	0.03	0.02	0.06	0.13	0.02	0.02
XAlm (= Fe/(Fe+Mg+M	0.70	0.74	0.74	0.74	0.73	0.73	0.73	0.73	0.78	0.77	0.72	0.63	0.76	0.78	0.72	0.65	0.79	0.76	0.71	0.66	0.76	0.79
XPy (= Mg/(Mg+Mn+C	0.10	0.13	0.14	0.12	0.14	0.13	0.13	0.12	0.13	0.13	0.11	0.08	0.11	0.13	0.10	0.08	0.11	0.13	0.11	0.08	0.14	0.12

Note: Analyses conducted on the same mineral grain (e.g. 1 core analysis and 2 rim analyses on a specific garnet grain) are highlighted in the same colour and enclosed in the same thick black box.

Garnets cont.

Analysis Label (Specimen_mineral_grain/zone:spot number)	ma29_gt_1o	ma29_gt_1n	ma29_gt_1q	ma29_gt_1r	ma29_gt_2a	ma29_gt_2c	ma29_gt_2b	ma29_gt_2d	ma29_gt_2g	ma29_gt_2f	ma29_gt_2e	ma29_gt_2h	ma29_gt_2k	ma29_gt_2i	ma29_gt_2h2	ma29_gt_2j	ma29_gt_2m	ma29_gt_2l	ma29_gt_2p	ma29_gt_2q	ma29_gt_2o	ma29_gt_2n
Mineral Probed: Core/Int/Rim:	gt Int	gt Core	gt Int	gt Rim	gt Rim	gt Int	gt Core	gt Rim	gt Rim	gt Int	gt Core	gt Rim	gt Rim	gt Int	gt Core	gt Int	gt Rim	gt Core	gt Rim	gt Rim	gt Int	gt Core
EMP Initial Results:																						
Oxide conc. (wt%)																						
SiO2	37.78	37.67	37.59	37.50	37.75	37.45	37.80	37.90	37.79	37.61	37.42	37.50	37.85	37.62	37.36	37.56	37.35	37.60	37.65	37.49	37.47	37.42
TiO2	0.01	0.12	0.05	0.02	0.02	0.11	0.08	0.02	0.00	0.07	0.09	0.03	0.00	0.27	0.12	0.11	0.02	0.01	0.01	0.00	0.08	0.08
Al2O3	21.77	21.47	21.76	21.87	21.98	21.71	21.73	21.67	21.95	21.59	21.79	21.65	22.00	21.47	21.80	21.32	21.63	22.12	21.74	21.74	21.56	21.72
Cr2O3	0.04	0.00	0.04	0.00	0.02	0.04	0.03	0.05	0.01	0.00	0.03	0.00	0.00	0.03	0.02	0.03	0.01	0.02	0.00	0.05	0.01	0.01
FeO	31.94	28.96	32.40	34.58	33.38	31.10	28.17	34.13	34.19	29.39	26.59	32.96	34.00	26.91	26.78	26.82	33.82	32.70	33.92	34.46	28.38	28.36
MnO	2.05	5.46	2.03	0.81	0.74	2.88	6.15	0.86	0.80	4.81	7.67	1.19	0.79	7.55	7.77	6.94	0.88	1.32	0.84	0.79	5.45	5.92
MgO	2.88	2.07	3.00	3.01	3.19	2.53	1.86	3.09	3.37	2.06	1.70	3.21	3.30	1.59	1.65	1.64	3.19	3.30	3.14	3.18	1.99	1.91
CaO	4.09	4.80	3.79	2.55	3.02	4.46	4.95	2.65	2.59	4.03	4.70	3.43	2.81	5.16	5.14	5.52	2.66	3.62	2.54	2.65	5.15	4.87
Na2O	0.05	0.03	0.01	0.03	0.02	0.05	0.04	0.01	0.01	0.02	0.02	0.04	0.05	0.04	0.00	0.00	0.05	0.00	0.04	0.01	0.00	0.01
K2O	0.00	0.00	0.00	0.00	0.00	0.00	0.00	0.00	0.00	0.00	0.00	0.00	0.00	0.00	0.00	0.00	0.00	0.00	0.00	0.00	0.00	0.00
Total	100.61	100.58	100.68	100.37	100.12	100.33	100.81	100.38	100.71	99.57	100.01	100.01	100.80	100.65	100.64	99.95	99.61	100.69	99.88	100.36	100.09	100.30
Cations:																						
Si	3.00	3.00	2.98	2.99	3.00	2.99	3.00	3.01	2.99	3.02	3.00	2.99	2.99	3.00	2.98	3.01	2.99	2.98	3.01	2.99	3.00	2.99
Ti	0.00	0.01	0.00	0.00	0.00	0.01	0.00	0.00	0.00	0.00	0.01	0.00	0.00	0.02	0.01	0.01	0.00	0.00	0.00	0.00	0.00	0.01
Al	2.04	2.02	2.04	2.05	2.06	2.04	2.03	2.03	2.05	2.04	2.06	2.04	2.05	2.02	2.05	2.01	2.04	2.06	2.05	2.04	2.03	2.05
Cr	0.00	0.00	0.00	0.00	0.00	0.00	0.00	0.00	0.00	0.00	0.00	0.00	0.00	0.00	0.00	0.00	0.00	0.00	0.00	0.00	0.00	0.00
Fe	2.12	1.93	2.15	2.31	2.22	2.07	1.87	2.27	2.27	1.97	1.78	2.20	2.25	1.79	1.79	1.80	2.27	2.16	2.27	2.30	1.90	1.90
Mn	0.14	0.37	0.14	0.05	0.05	0.19	0.41	0.06	0.05	0.33	0.52	0.08	0.05	0.51	0.53	0.47	0.06	0.09	0.06	0.05	0.37	0.40
Mg	0.34	0.25	0.36	0.36	0.38	0.30	0.22	0.37	0.40	0.25	0.20	0.38	0.39	0.19	0.20	0.20	0.38	0.39	0.37	0.38	0.24	0.23
Ca	0.35	0.41	0.32	0.22	0.26	0.38	0.42	0.23	0.22	0.35	0.40	0.29	0.24	0.44	0.44	0.47	0.23	0.31	0.22	0.23	0.44	0.42
Na	0.01	0.00	0.00	0.00	0.00	0.01	0.01	0.00	0.00	0.00	0.00	0.01	0.01	0.01	0.00	0.00	0.01	0.00	0.01	0.00	0.00	0.00
K	0.00	0.00	0.00	0.00	0.00	0.00	0.00	0.00	0.00	0.00	0.00	0.00	0.00	0.00	0.00	0.00	0.00	0.00	0.00	0.00	0.00	0.00
Total (All)	7.99	7.98	7.99	7.98	7.97	7.99	7.98	7.97	7.98	7.96	7.97	7.99	7.98	7.98	7.99	7.97	7.99	7.99	7.97	7.99	7.98	7.98
Total (Majors ONLY)	7.98	7.98	7.99	7.98	7.97	7.99	7.98	7.97	7.98	7.96	7.97	7.99	7.98	7.98	7.99	7.97	7.99	7.99	7.97	7.99	7.98	7.98
XGrss (= Ca/(Ca+Fe+M	0.12	0.14	0.11	0.07	0.09	0.13	0.14	0.08	0.07	0.12	0.14	0.10	0.08	0.15	0.15	0.16	0.08	0.10	0.07	0.08	0.15	0.14
XSpss (= Mn/(Mn+Fe+	0.05	0.12	0.05	0.02	0.02	0.07	0.14	0.02	0.02	0.11	0.18	0.03	0.02	0.17	0.18	0.16	0.02	0.03	0.02	0.02	0.13	0.14
XAlm (= Fe/(Fe+Mg+M	0.72	0.65	0.73	0.79	0.76	0.70	0.64	0.78	0.77	0.68	0.61	0.74	0.77	0.61	0.61	0.61	0.77	0.73	0.78	0.78	0.64	0.64
XPy (= Mg/(Mg+Mn+C	0.12	0.08	0.12	0.12	0.13	0.10	0.08	0.13	0.14	0.09	0.07	0.13	0.13	0.06	0.07	0.07	0.13	0.13	0.13	0.13	0.08	0.08

Note: Analyses conducted on the same mineral grain (e.g. 1 core analysis and 2 rim analyses on a specific garnet grain) are highlighted in the same colour and enclosed in the same thick black box.

Garnets cont.

Analysis Label (Specimen_mineral_grain/zone:spot number)	ma29_gt_2r	ma29_gt_2u	ma29_gt_2v	ma29_gt_2t	ma29_gt_2s	ma29_gt_2w	ma29_gt_2z	ma29_gt_2za	ma29_gt_2y	ma29_gt_2x	ma29_gt_2zb	ma29_gt_3c	ma29_gt_3b	ma29_gt_3a	ma29_gt_4c	ma29_gt_4a	ma29_gt_5c	ma29_gt_5b	ma29_gt_5a	ma29_gt_6c	ma29_gt_6b	ma29_gt_6a
Mineral Probed:	gt	gt	gt	gt	gt	gt	gt	gt	gt	gt	gt	gt	gt	gt	gt	gt	gt	gt	gt	gt	gt	gt
Core/Int/Rim:	Rim	Rim	Rim	Int	Core	Rim	Rim	Rim	Int	Core	Rim	Rim	Int	Core	Rim	Core	Rim	Int	Core	Rim	Int	Core
EMP Initial Results:																						
Oxide conc. (wt%)																						
SiO2	37.33	37.66	37.63	37.51	37.55	37.65	37.65	37.83	37.48	36.80	37.56	37.83	37.82	37.24	37.37	37.59	37.52	37.61	37.79	37.67	37.44	37.31
TiO2	0.02	0.05	0.01	0.01	0.03	0.04	0.03	0.07	0.42	0.07	0.04	0.04	0.07	0.06	0.03	0.05	0.02	0.00	0.03	0.00	0.05	0.05
Al2O3	21.64	21.79	21.75	21.90	21.57	21.84	21.99	21.79	21.49	21.04	21.90	21.86	21.70	21.57	21.65	21.70	22.04	21.95	21.77	21.91	21.62	21.63
Cr2O3	0.00	0.00	0.03	0.01	0.02	0.01	0.00	0.03	0.04	0.02	0.01	0.00	0.00	0.00	0.02	0.00	0.02	0.04	0.02	0.01	0.02	0.02
FeO	33.92	33.18	33.49	31.26	29.79	33.87	33.81	33.26	27.40	25.81	33.98	33.37	28.96	25.32	33.06	29.11	34.07	32.57	31.50	32.54	28.46	26.54
MnO	0.93	0.87	0.88	3.09	5.01	0.82	0.66	0.77	6.21	7.94	0.82	0.98	5.30	8.43	1.13	5.40	0.82	1.52	2.90	1.49	5.53	8.15
MgO	3.06	3.26	3.27	2.56	2.06	3.12	3.50	3.43	1.86	1.66	3.18	3.22	1.99	1.55	3.40	1.99	3.09	3.11	2.53	3.18	1.94	1.67
CaO	2.93	3.21	3.23	4.23	4.51	3.08	2.96	3.21	4.87	6.25	2.94	3.46	4.91	5.27	3.18	4.74	2.67	3.74	4.26	3.09	4.93	4.84
Na2O	0.04	0.00	0.03	0.04	0.01	0.00	0.02	0.04	0.00	0.06	0.04	0.02	0.01	0.10	0.02	0.08	0.07	0.03	0.04	0.04	0.02	0.04
K2O	0.00	0.00	0.00	0.00	0.00	0.00	0.00	0.00	0.00	0.00	0.00	0.00	0.00	0.00	0.00	0.00	0.00	0.00	0.00	0.00	0.00	0.00
Total	99.86	100.02	100.33	100.61	100.55	100.44	100.61	100.43	99.77	99.65	100.47	100.78	100.76	99.54	99.86	100.66	100.32	100.57	100.84	99.94	100.00	100.25
Cations:																						
Si	2.99	3.00	2.99	2.98	3.00	2.99	2.98	3.00	3.00	2.97	2.99	2.99	3.00	3.00	2.99	2.99	2.99	2.98	3.00	3.00	3.00	2.99
Ti	0.00	0.00	0.00	0.00	0.00	0.00	0.00	0.00	0.03	0.00	0.00	0.00	0.00	0.00	0.00	0.00	0.00	0.00	0.00	0.00	0.00	0.00
Al	2.04	2.05	2.04	2.05	2.03	2.05	2.05	2.04	2.03	2.00	2.05	2.04	2.03	2.05	2.04	2.04	2.07	2.05	2.03	2.06	2.04	2.04
Cr	0.00	0.00	0.00	0.00	0.00	0.00	0.00	0.00	0.00	0.00	0.00	0.00	0.00	0.00	0.00	0.00	0.00	0.00	0.00	0.00	0.00	0.00
Fe	2.27	2.21	2.23	2.08	1.99	2.25	2.24	2.20	1.84	1.74	2.26	2.21	1.92	1.70	2.21	1.94	2.27	2.16	2.09	2.17	1.91	1.78
Mn	0.06	0.06	0.06	0.21	0.34	0.06	0.04	0.05	0.42	0.54	0.06	0.07	0.36	0.57	0.08	0.36	0.06	0.10	0.19	0.10	0.38	0.55
Mg	0.37	0.39	0.39	0.30	0.25	0.37	0.41	0.41	0.22	0.20	0.38	0.38	0.24	0.19	0.40	0.24	0.37	0.37	0.30	0.38	0.23	0.20
Ca	0.25	0.27	0.28	0.36	0.39	0.26	0.25	0.27	0.42	0.54	0.25	0.29	0.42	0.45	0.27	0.40	0.23	0.32	0.36	0.26	0.42	0.42
Na	0.01	0.00	0.01	0.01	0.00	0.00	0.00	0.01	0.00	0.01	0.01	0.00	0.00	0.01	0.00	0.01	0.01	0.00	0.01	0.01	0.00	0.01
K	0.00	0.00	0.00	0.00	0.00	0.00	0.00	0.00	0.00	0.00	0.00	0.00	0.00	0.00	0.00	0.00	0.00	0.00	0.00	0.00	0.00	0.00
Total (All)	7.99	7.98	7.99	7.99	7.99	7.98	7.99	7.98	7.96	8.02	7.99	7.99	7.98	7.98	7.99	7.99	7.98	7.99	7.99	7.97	7.98	7.99
Total (Majors ONLY)	7.99	7.98	7.99	7.99	7.99	7.98	7.99	7.98	7.95	8.02	7.99	7.99	7.98	7.98	7.99	7.99	7.98	7.99	7.99	7.97	7.98	7.99
XGrss (= Ca/(Ca+Fe+M	0.09	0.09	0.09	0.12	0.13	0.09	0.09	0.09	0.14	0.18	0.09	0.10	0.14	0.16	0.09	0.14	0.08	0.11	0.12	0.09	0.14	0.14
XSpss (= Mn/(Mn+Fe+	0.02	0.02	0.02	0.07	0.11	0.02	0.01	0.02	0.15	0.18	0.02	0.02	0.12	0.20	0.03	0.12	0.02	0.03	0.07	0.03	0.13	0.19
XAlm (= Fe/(Fe+Mg+M	0.77	0.75	0.76	0.70	0.67	0.77	0.76	0.75	0.63	0.58	0.77	0.75	0.66	0.58	0.75	0.66	0.78	0.73	0.71	0.75	0.65	0.60
XPy (= Mg/(Mg+Mn+C	0.12	0.13	0.13	0.10	0.08	0.13	0.14	0.14	0.08	0.07	0.13	0.13	0.08	0.06	0.14	0.08	0.13	0.12	0.10	0.13	0.08	0.07

Note: Analyses conducted on the same mineral grain (e.g. 1 core analysis and 2 rim analyses on a specific garnet grain) are highlighted in the same colour and enclosed in the same thick black box.

Garnets cont.

Analysis Label (Specimen_mineral_grain/zone:spot number)	ma29_gt_6d	ma29_gt_6g	ma29_gt_6f	ma29_gt_6e	ma29_gt_6i	ma29_gt_6h	ma29_gt_7b	ma29_gt_7a	ma29_gt_7f	ma29_gt_7e	ma29_gt_7d	ma29_gt_7j	ma29_gt_7g	ma29_gt_7h	ma29_gt_7i	ma29_gt_7l	ma29_gt_7k	ma29_gt_7o	ma29_gt_7n	ma29_gt_7m	ma29_gt_7p	ma29_gt_7s
Mineral Probed: Core/Int/Rim:	gt Rim	gt Rim	gt Int	gt Core	gt Int	gt Core	gt Int	gt Core	gt Rim	gt Int	gt Core	gt Rim	gt Int	gt Core	gt Int	gt Rim	gt Core	gt Rim	gt Int	gt Core	gt Rim	gt Rim
EMP Initial Results:																						
Oxide conc. (wt%)																						
SiO2	37.75	37.78	37.68	37.80	37.28	37.28	37.57	37.76	37.70	37.47	37.48	37.62	37.63	37.57	37.34	37.82	37.60	37.48	37.80	37.52	37.29	37.50
TiO2	0.05	0.06	0.03	0.01	0.03	0.12	0.12	0.05	0.03	0.02	0.03	0.03	0.50	0.04	0.02	0.05	0.03	0.00	0.06	0.05	0.12	0.01
Al2O3	21.79	21.87	21.73	21.81	21.72	21.49	21.65	21.60	21.70	21.64	21.55	21.73	21.78	21.65	21.81	21.79	21.78	21.70	21.58	21.66	21.67	21.75
Cr2O3	0.00	0.00	0.02	0.00	0.01	0.01	0.00	0.01	0.01	0.00	0.00	0.01	0.04	0.00	0.00	0.00	0.04	0.00	0.00	0.04	0.00	0.02
FeO	31.41	32.27	30.81	31.07	31.86	27.81	29.08	26.49	33.66	30.20	28.75	33.59	31.82	30.65	30.68	34.14	33.22	33.43	28.65	27.56	33.35	34.35
MnO	2.52	1.29	2.89	2.56	2.29	6.15	4.50	7.06	0.99	3.90	5.59	0.74	2.10	3.64	3.21	1.00	0.82	0.88	5.36	6.83	0.95	1.01
MgO	2.58	3.21	2.73	2.65	2.68	1.84	2.12	1.65	3.14	2.21	1.90	3.34	2.74	2.34	2.39	3.06	3.38	3.12	2.00	1.77	3.14	2.94
CaO	4.03	3.56	4.06	4.47	3.98	4.99	5.17	5.44	2.57	4.51	4.81	2.91	3.80	4.42	4.36	2.56	3.13	3.03	4.91	4.83	3.13	2.45
Na2O	0.02	0.03	0.06	0.05	0.02	0.01	0.03	0.02	0.02	0.04	0.02	0.03	0.08	0.07	0.03	0.05	0.01	0.09	0.04	0.04	0.05	0.06
K2O	0.00	0.00	0.00	0.00	0.00	0.00	0.00	0.00	0.00	0.00	0.00	0.00	0.00	0.00	0.00	0.00	0.00	0.00	0.00	0.00	0.00	0.00
Total	100.15	100.07	100.01	100.42	99.87	99.70	100.24	100.08	99.83	99.99	100.13	100.00	100.49	100.37	99.84	100.47	100.01	99.73	100.39	100.30	99.70	100.08
Cations:																						
Si	3.01	3.00	3.00	3.00	2.98	3.00	3.00	3.02	3.01	3.00	3.00	3.00	2.99	3.00	2.99	3.01	2.99	3.00	3.01	3.00	2.99	3.00
Ti	0.00	0.00	0.00	0.00	0.00	0.01	0.01	0.00	0.00	0.00	0.00	0.00	0.03	0.00	0.00	0.00	0.00	0.00	0.00	0.00	0.01	0.00
Al	2.05	2.05	2.04	2.04	2.05	2.04	2.04	2.03	2.04	2.04	2.03	2.04	2.04	2.04	2.06	2.04	2.04	2.05	2.03	2.04	2.05	2.05
Cr	0.00	0.00	0.00	0.00	0.00	0.00	0.00	0.00	0.00	0.00	0.00	0.00	0.00	0.00	0.00	0.00	0.00	0.00	0.00	0.00	0.00	0.00
Fe	2.09	2.14	2.05	2.06	2.13	1.87	1.94	1.77	2.25	2.02	1.92	2.24	2.11	2.04	2.05	2.27	2.21	2.24	1.91	1.84	2.23	2.30
Mn	0.17	0.09	0.20	0.17	0.16	0.42	0.30	0.48	0.07	0.26	0.38	0.05	0.14	0.25	0.22	0.07	0.06	0.06	0.36	0.46	0.06	0.07
Mg	0.31	0.38	0.32	0.31	0.32	0.22	0.25	0.20	0.37	0.26	0.23	0.40	0.32	0.28	0.29	0.36	0.40	0.37	0.24	0.21	0.37	0.35
Ca	0.34	0.30	0.35	0.38	0.34	0.43	0.44	0.47	0.22	0.39	0.41	0.25	0.32	0.38	0.37	0.22	0.27	0.26	0.42	0.41	0.27	0.21
Na	0.00	0.00	0.01	0.01	0.00	0.00	0.00	0.00	0.00	0.01	0.00	0.00	0.01	0.01	0.00	0.01	0.00	0.01	0.01	0.01	0.01	0.01
K	0.00	0.00	0.00	0.00	0.00	0.00	0.00	0.00	0.00	0.00	0.00	0.00	0.00	0.00	0.00	0.00	0.00	0.00	0.00	0.00	0.00	0.00
Total (All)	7.97	7.97	7.98	7.98	7.99	7.98	7.98	7.97	7.97	7.98	7.98	7.98	7.97	7.99	7.98	7.98	7.98	7.99	7.97	7.98	7.99	7.98
Total (Majors ONLY)	7.97	7.97	7.98	7.98	7.99	7.98	7.98	7.96	7.97	7.98	7.98	7.98	7.97	7.99	7.98	7.98	7.98	7.99	7.97	7.98	7.99	7.98
XGrss (= Ca/(Ca+Fe+M	0.12	0.10	0.12	0.13	0.12	0.15	0.15	0.16	0.08	0.13	0.14	0.08	0.11	0.13	0.13	0.07	0.09	0.09	0.14	0.14	0.09	0.07
XSpss (= Mn/(Mn+Fe+	0.06	0.03	0.07	0.06	0.05	0.14	0.10	0.16	0.02	0.09	0.13	0.02	0.05	0.08	0.07	0.02	0.02	0.02	0.12	0.16	0.02	0.02
XAlm (= Fe/(Fe+Mg+M	0.72	0.74	0.70	0.70	0.72	0.64	0.66	0.61	0.77	0.69	0.65	0.76	0.73	0.69	0.70	0.78	0.75	0.76	0.65	0.63	0.76	0.79
XPy (= Mg/(Mg+Mn+C	0.11	0.13	0.11	0.11	0.11	0.08	0.09	0.07	0.13	0.09	0.08	0.14	0.11	0.09	0.10	0.12	0.14	0.13	0.08	0.07	0.13	0.12

Note: Analyses conducted on the same mineral grain (e.g. 1 core analysis and 2 rim analyses on a specific garnet grain) are highlighted in the same colour and enclosed in the same thick black box.

Garnets cont.

Analysis Label (Specimen_mineral_grain/zone:spot number)	ma29_gt_7r	ma29_gt_7q	ma29_gt_7t	ma29_gt_8c	ma29_gt_8b	ma29_gt_8a	ma29_gt_9b	ma29_gt_9a	ma29_gt_9f	ma29_gt_9e	ma29_gt_9d	ma29_gt_9g	ma31_gt_1a	ma31_gt_3b	ma31_gt_4a	ma31_gt_4b	ma31_gt_4c	ma31_gt_4d	ma31_gt_4e	ma31_gt_6c	ma31_gt_6b	ma31_gt_6a
Mineral Probed:	gt	gt	gt	gt	gt	gt	gt	gt	gt	gt	gt	gt	gt	gt	gt	gt	gt	gt	gt	gt	gt	gt
Core/Int/Rim:	Int	Core	Rim	Rim	Int	Core	Int	Core	Rim	Int	Core	Int	Core	Rim	Rim	Int	Core	Int	Rim	Rim	Int	Core
EMP Initial Results:																						
Oxide conc. (wt%)																						
SiO2	37.43	37.41	37.80	37.53	37.52	37.49	37.47	37.34	37.73	37.40	37.61	37.42	37.66	37.71	37.68	37.79	37.57	37.74	37.66	38.11	37.70	37.92
TiO2	0.05	0.09	0.28	0.00	0.02	0.22	0.05	0.12	0.03	0.05	0.49	0.62	0.15	0.08	0.00	0.56	0.18	0.08	0.05	0.07	0.06	0.07
Al2O3	21.66	21.39	21.63	21.58	21.61	21.42	21.46	21.30	21.68	21.52	21.59	21.53	21.39	21.49	21.90	21.70	21.36	21.46	21.77	21.98	21.71	21.63
Cr2O3	0.03	0.00	0.01	0.00	0.00	0.00	0.02	0.02	0.00	0.01	0.03	0.03	0.04	0.05	0.04	0.05	0.02	0.00	0.05	0.02	0.04	0.03
FeO	29.07	25.97	32.22	32.93	29.89	25.88	29.94	27.37	33.94	30.47	26.24	28.04	26.32	29.67	32.03	28.45	26.03	28.46	32.01	31.22	28.64	25.54
MnO	4.71	8.03	2.12	1.14	3.88	8.35	3.66	6.95	0.63	3.50	7.65	6.20	6.78	3.26	1.61	4.37	7.17	4.75	1.68	1.77	4.85	7.40
MgO	2.06	1.57	2.77	3.23	2.24	1.55	2.23	1.73	3.26	2.31	1.65	1.91	1.91	2.63	3.30	2.43	1.87	2.13	3.24	3.44	2.16	1.74
CaO	4.81	5.28	3.69	3.52	4.70	5.29	4.66	5.12	2.75	4.31	4.94	4.93	5.58	5.31	3.41	5.67	5.79	5.35	3.34	4.37	5.67	6.35
Na2O	0.01	0.04	0.03	0.06	0.01	0.05	0.04	0.04	0.07	0.07	0.05	0.02	0.03	0.05	0.06	0.00	0.05	0.03	0.07	0.02	0.04	0.00
K2O	0.00	0.00	0.00	0.00	0.00	0.00	0.00	0.00	0.00	0.00	0.00	0.00	0.00	0.00	0.00	0.00	0.00	0.00	0.00	0.00	0.00	0.00
Total	99.83	99.78	100.55	99.99	99.87	100.25	99.53	99.99	100.10	99.64	100.25	100.69	99.86	100.25	100.03	101.02	100.04	99.99	99.86	101.00	100.86	100.68
Cations:																						
Si	3.00	3.01	3.00	3.00	3.00	3.00	3.01	3.00	3.01	3.00	3.00	2.98	3.01	3.00	3.00	2.98	3.00	3.01	3.00	3.00	2.99	3.01
Ti	0.00	0.01	0.02	0.00	0.00	0.01	0.00	0.01	0.00	0.00	0.03	0.04	0.01	0.00	0.00	0.03	0.01	0.00	0.00	0.00	0.00	0.00
Al	2.05	2.03	2.02	2.03	2.04	2.02	2.03	2.02	2.04	2.04	2.03	2.02	2.02	2.02	2.05	2.02	2.01	2.02	2.04	2.04	2.03	2.02
Cr	0.00	0.00	0.00	0.00	0.00	0.00	0.00	0.00	0.00	0.00	0.00	0.00	0.00	0.00	0.00	0.00	0.00	0.00	0.00	0.00	0.00	0.00
Fe	1.95	1.75	2.14	2.20	2.00	1.73	2.01	1.84	2.26	2.05	1.75	1.87	1.76	1.97	2.13	1.88	1.74	1.90	2.13	2.05	1.90	1.69
Mn	0.32	0.55	0.14	0.08	0.26	0.57	0.25	0.47	0.04	0.24	0.52	0.42	0.46	0.22	0.11	0.29	0.49	0.32	0.11	0.12	0.33	0.50
Mg	0.25	0.19	0.33	0.38	0.27	0.18	0.27	0.21	0.39	0.28	0.20	0.23	0.23	0.31	0.39	0.29	0.22	0.25	0.38	0.40	0.26	0.21
Ca	0.41	0.45	0.31	0.30	0.40	0.45	0.40	0.44	0.23	0.37	0.42	0.42	0.48	0.45	0.29	0.48	0.50	0.46	0.29	0.37	0.48	0.54
Na	0.00	0.01	0.00	0.01	0.00	0.01	0.01	0.01	0.01	0.01	0.01	0.00	0.00	0.01	0.01	0.00	0.01	0.00	0.01	0.00	0.01	0.00
K	0.00	0.00	0.00	0.00	0.00	0.00	0.00	0.00	0.00	0.00	0.00	0.00	0.00	0.00	0.00	0.00	0.00	0.00	0.00	0.00	0.00	0.00
Total (All)	7.98	7.98	7.97	7.99	7.98	7.98	7.98	7.99	7.98	7.98	7.96	7.97	7.97	7.99	7.98	7.97	7.98	7.97	7.98	7.98	7.99	7.97
Total (Majors ONLY)	7.97	7.98	7.97	7.99	7.98	7.98	7.97	7.99	7.98	7.98	7.96	7.97	7.97	7.99	7.98	7.97	7.98	7.97	7.98	7.98	7.99	7.97
XGrss (= Ca/(Ca+Fe+M	0.14	0.15	0.11	0.10	0.14	0.15	0.14	0.15	0.08	0.13	0.15	0.14	0.16	0.15	0.10	0.16	0.17	0.16	0.10	0.13	0.16	0.18
XSpss (= Mn/(Mn+Fe+	0.11	0.19	0.05	0.03	0.09	0.19	0.09	0.16	0.01	0.08	0.18	0.14	0.16	0.07	0.04	0.10	0.16	0.11	0.04	0.04	0.11	0.17
XAlm (= Fe/(Fe+Mg+M	0.67	0.59	0.73	0.74	0.68	0.59	0.69	0.62	0.77	0.70	0.61	0.64	0.60	0.67	0.73	0.64	0.59	0.65	0.73	0.70	0.64	0.58
XPy (= Mg/(Mg+Mn+C	0.08	0.06	0.11	0.13	0.09	0.06	0.09	0.07	0.13	0.09	0.07	0.08	0.08	0.11	0.13	0.10	0.08	0.09	0.13	0.14	0.09	0.07

Note: Analyses conducted on the same mineral grain (e.g. 1 core analysis and 2 rim analyses on a specific garnet grain) are highlighted in the same colour and enclosed in the same thick black box.

Garnets cont.

Analysis Label (Specimen_mineral_grain/zone:spot number)	ma31_gt_8f	ma31_gt_8e	ma31_gt_8d	ma31_gt_8g	ma31_gt_8c	ma31_gt_8b	ma31_gt_8a	ma31_gt_7c	ma31_gt_7b	ma31_gt_7a	ma31_gt_7d	ma38(b)_gt_1c	ma38(b)_gt_1b	ma38(b)_gt_1d	ma38(b)_gt_1h	ma38(b)_gt_1f	ma38(b)_gt_1e	ma38(b)_gt_1g	ma38(a)_gt_1c	ma38(a)_gt_1d	ma38(a)_gt_1b	ma38(a)_gt_1a
Mineral Probed:	gt	gt	gt	gt	gt	gt	gt	gt	gt	gt	gt	gt	gt	gt	gt	gt	gt	gt	gt	gt	gt	gt
Core/Int/Rim:	Rim	Int	Core	Int	Rim	Int	Core	Rim	Int	Core	Int	Rim	Int	Rim	Rim	Int	Core	Int	Rim	Rim	Int	Core
EMP Initial Results:																						
Oxide conc. (wt%)																						
SiO2	37.86	37.70	37.77	37.82	37.71	37.74	37.48	37.15	37.80	37.52	37.50	37.65	37.11	37.41	37.61	37.17	37.69	37.59	37.45	37.94	37.55	37.00
TiO2	0.01	0.08	0.08	0.42	0.04	0.07	0.13	0.05	0.07	0.08	0.21	0.07	0.11	0.29	0.12	0.08	0.12	0.05	0.04	0.01	0.05	0.11
Al2O3	22.01	21.47	21.81	21.73	21.77	22.02	21.44	21.13	21.66	21.36	21.35	21.60	21.54	21.65	21.76	21.52	21.64	22.17	21.83	21.53	21.60	21.67
Cr2O3	0.02	0.00	0.04	0.02	0.03	0.03	0.00	0.02	0.02	0.00	0.03	0.00	0.03	0.01	0.01	0.00	0.00	0.00	0.00	0.00	0.00	0.00
FeO	32.17	28.00	25.95	30.24	31.05	29.13	26.30	30.05	29.89	26.67	26.96	31.38	29.28	31.78	30.57	30.68	28.91	32.00	31.52	32.10	30.37	29.21
MnO	1.97	4.81	6.52	3.02	1.48	4.05	6.90	2.21	3.59	6.32	6.23	2.90	6.13	3.05	3.71	4.35	5.82	2.78	2.81	3.01	4.29	6.37
MgO	3.30	2.22	1.85	2.46	3.54	2.26	1.80	3.19	2.29	2.00	2.07	3.51	2.50	3.16	3.20	2.89	2.42	3.34	3.25	2.86	2.79	2.42
CaO	3.25	5.51	6.35	5.11	3.79	5.60	6.28	5.96	4.93	5.72	5.58	2.90	3.39	2.87	3.09	2.99	3.48	2.53	2.98	2.29	3.29	3.39
Na2O	0.00	0.03	0.01	0.03	0.04	0.01	0.03	0.02	0.03	0.03	0.00	0.09	0.01	0.03	0.04	0.05	0.04	0.04	0.03	0.11	0.03	0.01
K2O	0.00	0.00	0.00	0.00	0.00	0.00	0.00	0.00	0.00	0.00	0.00	0.00	0.00	0.00	0.00	0.00	0.00	0.00	0.00	0.00	0.00	0.00
Total	100.59	99.82	100.38	100.85	99.45	100.90	100.36	99.78	100.28	99.70	99.93	100.10	100.10	100.26	100.12	99.73	100.12	100.50	99.91	99.84	99.97	100.18
Cations:																						
Si	3.00	3.01	3.00	2.99	3.00	2.99	2.99	2.97	3.01	3.01	3.00	3.00	2.98	2.98	2.99	2.99	3.01	2.98	2.99	3.03	3.00	2.97
Ti	0.00	0.00	0.00	0.02	0.00	0.00	0.01	0.00	0.00	0.00	0.01	0.00	0.01	0.02	0.01	0.00	0.01	0.00	0.00	0.00	0.00	0.01
Al	2.05	2.02	2.04	2.03	2.04	2.05	2.02	1.99	2.03	2.02	2.01	2.03	2.04	2.03	2.04	2.04	2.04	2.07	2.05	2.03	2.04	2.05
Cr	0.00	0.00	0.00	0.00	0.00	0.00	0.00	0.00	0.00	0.00	0.00	0.00	0.00	0.00	0.00	0.00	0.00	0.00	0.00	0.00	0.00	0.00
Fe	2.13	1.87	1.72	2.00	2.07	1.93	1.76	2.01	1.99	1.79	1.80	2.09	1.96	2.12	2.04	2.06	1.93	2.12	2.10	2.15	2.03	1.96
Mn	0.13	0.33	0.44	0.20	0.10	0.27	0.47	0.15	0.24	0.43	0.42	0.20	0.42	0.21	0.25	0.30	0.39	0.19	0.19	0.20	0.29	0.43
Mg	0.39	0.26	0.22	0.29	0.42	0.27	0.21	0.38	0.27	0.24	0.25	0.42	0.30	0.38	0.38	0.35	0.29	0.39	0.39	0.34	0.33	0.29
Ca	0.28	0.47	0.54	0.43	0.32	0.47	0.54	0.51	0.42	0.49	0.48	0.25	0.29	0.25	0.26	0.26	0.30	0.22	0.25	0.20	0.28	0.29
Na	0.00	0.00	0.00	0.01	0.01	0.00	0.00	0.00	0.01	0.01	0.00	0.01	0.00	0.01	0.01	0.01	0.01	0.01	0.00	0.02	0.00	0.00
K	0.00	0.00	0.00	0.00	0.00	0.00	0.00	0.00	0.00	0.00	0.00	0.00	0.00	0.00	0.00	0.00	0.00	0.00	0.00	0.00	0.00	0.00
Total (All)	7.98	7.98	7.97	7.97	7.97	7.98	7.99	8.03	7.97	7.98	7.98	7.99	8.00	7.99	7.98	8.00	7.97	7.98	7.98	7.96	7.98	8.00
Total (Majors ONLY)	7.98	7.97	7.97	7.97	7.97	7.98	7.99	8.03	7.97	7.98	7.98	7.99	8.00	7.98	7.98	8.00	7.97	7.98	7.98	7.96	7.98	8.00
XGrss (= Ca/(Ca+Fe+M	0.09	0.16	0.18	0.15	0.11	0.16	0.18	0.17	0.14	0.17	0.16	0.08	0.10	0.08	0.09	0.09	0.10	0.07	0.09	0.07	0.10	0.10
XSpss (= Mn/(Mn+Fe+	0.05	0.11	0.15	0.07	0.03	0.09	0.16	0.05	0.08	0.15	0.14	0.07	0.14	0.07	0.09	0.10	0.14	0.06	0.06	0.07	0.10	0.15
XAlm (= Fe/(Fe+Mg+M	0.73	0.64	0.59	0.68	0.71	0.66	0.59	0.66	0.68	0.61	0.61	0.71	0.66	0.72	0.69	0.70	0.66	0.73	0.72	0.74	0.69	0.66
XPy (= Mg/(Mg+Mn+C	0.13	0.09	0.07	0.10	0.14	0.09	0.07	0.12	0.09	0.08	0.08	0.14	0.10	0.13	0.13	0.12	0.10	0.14	0.13	0.12	0.11	0.10

Note: Analyses conducted on the same mineral grain (e.g. 1 core analysis and 2 rim analyses on a specific garnet grain) are highlighted in the same colour and enclosed in the same thick black box.

Garnets cont.

Analysis Label (Specimen_mineral_grain/zone:spot number)	ma38(a)_gt_1f	ma38(a)_gt_1e	ma38(a)_gt_1h	ma38(a)_gt_1g	ma40_gt_1b	ma40_gt_1a	ma40_gt_1c	ma40_gt_2c	ma40_gt_2b	ma40_gt_2a	ma40_gt_3c	ma40_gt_3b	ma40_gt_3a	ma40_gt_4c	ma40_gt_4a	ma40_gt_5c	ma40_gt_5b	ma40_gt_5a	ma40_gt_6c	ma40_gt_6d	ma40_gt_6a	ma40_gt_7c
Mineral Probed:	gt	gt	gt	gt	gt	gt	gt	gt	gt	gt	gt	gt	gt	gt	gt	gt	gt	gt	gt	gt	gt	gt
Core/Int/Rim:	Int	Rim	Int	Core	Rim	Core	Rim	Rim	Int	Core	Rim	Int	Core	Rim	Core	Rim	Int	Core	Rim	Int	Core	Rim
EMP Initial Results:																						
Oxide conc. (wt%)																						
SiO2	37.55	37.71	37.70	37.43	37.23	37.70	37.60	37.41	37.73	37.50	37.93	37.97	37.54	37.79	37.65	37.66	37.65	37.64	37.71	37.88	38.10	37.60
TiO2	0.11	0.06	0.06	0.11	0.14	0.07	0.01	0.01	0.12	0.10	0.08	0.05	0.05	0.03	0.15	0.04	0.00	0.04	0.02	0.22	0.10	0.00
Al2O3	21.74	21.66	21.94	21.44	21.78	22.02	21.58	21.74	21.87	21.73	21.85	21.67	21.78	21.77	21.62	21.59	21.62	21.71	21.67	21.68	21.87	21.42
Cr2O3	0.00	0.00	0.00	0.01	0.02	0.01	0.01	0.02	0.03	0.05	0.00	0.01	0.00	0.05	0.04	0.02	0.04	0.00	0.05	0.02	0.01	0.00
FeO	30.64	31.72	31.31	29.59	33.01	32.62	33.30	32.72	28.82	27.35	32.60	31.44	29.86	31.93	26.97	32.90	30.65	29.92	33.02	30.85	29.81	32.86
MnO	3.02	2.73	3.85	5.45	2.01	2.11	2.24	2.25	5.20	7.20	2.02	2.58	3.52	1.98	6.54	2.38	3.37	3.99	2.17	2.83	3.97	2.03
MgO	3.40	3.58	2.88	2.62	3.21	3.30	3.07	3.08	2.25	2.00	3.34	2.97	2.70	3.39	1.93	2.86	2.81	2.45	3.19	2.90	2.25	3.14
CaO	3.56	2.55	3.19	3.33	2.66	3.03	2.53	2.59	4.84	4.62	2.62	3.63	4.32	2.80	5.59	2.43	3.87	4.44	2.40	3.58	4.80	2.55
Na2O	0.02	0.04	0.03	0.02	0.02	0.01	0.02	0.05	0.03	0.07	0.00	0.00	0.03	0.01	0.04	0.03	0.04	0.00	0.01	0.03	0.02	0.00
K2O	0.00	0.00	0.00	0.00	0.00	0.00	0.00	0.00	0.00	0.00	0.00	0.00	0.00	0.00	0.00	0.00	0.00	0.00	0.00	0.00	0.00	0.00
Total	100.05	100.05	100.96	100.00	100.07	100.86	100.35	99.86	100.89	100.63	100.44	100.31	99.80	99.75	100.54	99.90	100.05	100.19	100.24	99.99	100.93	99.60
Cations:																						
Si	2.99	3.00	2.99	3.00	2.98	2.98	3.00	2.99	2.99	2.99	3.01	3.01	3.00	3.01	3.00	3.01	3.00	3.00	3.00	3.01	3.01	3.01
Ti	0.01	0.00	0.00	0.01	0.01	0.00	0.00	0.00	0.01	0.01	0.00	0.00	0.00	0.00	0.01	0.00	0.00	0.00	0.00	0.01	0.01	0.00
Al	2.04	2.03	2.05	2.02	2.05	2.05	2.03	2.05	2.04	2.04	2.04	2.03	2.05	2.04	2.03	2.04	2.03	2.04	2.04	2.03	2.04	2.02
Cr	0.00	0.00	0.00	0.00	0.00	0.00	0.00	0.00	0.00	0.00	0.00	0.00	0.00	0.00	0.00	0.00	0.00	0.00	0.00	0.00	0.00	0.00
Fe	2.04	2.11	2.07	1.98	2.21	2.16	2.22	2.19	1.91	1.82	2.16	2.09	1.99	2.13	1.79	2.20	2.04	1.99	2.20	2.05	1.97	2.20
Mn	0.20	0.18	0.26	0.37	0.14	0.14	0.15	0.15	0.35	0.49	0.14	0.17	0.24	0.13	0.44	0.16	0.23	0.27	0.15	0.19	0.27	0.14
Mg	0.40	0.42	0.34	0.31	0.38	0.39	0.37	0.37	0.27	0.24	0.39	0.35	0.32	0.40	0.23	0.34	0.33	0.29	0.38	0.34	0.27	0.38
Ca	0.30	0.22	0.27	0.29	0.23	0.26	0.22	0.22	0.41	0.39	0.22	0.31	0.37	0.24	0.48	0.21	0.33	0.38	0.20	0.31	0.41	0.22
Na	0.00	0.01	0.00	0.00	0.00	0.00	0.00	0.01	0.00	0.01	0.00	0.00	0.00	0.00	0.01	0.00	0.01	0.00	0.00	0.00	0.00	0.00
K	0.00	0.00	0.00	0.00	0.00	0.00	0.00	0.00	0.00	0.00	0.00	0.00	0.00	0.00	0.00	0.00	0.00	0.00	0.00	0.00	0.00	0.00
Total (All)	7.99	7.98	7.99	7.98	7.99	7.99	7.99	7.98	7.98	7.99	7.97	7.97	7.98	7.96	7.98	7.97	7.98	7.98	7.98	7.96	7.97	7.97
Total (Majors ONLY)	7.99	7.98	7.99	7.98	7.99	7.99	7.99	7.98	7.98	7.99	7.97	7.97	7.98	7.96	7.98	7.97	7.98	7.98	7.97	7.96	7.97	7.97
XGrss (= Ca/(Ca+Fe+	0.10	0.07	0.09	0.10	0.08	0.09	0.07	0.08	0.14	0.13	0.08	0.11	0.13	0.08	0.16	0.07	0.11	0.13	0.07	0.11	0.14	0.07
XSpss (= Mn/(Mn+Fe+	0.07	0.06	0.09	0.13	0.05	0.05	0.05	0.05	0.12	0.17	0.05	0.06	0.08	0.05	0.15	0.06	0.08	0.09	0.05	0.07	0.09	0.05
XAlm (= Fe/(Fe+Mg+M	0.69	0.72	0.70	0.67	0.75	0.73	0.75	0.75	0.65	0.62	0.74	0.71	0.68	0.73	0.61	0.76	0.70	0.68	0.75	0.71	0.68	0.75
XPy (= Mg/(Mg+Mn+C	0.14	0.14	0.12	0.11	0.13	0.13	0.12	0.13	0.09	0.08	0.14	0.12	0.11	0.14	0.08	0.12	0.11	0.10	0.13	0.12	0.09	0.13

Note: Analyses conducted on the same mineral grain (e.g. 1 core analysis and 2 rim analyses on a specific garnet grain) are highlighted in the same colour and enclosed in the same thick black box.

Garnets cont.

Analysis Label (Specimen_mineral_grain/zone:spot number)	ma40_gt_7b	ma40_gt_7a	ma40_gt_7d	ma40_gt_8c	ma40_gt_8b	ma40_gt_9c	ma40_gt_9b	ma40_gt_9a	ma40_gt_9d	ma40_gt_10c	ma40_gt_10b	ma40_gt_10a
Mineral Probed:	gt	gt	gt	gt	gt	gt	gt	gt	gt	gt	gt	gt
Core/Int/Rim:	Int	Core	Int	Rim	Int	Rim	Int	Core	Rim	Rim	Int	Core
EMP Initial Results:												
Oxide conc. (wt%)												
SiO2	37.97	37.88	37.57	37.56	37.73	37.82	37.70	37.54	37.59	37.45	37.59	37.50
TiO2	0.06	0.05	0.10	0.00	0.06	0.00	0.07	0.08	0.06	0.00	0.02	0.04
Al2O3	21.64	21.76	21.51	21.72	21.48	21.80	21.77	21.61	21.90	21.56	21.48	21.53
Cr2O3	0.01	0.02	0.05	0.03	0.03	0.04	0.02	0.04	0.01	0.02	0.10	0.01
FeO	30.19	27.01	28.40	32.89	29.32	32.74	29.73	26.73	32.95	32.64	30.81	29.96
MnO	3.64	7.01	5.14	1.98	4.10	1.94	4.24	6.64	2.10	1.95	3.26	3.99
MgO	2.51	1.91	2.17	3.32	2.32	3.21	2.42	1.85	2.92	3.19	2.74	2.43
CaO	4.32	4.86	4.91	2.68	4.84	2.73	4.42	5.25	2.52	2.84	3.99	4.69
Na2O	0.03	0.00	0.01	0.00	0.00	0.10	0.03	0.00	0.03	0.01	0.04	0.00
K2O	0.00	0.00	0.00	0.00	0.00	0.00	0.00	0.00	0.00	0.00	0.00	0.00
Total	100.37	100.49	99.86	100.18	99.88	100.38	100.41	99.74	100.08	99.67	100.02	100.15
Cations:												
Si	3.02	3.01	3.01	2.99	3.01	3.00	3.00	3.01	3.00	3.00	3.00	3.00
Ti	0.00	0.00	0.01	0.00	0.00	0.00	0.00	0.00	0.00	0.00	0.00	0.00
Al	2.03	2.04	2.03	2.04	2.02	2.04	2.04	2.04	2.06	2.04	2.02	2.03
Cr	0.00	0.00	0.00	0.00	0.00	0.00	0.00	0.00	0.00	0.00	0.01	0.00
Fe	2.01	1.80	1.90	2.19	1.96	2.18	1.98	1.79	2.20	2.19	2.06	2.00
Mn	0.24	0.47	0.35	0.13	0.28	0.13	0.29	0.45	0.14	0.13	0.22	0.27
Mg	0.30	0.23	0.26	0.39	0.28	0.38	0.29	0.22	0.35	0.38	0.33	0.29
Ca	0.37	0.41	0.42	0.23	0.41	0.23	0.38	0.45	0.22	0.24	0.34	0.40
Na	0.00	0.00	0.00	0.00	0.00	0.01	0.01	0.00	0.00	0.00	0.01	0.00
K	0.00	0.00	0.00	0.00	0.00	0.00	0.00	0.00	0.00	0.00	0.00	0.00
Total (All)	7.97	7.96	7.97	7.99	7.97	7.98	7.98	7.97	7.97	7.98	7.98	7.99
Total (Majors ONLY)	7.97	7.96	7.97	7.98	7.97	7.98	7.98	7.97	7.97	7.98	7.98	7.99
XGrss (= Ca/(Ca+Fe+M	0.13	0.14	0.14	0.08	0.14	0.08	0.13	0.15	0.07	0.08	0.12	0.14
XSpss (= Mn/(Mn+Fe+	0.08	0.16	0.12	0.05	0.09	0.04	0.10	0.15	0.05	0.04	0.07	0.09
XAlm (= Fe/(Fe+Mg+M	0.69	0.62	0.65	0.74	0.67	0.75	0.68	0.61	0.76	0.74	0.70	0.68
XPy (= Mg/(Mg+Mn+C	0.10	0.08	0.09	0.13	0.09	0.13	0.10	0.08	0.12	0.13	0.11	0.10

Note: Analyses conducted on the same mineral grain (e.g. 1 core analysis and 2 rim analyses on a specific garnet grain) are highlighted in the same colour and enclosed in the same thick black box.

Ilmenites and Magnetites

Analysis Label (Specimen_mineral grain/zone:spot number)	gb8_op_1a	gb8_op_1b	gb8_op_1f	gb8_op_1c	gb8_op_1e	gb8_op_2a	gb8_op_2d	gb8_op_2b	gb8_op_2e	gb8_op_3a	gb8_op_3d	gb8_op_3b	gb8_op_3e	gb8_op_4a	gb8_op_4d	gb8_op_4b	gb8_op_4e	gb8_op_4c	gb10_op_1a	gb10_op_1b	gb10_op_1d
Mineral Probed:	mt	mt	mt	mt	mt	mt	mt	mt	mt	mt	mt	mt	mt	mt	mt	mt	mt	mt	mt	mt	mt
Core/Int/Rim:	Rim	Rim	Int	Core	Rim	Rim	Int	Core	Rim	Rim	Rim	Core	Rim	Rim	Int	Core	Int	Rim	Rim	Rim	Int
EMP Initial Results:																					
Oxide conc. (wt%)																					
TiO2	0.07	0.06	0.12	0.04	0.09	0.18	0.07	0.10	0.10	0.14	0.09	0.08	0.14	0.05	0.08	0.06	0.09	0.07	0.05	0.02	0.05
Al2O3	0.20	0.16	0.17	0.22	0.16	0.18	0.11	0.18	0.24	0.20	0.20	0.37	0.15	0.16	0.21	0.19	0.19	0.19	0.20	0.05	0.09
Cr2O3	0.06	0.07	0.06	0.10	0.06	0.07	0.04	0.01	0.01	0.10	0.08	0.02	0.04	0.03	0.06	0.05	0.07	0.09	0.00	0.02	0.02
FeO	92.30	92.03	92.23	92.63	92.25	92.38	92.29	92.42	91.71	92.09	92.17	91.83	92.19	91.76	91.86	91.79	91.50	91.65	94.14	93.34	94.32
MnO	0.09	0.04	0.07	0.03	0.01	0.00	0.10	0.07	0.03	0.09	0.04	0.01	0.02	0.04	0.01	0.02	0.09	0.06	0.06	0.01	0.03
MgO	0.01	0.00	0.02	0.03	0.01	0.05	0.01	0.00	0.00	0.02	0.00	0.05	0.00	0.00	0.00	0.00	0.01	0.04	0.01	0.00	0.00
NiO	0.03	0.04	0.03	0.03	0.00	0.00	0.02	0.01	0.01	0.02	0.03	0.04	0.01	0.00	0.00	0.07	0.03	0.03	0.03	0.03	0.01
Total	92.75	92.41	92.70	93.08	92.57	92.86	92.65	92.79	92.11	92.65	92.61	92.40	92.55	92.04	92.21	92.18	91.98	92.12	94.49	93.46	94.53
Cations:																					
Ti	0.00	0.00	0.00	0.00	0.00	0.01	0.00	0.00	0.00	0.01	0.00	0.00	0.01	0.00	0.00	0.00	0.00	0.00	0.00	0.00	0.00
Al	0.01	0.01	0.01	0.01	0.01	0.01	0.01	0.01	0.01	0.01	0.01	0.02	0.01	0.01	0.01	0.01	0.01	0.01	0.01	0.00	0.01
Cr	0.00	0.00	0.00	0.00	0.00	0.00	0.00	0.00	0.00	0.00	0.00	0.00	0.00	0.00	0.00	0.00	0.00	0.00	0.00	0.00	0.00
Fe	3.97	3.97	3.97	3.97	3.97	3.96	3.98	3.97	3.97	3.96	3.97	3.95	3.97	3.98	3.97	3.97	3.97	3.97	3.97	3.99	3.98
Mn	0.00	0.00	0.00	0.00	0.00	0.00	0.00	0.00	0.00	0.00	0.00	0.00	0.00	0.00	0.00	0.00	0.00	0.00	0.00	0.00	0.00
Mg	0.00	0.00	0.00	0.00	0.00	0.00	0.00	0.00	0.00	0.00	0.00	0.00	0.00	0.00	0.00	0.00	0.00	0.00	0.00	0.00	0.00
Ni	0.00	0.00	0.00	0.00	0.00	0.00	0.00	0.00	0.00	0.00	0.00	0.00	0.00	0.00	0.00	0.00	0.00	0.00	0.00	0.00	0.00
Total (All)	3.99	3.99	3.99	3.99	3.99	3.99	3.99	3.99	3.99	3.99	3.99	3.99	3.99	3.99	3.99	3.99	3.99	3.99	3.99	4.00	3.99
Total (Majors ONLY)	3.99	3.99	3.99	3.98	3.99	3.98	3.99	3.99	3.99	3.98	3.98	3.98	3.99	3.99	3.99	3.99	3.99	3.99	3.99	4.00	3.99

Note: Analyses conducted on the same mineral grain (e.g. 1 core analysis and 2 rim analyses on a specific ilmenite or magnetite grain) are highlighted in the same colour and enclosed in the same thick black box.

Ilmenites and Magnetites cont.

Analysis Label (Specimen_mineral grain/zone:spot number)	gb10_op_1e	gb10_op_1h	gb10_op_1c	gb10_op_1f	ma29_op_1a	ma29_op_1c	ma29_op_2a	ma29_op_2b	ma29_op_4a	ma29_op_3a	ma29_op_5xz	ma31_op_2x	ma31_op_3x	ma31_op_4x	ma31_op_5x	ma31_op_6x	ma31_op_7x	ma31_op_8x	ma31_op_9x	ma31_op_10x	ma31_op_11x
Mineral Probed:	mt	mt	ilm	ilm	ilm	ilm	ilm	ilm	ilm	ilm	ilm	ilm	ilm	ilm	ilm	ilm	ilm	ilm	ilm	ilm	ilm
Core/Int/Rim:	Core	Core	Int	Rim	Core	Core	Core	Core	Core	Core	Core	Core	Core	Core	Core	Core	Core	Core	Core	Core	Core
EMP Initial Results:																					
Oxide conc. (wt%)																					
TiO2	0.04	0.03	45.90	47.51	52.08	52.22	52.04	52.12	51.03	51.38	51.28	51.65	51.16	51.76	52.01	51.87	51.06	51.29	51.39	51.59	51.44
Al2O3	0.14	0.49	0.01	0.03	0.05	0.03	0.00	0.01	0.00	0.00	0.00	0.01	0.00	0.02	0.00	0.00	0.26	0.00	0.01	0.00	0.01
Cr2O3	0.03	0.07	0.04	0.01	0.00	0.03	0.00	0.00	0.00	0.00	0.02	0.03	0.00	0.04	0.01	0.00	0.01	0.01	0.00	0.02	0.00
FeO	93.95	93.12	50.90	50.79	46.21	45.12	44.78	45.91	46.20	46.34	46.22	45.20	46.21	46.12	45.52	45.58	44.81	44.84	45.12	46.15	45.99
MnO	0.01	0.02	0.81	0.25	0.33	0.25	0.35	0.32	1.24	0.70	0.65	0.90	0.67	0.58	0.55	0.90	1.96	1.72	1.41	0.97	0.73
MgO	0.07	0.07	0.43	0.32	0.31	0.37	0.37	0.34	0.52	0.61	0.66	0.12	0.34	0.31	0.36	0.64	0.13	0.10	0.53	0.17	0.22
NiO	0.01	0.02	0.00	0.01	0.00	0.00	0.00	0.00	0.05	0.00	0.04	0.00	0.03	0.00	0.00	0.00	0.02	0.01	0.00	0.00	0.01
Total	94.25	93.82	98.10	98.92	98.98	98.01	97.54	98.69	99.05	99.04	98.86	97.91	98.41	98.83	98.45	99.00	98.26	97.97	98.45	98.90	98.40
Cations:																					
Ti	0.00	0.00	0.92	0.93	1.00	1.01	1.01	1.00	0.98	0.99	0.99	1.00	0.99	0.99	1.00	0.99	0.99	1.00	0.99	0.99	0.99
Al	0.01	0.03	0.00	0.00	0.00	0.00	0.00	0.00	0.00	0.00	0.00	0.00	0.00	0.00	0.00	0.00	0.01	0.00	0.00	0.00	0.00
Cr	0.00	0.00	0.00	0.00	0.00	0.00	0.00	0.00	0.00	0.00	0.00	0.00	0.00	0.00	0.00	0.00	0.00	0.00	0.00	0.00	0.00
Fe	3.98	3.94	1.13	1.11	0.98	0.97	0.96	0.98	0.99	0.99	0.99	0.97	0.99	0.98	0.97	0.97	0.96	0.97	0.97	0.99	0.99
Mn	0.00	0.00	0.02	0.01	0.01	0.01	0.01	0.01	0.03	0.02	0.01	0.02	0.01	0.01	0.01	0.02	0.04	0.04	0.03	0.02	0.02
Mg	0.01	0.01	0.02	0.01	0.01	0.01	0.01	0.01	0.02	0.02	0.03	0.00	0.01	0.01	0.01	0.02	0.01	0.00	0.02	0.01	0.01
Ni	0.00	0.00	0.00	0.00	0.00	0.00	0.00	0.00	0.00	0.00	0.00	0.00	0.00	0.00	0.00	0.00	0.00	0.00	0.00	0.00	0.00
Total (All)	3.99	3.98	2.08	2.06	2.00	1.99	1.99	2.00	2.02	2.01	2.01	2.00	2.01	2.01	2.00	2.01	2.01	2.00	2.01	2.01	2.01
Total (Majors ONLY)	3.99	3.98	2.08	2.06	2.00	1.99	1.99	2.00	2.02	2.01	2.01	2.00	2.01	2.00	2.00	2.01	2.01	2.00	2.01	2.01	2.01

Note: Analyses conducted on the same mineral grain (e.g. 1 core analysis and 2 rim analyses on a specific ilmenite or magnetite grain) are highlighted in the same colour and enclosed in the same thick black box.

Ilmenites and Magnetites cont.

Analysis Label (Specimen_mineral grain/zone:spot number)	ma31_op_12y	ma31_op_1a	ma31_op_1b	ma31_op_1c	ma38_op_op1	ma38_op_op2	ma38_op_op3	ma38_op_op4	ma38_op_op5	ma38_op_op6	ma38_op_op7	ma38_op_op11	ma38_op_op12	ma40_op_3x	ma40_op_4x	ma40_op_6x	ma40_op_7x	ma40_op_8x	ma40_op_9x	ma40_op_2b	ma40_op_1a	ma40_op_1b
Mineral Probed:	ilm	ilm	ilm	ilm	ilm	ilm	ilm	ilm	ilm	ilm	ilm	ilm	ilm	ilm	ilm	ilm	ilm	ilm	ilm	ilm	ilm	ilm
Core/Int/Rim:	Core	Core	Core	Core	Core	Core	Core	Core	Core	Core	Core	Core	Core	Core	Core	Core	Core	Core	Core	Core	Core	Core
EMP Initial Results:																						
Oxide conc. (wt%)																						
TiO2	51.87	51.83	51.89	50.80	52.17	51.72	51.93	51.11	51.14	51.82	51.85	52.12	51.29	51.69	51.55	51.59	51.44	51.62	51.10	51.27	50.81	51.60
Al2O3	0.01	0.00	0.00	0.00	0.10	0.00	0.03	0.00	0.01	0.00	0.00	0.01	0.00	0.02	0.04	0.12	0.00	0.00	0.00	0.01	1.22	0.02
Cr2O3	0.03	0.01	0.01	0.00	0.02	0.00	0.00	0.01	0.00	0.05	0.00	0.04	0.06	0.00	0.03	0.00	0.06	0.02	0.01	0.00	0.01	0.00
FeO	45.93	45.73	45.80	46.11	45.02	45.81	45.66	45.97	46.19	46.25	46.47	46.03	46.22	46.04	45.32	45.01	46.03	46.43	45.56	45.81	45.32	46.15
MnO	0.44	0.89	0.84	0.63	0.71	0.63	0.60	0.68	0.62	0.66	0.67	0.69	0.68	0.77	1.27	1.30	0.61	0.65	0.62	0.64	0.52	0.68
MgO	0.69	0.19	0.16	0.32	0.58	0.48	0.42	0.46	0.52	0.26	0.33	0.17	0.32	0.20	0.49	0.40	0.28	0.12	0.21	0.24	0.34	0.27
NiO	0.01	0.01	0.00	0.00	0.01	0.02	0.01	0.00	0.04	0.01	0.00	0.00	0.02	0.00	0.00	0.00	0.03	0.02	0.00	0.01	0.01	0.02
Total	98.97	98.66	98.70	97.87	98.61	98.66	98.64	98.23	98.52	99.04	99.32	99.06	98.59	98.71	98.71	98.42	98.45	98.86	97.50	97.98	98.24	98.74
Cations:																						
Ti	0.99	1.00	1.00	0.99	1.00	0.99	1.00	0.99	0.99	0.99	0.99	1.00	0.99	0.99	0.99	0.99	0.99	0.99	1.00	0.99	0.98	0.99
Al	0.00	0.00	0.00	0.00	0.00	0.00	0.00	0.00	0.00	0.00	0.00	0.00	0.00	0.00	0.00	0.00	0.00	0.00	0.00	0.00	0.04	0.00
Cr	0.00	0.00	0.00	0.00	0.00	0.00	0.00	0.00	0.00	0.00	0.00	0.00	0.00	0.00	0.00	0.00	0.00	0.00	0.00	0.00	0.00	0.00
Fe	0.98	0.98	0.98	1.00	0.96	0.98	0.97	0.99	0.99	0.99	0.99	0.98	0.99	0.99	0.97	0.96	0.99	0.99	0.99	0.99	0.97	0.99
Mn	0.01	0.02	0.02	0.01	0.02	0.01	0.01	0.01	0.01	0.01	0.01	0.01	0.01	0.02	0.03	0.03	0.01	0.01	0.01	0.01	0.01	0.01
Mg	0.03	0.01	0.01	0.01	0.02	0.02	0.02	0.02	0.02	0.01	0.01	0.01	0.01	0.01	0.02	0.02	0.01	0.00	0.01	0.01	0.01	0.01
Ni	0.00	0.00	0.00	0.00	0.00	0.00	0.00	0.00	0.00	0.00	0.00	0.00	0.00	0.00	0.00	0.00	0.00	0.00	0.00	0.00	0.00	0.00
Total (All)	2.01	2.00	2.00	2.01	2.00	2.01	2.00	2.01	2.01	2.01	2.01	2.00	2.01	2.00	2.01	2.00	2.01	2.01	2.00	2.01	2.01	2.01
Total (Majors ONLY)	2.01	2.00	2.00	2.01	2.00	2.01	2.00	2.01	2.01	2.00	2.01	2.00	2.01	2.00	2.01	2.00	2.00	2.01	2.00	2.01	2.01	2.01

Note: Analyses conducted on the same mineral grain (e.g. 1 core analysis and 2 rim analyses on a specific ilmenite or magnetite grain) are highlighted in the same colour and enclosed in the same thick black box.

Kyanites

Analysis Label (Specimen_mineral_grain/zone:spot number)	ma31_ky_1c	ma31_ky_1a	ma31_ky_1b	ma31_ky_2c	ma31_ky_2b	ma31_ky_2a	ma31_ky_2d	ma31_ky_3b	ma31_ky_3c	ma31_ky_3a	ma31_ky_3d	ma31_ky_3e	ma31_ky_4c	ma31_ky_4e	ma31_ky_4b	ma31_ky_4d	ma31_ky_4f	ma31_ky_4g	ma31_ky_4k	ma31_ky_4l	ma31_ky_4j
Mineral Probed:	ky	ky	ky	ky	ky	ky	ky	ky	ky	ky	ky	ky	ky	ky	ky	ky	ky	ky	ky	ky	ky
Core/Int/Rim:	Rim	Int	Core	Rim	Int	Core	Rim	Rim	Rim	Core	Core	Rim	Rim	Rim	Int	Int	Int	Rim	Int	Int	Core
EMP Initial Results:																					
Oxide conc. (wt%)																					
SiO2	36.68	36.86	37.13	36.56	36.81	36.79	37.06	36.49	36.79	36.44	36.55	37.05	36.81	36.55	36.62	36.57	36.79	36.28	36.34	36.50	36.77
TiO2	0.00	0.04	0.01	0.00	0.00	0.02	0.00	0.03	0.02	0.02	0.05	0.02	0.02	0.03	0.01	0.05	0.01	0.00	0.03	0.00	0.00
Al2O3	61.89	62.98	62.77	62.04	62.31	62.75	62.33	62.36	62.73	62.62	62.49	63.07	62.44	62.38	62.21	62.44	62.40	62.89	61.85	62.15	62.68
Cr2O3	0.02	0.00	0.01	0.00	0.00	0.06	0.00	0.02	0.04	0.03	0.01	0.00	0.04	0.02	0.02	0.05	0.00	0.03	0.08	0.02	0.06
FeO	0.23	0.10	0.21	0.19	0.20	0.19	0.26	0.23	0.24	0.16	0.14	0.15	0.29	0.18	0.20	0.35	0.21	0.19	0.23	0.21	0.12
MnO	0.04	0.01	0.02	0.03	0.01	0.05	0.04	0.00	0.05	0.02	0.03	0.03	0.01	0.02	0.01	0.04	0.04	0.04	0.05	0.03	0.00
MgO	0.01	0.01	0.04	0.00	0.02	0.05	0.00	0.00	0.02	0.00	0.02	0.00	0.03	0.00	0.03	0.02	0.03	0.02	0.02	0.02	0.00
CaO	0.01	0.00	0.01	0.01	0.01	0.01	0.01	0.01	0.01	0.01	0.00	0.00	0.00	0.00	0.00	0.00	0.01	0.02	0.00	0.02	0.01
Na2O	0.01	0.01	0.00	0.00	0.03	0.00	0.01	0.00	0.00	0.02	0.00	0.01	0.01	0.01	0.02	0.02	0.01	0.01	0.01	0.02	0.01
K2O	0.00	0.00	0.01	0.01	0.00	0.00	0.00	0.01	0.00	0.00	0.00	0.00	0.00	0.01	0.01	0.01	0.00	0.01	0.00	0.01	0.02
Total	98.90	100.01	100.21	98.84	99.39	99.91	99.73	99.14	99.90	99.33	99.29	100.33	99.66	99.20	99.12	99.54	99.51	99.49	98.61	98.98	99.67
Cations:																					
Si	1.00	0.99	1.00	1.00	1.00	0.99	1.00	0.99	1.00	0.99	0.99	1.00	1.00	1.00	1.00	0.99	1.00	0.99	1.00	1.00	1.00
Ti	0.00	0.00	0.00	0.00	0.00	0.00	0.00	0.00	0.00	0.00	0.00	0.00	0.00	0.00	0.00	0.00	0.00	0.00	0.00	0.00	0.00
Al	1.99	2.00	1.99	2.00	2.00	2.00	1.99	2.00	2.00	2.01	2.00	2.00	2.00	2.00	2.00	2.00	2.00	2.01	2.00	2.00	2.00
Cr	0.00	0.00	0.00	0.00	0.00	0.00	0.00	0.00	0.00	0.00	0.00	0.00	0.00	0.00	0.00	0.00	0.00	0.00	0.00	0.00	0.00
Fe	0.01	0.00	0.00	0.00	0.00	0.00	0.01	0.01	0.01	0.00	0.00	0.00	0.01	0.00	0.00	0.01	0.00	0.00	0.01	0.00	0.00
Mn	0.00	0.00	0.00	0.00	0.00	0.00	0.00	0.00	0.00	0.00	0.00	0.00	0.00	0.00	0.00	0.00	0.00	0.00	0.00	0.00	0.00
Mg	0.00	0.00	0.00	0.00	0.00	0.00	0.00	0.00	0.00	0.00	0.00	0.00	0.00	0.00	0.00	0.00	0.00	0.00	0.00	0.00	0.00
Ca	0.00	0.00	0.00	0.00	0.00	0.00	0.00	0.00	0.00	0.00	0.00	0.00	0.00	0.00	0.00	0.00	0.00	0.00	0.00	0.00	0.00
Na	0.00	0.00	0.00	0.00	0.00	0.00	0.00	0.00	0.00	0.00	0.00	0.00	0.00	0.00	0.00	0.00	0.00	0.00	0.00	0.00	0.00
K	0.00	0.00	0.00	0.00	0.00	0.00	0.00	0.00	0.00	0.00	0.00	0.00	0.00	0.00	0.00	0.00	0.00	0.00	0.00	0.00	0.00
Total (All)	3.00	3.00	3.00	3.00	3.00	3.00	3.00	3.00	3.00	3.01	3.00	3.00	3.00	3.00	3.00	3.01	3.00	3.01	3.00	3.00	3.00
Total (Majors ONLY)	3.00	3.00	3.00	3.00	3.00	3.00	3.00	3.00	3.00	3.00	3.00	3.00	3.00	3.00	3.00	3.00	3.00	3.01	3.00	3.00	3.00

Note: Analyses conducted on the same mineral grain (e.g. 1 core analysis and 2 rim analyses on a specific kyanite grain) are highlighted in the same colour and enclosed in the same thick black box.

Kyanites cont.

Analysis Label (Specimen_mineral_grain/zone:spot number)	ma31_ky_4i	ma31_ky_4h	ma38(b)_ky_1e	ma38(b)_ky_1d	ma38(b)_ky_1a	ma38(b)_ky_1c	ma38(b)_ky_2a	ma38(b)_ky_2e	ma38(b)_ky_2d	ma38(b)_ky_2b	ma38(b)_ky_2c	ma38(b)_ky_2f	ma38(a)_ky_1c	ma38(a)_ky_1b	ma38(a)_ky_1d	ma38(a)_ky_1a	ma38(a)_ky_1f	ma38(a)_ky_1e	ma38(a)_ky_1i	ma38(a)_ky_1g	ma38(a)_ky_1j
Mineral Probed:	ky	ky	ky	ky	ky	ky	ky	ky	ky	ky	ky	ky	ky	ky	ky	ky	ky	ky	ky	ky	ky
Core/Int/Rim:	Core	Int	Rim	Int	Core	Core	Rim	Rim	Int	Core	Core	Rim	Rim	Rim	Int	Core	Rim	Rim	Rim	Core	Rim
EMP Initial Results:																					
Oxide conc. (wt%)																					
SiO2	36.41	36.37	35.98	36.67	36.73	36.42	36.60	36.49	36.37	36.63	36.65	36.88	36.70	36.31	36.51	36.63	36.69	36.22	36.87	36.54	36.27
TiO2	0.00	0.01	0.00	0.02	0.03	0.04	0.16	0.03	0.04	0.00	0.04	0.02	0.07	0.00	0.00	0.02	0.00	0.03	0.02	0.04	0.00
Al2O3	62.48	62.33	62.21	62.27	62.93	63.04	62.58	62.66	61.87	63.00	62.50	62.62	62.39	62.38	62.61	62.00	62.37	62.06	62.99	62.22	61.97
Cr2O3	0.05	0.07	0.03	0.03	0.07	0.02	0.04	0.03	0.05	0.05	0.02	0.04	0.02	0.00	0.07	0.03	0.00	0.03	0.03	0.02	0.00
FeO	0.15	0.14	0.19	0.11	0.12	0.17	0.24	0.16	0.19	0.16	0.22	0.15	0.24	0.22	0.15	0.11	0.40	0.17	0.25	0.15	0.23
MnO	0.02	0.02	0.05	0.07	0.06	0.03	0.00	0.07	0.02	0.00	0.03	0.04	0.04	0.00	0.00	0.00	0.06	0.01	0.04	0.00	0.02
MgO	0.01	0.03	0.02	0.00	0.00	0.00	0.03	0.00	0.03	0.02	0.01	0.02	0.02	0.01	0.02	0.00	0.03	0.00	0.00	0.02	0.04
CaO	0.03	0.02	0.00	0.00	0.01	0.00	0.02	0.00	0.01	0.01	0.00	0.01	0.00	0.01	0.02	0.00	0.00	0.00	0.00	0.01	0.01
Na2O	0.02	0.05	0.03	0.00	0.01	0.04	0.00	0.00	0.03	0.04	0.02	0.01	0.02	0.01	0.02	0.00	0.00	0.01	0.00	0.07	0.01
K2O	0.00	0.00	0.00	0.00	0.01	0.01	0.00	0.02	0.00	0.01	0.00	0.01	0.00	0.00	0.01	0.00	0.00	0.00	0.00	0.01	0.00
Total	99.18	99.05	98.51	99.18	99.97	99.78	99.68	99.45	98.60	99.92	99.50	99.80	99.50	98.93	99.41	98.80	99.56	98.53	100.21	99.08	98.56
Cations:																					
Si	0.99	0.99	0.99	1.00	0.99	0.99	0.99	0.99	1.00	0.99	1.00	1.00	1.00	0.99	0.99	1.00	1.00	0.99	0.99	1.00	0.99
Ti	0.00	0.00	0.00	0.00	0.00	0.00	0.00	0.00	0.00	0.00	0.00	0.00	0.00	0.00	0.00	0.00	0.00	0.00	0.00	0.00	0.00
Al	2.01	2.00	2.01	2.00	2.00	2.01	2.00	2.01	2.00	2.01	2.00	2.00	2.00	2.01	2.01	2.00	2.00	2.01	2.00	2.00	2.00
Cr	0.00	0.00	0.00	0.00	0.00	0.00	0.00	0.00	0.00	0.00	0.00	0.00	0.00	0.00	0.00	0.00	0.00	0.00	0.00	0.00	0.00
Fe	0.00	0.00	0.00	0.00	0.00	0.00	0.01	0.00	0.00	0.00	0.00	0.00	0.01	0.00	0.00	0.00	0.01	0.00	0.01	0.00	0.01
Mn	0.00	0.00	0.00	0.00	0.00	0.00	0.00	0.00	0.00	0.00	0.00	0.00	0.00	0.00	0.00	0.00	0.00	0.00	0.00	0.00	0.00
Mg	0.00	0.00	0.00	0.00	0.00	0.00	0.00	0.00	0.00	0.00	0.00	0.00	0.00	0.00	0.00	0.00	0.00	0.00	0.00	0.00	0.00
Ca	0.00	0.00	0.00	0.00	0.00	0.00	0.00	0.00	0.00	0.00	0.00	0.00	0.00	0.00	0.00	0.00	0.00	0.00	0.00	0.00	0.00
Na	0.00	0.00	0.00	0.00	0.00	0.00	0.00	0.00	0.00	0.00	0.00	0.00	0.00	0.00	0.00	0.00	0.00	0.00	0.00	0.00	0.00
K	0.00	0.00	0.00	0.00	0.00	0.00	0.00	0.00	0.00	0.00	0.00	0.00	0.00	0.00	0.00	0.00	0.00	0.00	0.00	0.00	0.00
Total (All)	3.01	3.01	3.01	3.00	3.00	3.01	3.00	3.00	3.00	3.01	3.00	3.00	3.00	3.01	3.01	3.00	3.01	3.00	3.00	3.01	3.00
Total (Majors ONLY)	3.00	3.00	3.01	3.00	3.00	3.01	3.00	3.00	3.00	3.01	3.00	3.00	3.00	3.01	3.00	3.00	3.01	3.00	3.00	3.00	3.00

Note: Analyses conducted on the same mineral grain (e.g. 1 core analysis and 2 rim analyses on a specific kyanite grain) are highlighted in the same colour and enclosed in the same thick black box.

Kyanites cont.

Analysis Label (Specimen_mineral_grain/zone:spot number)	ma38(a)_ky_2c	ma38(a)_ky_2g	ma38(a)_ky_2b	ma38(a)_ky_2e	ma38(a)_ky_2a	ma38(a)_ky_2h	ma38(a)_ky_2f	ma38(a)_ky_2i	ma38(a)_ky_2j	ma40_ky_1b	ma40_ky_1c	ma40_ky_1a	ma40_ky_1d	ma40_ky_1e	ma40_ky_1g	ma40_ky_1i	ma40_ky_1f	ma40_ky_1h	ma40_ky_1k	ma40_ky_1j	ma40_ky_1m
Mineral Probed:	ky	ky	ky	ky	ky	ky	ky	ky	ky	ky	ky	ky	ky	ky	ky	ky	ky	ky	ky	ky	ky
Core/Int/Rim:	Rim	Rim	Int	Int	Core	Core	Int	Int	Rim	Rim	Int	Core	Int	Rim	Rim	Int	Core	Rim	Rim	Core	Int
EMP Initial Results:																					
Oxide conc. (wt%)																					
SiO2	36.94	36.29	36.73	36.37	37.08	36.83	36.65	36.78	36.75	36.69	37.16	36.95	36.82	36.83	37.03	36.61	36.54	36.62	36.96	37.08	36.56
TiO2	0.00	0.01	0.01	0.00	0.02	0.03	0.08	0.00	0.01	0.04	0.10	0.00	0.03	0.00	0.00	0.00	0.06	0.00	0.00	0.00	0.02
Al2O3	63.06	63.03	62.83	62.26	62.50	62.84	62.87	62.99	62.71	62.88	63.00	63.19	62.94	62.84	62.91	62.51	63.07	62.93	62.75	63.01	62.90
Cr2O3	0.08	0.10	0.10	0.05	0.08	0.00	0.07	0.06	0.08	0.04	0.02	0.00	0.02	0.00	0.00	0.05	0.00	0.03	0.03	0.06	0.07
FeO	0.18	0.32	0.16	0.11	0.16	0.11	0.28	0.08	0.18	0.18	0.22	0.15	0.28	0.17	0.17	0.20	0.15	0.17	0.19	0.20	0.23
MnO	0.01	0.03	0.03	0.03	0.00	0.00	0.03	0.01	0.04	0.04	0.00	0.03	0.02	0.07	0.00	0.00	0.06	0.00	0.03	0.00	0.03
MgO	0.01	0.02	0.01	0.02	0.00	0.00	0.03	0.00	0.00	0.00	0.01	0.02	0.02	0.00	0.00	0.00	0.02	0.01	0.02	0.03	0.00
CaO	0.01	0.00	0.00	0.01	0.00	0.01	0.02	0.00	0.01	0.00	0.01	0.00	0.01	0.01	0.00	0.00	0.00	0.02	0.01	0.02	0.00
Na2O	0.00	0.00	0.01	0.02	0.01	0.01	0.01	0.02	0.00	0.00	0.01	0.00	0.00	0.02	0.01	0.02	0.00	0.01	0.00	0.00	0.01
K2O	0.01	0.00	0.00	0.00	0.01	0.00	0.01	0.00	0.01	0.00	0.00	0.00	0.01	0.00	0.00	0.02	0.00	0.00	0.01	0.00	0.01
Total	100.31	99.80	99.88	98.86	99.87	99.84	100.04	99.94	99.79	99.87	100.54	100.34	100.16	99.95	100.13	99.41	99.91	99.79	100.00	100.41	99.84
Cations:																					
Si	0.99	0.98	0.99	0.99	1.00	1.00	0.99	0.99	0.99	0.99	1.00	0.99	0.99	1.00	1.00	0.99	0.99	0.99	1.00	1.00	0.99
Ti	0.00	0.00	0.00	0.00	0.00	0.00	0.00	0.00	0.00	0.00	0.00	0.00	0.00	0.00	0.00	0.00	0.00	0.00	0.00	0.00	0.00
Al	2.00	2.01	2.00	2.00	1.99	2.00	2.00	2.01	2.00	2.00	2.00	2.00	2.00	2.00	2.00	2.00	2.01	2.01	2.00	2.00	2.01
Cr	0.00	0.00	0.00	0.00	0.00	0.00	0.00	0.00	0.00	0.00	0.00	0.00	0.00	0.00	0.00	0.00	0.00	0.00	0.00	0.00	0.00
Fe	0.00	0.01	0.00	0.00	0.00	0.00	0.01	0.00	0.00	0.00	0.01	0.00	0.01	0.00	0.00	0.00	0.00	0.00	0.00	0.00	0.01
Mn	0.00	0.00	0.00	0.00	0.00	0.00	0.00	0.00	0.00	0.00	0.00	0.00	0.00	0.00	0.00	0.00	0.00	0.00	0.00	0.00	0.00
Mg	0.00	0.00	0.00	0.00	0.00	0.00	0.00	0.00	0.00	0.00	0.00	0.00	0.00	0.00	0.00	0.00	0.00	0.00	0.00	0.00	0.00
Ca	0.00	0.00	0.00	0.00	0.00	0.00	0.00	0.00	0.00	0.00	0.00	0.00	0.00	0.00	0.00	0.00	0.00	0.00	0.00	0.00	0.00
Na	0.00	0.00	0.00	0.00	0.00	0.00	0.00	0.00	0.00	0.00	0.00	0.00	0.00	0.00	0.00	0.00	0.00	0.00	0.00	0.00	0.00
K	0.00	0.00	0.00	0.00	0.00	0.00	0.00	0.00	0.00	0.00	0.00	0.00	0.00	0.00	0.00	0.00	0.00	0.00	0.00	0.00	0.00
Total (All)	3.00	3.01	3.00	3.00	3.00	3.00	3.01	3.00	3.00	3.00	3.00	3.00	3.00	3.00	3.00	3.00	3.01	3.00	3.00	3.00	3.01
Total (Majors ONLY)	3.00	3.01	3.00	3.00	3.00	3.00	3.00	3.00	3.00	3.00	3.00	3.00	3.00	3.00	3.00	3.00	3.01	3.00	3.00	3.00	3.00

Note: Analyses conducted on the same mineral grain (e.g. 1 core analysis and 2 rim analyses on a specific kyanite grain) are highlighted in the same colour and enclosed in the same thick black box.

Kyanites cont.

Analysis Label (Specimen_mineral_ grain/zone:spot number)	ma40_ky_1n	ma40_ky_1p	ma40_ky_1q	ma40_ky_1r	ma40_ky_1o	ma40_ky_1s
Mineral Probed:	ky	ky	ky	ky	ky	ky
Core/Int/Rim:	Core	Rim	Rim	Int	Core	Rim
EMP Initial Results:						
Oxide conc. (wt%)						
SiO2	36.41	36.48	36.55	36.87	36.67	36.37
TiO2	0.02	0.00	0.02	0.03	0.00	0.01
Al2O3	62.39	62.24	62.80	62.94	62.76	62.38
Cr2O3	0.02	0.04	0.05	0.02	0.02	0.03
FeO	0.14	0.22	0.18	0.22	0.12	0.16
MnO	0.00	0.04	0.02	0.00	0.02	0.03
MgO	0.00	0.00	0.01	0.05	0.02	0.01
CaO	0.00	0.00	0.01	0.00	0.01	0.02
Na2O	0.02	0.00	0.00	0.02	0.00	0.00
K2O	0.00	0.01	0.01	0.00	0.00	0.01
Total	99.00	99.03	99.65	100.14	99.63	99.00
Cations:						
Si	0.99	1.00	0.99	0.99	0.99	0.99
Ti	0.00	0.00	0.00	0.00	0.00	0.00
Al	2.01	2.00	2.01	2.00	2.00	2.01
Cr	0.00	0.00	0.00	0.00	0.00	0.00
Fe	0.00	0.00	0.00	0.00	0.00	0.00
Mn	0.00	0.00	0.00	0.00	0.00	0.00
Mg	0.00	0.00	0.00	0.00	0.00	0.00
Ca	0.00	0.00	0.00	0.00	0.00	0.00
Na	0.00	0.00	0.00	0.00	0.00	0.00
K	0.00	0.00	0.00	0.00	0.00	0.00
Total (All)	3.00	3.00	3.00	3.00	3.00	3.00
Total (Majors ONLY)	3.00	3.00	3.00	3.00	3.00	3.00

Note: Analyses conducted on the same mineral grain (e.g. 1 core analysis and 2 rim analyses on a specific kyanite grain) are highlighted in the same colour and enclosed in the same thick black box.

Muscovites

Analysis Label (Specimen_mineral_grain/zone:spot number)	gb8_mu_1b	gb8_mu_1a	gb8_mu_2a	gb8_mu_2b	gb10_mu_1a	gb10_mu_1c	gb10_mu_1d	gb10_mu_1e	gb10_mu_1f	gb10_mu_1g	gb10_mu_1h	gb10_mu_1i	gb10_mu_1j	gb10_mu_1k	gb10_mu_1l	gb10_mu_1n	gb10_mu_3b	gb10_mu_3a	gb10_mu_3c	gb10_mu_3d	gb10_mu_3e
Mineral Probed:	mu	mu	mu	mu	mu	mu	mu	mu	mu	mu	mu	mu	mu	mu	mu	mu	mu	mu	mu	mu	mu
Core/Int/Rim:	Rim	Core	Core	Core	Core	Core	Core	Core	Core	Core	Core	Core	Core	Core	Core	Core	Core	Core	Core	Core	Core
EMP Initial Results:																					
Oxide conc. (wt%)																					
SiO2	47.00	46.66	48.11	47.02	46.77	47.06	45.71	45.38	47.47	46.04	45.69	46.42	45.81	45.75	46.18	45.65	45.44	46.95	45.89	47.60	45.89
TiO2	0.30	0.28	0.35	0.21	0.37	0.39	0.25	0.25	0.37	0.28	0.33	0.33	0.19	0.27	0.28	0.28	0.38	0.30	0.49	0.36	0.30
Al2O3	36.57	36.75	34.80	37.11	34.71	33.99	36.98	36.86	33.74	36.46	36.32	35.53	36.38	36.78	36.08	36.70	36.57	35.18	36.71	34.13	36.81
Cr2O3	0.03	0.00	0.05	0.04	0.06	0.02	0.04	0.05	0.00	0.02	0.05	0.00	0.03	0.01	0.06	0.00	0.01	0.07	0.05	0.05	0.04
FeO	2.83	2.85	2.96	2.80	2.87	3.00	2.88	2.89	2.77	2.77	2.87	3.08	2.77	2.80	2.82	2.75	2.82	2.52	2.67	2.66	2.60
MnO	0.00	0.00	0.05	0.02	0.02	0.07	0.03	0.03	0.02	0.04	0.06	0.00	0.00	0.00	0.02	0.07	0.03	0.05	0.01	0.06	0.00
MgO	0.67	0.73	1.30	0.64	1.23	1.42	0.66	0.61	1.39	0.69	0.78	1.47	0.78	0.75	0.99	0.74	0.73	1.18	0.73	1.41	0.71
CaO	0.00	0.00	0.00	0.01	0.00	0.02	0.00	0.00	0.00	0.00	0.01	0.00	0.00	0.00	0.00	0.00	0.00	0.00	0.00	0.00	0.00
NaO	1.73	1.86	1.21	2.04	1.14	1.04	1.50	1.34	1.05	1.83	1.58	1.04	1.78	1.61	1.30	1.47	1.64	1.07	1.56	1.02	1.67
K2O	8.94	8.80	9.48	8.50	9.67	9.53	9.16	9.43	9.53	8.78	9.01	9.58	8.88	9.01	9.40	9.11	9.04	9.72	9.13	9.60	9.14
Total	98.07	97.93	98.31	98.40	96.84	96.54	97.21	96.85	96.34	96.90	96.70	97.45	96.63	96.98	97.13	96.77	96.66	97.04	97.24	96.89	97.17
Cations:																					
Si	3.04	3.03	3.11	3.03	3.08	3.11	2.99	2.99	3.13	3.02	3.01	3.04	3.01	3.00	3.03	3.00	2.99	3.08	3.00	3.12	3.00
Ti	0.01	0.01	0.02	0.01	0.02	0.02	0.01	0.01	0.02	0.01	0.02	0.02	0.01	0.01	0.01	0.01	0.02	0.01	0.02	0.02	0.01
Al	2.79	2.81	2.65	2.82	2.69	2.65	2.85	2.86	2.62	2.82	2.82	2.74	2.82	2.84	2.79	2.84	2.84	2.72	2.83	2.64	2.84
Cr	0.00	0.00	0.00	0.00	0.00	0.00	0.00	0.00	0.00	0.00	0.00	0.00	0.00	0.00	0.00	0.00	0.00	0.00	0.00	0.00	0.00
Fe	0.15	0.15	0.16	0.15	0.16	0.17	0.16	0.16	0.15	0.15	0.16	0.17	0.15	0.15	0.15	0.15	0.16	0.14	0.15	0.15	0.14
Mn	0.00	0.00	0.00	0.00	0.00	0.00	0.00	0.00	0.00	0.00	0.00	0.00	0.00	0.00	0.00	0.00	0.00	0.00	0.00	0.00	0.00
Mg	0.07	0.07	0.12	0.06	0.12	0.14	0.06	0.06	0.14	0.07	0.08	0.14	0.08	0.07	0.10	0.07	0.07	0.11	0.07	0.14	0.07
Ca	0.00	0.00	0.00	0.00	0.00	0.00	0.00	0.00	0.00	0.00	0.00	0.00	0.00	0.00	0.00	0.00	0.00	0.00	0.00	0.00	0.00
Na	0.22	0.23	0.15	0.25	0.15	0.13	0.19	0.17	0.14	0.23	0.20	0.13	0.23	0.20	0.17	0.19	0.21	0.14	0.20	0.13	0.21
K	0.74	0.73	0.78	0.70	0.81	0.80	0.77	0.79	0.80	0.73	0.76	0.80	0.75	0.75	0.79	0.76	0.76	0.81	0.76	0.80	0.76
Total (All)	7.02	7.04	7.01	7.03	7.03	7.02	7.04	7.05	7.00	7.04	7.04	7.04	7.05	7.04	7.04	7.04	7.05	7.02	7.04	7.00	7.05
Total (Majors ONLY)	7.02	7.04	7.01	7.03	7.03	7.02	7.04	7.05	7.00	7.04	7.04	7.04	7.05	7.04	7.03	7.04	7.05	7.02	7.03	7.00	7.05
Al(VI) (= (Si + Al) - 4)	1.83	1.84	1.77	1.85	1.77	1.75	1.85	1.85	1.76	1.84	1.83	1.78	1.84	1.84	1.82	1.85	1.83	1.80	1.83	1.76	1.84
Al(IV) (= Al - Al(VI))	0.96	0.97	0.89	0.97	0.92	0.89	1.01	1.01	0.87	0.98	0.99	0.96	0.99	1.00	0.97	1.00	1.01	0.92	1.00	0.88	1.00
Si (apfu)	3.04	3.03	3.11	3.03	3.08	3.11	2.99	2.99	3.13	3.02	3.01	3.04	3.01	3.00	3.03	3.00	2.99	3.08	3.00	3.12	3.00
Al (apfu)	2.79	2.81	2.65	2.82	2.69	2.65	2.85	2.86	2.62	2.82	2.82	2.74	2.82	2.84	2.79	2.84	2.84	2.72	2.83	2.64	2.84
XPa (= Na / (Na + K))	0.23	0.24	0.16	0.27	0.15	0.14	0.20	0.18	0.14	0.24	0.21	0.14	0.23	0.21	0.17	0.20	0.22	0.14	0.21	0.14	0.22
XMu (= K / (K + Na))	0.77	0.76	0.84	0.73	0.85	0.86	0.80	0.82	0.86	0.76	0.79	0.86	0.77	0.79	0.83	0.80	0.78	0.86	0.79	0.86	0.78

Note: Analyses conducted on the same mineral grain (e.g. 1 core analysis and 2 rim analyses on a specific muscovite grain) are highlighted in the same colour and enclosed in the same thick black box.

Muscovites cont.

Analysis Label (Specimen_mineral_grain/zone:spot number)	gb10_mu_3f	gb10_mu_3g	gb10_mu_3i	gb10_mu_3j	gb10_mu_3k	gb13_mu_1b	gb13_mu_1c	gb13_mu_3b	gb13_mu_3a	gb13_mu_3c	ma29_mu_1x	ma29_mu_2x	ma29_mu_3x	ma29_mu_4x	ma29_mu_4y	ma29_mu_5y	ma29_mu_5x	ma29_mu_6y	ma29_mu_7x	ma29_mu_test	ma31_mu_1d
Mineral Probed:	mu	mu	mu	mu	mu	mu	mu	mu	mu	mu	mu	mu	mu	mu	mu	mu	mu	mu	mu	mu	mu
Core/Int/Rim:	Core	Core	Core	Core	Core	Core	Core	Rim	Core	Core	Core	Core	Core	Core	Core	Core	Core	Core	Core	Core	Core
EMP Initial Results:																					
Oxide conc. (wt%)																					
SiO2	47.51	45.39	45.84	45.75	45.97	47.56	47.05	46.21	46.26	46.04	46.50	46.61	48.76	47.69	46.13	46.80	47.30	46.70	46.48	47.58	46.02
TiO2	0.33	0.54	0.23	0.31	0.31	0.35	0.32	0.41	0.25	0.31	0.35	0.32	0.49	0.37	0.29	0.37	0.45	0.33	0.35	0.34	0.47
Al2O3	33.89	36.90	36.66	36.94	36.82	35.19	34.90	37.52	37.95	37.68	38.92	38.70	33.68	36.41	38.07	38.63	36.63	37.92	38.15	38.03	37.70
Cr2O3	0.03	0.02	0.05	0.07	0.03	0.04	0.00	0.03	0.06	0.00	0.08	0.01	0.04	0.08	0.05	0.05	0.05	0.01	0.06	0.02	0.02
FeO	2.95	2.58	2.59	2.64	2.43	2.12	2.06	1.79	1.86	1.68	1.03	0.93	1.33	1.23	0.90	1.15	1.15	1.08	1.14	0.97	0.86
MnO	0.05	0.00	0.05	0.08	0.04	0.04	0.00	0.00	0.00	0.02	0.04	0.04	0.02	0.06	0.01	0.05	0.01	0.02	0.02	0.08	0.00
MgO	1.47	0.66	0.67	0.66	0.75	1.37	1.30	0.76	0.67	0.71	0.61	0.59	1.73	1.15	0.57	0.63	1.07	0.79	0.61	0.88	0.71
CaO	0.00	0.00	0.00	0.00	0.00	0.00	0.00	0.00	0.00	0.00	0.01	0.00	0.00	0.00	0.00	0.00	0.00	0.00	0.00	0.00	0.00
NaO	1.12	1.45	1.75	1.58	1.41	0.98	0.91	1.38	1.45	1.45	1.74	1.17	0.72	1.15	1.60	1.36	1.23	1.64	1.56	1.28	1.53
K2O	9.40	9.19	8.95	9.26	9.26	9.80	9.89	9.33	9.11	9.32	8.87	9.60	9.91	9.43	9.13	9.39	9.41	8.92	9.02	9.40	9.11
Total	96.75	96.74	96.79	97.29	97.02	97.44	96.42	97.43	97.60	97.21	98.16	97.96	96.69	97.58	96.76	98.42	97.30	97.41	97.40	98.58	96.42
Cations:																					
Si	3.12	2.98	3.01	2.99	3.01	3.10	3.10	3.00	3.00	3.00	2.98	3.00	3.18	3.08	3.00	3.00	3.06	3.02	3.00	3.04	3.00
Ti	0.02	0.03	0.01	0.02	0.02	0.02	0.02	0.02	0.01	0.02	0.02	0.02	0.02	0.02	0.01	0.02	0.02	0.02	0.02	0.02	0.02
Al	2.63	2.86	2.84	2.85	2.84	2.70	2.71	2.87	2.90	2.89	2.94	2.93	2.59	2.77	2.92	2.92	2.80	2.89	2.91	2.86	2.90
Cr	0.00	0.00	0.00	0.00	0.00	0.00	0.00	0.00	0.00	0.00	0.00	0.00	0.00	0.00	0.00	0.00	0.00	0.00	0.00	0.00	0.00
Fe	0.16	0.14	0.14	0.14	0.13	0.12	0.11	0.10	0.10	0.09	0.06	0.05	0.07	0.07	0.05	0.06	0.06	0.06	0.06	0.05	0.05
Mn	0.00	0.00	0.00	0.00	0.00	0.00	0.00	0.00	0.00	0.00	0.00	0.00	0.00	0.00	0.00	0.00	0.00	0.00	0.00	0.00	0.00
Mg	0.14	0.07	0.07	0.06	0.07	0.13	0.13	0.07	0.06	0.07	0.06	0.06	0.17	0.11	0.06	0.06	0.10	0.08	0.06	0.08	0.07
Ca	0.00	0.00	0.00	0.00	0.00	0.00	0.00	0.00	0.00	0.00	0.00	0.00	0.00	0.00	0.00	0.00	0.00	0.00	0.00	0.00	0.00
Na	0.14	0.18	0.22	0.20	0.18	0.12	0.12	0.17	0.18	0.18	0.22	0.15	0.09	0.14	0.20	0.17	0.16	0.21	0.20	0.16	0.19
K	0.79	0.77	0.75	0.77	0.77	0.81	0.83	0.77	0.75	0.77	0.73	0.79	0.82	0.78	0.76	0.77	0.78	0.73	0.74	0.77	0.76
Total (All)	7.01	7.04	7.04	7.05	7.03	7.00	7.01	7.01	7.01	7.02	7.00	6.99	6.96	6.97	7.00	6.99	6.98	6.99	6.99	6.98	7.00
Total (Majors ONLY)	7.01	7.03	7.04	7.05	7.03	7.00	7.01	7.01	7.01	7.02	7.00	6.99	6.95	6.97	7.00	6.99	6.98	6.99	6.99	6.98	7.00
Al(VI) (= (Si + Al) - 4)	1.75	1.84	1.85	1.84	1.85	1.80	1.80	1.87	1.89	1.89	1.92	1.93	1.77	1.85	1.92	1.91	1.86	1.90	1.91	1.90	1.91
Al(IV) (= Al - Al(VI))	0.88	1.02	0.99	1.01	0.99	0.90	0.90	1.00	1.00	1.00	1.02	1.00	0.82	0.92	1.00	1.00	0.94	0.98	1.00	0.96	1.00
Si (apfu)	3.12	2.98	3.01	2.99	3.01	3.10	3.10	3.00	3.00	3.00	2.98	3.00	3.18	3.08	3.00	3.00	3.06	3.02	3.00	3.04	3.00
Al (apfu)	2.63	2.86	2.84	2.85	2.84	2.70	2.71	2.87	2.90	2.89	2.94	2.93	2.59	2.77	2.92	2.92	2.80	2.89	2.91	2.86	2.90
XPa (= Na / (Na + K))	0.15	0.19	0.23	0.21	0.19	0.13	0.12	0.18	0.19	0.19	0.23	0.16	0.10	0.16	0.21	0.18	0.17	0.22	0.21	0.17	0.20
XMu (= K / (K + Na))	0.85	0.81	0.77	0.79	0.81	0.87	0.88	0.82	0.81	0.81	0.77	0.84	0.90	0.84	0.79	0.82	0.83	0.78	0.79	0.83	0.80

Note: Analyses conducted on the same mineral grain (e.g. 1 core analysis and 2 rim analyses on a specific muscovite grain) are highlighted in the same colour and enclosed in the same thick black box.

Muscovites cont.

Analysis Label (Specimen_mineral_grain/zone:spot number)	ma31_mu_1a	ma31_mu_1c	ma31_mu_1f	ma31_mu_2b	ma31_mu_2c	ma31_mu_2a	ma31_mu_2d	ma31_mu_2f	ma31_mu_2g	ma31_mu_3c	ma31_mu_3d	ma31_mu_3i	ma31_mu_3g	ma31_mu_3h	ma31_mu_3f	ma38_mu_m7	ma38_mu_m5	ma38_mu_m4b	ma38_chl_3c	ma38_unk	ma40_mu_1v
Mineral Probed:	mu	mu	mu	mu	mu	mu	mu	mu	mu	mu	mu	mu	mu	mu	mu	mu	mu	mu	mu	mu	mu
Core/Int/Rim:	Core	Core	Core	Core	Core	Core	Core	Core	Core	Core	Core	Core	Core	Core	Core	Core	Core	Core	Rim	Core	Core
EMP Initial Results:																					
Oxide conc. (wt%)																					
SiO2	46.23	46.32	45.68	46.16	45.27	45.89	45.98	46.29	45.92	46.45	47.30	46.36	46.17	46.52	46.38	47.00	46.53	46.80	46.64	46.14	46.77
TiO2	0.32	0.37	0.55	0.41	0.43	0.32	0.31	0.40	0.32	0.48	0.40	0.42	0.38	0.47	0.46	0.27	0.40	0.28	0.29	0.36	0.32
Al2O3	36.93	38.07	37.76	38.25	37.32	38.76	38.48	37.96	38.26	38.23	36.09	38.50	37.83	37.89	37.94	39.09	38.85	38.96	38.12	38.49	39.05
Cr2O3	0.03	0.03	0.03	0.06	0.06	0.00	0.00	0.04	0.02	0.05	0.00	0.02	0.01	0.04	0.04	0.01	0.04	0.00	0.02	0.06	0.00
FeO	1.11	1.03	1.04	0.80	0.91	0.99	0.85	1.04	0.93	0.94	1.17	0.91	0.77	0.87	0.86	0.88	1.12	0.82	1.29	0.75	0.92
MnO	0.00	0.03	0.09	0.05	0.04	0.03	0.00	0.07	0.00	0.02	0.04	0.04	0.03	0.06	0.00	0.03	0.00	0.00	0.05	0.00	0.00
MgO	0.85	0.66	0.60	0.58	0.62	0.55	0.53	0.64	0.57	0.68	1.11	0.65	0.71	0.72	0.73	0.49	0.58	0.51	0.64	0.66	0.55
CaO	0.00	0.00	0.00	0.00	0.86	0.00	0.00	0.00	0.00	0.00	0.01	0.00	0.00	0.00	0.00	0.00	0.00	0.00	0.00	0.00	0.00
NaO	1.27	1.53	1.28	1.46	1.38	1.71	1.62	1.44	1.50	1.44	0.85	1.55	1.37	1.51	1.40	1.69	1.65	1.79	1.24	1.78	1.44
K2O	9.25	8.98	9.18	9.29	9.13	8.91	8.15	8.50	9.15	8.48	9.41	8.09	9.23	8.13	8.23	7.13	7.47	6.98	7.86	8.97	8.01
Total	95.99	97.02	96.22	97.07	96.02	97.16	95.92	96.37	96.68	96.77	96.38	96.55	96.50	96.22	96.05	96.59	96.64	96.14	96.15	97.21	97.06
Cations:																					
Si	3.03	3.00	2.99	2.99	2.98	2.97	3.00	3.01	2.99	3.01	3.09	3.00	3.01	3.02	3.02	3.02	3.00	3.02	3.03	2.99	3.01
Ti	0.02	0.02	0.03	0.02	0.02	0.02	0.02	0.02	0.02	0.02	0.02	0.02	0.02	0.02	0.02	0.01	0.02	0.01	0.01	0.02	0.02
Al	2.86	2.91	2.92	2.92	2.90	2.96	2.96	2.91	2.94	2.92	2.78	2.94	2.91	2.90	2.91	2.96	2.95	2.96	2.92	2.94	2.96
Cr	0.00	0.00	0.00	0.00	0.00	0.00	0.00	0.00	0.00	0.00	0.00	0.00	0.00	0.00	0.00	0.00	0.00	0.00	0.00	0.00	0.00
Fe	0.06	0.06	0.06	0.04	0.05	0.05	0.05	0.06	0.05	0.05	0.06	0.05	0.04	0.05	0.05	0.05	0.06	0.04	0.07	0.04	0.05
Mn	0.00	0.00	0.01	0.00	0.00	0.00	0.00	0.00	0.00	0.00	0.00	0.00	0.00	0.00	0.00	0.00	0.00	0.00	0.00	0.00	0.00
Mg	0.08	0.06	0.06	0.06	0.06	0.05	0.05	0.06	0.06	0.07	0.11	0.06	0.07	0.07	0.07	0.05	0.06	0.05	0.06	0.06	0.05
Ca	0.00	0.00	0.00	0.00	0.06	0.00	0.00	0.00	0.00	0.00	0.00	0.00	0.00	0.00	0.00	0.00	0.00	0.00	0.00	0.00	0.00
Na	0.16	0.19	0.16	0.18	0.18	0.21	0.20	0.18	0.19	0.18	0.11	0.19	0.17	0.19	0.18	0.21	0.21	0.22	0.16	0.22	0.18
K	0.77	0.74	0.77	0.77	0.77	0.74	0.68	0.71	0.76	0.70	0.78	0.67	0.77	0.67	0.68	0.58	0.61	0.57	0.65	0.74	0.66
Total (All)	6.99	6.99	6.99	7.00	7.02	7.01	6.95	6.95	7.00	6.95	6.95	6.94	6.99	6.93	6.93	6.88	6.91	6.89	6.90	7.01	6.92
Total (Majors ONLY)	6.99	6.99	6.99	6.99	7.02	7.01	6.95	6.95	7.00	6.95	6.95	6.94	6.99	6.93	6.93	6.88	6.91	6.89	6.90	7.01	6.92
Al(VI) (= (Si + Al) - 4)	1.89	1.91	1.91	1.92	1.88	1.93	1.95	1.92	1.93	1.92	1.86	1.94	1.92	1.92	1.93	1.98	1.95	1.98	1.95	1.92	1.96
Al(IV) (= Al - Al(VI))	0.97	1.00	1.01	1.01	1.02	1.03	1.00	0.99	1.01	0.99	0.91	1.00	0.99	0.98	0.98	0.98	1.00	0.98	0.97	1.01	0.99
Si (apfu)	3.03	3.00	2.99	2.99	2.98	2.97	3.00	3.01	2.99	3.01	3.09	3.00	3.01	3.02	3.02	3.02	3.00	3.02	3.03	2.99	3.01
Al (apfu)	2.86	2.91	2.92	2.92	2.90	2.96	2.96	2.91	2.94	2.92	2.78	2.94	2.91	2.90	2.91	2.96	2.95	2.96	2.92	2.94	2.96
XPa (= Na / (Na + K))	0.17	0.21	0.18	0.19	0.19	0.23	0.23	0.20	0.20	0.21	0.12	0.23	0.18	0.22	0.21	0.26	0.25	0.28	0.19	0.23	0.21
XMu (= K / (K + Na))	0.83	0.79	0.82	0.81	0.81	0.77	0.77	0.80	0.80	0.79	0.88	0.77	0.82	0.78	0.79	0.74	0.75	0.72	0.81	0.77	0.79

Note: Analyses conducted on the same mineral grain (e.g. 1 core analysis and 2 rim analyses on a specific muscovite grain) are highlighted in the same colour and enclosed in the same thick black box.

Muscovites cont.

Analysis Label (Specimen_mineral_grain/zone:spot number)	ma40_mu_2u	ma40_mu_2w	ma40_mu_2x	ma40_mu_3v	ma40_mu_5w	ma40_mu_6v	ma40_mu_6u	ma40_mu_6w	ma40_mu_6x	ma40_mu_6y	ma40_mu_6z	ma40_chl_1d
Mineral Probed:	mu	mu	mu	mu	mu	mu	mu	mu	mu	mu	mu	mu
Core/Int/Rim:	Core	Core	Core	Core	Core	Core	Core	Core	Core	Core	Core	Rim
EMP Initial Results:												
Oxide conc. (wt%)												
SiO2	47.08	47.25	46.25	46.00	46.42	47.27	46.49	47.09	46.37	47.14	46.30	46.25
TiO2	0.42	0.36	0.32	0.46	0.33	0.39	0.27	0.29	0.30	0.35	0.32	0.16
Al2O3	38.69	37.02	37.98	37.96	38.55	36.67	38.73	38.60	38.54	38.65	38.25	39.26
Cr2O3	0.00	0.07	0.02	0.01	0.04	0.05	0.05	0.03	0.03	0.03	0.03	0.05
FeO	1.05	1.17	1.06	1.02	0.91	1.25	0.95	1.08	0.90	0.95	0.90	0.76
MnO	0.00	0.02	0.00	0.02	0.05	0.00	0.05	0.04	0.00	0.03	0.05	0.03
MgO	0.59	0.97	0.67	0.64	0.56	0.97	0.58	0.72	0.63	0.63	0.56	0.51
CaO	0.00	0.00	0.01	0.06	0.01	0.00	0.01	0.00	0.03	0.02	0.00	0.01
NaO	1.29	1.08	1.43	1.60	1.32	0.88	1.62	1.46	1.53	1.31	1.54	1.31
K2O	8.30	9.57	8.47	8.26	8.15	8.83	7.72	7.89	7.91	7.62	8.22	9.47
Total	97.42	97.50	96.22	96.03	96.34	96.32	96.47	97.22	96.23	96.73	96.18	97.81
Cations:												
Si	3.02	3.05	3.01	3.00	3.01	3.08	3.01	3.02	3.01	3.03	3.01	2.98
Ti	0.02	0.02	0.02	0.02	0.02	0.02	0.01	0.01	0.01	0.02	0.02	0.01
Al	2.92	2.82	2.92	2.92	2.95	2.81	2.95	2.92	2.95	2.93	2.93	2.98
Cr	0.00	0.00	0.00	0.00	0.00	0.00	0.00	0.00	0.00	0.00	0.00	0.00
Fe	0.06	0.06	0.06	0.06	0.05	0.07	0.05	0.06	0.05	0.05	0.05	0.04
Mn	0.00	0.00	0.00	0.00	0.00	0.00	0.00	0.00	0.00	0.00	0.00	0.00
Mg	0.06	0.09	0.07	0.06	0.05	0.09	0.06	0.07	0.06	0.06	0.05	0.05
Ca	0.00	0.00	0.00	0.00	0.00	0.00	0.00	0.00	0.00	0.00	0.00	0.00
Na	0.16	0.13	0.18	0.20	0.17	0.11	0.20	0.18	0.19	0.16	0.19	0.16
K	0.68	0.79	0.70	0.69	0.67	0.73	0.64	0.65	0.65	0.63	0.68	0.78
Total (All)	6.92	6.98	6.95	6.96	6.92	6.92	6.92	6.92	6.93	6.88	6.94	7.00
Total (Majors ONLY)	6.92	6.97	6.95	6.96	6.92	6.92	6.92	6.91	6.93	6.88	6.94	6.99
Al(VI) (= (Si + Al) - 4)	1.94	1.88	1.93	1.92	1.96	1.89	1.96	1.94	1.95	1.96	1.94	1.95
Al(IV) (= Al - Al(VI))	0.98	0.95	0.99	1.00	0.99	0.92	0.99	0.98	0.99	0.97	0.99	1.02
Si (apfu)	3.02	3.05	3.01	3.00	3.01	3.08	3.01	3.02	3.01	3.03	3.01	2.98
Al (apfu)	2.92	2.82	2.92	2.92	2.95	2.81	2.95	2.92	2.95	2.93	2.93	2.98
XPa (= Na / (Na + K))	0.19	0.15	0.20	0.23	0.20	0.13	0.24	0.22	0.23	0.21	0.22	0.17
XMu (= K / (K + Na))	0.81	0.85	0.80	0.77	0.80	0.87	0.76	0.78	0.77	0.79	0.78	0.83

Note: Analyses conducted on the same mineral grain (e.g. 1 core analysis and 2 rim analyses on a specific muscovite grain) are highlighted in the same colour and enclosed in the same thick black box.

Plagioclases

Analysis Label (Specimen_mineral_grain/zone:spot number)	gb10_mu_1b	gb10_mu_1m	gb10_mu_1o	ma29_bi_5b	ma31_mu_3b	ma31_mu_4c	ma31_gt_1b	ma40_fsp_f3	ma40_fsp_f1	ma40_fsp_f2	ma40_mu_3w	ma44_qtz_1b	ma44_plag_1a	ma44_plag_2a	ma44_plag_2b	ma44_plag_2d	ma44_plag_2c	ma44_plag_2f	ma44_plag_2e	ma44_plag_2h	ma44_plag_2g
Mineral Probed:	pl	pl	pl	pl	pl	pl	pl	pl	pl	pl	pl	pl	pl	pl	pl	pl	pl	pl	pl	pl	pl
Core/Int/Rim:	Core	Core	Core	Rim	Core	Core	Rim	Core	Core	Core	Core	Core	Core	Rim	Core	Rim	Core	Rim	Core	Rim	Core
EMP Initial Results:																					
Oxide conc. (wt%)																					
SiO2	59.11	60.08	60.24	61.79	64.83	60.39	58.90	61.11	59.42	60.97	60.94	58.60	58.29	58.85	60.18	57.22	60.09	57.62	60.12	57.53	60.48
TiO2	0.06	0.01	0.00	0.02	0.03	0.00	0.00	0.01	0.02	0.01	0.05	0.03	0.00	0.01	0.01	0.00	0.01	0.01	0.01	0.02	0.00
Al2O3	27.29	26.48	26.75	25.69	19.44	26.83	25.07	25.07	26.53	25.43	25.88	25.11	26.23	25.53	24.46	26.33	24.70	26.26	24.38	26.70	24.50
Cr2O3	0.00	0.02	0.00	0.03	0.00	0.00	0.02	0.00	0.00	0.00	0.00	0.00	0.00	0.00	0.00	0.00	0.00	0.00	0.00	0.00	0.00
FeO	0.32	0.20	0.20	0.39	0.08	0.11	0.28	0.05	0.01	0.06	0.11	0.09	0.27	0.17	0.11	0.17	0.11	0.12	0.14	0.22	0.09
MnO	0.02	0.03	0.00	0.01	0.00	0.02	0.01	0.06	0.02	0.04	0.02	0.00	0.06	0.03	0.02	0.00	0.00	0.03	0.00	0.03	0.05
MgO	0.01	0.00	0.00	0.02	0.01	0.04	0.00	0.01	0.00	0.00	0.05	0.01	0.03	0.01	0.00	0.00	0.00	0.02	0.00	0.02	0.00
CaO	7.40	6.56	6.70	5.53	0.00	6.16	6.54	5.48	7.27	5.90	5.51	6.30	6.87	6.09	4.93	7.14	4.96	7.00	4.83	7.13	4.85
Na2O	7.60	8.12	8.16	8.68	0.05	7.83	8.00	8.20	7.20	8.24	8.31	7.46	7.15	7.56	7.85	7.09	7.93	7.11	8.25	7.23	8.05
K2O	0.08	0.08	0.05	0.08	14.93	0.12	0.00	0.15	0.07	0.08	0.41	0.00	0.04	0.05	0.03	0.05	0.04	0.04	0.05	0.04	0.04
Total	101.89	101.58	102.11	102.24	99.38	101.49	98.83	100.15	100.53	100.73	101.27	97.60	98.93	98.29	97.59	98.00	97.84	98.20	97.77	98.91	98.06
Cations:																					
Si	2.60	2.64	2.63	2.69	2.99	2.65	2.66	2.71	2.63	2.69	2.68	2.67	2.63	2.66	2.73	2.61	2.72	2.62	2.72	2.60	2.73
Ti	0.00	0.00	0.00	0.00	0.00	0.00	0.00	0.00	0.00	0.00	0.00	0.00	0.00	0.00	0.00	0.00	0.00	0.00	0.00	0.00	0.00
Al	1.41	1.37	1.38	1.32	1.06	1.39	1.33	1.31	1.39	1.32	1.34	1.35	1.39	1.36	1.31	1.41	1.32	1.40	1.30	1.42	1.30
Cr	0.00	0.00	0.00	0.00	0.00	0.00	0.00	0.00	0.00	0.00	0.00	0.00	0.00	0.00	0.00	0.00	0.00	0.00	0.00	0.00	0.00
Fe	0.01	0.01	0.01	0.01	0.00	0.00	0.01	0.00	0.00	0.00	0.00	0.00	0.01	0.01	0.00	0.01	0.00	0.00	0.01	0.01	0.00
Mn	0.00	0.00	0.00	0.00	0.00	0.00	0.00	0.00	0.00	0.00	0.00	0.00	0.00	0.00	0.00	0.00	0.00	0.00	0.00	0.00	0.00
Mg	0.00	0.00	0.00	0.00	0.00	0.00	0.00	0.00	0.00	0.00	0.00	0.00	0.00	0.00	0.00	0.00	0.00	0.00	0.00	0.00	0.00
Ca	0.35	0.31	0.31	0.26	0.00	0.29	0.32	0.26	0.35	0.28	0.26	0.31	0.33	0.30	0.24	0.35	0.24	0.34	0.23	0.34	0.23
Na	0.65	0.69	0.69	0.73	0.00	0.66	0.70	0.70	0.62	0.70	0.71	0.66	0.62	0.66	0.69	0.63	0.70	0.63	0.72	0.63	0.70
K	0.00	0.00	0.00	0.00	0.88	0.01	0.00	0.01	0.00	0.00	0.02	0.00	0.00	0.00	0.00	0.00	0.00	0.00	0.00	0.00	0.00
Total (All)	5.02	5.02	5.03	5.02	4.93	5.00	5.02	4.99	4.99	5.00	5.02	4.99	4.99	4.99	4.97	5.00	4.97	5.00	4.99	5.01	4.97
Total (Majors ONLY)	5.02	5.02	5.03	5.02	4.93	5.00	5.02	4.99	4.99	5.00	5.02	4.99	4.99	4.99	4.97	5.00	4.97	5.00	4.99	5.01	4.97
An (= Ca / (Ca + Na + K	0.35	0.31	0.31	0.26	0.00	0.30	0.31	0.27	0.36	0.28	0.26	0.32	0.35	0.31	0.26	0.36	0.26	0.35	0.24	0.35	0.25
Ab (= Na / (Na + Ca + K	0.65	0.69	0.69	0.74	0.01	0.69	0.69	0.72	0.64	0.71	0.71	0.68	0.65	0.69	0.74	0.64	0.74	0.65	0.75	0.65	0.75
Or (= K / (K + Ca + Na)	0.00	0.00	0.00	0.00	0.99	0.01	0.00	0.01	0.00	0.00	0.02	0.00	0.00	0.00	0.00	0.00	0.00	0.00	0.00	0.00	0.00

Note: Analyses conducted on the same mineral grain (e.g. 1 core analysis and 2 rim analyses on a specific plagioclase grain) are highlighted in the same colour and enclosed in the same thick black box.

Quartzs

Analysis Label (Specimen_mineral grain/zone:spot number)	gb8_qtz_2c	gb8_qtz_2d	gb10_qtz_2a	gb10_qtz_1a	gb10_qtz_3x	gb10_qtz_3y	gb10_st_11m	gb10_st_12a	gb10_st_12b	gb10_st_13d	gb13_qtz_1x	gb13_qtz_1y	gb13_qtz_2x	gb13_qtz_2y	gb13_qtz_3x	gb13_qtz_3y	gb13_qtz_4x	gb13_qtz_5x	gb13_mu_1h	gb13_mu_1g	gb13_mu_1f
Mineral Probed:	qtz	qtz	qtz	qtz	qtz	qtz	qtz	qtz	qtz	qtz	qtz	qtz	qtz	qtz	qtz	qtz	qtz	qtz	qtz	qtz	qtz
Core/Int/Rim:	Core	Core	Core	Core	Core	Core	Rim	Rim	Rim	Rim	Core	Core	Core	Core	Core	Core	Core	Core	Core	Core	Core
EMP Initial Results:																					
Oxide conc. (wt%)																					
SiO2	100.00	99.99	99.49	98.42	98.62	98.36	98.90	99.03	99.37	98.90	99.68	99.62	99.66	99.90	98.75	98.48	98.82	99.57	99.51	99.51	99.86
TiO2	0.00	0.00	0.00	0.01	0.00	0.00	0.00	0.01	0.00	0.00	0.01	0.00	0.01	0.00	0.00	0.00	0.00	0.00	0.00	0.00	0.02
Al2O3	0.02	0.01	0.02	0.01	0.00	0.02	0.02	0.02	0.01	0.01	0.00	0.00	0.00	0.02	0.01	0.00	0.00	0.01	0.02	0.01	0.03
Cr2O3	0.02	0.00	0.00	0.02	0.01	0.00	0.00	0.00	0.00	0.00	0.00	0.04	0.03	0.02	0.00	0.00	0.01	0.00	0.04	0.04	0.00
FeO	0.04	0.06	0.01	0.00	0.09	0.06	0.37	0.24	0.14	0.15	0.04	0.03	0.05	0.06	0.16	0.17	0.13	0.15	0.15	0.09	0.02
MnO	0.03	0.06	0.02	0.05	0.08	0.00	0.00	0.01	0.00	0.03	0.05	0.04	0.03	0.05	0.07	0.06	0.00	0.05	0.00	0.02	0.06
MgO	0.01	0.00	0.01	0.00	0.00	0.00	0.00	0.00	0.00	0.00	0.00	0.00	0.00	0.00	0.00	0.02	0.00	0.00	0.01	0.00	0.00
CaO	0.00	0.01	0.00	0.02	0.01	0.01	0.01	0.00	0.00	0.00	0.00	0.01	0.01	0.00	0.00	0.00	0.01	0.01	0.00	0.02	0.00
Na2O	0.02	0.01	0.02	0.01	0.04	0.01	0.00	0.00	0.00	0.00	0.02	0.00	0.00	0.00	0.02	0.01	0.01	0.04	0.04	0.01	0.00
K2O	0.00	0.00	0.00	0.00	0.00	0.00	0.00	0.03	0.00	0.02	0.00	0.00	0.00	0.00	0.00	0.00	0.00	0.00	0.02	0.01	0.01
ZnO	0.00	0.00	0.00	0.00	0.00	0.00	0.05	0.05	0.00	0.06	0.00	0.00	0.00	0.00	0.00	0.00	0.00	0.00	0.00	0.00	0.00
NiO	0.00	0.00	0.00	0.00	0.00	0.00	0.00	0.00	0.00	0.00	0.00	0.00	0.00	0.00	0.00	0.00	0.00	0.00	0.00	0.00	0.00
Total	100.13	100.14	99.57	98.54	98.85	98.47	99.35	99.38	99.53	99.16	99.80	99.74	99.78	100.06	99.01	98.73	98.99	99.83	99.78	99.70	100.00
Cations:																					
Si	1.00	1.00	1.00	1.00	1.00	1.00	1.00	1.00	1.00	1.00	1.00	1.00	1.00	1.00	1.00	1.00	1.00	1.00	1.00	1.00	1.00
Ti	0.00	0.00	0.00	0.00	0.00	0.00	0.00	0.00	0.00	0.00	0.00	0.00	0.00	0.00	0.00	0.00	0.00	0.00	0.00	0.00	0.00
Al	0.00	0.00	0.00	0.00	0.00	0.00	0.00	0.00	0.00	0.00	0.00	0.00	0.00	0.00	0.00	0.00	0.00	0.00	0.00	0.00	0.00
Cr	0.00	0.00	0.00	0.00	0.00	0.00	0.00	0.00	0.00	0.00	0.00	0.00	0.00	0.00	0.00	0.00	0.00	0.00	0.00	0.00	0.00
Fe	0.00	0.00	0.00	0.00	0.00	0.00	0.00	0.00	0.00	0.00	0.00	0.00	0.00	0.00	0.00	0.00	0.00	0.00	0.00	0.00	0.00
Mn	0.00	0.00	0.00	0.00	0.00	0.00	0.00	0.00	0.00	0.00	0.00	0.00	0.00	0.00	0.00	0.00	0.00	0.00	0.00	0.00	0.00
Mg	0.00	0.00	0.00	0.00	0.00	0.00	0.00	0.00	0.00	0.00	0.00	0.00	0.00	0.00	0.00	0.00	0.00	0.00	0.00	0.00	0.00
Ca	0.00	0.00	0.00	0.00	0.00	0.00	0.00	0.00	0.00	0.00	0.00	0.00	0.00	0.00	0.00	0.00	0.00	0.00	0.00	0.00	0.00
Na	0.00	0.00	0.00	0.00	0.00	0.00	0.00	0.00	0.00	0.00	0.00	0.00	0.00	0.00	0.00	0.00	0.00	0.00	0.00	0.00	0.00
K	0.00	0.00	0.00	0.00	0.00	0.00	0.00	0.00	0.00	0.00	0.00	0.00	0.00	0.00	0.00	0.00	0.00	0.00	0.00	0.00	0.00
Zn	0.00	0.00	0.00	0.00	0.00	0.00	0.00	0.00	0.00	0.00	0.00	0.00	0.00	0.00	0.00	0.00	0.00	0.00	0.00	0.00	0.00
Ni	0.00	0.00	0.00	0.00	0.00	0.00	0.00	0.00	0.00	0.00	0.00	0.00	0.00	0.00	0.00	0.00	0.00	0.00	0.00	0.00	0.00
Total (All)	1.00	1.00	1.00	1.00	1.00	1.00	1.00	1.00	1.00	1.00	1.00	1.00	1.00	1.00	1.00	1.00	1.00	1.00	1.00	1.00	1.00
Total (Majors ONLY)	1.00	1.00	1.00	1.00	1.00	1.00	1.00	1.00	1.00	1.00	1.00	1.00	1.00	1.00	1.00	1.00	1.00	1.00	1.00	1.00	1.00

Note: Analyses conducted on the same mineral grain (e.g. 1 core analysis and 2 rim analyses on a specific quartz grain) are highlighted in the same colour and enclosed in the same thick black box.

Quartz cont.

Analysis Label (Specimen_mineral grain/zone:spot number)	gb13_mu_1a	gb13_mu_2a	gb13_mu_2b	gb13_mu_2c	gb13_mu_2d	gb13_mu_2e	gb13_gt_4c	gb13_gt_10h	ma29_qtz_1a	ma29_qtz_1b	ma31_qtz_q1	ma31_qtz_q2	ma31_fsp_1zv	ma38_chl_2b	ma38_chl_2a	ma40_qtz_q1	ma40_qtz_q2
Mineral Probed:	qtz	qtz	qtz	qtz	qtz	qtz	qtz	qtz	qtz	qtz	qtz	qtz	qtz	qtz	qtz	qtz	qtz
Core/Int/Rim:	Core	Core	Core	Core	Core	Core	Rim	Core	Core	Core	Core	Core	Core	Rim	Core	Core	Core
EMP Initial Results:																	
Oxide conc. (wt%)																	
SiO2	99.77	99.62	99.25	99.82	99.10	99.81	98.53	98.93	99.58	99.55	98.85	98.71	100.37	100.21	99.92	99.14	99.56
TiO2	0.00	0.01	0.00	0.01	0.00	0.00	0.02	0.03	0.00	0.00	0.04	0.01	0.03	0.02	0.00	0.02	0.00
Al2O3	0.01	0.02	0.04	0.00	0.02	0.02	0.05	0.00	0.00	0.01	0.01	0.01	0.00	0.00	0.00	0.03	0.03
Cr2O3	0.00	0.00	0.00	0.00	0.01	0.00	0.03	0.03	0.01	0.01	0.00	0.00	0.00	0.00	0.01	0.00	0.00
FeO	0.10	0.02	0.08	0.08	0.12	0.10	0.34	0.26	0.01	0.02	0.00	0.00	0.01	0.15	0.01	0.04	0.06
MnO	0.02	0.03	0.01	0.06	0.05	0.04	0.00	0.09	0.02	0.03	0.00	0.02	0.04	0.02	0.05	0.05	0.00
MgO	0.01	0.00	0.00	0.01	0.00	0.00	0.02	0.00	0.01	0.00	0.02	0.00	0.00	0.01	0.00	0.00	0.00
CaO	0.01	0.00	0.01	0.00	0.00	0.01	0.01	0.02	0.01	0.00	0.00	0.01	0.00	0.00	0.03	0.00	0.01
Na2O	0.00	0.00	0.00	0.01	0.00	0.00	0.02	0.01	0.00	0.00	0.02	0.01	0.02	0.00	0.05	0.01	0.02
K2O	0.00	0.01	0.02	0.02	0.02	0.02	0.00	0.00	0.00	0.00	0.00	0.00	0.01	0.00	0.01	0.00	0.00
ZnO	0.00	0.00	0.00	0.00	0.00	0.00	0.00	0.00	0.00	0.00	0.00	0.00	0.00	0.00	0.00	0.00	0.00
NiO	0.00	0.00	0.00	0.00	0.00	0.00	0.00	0.00	0.00	0.00	0.00	0.00	0.00	0.00	0.00	0.00	0.00
Total	99.94	99.72	99.40	100.00	99.31	99.99	99.02	99.37	99.64	99.62	98.94	98.76	100.49	100.40	100.07	99.28	99.68
Cations:																	
Si	1.00	1.00	1.00	1.00	1.00	1.00	1.00	1.00	1.00	1.00	1.00	1.00	1.00	1.00	1.00	1.00	1.00
Ti	0.00	0.00	0.00	0.00	0.00	0.00	0.00	0.00	0.00	0.00	0.00	0.00	0.00	0.00	0.00	0.00	0.00
Al	0.00	0.00	0.00	0.00	0.00	0.00	0.00	0.00	0.00	0.00	0.00	0.00	0.00	0.00	0.00	0.00	0.00
Cr	0.00	0.00	0.00	0.00	0.00	0.00	0.00	0.00	0.00	0.00	0.00	0.00	0.00	0.00	0.00	0.00	0.00
Fe	0.00	0.00	0.00	0.00	0.00	0.00	0.00	0.00	0.00	0.00	0.00	0.00	0.00	0.00	0.00	0.00	0.00
Mn	0.00	0.00	0.00	0.00	0.00	0.00	0.00	0.00	0.00	0.00	0.00	0.00	0.00	0.00	0.00	0.00	0.00
Mg	0.00	0.00	0.00	0.00	0.00	0.00	0.00	0.00	0.00	0.00	0.00	0.00	0.00	0.00	0.00	0.00	0.00
Ca	0.00	0.00	0.00	0.00	0.00	0.00	0.00	0.00	0.00	0.00	0.00	0.00	0.00	0.00	0.00	0.00	0.00
Na	0.00	0.00	0.00	0.00	0.00	0.00	0.00	0.00	0.00	0.00	0.00	0.00	0.00	0.00	0.00	0.00	0.00
K	0.00	0.00	0.00	0.00	0.00	0.00	0.00	0.00	0.00	0.00	0.00	0.00	0.00	0.00	0.00	0.00	0.00
Zn	0.00	0.00	0.00	0.00	0.00	0.00	0.00	0.00	0.00	0.00	0.00	0.00	0.00	0.00	0.00	0.00	0.00
Ni	0.00	0.00	0.00	0.00	0.00	0.00	0.00	0.00	0.00	0.00	0.00	0.00	0.00	0.00	0.00	0.00	0.00
Total (All)	1.00	1.00	1.00	1.00	1.00	1.00	1.00	1.00	1.00	1.00	1.00	1.00	1.00	1.00	1.00	1.00	1.00
Total (Majors ONLY)	1.00	1.00	1.00	1.00	1.00	1.00	1.00	1.00	1.00	1.00	1.00	1.00	1.00	1.00	1.00	1.00	1.00

Note: Analyses conducted on the same mineral grain (e.g. 1 core analysis and 2 rim analyses on a specific quartz grain) are highlighted in the same colour and enclosed in the same thick black box.

Rutiles

Analysis Label (Specimen_mineral_grain/zone:spot number)	ma31_ru_r1	ma31_ru_r2	ma31_ru_r4	ma31_ru_r5	ma38_ru_ru3	ma38_ru_ru2	ma38_ru_ru4	ma38_ru_ru6	ma38_ru_ru7
Mineral Probed:	ru	ru	ru	ru	ru	ru	ru	ru	ru
Core/Int/Rim:	Core	Core	Core	Core	Rim	Core	Core	Core	Core
EMP Initial Results:									
Oxide conc. (wt%)									
TiO2	95.76	95.13	96.12	95.83	94.52	95.35	94.65	95.99	94.95
Al2O3	0.02	0.01	0.01	0.00	0.03	0.01	0.09	0.00	0.00
Cr2O3	0.08	0.04	0.03	0.17	0.11	0.08	0.15	0.16	0.17
FeO	0.73	0.71	0.30	0.47	0.61	0.47	0.63	0.23	0.45
MnO	0.07	0.08	0.06	0.04	0.03	0.04	0.00	0.08	0.01
MgO	0.00	0.00	0.01	0.00	0.02	0.02	0.02	0.01	0.01
NiO	0.00	0.00	0.00	0.03	0.01	0.02	0.02	0.00	0.02
Total	96.66	95.98	96.54	96.54	95.34	95.98	95.57	96.47	95.61
Cations:									
Ti	0.99	0.99	1.00	1.00	0.99	1.00	0.99	1.00	1.00
Al	0.00	0.00	0.00	0.00	0.00	0.00	0.00	0.00	0.00
Cr	0.00	0.00	0.00	0.00	0.00	0.00	0.00	0.00	0.00
Fe	0.01	0.01	0.00	0.01	0.01	0.01	0.01	0.00	0.01
Mn	0.00	0.00	0.00	0.00	0.00	0.00	0.00	0.00	0.00
Mg	0.00	0.00	0.00	0.00	0.00	0.00	0.00	0.00	0.00
Ni	0.00	0.00	0.00	0.00	0.00	0.00	0.00	0.00	0.00
Total (All)	1.00	1.00	1.00	1.00	1.00	1.00	1.00	1.00	1.00
Total (Majors ONLY)	1.00	1.00	1.00	1.00	1.00	1.00	1.00	1.00	1.00

Note: Analyses conducted on the same mineral grain (e.g. 1 core analysis and 2 rim analyses on a specific rutile grain) are highlighted in the same colour and enclosed in the same thick black box.

Sphenes

Analysis Label (Specimen_mineral_grain/zone:spot number)	ma44_amph_5c	ma44_amph_5d
Mineral Probed:	sph	sph
Core/Int/Rim:	Core	Core
EMP Initial Results:		
Oxide conc. (wt%)		
SiO2	29.55	29.63
TiO2	38.58	37.63
Al2O3	1.03	1.30
Cr2O3	0.02	0.00
FeO	0.42	0.38
MnO	0.07	0.08
MgO	0.00	0.03
CaO	28.30	28.02
Na2O	0.05	0.00
K2O	0.01	0.01
Total	98.03	97.07
Cations:		
Si	0.99	1.00
Ti	0.97	0.95
Al	0.04	0.05
Cr	0.00	0.00
Fe	0.01	0.01
Mn	0.00	0.00
Mg	0.00	0.00
Ca	1.01	1.01
Na	0.00	0.00
K	0.00	0.00
Total (All)	3.03	3.03
Total (Majors ONLY)	3.03	3.03

Note: Analyses conducted on the same mineral grain (e.g. 1 core analysis and 2 rim analyses on a specific sphene grain) are highlighted in the same colour and enclosed in the same thick black box.

Staurolites

Analysis Label (Specimen_mineral_grain/zone:spot number)	gb8_st_1a	gb8_st_1e	gb8_st_1b	gb8_st_1c	gb8_st_1g	gb8_st_1h	gb8_st_1d	gb8_st_1f	gb8_st_1i	gb8_st_1j	gb8_st_1l	gb8_st_1k	gb8_st_1o	gb8_st_1t	gb8_st_1y	gb8_st_1m	gb8_st_1r	gb8_st_1u	gb8_st_1x	gb8_st_1z	gb8_st_1p
Mineral Probed:	st	st	st	st	st	st	st	st	st	st	st	st	st	st	st	st	st	st	st	st	st
Core/Int/Rim:	Rim	Rim	Int	Core	Core	Core	Int	Rim	Rim	Rim	Int	Int	Int	Core	Core	Core	Int	Int	Rim	Rim	Rim
EMP Initial Results:																					
Oxide conc. (wt%)																					
SiO2	27.97	27.93	28.03	28.22	28.41	28.13	27.63	28.37	28.30	28.15	28.20	27.91	28.03	27.86	28.36	28.17	28.15	28.05	28.14	28.14	27.92
TiO2	0.51	0.44	0.56	0.51	0.48	0.47	0.45	0.55	0.52	0.44	0.45	0.46	0.56	0.51	0.48	0.45	0.56	0.45	0.56	0.53	0.45
Al2O3	54.19	54.25	54.52	54.46	54.37	53.93	54.11	54.31	54.02	53.36	53.34	53.74	53.74	53.88	53.27	53.34	53.68	53.40	53.57	53.72	53.66
FeO	14.42	14.04	14.05	14.22	14.16	14.32	14.43	14.38	14.24	14.24	14.21	14.27	14.63	14.08	14.29	14.18	14.33	14.37	14.44	14.44	14.51
MnO	0.10	0.15	0.14	0.10	0.13	0.20	0.14	0.13	0.16	0.08	0.12	0.13	0.14	0.07	0.12	0.08	0.09	0.07	0.03	0.08	0.10
MgO	1.39	1.24	1.29	1.32	1.31	1.47	1.36	1.27	1.42	2.02	2.10	2.06	2.02	2.12	2.03	2.06	2.08	2.00	2.04	2.07	2.03
CaO	0.01	0.02	0.00	0.00	0.01	0.00	0.01	0.03	0.03	0.02	0.00	0.02	0.01	0.03	0.02	0.04	0.03	0.01	0.01	0.02	0.02
ZnO	0.87	0.93	1.11	1.05	0.94	1.08	1.02	0.98	0.95	0.98	0.94	0.99	0.96	0.89	0.93	0.83	0.87	0.92	0.91	0.81	0.90
Total	99.46	99.00	99.70	99.88	99.82	99.61	99.15	100.01	99.64	99.30	99.35	99.58	100.09	99.43	99.50	99.14	99.78	99.27	99.70	99.81	99.59
Cations:																					
Si	7.69	7.70	7.68	7.72	7.77	7.73	7.63	7.75	7.76	7.75	7.76	7.67	7.67	7.65	7.79	7.76	7.71	7.73	7.72	7.71	7.68
Ti	0.11	0.09	0.12	0.11	0.10	0.10	0.09	0.11	0.11	0.09	0.09	0.09	0.11	0.11	0.10	0.09	0.12	0.09	0.12	0.11	0.09
Al	17.55	17.63	17.61	17.55	17.52	17.46	17.61	17.49	17.46	17.32	17.30	17.41	17.34	17.45	17.25	17.32	17.34	17.34	17.32	17.35	17.39
Fe	3.31	3.24	3.22	3.25	3.24	3.29	3.33	3.29	3.26	3.28	3.27	3.28	3.35	3.24	3.28	3.27	3.28	3.31	3.31	3.31	3.34
Mn	0.02	0.03	0.03	0.02	0.03	0.05	0.03	0.03	0.04	0.02	0.03	0.03	0.03	0.02	0.03	0.02	0.02	0.02	0.01	0.02	0.02
Mg	0.57	0.51	0.52	0.54	0.53	0.60	0.56	0.52	0.58	0.83	0.86	0.84	0.82	0.87	0.83	0.85	0.85	0.82	0.83	0.85	0.83
Ca	0.00	0.01	0.00	0.00	0.00	0.00	0.00	0.01	0.01	0.01	0.00	0.01	0.00	0.01	0.01	0.01	0.01	0.00	0.00	0.01	0.01
Zn	0.18	0.19	0.22	0.21	0.19	0.22	0.21	0.20	0.19	0.20	0.19	0.20	0.19	0.18	0.19	0.17	0.18	0.19	0.18	0.16	0.18
Total (All)	29.43	29.39	29.40	29.40	29.38	29.45	29.47	29.39	29.41	29.50	29.50	29.53	29.54	29.52	29.48	29.49	29.50	29.51	29.50	29.51	29.54
Total (Majors ONLY)	29.26	29.21	29.18	29.19	29.19	29.23	29.26	29.19	29.21	29.30	29.31	29.33	29.34	29.34	29.29	29.32	29.33	29.32	29.32	29.34	29.35
XMg (= Mg / (Mg + Fe)	0.15	0.14	0.14	0.14	0.14	0.15	0.14	0.14	0.15	0.20	0.21	0.20	0.20	0.21	0.20	0.21	0.21	0.20	0.20	0.20	0.20

Note: Analyses conducted on the same mineral grain (e.g. 1 core analysis and 2 rim analyses on a specific staurolite grain) are highlighted in the same colour and enclosed in the same thick black box.

Staurolites cont.

Analysis Label (Specimen_mineral_grain/zone:spot number)	gb8_st_2a	gb8_st_2b	gb8_st_2e	gb8_st_2f	gb8_st_3a	gb8_st_3c	gb8_st_3b	gb8_st_3f	gb8_st_3h	gb8_st_4a	gb8_st_4b	gb8_st_4c	gb8_st_4d	gb8_st_4f	gb8_st_4e	gb8_st_4g	gb8_st_4i	gb8_st_4k	gb8_st_4l	gb8_st_4m	gb8_st_5a
Mineral Probed:	st	st	st	st	st	st	st	st	st	st	st	st	st	st	st	st	st	st	st	st	st
Core/Int/Rim:	Rim	Core	Core	Rim	Rim	Core	Rim	Rim	Core	Rim	Int	Core	Rim	Rim	Core	Rim	Core	Rim	Core	Rim	Rim
EMP Initial Results:																					
Oxide conc. (wt%)																					
SiO2	28.29	28.26	28.47	28.43	28.37	28.21	28.48	28.34	28.37	28.32	28.56	28.54	28.32	28.38	28.38	28.26	28.39	28.13	28.54	28.34	28.31
TiO2	0.54	0.49	0.53	0.51	0.48	0.52	0.46	0.49	0.46	0.44	0.47	0.50	0.49	0.48	0.51	0.48	0.48	0.52	0.44	0.48	0.55
Al2O3	54.81	54.37	54.97	54.72	55.05	54.90	55.07	54.89	53.78	55.57	55.23	55.17	55.14	55.55	55.02	54.96	55.08	55.16	54.96	54.76	54.96
FeO	14.03	13.83	13.61	13.45	12.75	12.80	12.92	12.70	13.13	12.70	12.96	12.65	12.69	12.57	12.64	12.66	12.68	12.58	12.46	12.65	12.89
MnO	0.09	0.12	0.11	0.08	0.09	0.10	0.05	0.05	0.11	0.05	0.07	0.09	0.02	0.13	0.07	0.10	0.08	0.10	0.09	0.04	0.09
MgO	1.32	1.35	1.32	1.29	1.28	1.23	1.18	1.17	1.48	1.20	1.22	1.26	1.16	1.16	1.17	1.11	1.21	1.17	1.16	1.12	1.12
CaO	0.02	0.02	0.02	0.02	0.02	0.00	0.00	0.00	0.02	0.00	0.02	0.00	0.00	0.00	0.00	0.04	0.00	0.00	0.01	0.00	0.00
ZnO	0.94	0.99	1.06	1.18	1.58	1.58	1.38	1.67	1.65	1.73	1.62	1.68	1.63	1.75	1.67	1.69	1.54	1.86	1.94	1.89	1.66
Total	100.04	99.44	100.09	99.69	99.61	99.34	99.54	99.31	99.00	100.01	100.14	99.89	99.45	100.02	99.45	99.30	99.46	99.52	99.59	99.28	99.59
Cations:																					
Si	7.71	7.75	7.74	7.76	7.74	7.72	7.77	7.76	7.81	7.70	7.76	7.76	7.73	7.71	7.75	7.74	7.75	7.69	7.79	7.76	7.73
Ti	0.11	0.10	0.11	0.10	0.10	0.11	0.09	0.10	0.09	0.09	0.10	0.10	0.10	0.10	0.10	0.10	0.10	0.11	0.09	0.10	0.11
Al	17.61	17.57	17.62	17.61	17.70	17.71	17.71	17.70	17.46	17.80	17.68	17.68	17.75	17.79	17.72	17.74	17.72	17.77	17.68	17.68	17.70
Fe	3.20	3.17	3.10	3.07	2.91	2.93	2.95	2.91	3.02	2.89	2.94	2.88	2.90	2.86	2.89	2.90	2.90	2.88	2.84	2.90	2.94
Mn	0.02	0.03	0.02	0.02	0.02	0.02	0.01	0.01	0.03	0.01	0.02	0.02	0.00	0.03	0.02	0.02	0.02	0.02	0.02	0.01	0.02
Mg	0.54	0.55	0.54	0.53	0.52	0.50	0.48	0.48	0.61	0.49	0.49	0.51	0.47	0.47	0.47	0.45	0.49	0.48	0.47	0.46	0.46
Ca	0.01	0.01	0.01	0.01	0.00	0.00	0.00	0.00	0.01	0.00	0.00	0.00	0.00	0.00	0.00	0.01	0.00	0.00	0.00	0.00	0.00
Zn	0.19	0.20	0.21	0.24	0.32	0.32	0.28	0.34	0.34	0.35	0.32	0.34	0.33	0.35	0.34	0.34	0.31	0.38	0.39	0.38	0.33
Total (All)	29.38	29.37	29.34	29.33	29.31	29.32	29.28	29.29	29.36	29.32	29.31	29.29	29.29	29.30	29.29	29.30	29.29	29.32	29.28	29.29	29.30
Total (Majors ONLY)	29.19	29.17	29.13	29.09	28.99	29.00	29.01	28.96	29.03	28.97	28.99	28.96	28.96	28.95	28.95	28.96	28.98	28.94	28.89	28.91	28.97
XMg (= Mg / (Mg + Fe)	0.14	0.15	0.15	0.15	0.15	0.15	0.14	0.14	0.17	0.14	0.14	0.15	0.14	0.14	0.14	0.14	0.15	0.14	0.14	0.14	0.13

Note: Analyses conducted on the same mineral grain (e.g. 1 core analysis and 2 rim analyses on a specific staurolite grain) are highlighted in the same colour and enclosed in the same thick black box.

Staurolites cont.

Analysis Label (Specimen_mineral_grain/zone:spot number)	gb8_st_5c	gb8_st_5b	gb8_st_5d	gb8_st_5e	gb8_st_6a	gb8_st_6c	gb8_st_6b	gb8_st_6d	gb8_st_6e	gb8_st_6f	gb8_st_6g	gb8_st_6h	gb8_st_6i	gb8_st_7a	gb8_st_7b	gb8_st_7c	gb8_st_7d	gb8_st_7f	gb8_st_7j	gb8_st_8d	gb8_st_8b
Mineral Probed:	st	st	st	st	st	st	st	st	st	st	st	st	st	st	st	st	st	st	st	st	st
Core/Int/Rim:	Rim	Core	Core	Rim	Rim	Int	Core	Rim	Core	Core	Rim	Core	Rim	Rim	Core	Core	Rim	Int	Int	Rim	Int
EMP Initial Results:																					
Oxide conc. (wt%)																					
SiO2	28.24	28.27	28.59	28.33	28.36	28.43	28.01	28.54	28.15	28.44	28.35	28.09	28.48	28.16	28.21	28.04	28.37	28.33	28.28	28.50	28.30
TiO2	0.42	0.44	0.45	0.42	0.51	0.39	0.44	0.44	0.38	0.49	0.52	0.52	0.45	0.45	0.45	0.50	0.47	0.48	0.51	0.49	0.43
Al2O3	54.90	55.00	55.17	54.93	54.77	54.65	54.52	54.88	54.78	54.82	55.02	54.80	54.87	54.94	55.21	55.03	55.14	55.62	54.98	55.31	55.23
FeO	12.88	12.90	12.82	13.20	12.72	13.04	13.26	12.69	12.85	13.00	12.91	12.91	13.05	12.79	12.79	12.96	12.95	12.63	12.84	12.72	12.65
MnO	0.09	0.07	0.00	0.05	0.06	0.12	0.05	0.09	0.06	0.05	0.10	0.08	0.06	0.03	0.02	0.08	0.05	0.07	0.08	0.08	0.07
MgO	1.21	1.25	1.25	1.25	1.30	1.21	1.35	1.23	1.26	1.26	1.19	1.25	1.21	1.16	1.28	1.28	1.25	1.11	1.20	1.20	1.18
CaO	0.01	0.00	0.01	0.01	0.02	0.02	0.00	0.01	0.00	0.00	0.01	0.00	0.00	0.02	0.01	0.00	0.02	0.01	0.02	0.00	0.01
ZnO	1.55	1.31	1.41	1.36	1.75	1.89	1.67	1.73	1.67	1.74	1.55	1.67	1.63	1.67	1.71	1.76	1.62	1.59	1.65	1.40	1.61
Total	99.30	99.24	99.71	99.55	99.48	99.75	99.31	99.60	99.15	99.80	99.65	99.32	99.77	99.22	99.69	99.65	99.88	99.85	99.57	99.69	99.48
Cations:																					
Si	7.73	7.74	7.78	7.74	7.75	7.77	7.69	7.79	7.72	7.76	7.74	7.70	7.77	7.72	7.70	7.67	7.73	7.70	7.73	7.76	7.73
Ti	0.09	0.09	0.09	0.09	0.11	0.08	0.09	0.09	0.08	0.10	0.11	0.11	0.09	0.09	0.09	0.10	0.10	0.10	0.11	0.10	0.09
Al	17.72	17.74	17.70	17.69	17.65	17.61	17.65	17.65	17.72	17.63	17.70	17.71	17.64	17.75	17.75	17.74	17.70	17.82	17.70	17.74	17.77
Fe	2.95	2.95	2.92	3.02	2.91	2.98	3.05	2.90	2.95	2.97	2.95	2.96	2.98	2.93	2.92	2.96	2.95	2.87	2.93	2.89	2.89
Mn	0.02	0.02	0.00	0.01	0.01	0.03	0.01	0.02	0.01	0.01	0.02	0.02	0.01	0.01	0.01	0.02	0.01	0.02	0.02	0.02	0.02
Mg	0.49	0.51	0.51	0.51	0.53	0.49	0.55	0.50	0.52	0.51	0.49	0.51	0.49	0.47	0.52	0.52	0.51	0.45	0.49	0.49	0.48
Ca	0.00	0.00	0.00	0.00	0.00	0.01	0.00	0.00	0.00	0.00	0.00	0.00	0.00	0.00	0.00	0.00	0.01	0.00	0.01	0.00	0.00
Zn	0.31	0.26	0.28	0.27	0.35	0.38	0.34	0.35	0.34	0.35	0.31	0.34	0.33	0.34	0.34	0.36	0.33	0.32	0.33	0.28	0.32
Total (All)	29.32	29.31	29.28	29.33	29.32	29.35	29.39	29.30	29.34	29.33	29.31	29.34	29.32	29.31	29.33	29.36	29.33	29.29	29.32	29.28	29.30
Total (Majors ONLY)	29.01	29.04	29.00	29.05	28.96	28.97	29.05	28.95	29.00	28.98	29.00	29.00	28.99	28.98	28.99	29.01	29.00	28.97	28.98	28.99	28.98
XMg (= Mg / (Mg + Fe)	0.14	0.15	0.15	0.14	0.15	0.14	0.15	0.15	0.15	0.15	0.14	0.15	0.14	0.14	0.15	0.15	0.15	0.14	0.14	0.14	0.14

Note: Analyses conducted on the same mineral grain (e.g. 1 core analysis and 2 rim analyses on a specific staurolite grain) are highlighted in the same colour and enclosed in the same thick black box.

Staurolites cont.

Analysis Label (Specimen_mineral_grain/zone:spot number)	gb8_st_8c	gb8_st_8h	gb8_st_8i	gb8_st_8g	gb8_st_8j	gb8_st_9b	gb8_st_9e	gb8_st_9g	gb8_st_9d	gb8_st_9f	gb8_st_9m	gb8_st_9i	gb8_st_9j	gb8_st_9l	gb8_st_9h	gb8_st_9p	gb8_st_9r	gb8_st_9q	gb8_st_9t	gb8_st_9s	gb8_st_9x
Mineral Probed:	st	st	st	st	st	st	st	st	st	st	st	st	st	st	st	st	st	st	st	st	st
Core/Int/Rim:	Core	Rim	Rim	Core	Rim	Rim	Rim	Rim	Int	Core	Core	Core	Rim	Rim	Rim	Rim	Core	Rim	Rim	Core	Rim
EMP Initial Results:																					
Oxide conc. (wt%)																					
SiO2	28.14	28.19	28.16	28.46	28.41	28.17	28.18	28.34	28.40	28.08	28.52	28.08	28.19	28.38	28.26	28.16	28.23	28.22	28.44	28.39	28.71
TiO2	0.46	0.42	0.49	0.45	0.49	0.48	0.52	0.45	0.38	0.47	0.50	0.43	0.57	0.44	0.47	0.43	0.51	0.50	0.51	0.52	0.50
Al2O3	55.03	55.33	55.05	54.92	54.77	54.96	55.20	55.34	55.00	55.00	55.13	54.92	55.11	55.48	55.40	55.20	55.20	55.25	55.45	55.05	54.53
FeO	13.04	12.65	12.99	12.98	12.59	12.43	13.17	13.05	13.01	13.17	13.13	13.62	12.91	13.08	12.73	12.53	12.70	12.79	12.73	12.93	12.47
MnO	0.11	0.05	0.09	0.12	0.08	0.06	0.11	0.02	0.07	0.09	0.07	0.10	0.03	0.03	0.07	0.07	0.04	0.16	0.09	0.07	0.05
MgO	1.21	1.18	1.22	1.25	1.21	1.27	1.23	1.18	1.39	1.39	1.35	1.45	1.14	1.22	1.22	1.18	1.21	1.19	1.25	1.26	1.16
CaO	0.00	0.02	0.04	0.01	0.00	0.01	0.01	0.01	0.02	0.00	0.00	0.01	0.00	0.01	0.06	0.01	0.00	0.02	0.02	0.01	0.00
ZnO	1.57	1.88	1.50	1.66	1.75	1.64	1.64	1.30	1.51	1.37	1.26	1.17	1.13	1.33	1.68	1.70	1.73	1.74	1.26	1.23	1.73
Total	99.57	99.72	99.54	99.86	99.30	99.02	100.05	99.70	99.78	99.58	99.96	99.78	99.08	99.97	99.89	99.29	99.62	99.87	99.74	99.46	99.15
Cations:																					
Si	7.69	7.69	7.70	7.76	7.78	7.72	7.68	7.72	7.74	7.68	7.75	7.67	7.72	7.71	7.69	7.70	7.70	7.69	7.73	7.75	7.86
Ti	0.10	0.09	0.10	0.09	0.10	0.10	0.11	0.09	0.08	0.10	0.10	0.09	0.12	0.09	0.10	0.09	0.11	0.10	0.10	0.11	0.10
Al	17.73	17.79	17.74	17.64	17.67	17.76	17.72	17.77	17.67	17.72	17.66	17.68	17.78	17.77	17.77	17.80	17.76	17.75	17.77	17.71	17.59
Fe	2.98	2.89	2.97	2.96	2.88	2.85	3.00	2.97	2.97	3.01	2.98	3.11	2.96	2.97	2.90	2.87	2.90	2.92	2.89	2.95	2.85
Mn	0.03	0.01	0.02	0.03	0.02	0.01	0.02	0.00	0.02	0.02	0.02	0.02	0.01	0.01	0.02	0.02	0.01	0.04	0.02	0.02	0.01
Mg	0.49	0.48	0.50	0.51	0.49	0.52	0.50	0.48	0.57	0.56	0.55	0.59	0.46	0.50	0.49	0.48	0.49	0.48	0.51	0.51	0.47
Ca	0.00	0.01	0.01	0.00	0.00	0.00	0.00	0.00	0.01	0.00	0.00	0.00	0.00	0.00	0.02	0.00	0.00	0.00	0.00	0.00	0.00
Zn	0.32	0.38	0.30	0.33	0.35	0.33	0.33	0.26	0.30	0.28	0.25	0.24	0.23	0.27	0.34	0.34	0.35	0.35	0.25	0.25	0.35
Total (All)	29.34	29.33	29.34	29.33	29.29	29.30	29.36	29.30	29.35	29.37	29.32	29.40	29.27	29.31	29.32	29.31	29.31	29.33	29.28	29.29	29.24
Total (Majors ONLY)	29.03	28.95	29.03	28.99	28.94	28.97	29.03	29.04	29.04	29.09	29.06	29.17	29.05	29.05	28.99	28.96	28.96	28.98	29.03	29.04	28.89
XMg (= Mg / (Mg + Fe)	0.14	0.14	0.14	0.15	0.15	0.15	0.14	0.14	0.16	0.16	0.15	0.16	0.14	0.14	0.15	0.14	0.15	0.14	0.15	0.15	0.14

Note: Analyses conducted on the same mineral grain (e.g. 1 core analysis and 2 rim analyses on a specific staurolite grain) are highlighted in the same colour and enclosed in the same thick black box.

Staurolites cont.

Analysis Label (Specimen_mineral_grain/zone:spot number)	gb8_st_10a	gb8_st_10c	gb8_st_10f	gb8_st_11a	gb8_st_11e	gb8_st_11d	gb8_st_12a	gb8_st_13a	gb8_st_13d	gb8_st_13b	gb8_st_13c	gb8_st_13e	gb8_st_13f	gb10_st_2a	gb10_st_2b	gb10_st_2c	gb10_st_2d	gb10_st_2e	gb10_st_2h	gb10_st_2g	gb10_st_2f
Mineral Probed:	st	st	st	st	st	st	st	st	st	st	st	st	st	st	st	st	st	st	st	st	st
Core/Int/Rim:	Rim	Core	Core	Core	Rim	Core	Core	Rim	Rim	Core	Core	Rim	Rim	Rim	Core	Rim	Rim	Int	Core	Int	Rim
EMP Initial Results:																					
Oxide conc. (wt%)																					
SiO2	28.45	28.35	28.45	28.50	28.68	28.39	28.57	28.47	28.31	28.30	28.56	29.01	28.47	28.13	28.06	27.90	27.93	27.97	27.88	27.73	28.23
TiO2	0.50	0.45	0.45	0.38	0.46	0.44	0.46	0.42	0.42	0.34	0.41	0.36	0.41	0.51	0.50	0.49	0.41	0.42	0.35	0.48	0.48
Al2O3	54.96	55.87	55.37	55.47	55.28	55.45	55.24	55.14	55.14	55.32	55.00	54.47	55.06	54.09	53.69	53.70	54.18	53.72	53.60	53.67	53.74
FeO	12.83	12.82	12.69	12.63	12.20	12.60	12.25	12.64	12.36	12.47	12.67	11.92	12.23	14.08	14.51	14.83	14.66	14.84	14.73	14.69	14.85
MnO	0.10	0.07	0.06	0.10	0.06	0.06	0.10	0.08	0.07	0.12	0.09	0.07	0.12	0.07	0.06	0.09	0.14	0.12	0.09	0.15	0.15
MgO	1.20	1.15	1.29	1.21	1.21	1.29	1.27	1.43	1.30	1.45	1.48	1.35	1.28	1.93	2.11	2.12	2.13	2.08	2.07	2.06	2.04
CaO	0.01	0.00	0.00	0.00	0.01	0.01	0.01	0.01	0.01	0.00	0.00	0.01	0.01	0.00	0.01	0.00	0.02	0.02	0.00	0.00	0.02
ZnO	1.37	1.44	1.48	1.74	1.92	1.79	1.78	1.77	2.02	1.70	1.71	1.96	1.98	0.52	0.42	0.46	0.53	0.43	0.56	0.50	0.49
Total	99.41	100.15	99.79	100.03	99.82	100.03	99.68	99.96	99.63	99.70	99.92	99.16	99.56	99.33	99.36	99.60	100.00	99.59	99.28	99.28	99.99
Cations:																					
Si	7.77	7.68	7.74	7.74	7.79	7.71	7.77	7.74	7.72	7.71	7.77	7.93	7.77	7.71	7.71	7.66	7.64	7.68	7.68	7.64	7.72
Ti	0.10	0.09	0.09	0.08	0.09	0.09	0.09	0.09	0.09	0.07	0.08	0.07	0.08	0.10	0.10	0.10	0.08	0.09	0.07	0.10	0.10
Al	17.69	17.85	17.75	17.76	17.71	17.76	17.72	17.67	17.73	17.76	17.63	17.54	17.70	17.48	17.38	17.39	17.46	17.39	17.41	17.43	17.33
Fe	2.93	2.91	2.89	2.87	2.77	2.86	2.79	2.87	2.82	2.84	2.88	2.72	2.79	3.23	3.33	3.41	3.35	3.41	3.39	3.39	3.40
Mn	0.02	0.02	0.01	0.02	0.01	0.01	0.02	0.02	0.02	0.03	0.02	0.02	0.03	0.02	0.01	0.02	0.03	0.03	0.02	0.03	0.03
Mg	0.49	0.46	0.52	0.49	0.49	0.52	0.52	0.58	0.53	0.59	0.60	0.55	0.52	0.79	0.86	0.87	0.87	0.85	0.85	0.85	0.83
Ca	0.00	0.00	0.00	0.00	0.00	0.00	0.00	0.00	0.00	0.00	0.00	0.00	0.00	0.00	0.00	0.00	0.01	0.00	0.00	0.00	0.00
Zn	0.28	0.29	0.30	0.35	0.39	0.36	0.36	0.36	0.41	0.34	0.34	0.40	0.40	0.11	0.08	0.09	0.11	0.09	0.11	0.10	0.10
Total (All)	29.28	29.30	29.30	29.30	29.26	29.32	29.27	29.34	29.32	29.34	29.33	29.23	29.30	29.44	29.50	29.54	29.55	29.54	29.54	29.54	29.51
Total (Majors ONLY)	29.01	29.01	29.00	28.95	28.87	28.96	28.92	28.98	28.91	29.00	28.99	28.83	28.90	29.33	29.41	29.45	29.44	29.45	29.43	29.44	29.42
XMg (= Mg / (Mg + Fe)	0.14	0.14	0.15	0.15	0.15	0.15	0.16	0.17	0.16	0.17	0.17	0.17	0.16	0.20	0.21	0.20	0.21	0.20	0.20	0.20	0.20

Note: Analyses conducted on the same mineral grain (e.g. 1 core analysis and 2 rim analyses on a specific staurolite grain) are highlighted in the same colour and enclosed in the same thick black box.

Staurolites cont.

Analysis Label (Specimen_mineral_grain/zone:spot number)	gb10_st_2j	gb10_st_2i	gb10_st_2k	gb10_st_2n	gb10_st_2l	gb10_st_2o	gb10_st_2q	gb10_st_2p	gb10_st_2y	gb10_st_2r	gb10_st_2s	gb10_st_2z	gb10_st_2t	gb10_st_2u	gb10_st_2w	gb10_st_2v	gb10_st_2x	gb10_st_2za	gb10_st_2zb	gb10_st_2zd	gb10_st_2zc
Mineral Probed:	st	st	st	st	st	st	st	st	st	st	st	st	st	st	st	st	st	st	st	st	st
Core/Int/Rim:	Rim	Core	Rim	Int	Rim	Rim	Rim	Int	Int	Core	Int	Rim	Rim	Rim	Int	Core	Int	Core	Core	Rim	Core
EMP Initial Results:																					
Oxide conc. (wt%)																					
SiO2	27.83	27.96	27.94	27.83	27.92	28.21	28.16	27.87	27.90	27.91	28.06	27.99	27.70	27.78	28.01	27.72	27.85	28.06	27.92	27.81	27.81
TiO2	0.40	0.54	0.53	0.53	0.53	0.32	0.41	0.37	0.39	0.39	0.38	0.38	0.37	0.30	0.41	0.38	0.39	0.46	0.39	0.43	0.34
Al2O3	54.06	54.05	53.99	53.88	54.03	53.70	53.70	54.07	53.94	53.70	53.57	54.25	53.65	53.59	54.34	54.03	54.45	53.78	53.82	54.30	53.79
FeO	15.03	15.00	14.70	14.69	14.50	14.77	14.51	14.78	15.00	14.64	14.65	14.54	14.83	14.79	14.40	14.66	14.55	14.69	14.85	14.50	14.68
MnO	0.09	0.09	0.16	0.12	0.10	0.11	0.10	0.12	0.09	0.04	0.11	0.09	0.07	0.07	0.06	0.12	0.06	0.09	0.13	0.04	0.08
MgO	1.83	1.88	2.06	2.02	2.01	2.07	2.15	2.05	2.04	2.02	2.08	1.82	1.96	2.14	2.05	2.07	1.99	1.85	2.02	1.92	2.07
CaO	0.03	0.01	0.02	0.01	0.01	0.00	0.00	0.00	0.01	0.00	0.00	0.01	0.02	0.00	0.01	0.00	0.00	0.02	0.00	0.00	0.00
ZnO	0.52	0.51	0.46	0.47	0.41	0.44	0.47	0.47	0.49	0.44	0.39	0.51	0.46	0.35	0.38	0.44	0.41	0.54	0.45	0.45	0.46
Total	99.78	100.04	99.85	99.56	99.52	99.62	99.50	99.73	99.86	99.13	99.24	99.58	99.06	99.02	99.67	99.42	99.70	99.49	99.58	99.45	99.23
Cations:																					
Si	7.64	7.65	7.65	7.64	7.66	7.74	7.73	7.64	7.65	7.69	7.72	7.67	7.65	7.67	7.66	7.62	7.62	7.71	7.67	7.63	7.66
Ti	0.08	0.11	0.11	0.11	0.11	0.07	0.09	0.08	0.08	0.08	0.08	0.08	0.08	0.06	0.09	0.08	0.08	0.10	0.08	0.09	0.07
Al	17.49	17.43	17.43	17.44	17.47	17.36	17.37	17.48	17.43	17.44	17.38	17.53	17.47	17.44	17.52	17.51	17.57	17.42	17.43	17.56	17.46
Fe	3.45	3.43	3.37	3.37	3.33	3.39	3.33	3.39	3.44	3.37	3.37	3.33	3.43	3.41	3.29	3.37	3.33	3.38	3.41	3.33	3.38
Mn	0.02	0.02	0.04	0.03	0.02	0.03	0.02	0.03	0.02	0.01	0.02	0.02	0.02	0.02	0.01	0.03	0.01	0.02	0.03	0.01	0.02
Mg	0.75	0.77	0.84	0.83	0.82	0.85	0.88	0.84	0.83	0.83	0.85	0.74	0.81	0.88	0.84	0.85	0.81	0.76	0.83	0.79	0.85
Ca	0.01	0.00	0.01	0.00	0.00	0.00	0.00	0.00	0.00	0.00	0.00	0.00	0.01	0.00	0.00	0.00	0.00	0.00	0.00	0.00	0.00
Zn	0.10	0.10	0.09	0.10	0.08	0.09	0.09	0.09	0.10	0.09	0.08	0.10	0.09	0.07	0.08	0.09	0.08	0.11	0.09	0.09	0.09
Total (All)	29.54	29.52	29.53	29.53	29.50	29.52	29.51	29.54	29.55	29.51	29.51	29.48	29.54	29.55	29.49	29.55	29.51	29.49	29.54	29.50	29.54
Total (Majors ONLY)	29.43	29.42	29.43	29.43	29.41	29.43	29.41	29.45	29.46	29.42	29.43	29.38	29.45	29.48	29.42	29.46	29.43	29.38	29.45	29.41	29.44
XMg (= Mg / (Mg + Fe)	0.18	0.18	0.20	0.20	0.20	0.20	0.21	0.20	0.20	0.20	0.20	0.18	0.19	0.21	0.20	0.20	0.20	0.18	0.20	0.19	0.20

Note: Analyses conducted on the same mineral grain (e.g. 1 core analysis and 2 rim analyses on a specific staurolite grain) are highlighted in the same colour and enclosed in the same thick black box.

Staurolites cont.

Analysis Label (Specimen_mineral_grain/zone:spot number)	gb10_st_3a	gb10_st_3b	gb10_st_3c	gb10_st_3d	gb10_st_3f	gb10_st_3e	gb10_st_3h	gb10_st_3g	gb10_st_3i	gb10_st_3j	gb10_st_3k	gb10_st_3l	gb10_st_3m	gb10_st_3o	gb10_st_3n	gb10_st_3q	gb10_st_3p	gb10_st_3r	gb10_st_4b	gb10_st_4a	gb10_st_4e
Mineral Probed:	st	st	st	st	st	st	st	st	st	st	st	st	st	st	st	st	st	st	st	st	st
Core/Int/Rim:	Core	Core	Core	Rim	Rim	Core	Core	Rim	Rim	Core	Rim	Rim	Core	Rim	Core	Core	Rim	Rim	Rim	Core	Rim
EMP Initial Results:																					
Oxide conc. (wt%)																					
SiO2	27.97	27.94	27.81	28.05	27.74	27.90	27.88	28.29	27.98	27.83	27.88	28.11	27.84	28.13	27.91	27.73	28.21	28.06	28.09	27.97	28.25
TiO2	0.45	0.46	0.50	0.44	0.49	0.51	0.45	0.41	0.45	0.48	0.50	0.43	0.47	0.45	0.52	0.48	0.48	0.52	0.39	0.47	0.59
Al2O3	53.93	54.53	53.39	54.18	53.69	53.64	53.77	54.56	53.58	53.89	54.49	53.87	53.55	54.36	54.13	53.89	54.40	53.63	54.36	54.33	54.46
FeO	14.48	13.97	14.72	14.43	14.70	14.84	14.49	14.03	14.74	14.67	14.64	14.38	14.69	14.05	14.33	14.62	14.24	14.52	14.81	14.70	14.15
MnO	0.08	0.10	0.06	0.05	0.09	0.06	0.08	0.10	0.07	0.08	0.06	0.11	0.08	0.11	0.14	0.10	0.12	0.07	0.13	0.10	0.16
MgO	2.15	2.01	2.07	1.97	2.02	2.19	1.94	1.91	2.07	2.07	2.01	1.99	2.10	1.64	1.89	1.98	1.78	2.01	2.00	1.97	1.75
CaO	0.02	0.00	0.00	0.01	0.01	0.00	0.00	0.00	0.00	0.02	0.00	0.01	0.01	0.02	0.01	0.02	0.00	0.01	0.00	0.01	0.01
ZnO	0.51	0.53	0.41	0.42	0.38	0.30	0.50	0.42	0.43	0.46	0.43	0.36	0.48	0.55	0.49	0.47	0.41	0.48	0.42	0.43	0.41
Total	99.59	99.55	98.97	99.55	99.12	99.44	99.10	99.72	99.33	99.50	100.01	99.26	99.22	99.30	99.41	99.29	99.65	99.30	100.20	99.98	99.78
Cations:																					
Si	7.67	7.64	7.68	7.68	7.65	7.67	7.68	7.72	7.70	7.65	7.61	7.72	7.67	7.71	7.66	7.63	7.71	7.72	7.66	7.64	7.71
Ti	0.09	0.09	0.10	0.09	0.10	0.11	0.09	0.08	0.09	0.10	0.10	0.09	0.10	0.09	0.11	0.10	0.10	0.11	0.08	0.10	0.12
Al	17.43	17.58	17.38	17.49	17.45	17.38	17.46	17.54	17.38	17.45	17.54	17.44	17.39	17.57	17.51	17.49	17.53	17.38	17.47	17.50	17.52
Fe	3.32	3.20	3.40	3.31	3.39	3.41	3.34	3.20	3.39	3.37	3.34	3.30	3.39	3.22	3.29	3.37	3.26	3.34	3.38	3.36	3.23
Mn	0.02	0.02	0.01	0.01	0.02	0.01	0.02	0.02	0.02	0.02	0.01	0.02	0.02	0.03	0.03	0.02	0.03	0.02	0.03	0.02	0.04
Mg	0.88	0.82	0.85	0.80	0.83	0.90	0.80	0.78	0.85	0.85	0.82	0.81	0.86	0.67	0.77	0.81	0.73	0.82	0.81	0.80	0.71
Ca	0.00	0.00	0.00	0.00	0.00	0.00	0.00	0.00	0.00	0.01	0.00	0.00	0.00	0.01	0.00	0.01	0.00	0.00	0.00	0.00	0.00
Zn	0.10	0.11	0.08	0.08	0.08	0.06	0.10	0.08	0.09	0.09	0.09	0.07	0.10	0.11	0.10	0.10	0.08	0.10	0.08	0.09	0.08
Total (All)	29.52	29.47	29.52	29.48	29.52	29.54	29.49	29.43	29.52	29.53	29.52	29.47	29.53	29.41	29.48	29.52	29.43	29.48	29.52	29.51	29.41
Total (Majors ONLY)	29.42	29.36	29.44	29.39	29.45	29.48	29.39	29.34	29.43	29.44	29.43	29.40	29.44	29.30	29.38	29.43	29.35	29.39	29.44	29.43	29.33
XMg (= Mg / (Mg + Fe)	0.21	0.20	0.20	0.20	0.20	0.21	0.19	0.20	0.20	0.20	0.20	0.20	0.20	0.17	0.19	0.19	0.18	0.20	0.19	0.19	0.18

Note: Analyses conducted on the same mineral grain (e.g. 1 core analysis and 2 rim analyses on a specific staurolite grain) are highlighted in the same colour and enclosed in the same thick black box.

Staurolites cont.

Analysis Label (Specimen_mineral_grain/zone:spot number)	gb10_st_4d	gb10_st_4c	gb10_st_4f	gb10_st_4g	gb10_st_4i	gb10_st_4h	gb10_st_5c	gb10_st_5d	gb10_st_5e	gb10_st_5f	gb10_st_5g	gb10_st_5j	gb10_st_5k	gb10_st_5l	gb10_st_5m	gb10_st_5n	gb10_st_5o	gb10_st_5p	gb10_st_5q	gb10_st_5r	gb10_st_5t
Mineral Probed:	st	st	st	st	st	st	st	st	st	st	st	st	st	st	st	st	st	st	st	st	st
Core/Int/Rim:	Int	Core	Rim	Core	Rim	Core	Rim	Int	Rim	Core	Rim	Rim	Rim	Core	Rim	Rim	Core	Rim	Core	Core	Rim
EMP Initial Results:																					
Oxide conc. (wt%)																					
SiO2	27.89	28.02	27.99	27.90	28.13	27.98	27.85	27.76	28.09	28.20	27.93	28.11	28.04	27.94	28.00	28.05	27.98	28.06	27.83	28.01	28.22
TiO2	0.47	0.39	0.52	0.36	0.50	0.43	0.50	0.54	0.54	0.37	0.46	0.46	0.46	0.44	0.45	0.44	0.56	0.47	0.46	0.49	0.47
Al2O3	54.58	54.21	53.88	54.49	54.23	54.13	54.62	54.33	55.05	54.62	54.56	54.20	54.03	53.86	54.35	54.24	53.69	54.54	54.06	54.18	54.46
FeO	14.50	14.47	14.55	14.34	14.62	14.73	14.79	14.71	14.16	14.40	14.79	14.45	14.39	14.81	14.08	14.20	14.82	14.23	14.88	14.55	14.15
MnO	0.12	0.14	0.03	0.12	0.13	0.09	0.13	0.07	0.10	0.10	0.13	0.09	0.11	0.11	0.09	0.09	0.10	0.15	0.06	0.11	0.14
MgO	1.94	2.06	1.94	1.98	1.80	1.89	1.77	1.86	1.62	1.88	2.00	1.82	1.86	1.92	1.89	1.80	1.98	1.76	1.98	2.02	1.87
CaO	0.00	0.00	0.04	0.01	0.01	0.00	0.01	0.04	0.00	0.00	0.00	0.00	0.00	0.01	0.01	0.02	0.02	0.01	0.01	0.02	0.01
ZnO	0.49	0.49	0.54	0.60	0.51	0.53	0.50	0.52	0.57	0.40	0.32	0.48	0.45	0.31	0.49	0.47	0.36	0.33	0.44	0.44	0.34
Total	100.00	99.77	99.49	99.80	99.93	99.77	100.17	99.83	100.13	99.97	100.19	99.61	99.34	99.40	99.37	99.31	99.51	99.54	99.72	99.82	99.66
Cations:																					
Si	7.61	7.67	7.68	7.63	7.69	7.67	7.60	7.60	7.64	7.69	7.62	7.70	7.70	7.68	7.67	7.70	7.69	7.68	7.63	7.66	7.71
Ti	0.10	0.08	0.11	0.07	0.10	0.09	0.10	0.11	0.11	0.08	0.09	0.09	0.10	0.09	0.09	0.09	0.11	0.10	0.10	0.10	0.10
Al	17.56	17.48	17.44	17.57	17.47	17.48	17.57	17.54	17.65	17.55	17.53	17.50	17.49	17.45	17.56	17.54	17.39	17.59	17.48	17.47	17.53
Fe	3.31	3.31	3.34	3.28	3.34	3.37	3.38	3.37	3.22	3.28	3.37	3.31	3.30	3.40	3.23	3.26	3.41	3.26	3.41	3.33	3.23
Mn	0.03	0.03	0.01	0.03	0.03	0.02	0.03	0.02	0.02	0.02	0.03	0.02	0.02	0.03	0.02	0.02	0.02	0.03	0.01	0.03	0.03
Mg	0.79	0.84	0.79	0.81	0.73	0.77	0.72	0.76	0.66	0.76	0.81	0.74	0.76	0.79	0.77	0.74	0.81	0.72	0.81	0.82	0.76
Ca	0.00	0.00	0.01	0.00	0.00	0.00	0.00	0.01	0.00	0.00	0.00	0.00	0.00	0.00	0.00	0.01	0.01	0.00	0.00	0.01	0.00
Zn	0.10	0.10	0.11	0.12	0.10	0.11	0.10	0.10	0.11	0.08	0.06	0.10	0.09	0.06	0.10	0.10	0.07	0.07	0.09	0.09	0.07
Total (All)	29.51	29.51	29.49	29.51	29.47	29.51	29.51	29.52	29.42	29.46	29.52	29.46	29.46	29.50	29.45	29.44	29.51	29.43	29.53	29.50	29.43
Total (Majors ONLY)	29.41	29.41	29.38	29.39	29.37	29.40	29.41	29.41	29.31	29.38	29.46	29.36	29.37	29.44	29.35	29.35	29.43	29.37	29.45	29.41	29.36
XMg (= Mg / (Mg + Fe)	0.19	0.20	0.19	0.20	0.18	0.19	0.18	0.18	0.17	0.19	0.19	0.18	0.19	0.19	0.19	0.18	0.19	0.18	0.19	0.20	0.19

Note: Analyses conducted on the same mineral grain (e.g. 1 core analysis and 2 rim analyses on a specific staurolite grain) are highlighted in the same colour and enclosed in the same thick black box.

Staurolites cont.

Analysis Label (Specimen_mineral_grain/zone:spot number)	gb10_st_5u	gb10_st_5v	gb10_st_5w	gb10_st_5x	gb10_st_6a	gb10_st_6b	gb10_st_6d	gb10_st_6e	gb10_st_6f	gb10_st_6h	gb10_st_6g	gb10_st_6i	gb10_st_7a	gb10_st_7b	gb10_st_7e	gb10_st_7f	gb10_st_7g	gb10_st_8a	gb10_st_8c	gb10_st_8b	gb10_st_8f
Mineral Probed:	st	st	st	st	st	st	st	st	st	st	st	st	st	st	st	st	st	st	st	st	st
Core/Int/Rim:	Rim	Core	Rim	Core	Core	Core	Rim	Core	Rim	Rim	Int	Core	Rim	Core	Rim	Int	Core	Rim	Rim	Int	Core
EMP Initial Results:																					
Oxide conc. (wt%)																					
SiO2	28.06	28.28	28.20	27.87	27.94	28.04	28.19	27.78	28.06	28.16	27.98	27.85	28.00	28.06	28.20	28.02	28.29	28.24	28.07	28.28	27.87
TiO2	0.42	0.42	0.42	0.39	0.45	0.48	0.48	0.52	0.47	0.50	0.47	0.47	0.48	0.46	0.47	0.54	0.46	0.43	0.48	0.50	0.41
Al2O3	54.20	54.17	54.86	54.34	54.63	54.49	54.21	54.21	54.09	54.51	54.42	54.21	54.27	54.09	54.89	54.06	54.21	54.82	54.01	54.38	53.87
FeO	14.67	14.23	14.31	14.36	14.66	14.69	14.80	14.76	14.84	14.15	14.63	14.68	14.27	14.16	14.28	15.12	14.35	14.06	14.45	13.99	14.35
MnO	0.12	0.05	0.14	0.11	0.11	0.10	0.14	0.06	0.09	0.07	0.16	0.07	0.11	0.13	0.07	0.08	0.14	0.12	0.14	0.07	0.11
MgO	1.79	1.94	1.67	1.91	1.81	1.85	1.78	1.99	1.92	1.77	1.88	1.93	1.86	1.91	1.72	1.99	1.73	1.67	1.81	1.89	2.01
CaO	0.02	0.02	0.02	0.01	0.00	0.00	0.00	0.01	0.03	0.01	0.00	0.01	0.00	0.00	0.01	0.00	0.02	0.01	0.00	0.00	0.00
ZnO	0.41	0.38	0.54	0.50	0.46	0.55	0.40	0.52	0.44	0.48	0.35	0.40	0.37	0.54	0.39	0.39	0.61	0.42	0.35	0.46	0.41
Total	99.69	99.49	100.15	99.50	100.07	100.20	100.00	99.85	99.93	99.65	99.89	99.62	99.37	99.34	100.03	100.19	99.81	99.78	99.31	99.57	99.03
Cations:																					
Si	7.69	7.74	7.68	7.64	7.63	7.65	7.70	7.61	7.68	7.69	7.65	7.64	7.68	7.70	7.68	7.65	7.73	7.70	7.71	7.73	7.68
Ti	0.09	0.09	0.09	0.08	0.09	0.10	0.10	0.11	0.10	0.10	0.10	0.10	0.10	0.09	0.10	0.11	0.09	0.09	0.10	0.10	0.08
Al	17.50	17.47	17.60	17.56	17.57	17.52	17.45	17.50	17.44	17.56	17.53	17.52	17.54	17.49	17.61	17.41	17.47	17.62	17.48	17.51	17.49
Fe	3.36	3.26	3.26	3.29	3.35	3.35	3.38	3.38	3.40	3.23	3.34	3.37	3.27	3.25	3.25	3.45	3.28	3.21	3.32	3.20	3.31
Mn	0.03	0.01	0.03	0.02	0.03	0.02	0.03	0.01	0.02	0.02	0.04	0.02	0.03	0.03	0.02	0.02	0.03	0.03	0.03	0.02	0.03
Mg	0.73	0.79	0.68	0.78	0.74	0.75	0.72	0.81	0.78	0.72	0.77	0.79	0.76	0.78	0.70	0.81	0.70	0.68	0.74	0.77	0.83
Ca	0.01	0.01	0.01	0.00	0.00	0.00	0.00	0.00	0.01	0.00	0.00	0.00	0.00	0.00	0.00	0.00	0.01	0.00	0.00	0.00	0.00
Zn	0.08	0.08	0.11	0.10	0.09	0.11	0.08	0.10	0.09	0.10	0.07	0.08	0.07	0.11	0.08	0.08	0.12	0.09	0.07	0.09	0.08
Total (All)	29.48	29.44	29.44	29.49	29.49	29.50	29.47	29.53	29.51	29.42	29.49	29.51	29.45	29.46	29.42	29.53	29.44	29.40	29.45	29.42	29.49
Total (Majors ONLY)	29.40	29.36	29.33	29.39	29.40	29.39	29.39	29.43	29.42	29.33	29.42	29.43	29.38	29.35	29.35	29.45	29.32	29.32	29.38	29.32	29.41
XMg (= Mg / (Mg + Fe)	0.18	0.20	0.17	0.19	0.18	0.18	0.18	0.19	0.19	0.18	0.19	0.19	0.19	0.19	0.18	0.19	0.18	0.17	0.18	0.19	0.20

Note: Analyses conducted on the same mineral grain (e.g. 1 core analysis and 2 rim analyses on a specific staurolite grain) are highlighted in the same colour and enclosed in the same thick black box.

Staurolites cont.

Analysis Label (Specimen_mineral grain/zone:spot number)	gb10_st_8d	gb10_st_8e	gb10_st_9a	gb10_st_9b	gb10_st_9c	gb10_st_9f	gb10_st_9e	gb10_st_9g	gb10_st_10d	gb10_st_10b	gb10_st_10c	gb10_st_11a	gb10_st_11b	gb10_st_11c	gb10_st_11d	gb10_st_11g	gb10_st_11i	gb10_st_11e	gb10_st_11f	gb10_st_11h	gb10_st_11j
Mineral Probed:	st	st	st	st	st	st	st	st	st	st	st	st	st	st	st	st	st	st	st	st	st
Core/Int/Rim:	Core	Rim	Rim	Core	Core	Rim	Int	Rim	Rim	Int	Core	Rim	Core	Core	Rim	Rim	Int	Core	Core	Core	Core
EMP Initial Results:																					
Oxide conc. (wt%)																					
SiO2	27.86	27.97	28.13	27.76	27.94	27.59	28.03	28.01	28.23	27.83	28.00	28.12	28.05	28.12	27.80	27.68	28.01	28.01	27.70	28.03	27.74
TiO2	0.49	0.46	0.49	0.48	0.44	0.42	0.44	0.49	0.49	0.47	0.43	0.45	0.38	0.44	0.44	0.48	0.49	0.37	0.37	0.44	0.36
Al2O3	54.09	54.25	54.31	54.35	53.65	54.40	53.76	54.30	54.21	53.85	53.96	54.38	54.38	54.42	54.38	54.02	54.12	53.77	54.39	53.80	54.26
FeO	14.43	14.55	14.61	14.80	14.85	14.68	14.74	14.98	14.37	14.86	14.79	14.01	14.73	14.64	14.55	14.84	14.74	14.96	15.02	14.92	14.78
MnO	0.08	0.12	0.08	0.13	0.06	0.10	0.13	0.04	0.14	0.13	0.13	0.01	0.14	0.09	0.12	0.13	0.12	0.10	0.08	0.11	0.12
MgO	2.01	1.70	1.79	1.89	1.88	1.92	1.91	1.81	1.84	1.97	2.08	1.81	1.94	1.96	1.86	1.89	1.86	2.11	2.00	1.90	1.94
CaO	0.00	0.01	0.00	0.00	0.01	0.00	0.00	0.00	0.00	0.01	0.02	0.02	0.01	0.00	0.01	0.02	0.00	0.01	0.00	0.00	0.00
ZnO	0.38	0.47	0.43	0.41	0.30	0.37	0.29	0.37	0.42	0.33	0.32	0.37	0.32	0.34	0.39	0.34	0.33	0.37	0.35	0.45	0.38
Total	99.34	99.52	99.84	99.83	99.13	99.48	99.30	100.00	99.71	99.44	99.72	99.17	99.94	100.00	99.54	99.40	99.67	99.70	99.92	99.65	99.58
Cations:																					
Si	7.65	7.67	7.69	7.60	7.70	7.58	7.71	7.66	7.72	7.65	7.67	7.71	7.66	7.67	7.62	7.61	7.67	7.68	7.58	7.69	7.61
Ti	0.10	0.10	0.10	0.10	0.09	0.09	0.09	0.10	0.10	0.10	0.09	0.09	0.08	0.09	0.09	0.10	0.10	0.08	0.08	0.09	0.07
Al	17.51	17.54	17.50	17.55	17.43	17.61	17.43	17.49	17.47	17.45	17.43	17.57	17.51	17.50	17.58	17.52	17.48	17.39	17.55	17.41	17.55
Fe	3.31	3.34	3.34	3.39	3.42	3.37	3.39	3.42	3.29	3.42	3.39	3.21	3.37	3.34	3.34	3.41	3.38	3.43	3.44	3.43	3.39
Mn	0.02	0.03	0.02	0.03	0.01	0.02	0.03	0.01	0.03	0.03	0.03	0.00	0.03	0.02	0.03	0.03	0.03	0.02	0.02	0.03	0.03
Mg	0.82	0.70	0.73	0.77	0.77	0.79	0.78	0.74	0.75	0.81	0.85	0.74	0.79	0.80	0.76	0.78	0.76	0.86	0.82	0.78	0.79
Ca	0.00	0.00	0.00	0.00	0.00	0.00	0.00	0.00	0.00	0.00	0.00	0.01	0.00	0.00	0.00	0.01	0.00	0.00	0.00	0.00	0.00
Zn	0.08	0.09	0.09	0.08	0.06	0.08	0.06	0.07	0.08	0.07	0.06	0.08	0.06	0.07	0.08	0.07	0.07	0.07	0.07	0.09	0.08
Total (All)	29.49	29.46	29.46	29.52	29.49	29.53	29.49	29.50	29.44	29.53	29.53	29.41	29.50	29.49	29.50	29.53	29.49	29.55	29.56	29.51	29.53
Total (Majors ONLY)	29.42	29.37	29.37	29.44	29.43	29.46	29.43	29.42	29.36	29.46	29.46	29.34	29.44	29.42	29.42	29.46	29.42	29.47	29.49	29.42	29.46
XMg (= Mg / (Mg + Fe)	0.20	0.17	0.18	0.19	0.18	0.19	0.19	0.18	0.19	0.19	0.20	0.19	0.19	0.19	0.19	0.19	0.18	0.20	0.19	0.18	0.19

Note: Analyses conducted on the same mineral grain (e.g. 1 core analysis and 2 rim analyses on a specific staurolite grain) are highlighted in the same colour and enclosed in the same thick black box.

Staurolites cont.

Analysis Label (Specimen_mineral_grain/zone:spot number)	gb10_st_11k	gb10_st_11l	gb10_st_11n	gb10_st_11q	gb10_st_11p	gb10_st_11r	gb10_st_11s	gb10_st_12f	gb10_st_12e	gb10_st_12d	gb10_st_12c	gb10_st_13a	gb10_st_13b	gb10_st_13c	gb10_st_13f	gb10_st_13g	gb10_st_13h	gb10_st_13i	gb10_st_13k	gb10_st_14a	gb10_st_14b
Mineral Probed:	st	st	st	st	st	st	st	st	st	st	st	st	st	st	st	st	st	st	st	st	st
Core/Int/Rim:	Rim	Core	Rim	Int	Core	Rim	Core	Rim	Int	Core	Core	Rim	Core	Core	Core	Core	Core	Core	Rim	Core	Rim
EMP Initial Results:																					
Oxide conc. (wt%)																					
SiO2	28.11	28.00	28.08	27.95	27.77	28.06	27.87	28.02	28.07	27.70	27.80	28.19	28.22	27.59	28.15	28.03	27.95	27.94	28.12	28.00	28.00
TiO2	0.45	0.32	0.50	0.49	0.45	0.50	0.45	0.41	0.43	0.45	0.43	0.50	0.46	0.41	0.52	0.45	0.47	0.46	0.48	0.38	0.55
Al2O3	54.13	54.45	54.25	54.04	54.20	54.28	54.03	54.03	54.72	54.20	53.85	54.25	54.13	54.13	54.55	54.32	54.40	54.92	54.50	54.05	54.03
FeO	14.83	14.66	14.32	14.87	14.68	14.87	15.08	14.85	14.63	15.03	14.68	14.42	14.62	14.76	13.84	15.10	15.01	14.49	14.27	14.64	14.85
MnO	0.12	0.11	0.10	0.12	0.12	0.19	0.14	0.06	0.15	0.12	0.09	0.07	0.13	0.05	0.07	0.10	0.08	0.12	0.09	0.10	0.05
MgO	2.05	1.99	1.72	1.83	1.87	1.79	1.88	1.91	1.85	1.97	1.93	1.75	1.88	1.96	1.88	1.80	1.88	1.80	1.92	1.87	1.80
CaO	0.03	0.00	0.01	0.01	0.01	0.02	0.00	0.00	0.01	0.01	0.02	0.01	0.03	0.01	0.02	0.01	0.03	0.00	0.03	0.01	0.00
ZnO	0.42	0.40	0.22	0.29	0.40	0.31	0.38	0.25	0.37	0.35	0.48	0.39	0.32	0.29	0.37	0.38	0.38	0.38	0.36	0.49	0.41
Total	100.13	99.94	99.20	99.60	99.49	100.02	99.85	99.53	100.23	99.82	99.28	99.58	99.79	99.20	99.41	100.20	100.20	100.12	99.78	99.54	99.69
Cations:																					
Si	7.67	7.65	7.71	7.67	7.63	7.67	7.64	7.69	7.64	7.59	7.65	7.72	7.72	7.60	7.70	7.65	7.63	7.61	7.68	7.68	7.68
Ti	0.09	0.07	0.10	0.10	0.09	0.10	0.09	0.08	0.09	0.09	0.09	0.10	0.10	0.09	0.11	0.09	0.10	0.10	0.10	0.08	0.11
Al	17.42	17.53	17.55	17.47	17.54	17.48	17.46	17.47	17.56	17.52	17.48	17.50	17.44	17.57	17.58	17.48	17.50	17.63	17.54	17.48	17.46
Fe	3.39	3.35	3.29	3.41	3.37	3.40	3.46	3.41	3.33	3.45	3.38	3.30	3.34	3.40	3.16	3.45	3.43	3.30	3.26	3.36	3.40
Mn	0.03	0.03	0.02	0.03	0.03	0.04	0.03	0.01	0.03	0.03	0.02	0.02	0.03	0.01	0.02	0.02	0.02	0.03	0.02	0.02	0.01
Mg	0.83	0.81	0.70	0.75	0.77	0.73	0.77	0.78	0.75	0.81	0.79	0.71	0.77	0.80	0.77	0.73	0.76	0.73	0.78	0.76	0.74
Ca	0.01	0.00	0.00	0.00	0.00	0.00	0.00	0.00	0.00	0.00	0.01	0.00	0.01	0.00	0.01	0.00	0.01	0.00	0.01	0.00	0.00
Zn	0.08	0.08	0.05	0.06	0.08	0.06	0.08	0.05	0.08	0.07	0.10	0.08	0.06	0.06	0.08	0.08	0.08	0.08	0.07	0.10	0.08
Total (All)	29.52	29.52	29.42	29.49	29.51	29.49	29.53	29.49	29.49	29.55	29.52	29.43	29.47	29.53	29.41	29.51	29.52	29.48	29.46	29.50	29.48
Total (Majors ONLY)	29.44	29.44	29.37	29.43	29.43	29.43	29.46	29.44	29.41	29.48	29.42	29.35	29.40	29.47	29.33	29.44	29.45	29.40	29.38	29.40	29.40
XMg (= Mg / (Mg + Fe)	0.20	0.19	0.18	0.18	0.19	0.18	0.18	0.19	0.18	0.19	0.19	0.18	0.19	0.19	0.19	0.18	0.18	0.18	0.19	0.19	0.18

Note: Analyses conducted on the same mineral grain (e.g. 1 core analysis and 2 rim analyses on a specific staurolite grain) are highlighted in the same colour and enclosed in the same thick black box.

Staurolites cont.

Analysis Label (Specimen_mineral_grain/zone:spot number)	gb10_st_14c	gb10_st_14d	gb10_st_14e	gb10_st_14f	gb10_st_14h	gb10_st_14g	gb10_st_14j	gb10_st_14i	gb10_st_14l	gb10_st_14k	gb13_st_1b	gb13_st_1d	gb13_st_3d	gb13_st_3c	gb13_st_3f	gb13_st_3g	gb13_st_3k	gb13_st_3l	gb13_st_3n	gb13_st_3o	gb13_st_3p
Mineral Probed:	st	st	st	st	st	st	st	st	st	st	st	st	st	st	st	st	st	st	st	st	st
Core/Int/Rim:	Core	Rim	Rim	Core	Core	Rim	Rim	Core	Rim	Core	Rim	Rim	Rim	Core	Core	Core	Rim	Core	Rim	Rim	Core
EMP Initial Results:																					
Oxide conc. (wt%)																					
SiO2	28.11	28.12	27.97	28.12	28.11	28.17	28.42	28.17	28.10	28.19	27.97	28.16	28.12	27.96	27.87	27.86	28.16	27.93	28.17	28.02	28.06
TiO2	0.47	0.44	0.52	0.48	0.53	0.46	0.42	0.44	0.46	0.44	0.52	0.46	0.60	0.54	0.50	0.52	0.58	0.50	0.58	0.46	0.55
Al2O3	54.03	54.27	53.73	54.36	53.69	54.30	54.03	54.28	54.29	53.75	54.65	54.22	54.35	54.13	53.87	54.46	54.37	54.37	54.24	54.41	54.12
FeO	15.10	14.52	14.80	14.66	14.91	14.52	14.45	14.94	14.84	14.59	13.82	13.91	14.36	14.56	14.83	14.76	14.28	14.34	14.51	14.76	14.85
MnO	0.07	0.06	0.08	0.08	0.06	0.07	0.11	0.14	0.06	0.11	0.11	0.10	0.06	0.09	0.14	0.07	0.04	0.13	0.13	0.10	0.13
MgO	1.92	1.73	1.84	1.83	1.93	1.75	1.69	1.82	1.61	1.79	1.70	1.96	2.11	2.01	2.04	2.05	2.21	2.13	2.10	1.97	2.00
CaO	0.00	0.00	0.01	0.00	0.01	0.01	0.01	0.00	0.00	0.01	0.00	0.00	0.01	0.01	0.01	0.01	0.01	0.01	0.01	0.00	0.00
ZnO	0.28	0.25	0.30	0.42	0.31	0.33	0.34	0.40	0.40	0.35	0.69	0.48	0.50	0.50	0.47	0.45	0.43	0.34	0.42	0.41	0.43
Total	99.98	99.39	99.25	99.95	99.55	99.62	99.47	100.19	99.76	99.24	99.45	99.30	100.11	99.80	99.73	100.18	100.07	99.74	100.17	100.13	100.14
Cations:																					
Si	7.69	7.71	7.70	7.68	7.72	7.71	7.78	7.69	7.69	7.75	7.66	7.72	7.66	7.65	7.65	7.60	7.67	7.64	7.68	7.64	7.66
Ti	0.10	0.09	0.11	0.10	0.11	0.10	0.09	0.09	0.09	0.09	0.11	0.09	0.12	0.11	0.10	0.11	0.12	0.10	0.12	0.10	0.11
Al	17.42	17.53	17.43	17.50	17.37	17.51	17.44	17.46	17.52	17.42	17.63	17.51	17.46	17.46	17.42	17.52	17.45	17.52	17.42	17.50	17.42
Fe	3.45	3.33	3.41	3.35	3.42	3.32	3.31	3.41	3.40	3.35	3.16	3.19	3.27	3.33	3.40	3.37	3.25	3.28	3.31	3.37	3.39
Mn	0.02	0.01	0.02	0.02	0.02	0.02	0.03	0.03	0.01	0.03	0.02	0.02	0.01	0.02	0.03	0.02	0.01	0.03	0.03	0.02	0.03
Mg	0.78	0.71	0.75	0.74	0.79	0.71	0.69	0.74	0.66	0.73	0.69	0.80	0.86	0.82	0.83	0.83	0.90	0.87	0.85	0.80	0.81
Ca	0.00	0.00	0.00	0.00	0.00	0.00	0.00	0.00	0.00	0.00	0.00	0.00	0.00	0.00	0.00	0.00	0.00	0.00	0.00	0.00	0.00
Zn	0.06	0.05	0.06	0.08	0.06	0.07	0.07	0.08	0.08	0.07	0.14	0.10	0.10	0.10	0.10	0.09	0.09	0.07	0.09	0.08	0.09
Total (All)	29.51	29.43	29.48	29.47	29.49	29.44	29.41	29.49	29.45	29.45	29.42	29.43	29.49	29.50	29.54	29.53	29.49	29.50	29.49	29.51	29.52
Total (Majors ONLY)	29.45	29.38	29.42	29.39	29.43	29.37	29.34	29.41	29.37	29.38	29.28	29.34	29.39	29.40	29.44	29.44	29.40	29.43	29.41	29.43	29.43
XMg (= Mg / (Mg + Fe)	0.18	0.18	0.18	0.18	0.19	0.18	0.17	0.18	0.16	0.18	0.18	0.20	0.21	0.20	0.20	0.20	0.22	0.21	0.21	0.19	0.19

Note: Analyses conducted on the same mineral grain (e.g. 1 core analysis and 2 rim analyses on a specific staurolite grain) are highlighted in the same colour and enclosed in the same thick black box.

Staurolites cont.

Analysis Label (Specimen_mineral_grain/zone:spot number)	gb13_st_3q	gb13_st_3r	gb13_st_3t	gb13_st_4b	gb13_st_4e	gb13_st_4d	gb13_st_4g	gb13_st_4f	gb13_st_4i	gb13_st_4h	gb13_st_4j	gb13_st_4k	gb13_st_4m	gb13_st_4o	gb13_st_4n	gb13_st_4p	gb13_st_4q	gb13_st_5b	gb13_st_5a	gb13_st_5d	gb13_st_5e
Mineral Probed:	st	st	st	st	st	st	st	st	st	st	st	st	st	st	st	st	st	st	st	st	st
Core/Int/Rim:	Int	Core	Core	Rim	Rim	Core	Rim	Core	Rim	Core	Core	Rim	Core	Rim	Int	Rim	Core	Rim	Int	Rim	Core
EMP Initial Results:																					
Oxide conc. (wt%)																					
SiO2	28.02	27.92	27.76	28.32	27.93	27.93	27.91	28.13	28.17	28.04	28.22	28.23	27.97	27.87	28.07	28.06	28.00	28.19	28.17	27.94	27.64
TiO2	0.52	0.52	0.49	0.49	0.53	0.45	0.49	0.47	0.44	0.51	0.41	0.47	0.51	0.51	0.54	0.50	0.34	0.57	0.51	0.35	0.43
Al2O3	53.94	54.12	54.10	54.94	54.76	54.61	54.24	53.99	53.96	54.00	54.07	53.96	54.47	53.82	53.92	54.75	54.87	54.19	54.60	54.30	53.86
FeO	14.68	14.48	14.70	14.30	13.98	14.45	14.54	14.58	14.20	14.37	14.76	14.53	14.08	14.98	14.56	13.29	13.64	14.36	14.25	14.36	14.45
MnO	0.11	0.13	0.13	0.07	0.08	0.09	0.06	0.06	0.09	0.07	0.08	0.09	0.10	0.07	0.09	0.06	0.09	0.03	0.09	0.09	0.04
MgO	1.94	2.04	2.08	1.20	1.51	1.70	1.86	2.00	2.05	1.95	2.00	2.02	1.78	1.75	1.83	1.72	1.82	1.78	1.72	1.94	2.05
CaO	0.00	0.02	0.00	0.01	0.00	0.02	0.01	0.00	0.00	0.00	0.00	0.01	0.02	0.01	0.00	0.01	0.01	0.00	0.00	0.00	0.02
ZnO	0.48	0.51	0.44	0.63	0.77	0.59	0.68	0.65	0.61	0.52	0.51	0.63	0.81	0.62	0.66	0.64	0.83	0.63	0.65	0.61	0.59
Total	99.68	99.73	99.69	99.97	99.56	99.83	99.79	99.88	99.51	99.47	100.06	99.93	99.74	99.63	99.67	99.03	99.60	99.75	99.99	99.59	99.08
Cations:																					
Si	7.68	7.65	7.61	7.72	7.64	7.64	7.64	7.70	7.72	7.69	7.71	7.72	7.65	7.66	7.70	7.69	7.65	7.71	7.68	7.66	7.62
Ti	0.11	0.11	0.10	0.10	0.11	0.09	0.10	0.10	0.09	0.11	0.08	0.10	0.11	0.11	0.11	0.10	0.07	0.12	0.11	0.07	0.09
Al	17.43	17.47	17.49	17.65	17.67	17.60	17.51	17.41	17.43	17.46	17.41	17.39	17.56	17.44	17.43	17.68	17.67	17.47	17.55	17.54	17.51
Fe	3.37	3.32	3.37	3.26	3.20	3.30	3.33	3.34	3.25	3.30	3.37	3.32	3.22	3.44	3.34	3.05	3.12	3.28	3.25	3.29	3.33
Mn	0.03	0.03	0.03	0.02	0.02	0.02	0.01	0.01	0.02	0.02	0.02	0.02	0.02	0.02	0.02	0.01	0.02	0.01	0.02	0.02	0.01
Mg	0.79	0.83	0.85	0.49	0.62	0.69	0.76	0.82	0.84	0.80	0.81	0.82	0.73	0.72	0.75	0.70	0.74	0.73	0.70	0.79	0.84
Ca	0.00	0.01	0.00	0.00	0.00	0.00	0.00	0.00	0.00	0.00	0.00	0.00	0.00	0.00	0.00	0.00	0.00	0.00	0.00	0.00	0.00
Zn	0.10	0.10	0.09	0.13	0.16	0.12	0.14	0.13	0.12	0.11	0.10	0.13	0.16	0.13	0.13	0.13	0.17	0.13	0.13	0.12	0.12
Total (All)	29.50	29.51	29.54	29.36	29.41	29.47	29.50	29.50	29.48	29.47	29.51	29.49	29.46	29.51	29.48	29.37	29.44	29.44	29.44	29.50	29.53
Total (Majors ONLY)	29.40	29.41	29.45	29.23	29.26	29.35	29.36	29.37	29.35	29.37	29.40	29.37	29.30	29.39	29.35	29.24	29.28	29.31	29.31	29.38	29.41
XMg (= Mg / (Mg + Fe)	0.19	0.20	0.20	0.13	0.16	0.17	0.19	0.20	0.20	0.19	0.19	0.20	0.18	0.17	0.18	0.19	0.19	0.18	0.18	0.19	0.20

Note: Analyses conducted on the same mineral grain (e.g. 1 core analysis and 2 rim analyses on a specific staurolite grain) are highlighted in the same colour and enclosed in the same thick black box.

Staurolites cont.

Analysis Label (Specimen_mineral_grain/zone:spot number)	gb13_st_5g	gb13_st_5h	gb13_st_5i	gb13_st_5j	gb13_st_5n	gb13_st_5m	gb13_st_6a	gb13_st_6d	gb13_st_6c	gb13_st_6e	gb13_st_6f	gb13_st_6g	gb13_st_6h	gb13_st_6j	gb13_st_6i	gb13_st_12b	gb13_st_12c	gb13_st_12a	gb13_st_12d	gb13_st_12f	gb13_st_12e
Mineral Probed:	st	st	st	st	st	st	st	st	st	st	st	st	st	st	st	st	st	st	st	st	st
Core/Int/Rim:	Rim	Core	Rim	Core	Rim	Core	Core	Rim	Core	Core	Rim	Rim	Core	Int	Core	Rim	Int	Core	Rim	Rim	Core
EMP Initial Results:																					
Oxide conc. (wt%)																					
SiO2	28.23	28.04	28.11	27.91	28.02	27.83	27.98	28.20	27.82	27.72	27.89	27.88	28.02	28.19	27.75	28.01	27.95	27.78	27.89	27.92	27.94
TiO2	0.59	0.45	0.55	0.48	0.28	0.43	0.44	0.48	0.43	0.49	0.50	0.54	0.53	0.44	0.27	0.32	0.38	0.45	0.42	0.35	0.41
Al2O3	54.60	54.51	54.49	54.35	54.81	54.37	54.47	53.80	54.52	54.26	54.29	53.68	53.74	53.84	54.28	54.46	54.35	54.17	53.67	53.39	54.02
FeO	14.15	14.27	13.95	14.42	14.27	14.49	14.01	14.55	14.51	14.28	14.35	14.37	14.22	14.35	14.52	14.36	14.78	14.86	14.49	14.70	14.50
MnO	0.06	0.11	0.08	0.11	0.08	0.08	0.06	0.06	0.04	0.07	0.11	0.05	0.10	0.11	0.10	0.09	0.10	0.04	0.10	0.11	0.08
MgO	1.84	1.75	1.79	2.09	2.05	2.06	2.02	1.98	1.92	1.98	1.94	2.12	2.31	2.08	2.18	1.86	1.93	2.04	2.08	2.15	1.99
CaO	0.01	0.00	0.02	0.00	0.01	0.00	0.01	0.02	0.00	0.01	0.00	0.01	0.00	0.00	0.01	0.01	0.00	0.00	0.00	0.00	0.00
ZnO	0.64	0.69	0.63	0.61	0.48	0.70	0.56	0.65	0.72	0.51	0.54	0.47	0.53	0.53	0.58	0.67	0.72	0.63	0.56	0.61	0.60
Total	100.12	99.83	99.61	99.97	99.99	99.96	99.54	99.75	99.96	99.32	99.62	99.13	99.45	99.54	99.69	99.77	100.22	99.97	99.21	99.24	99.54
Cations:																					
Si	7.68	7.66	7.68	7.63	7.64	7.61	7.66	7.72	7.61	7.61	7.64	7.68	7.69	7.73	7.61	7.66	7.63	7.61	7.68	7.70	7.67
Ti	0.12	0.09	0.11	0.10	0.06	0.09	0.09	0.10	0.09	0.10	0.10	0.11	0.11	0.09	0.05	0.06	0.08	0.09	0.09	0.07	0.08
Al	17.52	17.56	17.56	17.50	17.61	17.53	17.57	17.37	17.57	17.57	17.53	17.42	17.38	17.39	17.54	17.56	17.50	17.48	17.42	17.35	17.47
Fe	3.22	3.26	3.19	3.30	3.25	3.31	3.21	3.33	3.32	3.28	3.29	3.31	3.26	3.29	3.33	3.29	3.38	3.40	3.34	3.39	3.33
Mn	0.01	0.03	0.02	0.03	0.02	0.02	0.01	0.02	0.01	0.02	0.03	0.01	0.02	0.02	0.02	0.02	0.02	0.01	0.02	0.03	0.02
Mg	0.75	0.71	0.73	0.85	0.83	0.84	0.82	0.81	0.78	0.81	0.79	0.87	0.94	0.85	0.89	0.76	0.79	0.83	0.85	0.88	0.81
Ca	0.00	0.00	0.00	0.00	0.00	0.00	0.00	0.01	0.00	0.00	0.00	0.00	0.00	0.00	0.00	0.00	0.00	0.00	0.00	0.00	0.00
Zn	0.13	0.14	0.13	0.12	0.10	0.14	0.11	0.13	0.15	0.10	0.11	0.10	0.11	0.11	0.12	0.14	0.15	0.13	0.11	0.12	0.12
Total (All)	29.44	29.46	29.42	29.52	29.50	29.54	29.47	29.49	29.52	29.50	29.49	29.50	29.51	29.48	29.57	29.49	29.54	29.56	29.52	29.55	29.51
Total (Majors ONLY)	29.31	29.32	29.30	29.40	29.41	29.40	29.36	29.36	29.37	29.40	29.38	29.40	29.41	29.38	29.45	29.36	29.39	29.43	29.41	29.43	29.39
XMg (= Mg / (Mg + Fe)	0.19	0.18	0.19	0.21	0.20	0.20	0.20	0.20	0.19	0.20	0.19	0.21	0.22	0.21	0.21	0.19	0.19	0.20	0.20	0.21	0.20

Note: Analyses conducted on the same mineral grain (e.g. 1 core analysis and 2 rim analyses on a specific staurolite grain) are highlighted in the same colour and enclosed in the same thick black box.

Staurolites cont.

Analysis Label (Specimen_mineral_grain/zone:spot number)	gb13_st_12h	gb13_st_12g	gb13_st_10b	gb13_st_10a	gb13_st_10e	gb13_st_10d	gb13_st_11b	gb13_st_11c	gb13_st_11a	gb13_st_11e	gb13_st_11d	gb13_st_11g	gb13_st_11f	gb13_st_11h	gb13_st_11j	gb13_st_11i	gb13_st_8b	gb13_st_8a	gb13_st_8g	gb13_st_8c	gb13_st_8e
Mineral Probed:	st	st	st	st	st	st	st	st	st	st	st	st	st	st	st	st	st	st	st	st	st
Core/Int/Rim:	Rim	Core	Rim	Core	Rim	Core	Rim	Int	Core	Rim	Core	Rim	Core	Core	Rim	Core	Rim	Core	Rim	Core	Rim
EMP Initial Results:																					
Oxide conc. (wt%)																					
SiO2	27.92	27.91	27.91	28.02	28.01	27.95	27.99	28.01	27.89	28.00	27.83	28.02	27.61	27.84	28.21	27.81	28.17	27.93	28.12	27.68	28.10
TiO2	0.44	0.46	0.39	0.38	0.53	0.51	0.40	0.46	0.47	0.53	0.47	0.67	0.46	0.50	0.37	0.39	0.48	0.47	0.51	0.49	0.39
Al2O3	54.00	54.06	54.30	54.42	53.70	54.45	54.10	54.33	54.41	54.22	53.99	53.41	54.37	54.56	54.22	54.01	54.13	54.45	54.32	53.91	54.13
FeO	14.58	14.60	14.66	14.60	14.76	14.44	14.73	14.44	14.57	13.87	14.55	14.56	14.52	14.42	14.45	14.71	14.43	14.45	14.64	14.95	14.77
MnO	0.12	0.06	0.10	0.04	0.05	0.09	0.08	0.12	0.10	0.04	0.05	0.09	0.11	0.09	0.01	0.05	0.09	0.12	0.12	0.08	0.14
MgO	1.98	1.90	2.09	2.03	1.85	1.89	1.78	1.79	1.98	1.71	1.88	2.01	1.89	1.78	1.87	1.91	1.84	2.12	1.85	1.93	1.88
CaO	0.00	0.02	0.00	0.01	0.02	0.01	0.00	0.01	0.00	0.00	0.00	0.00	0.01	0.00	0.00	0.00	0.01	0.00	0.01	0.03	0.01
ZnO	0.65	0.61	0.53	0.73	0.55	0.56	0.61	0.61	0.66	0.67	0.67	0.59	0.70	0.72	0.56	0.69	0.37	0.50	0.57	0.55	0.52
Total	99.69	99.61	99.98	100.24	99.48	99.90	99.69	99.76	100.09	99.04	99.44	99.34	99.67	99.92	99.69	99.58	99.52	100.04	100.14	99.62	99.94
Cations:																					
Si	7.66	7.66	7.63	7.64	7.70	7.64	7.68	7.67	7.62	7.70	7.65	7.71	7.58	7.61	7.72	7.64	7.72	7.62	7.67	7.61	7.69
Ti	0.09	0.09	0.08	0.08	0.11	0.11	0.08	0.10	0.10	0.11	0.10	0.14	0.09	0.10	0.08	0.08	0.10	0.10	0.11	0.10	0.08
Al	17.46	17.48	17.50	17.49	17.40	17.54	17.49	17.53	17.52	17.57	17.49	17.32	17.59	17.58	17.49	17.49	17.48	17.52	17.47	17.47	17.45
Fe	3.34	3.35	3.35	3.33	3.39	3.30	3.38	3.31	3.33	3.19	3.35	3.35	3.33	3.30	3.31	3.38	3.31	3.30	3.34	3.44	3.38
Mn	0.03	0.01	0.02	0.01	0.01	0.02	0.02	0.03	0.02	0.01	0.01	0.02	0.03	0.02	0.00	0.01	0.02	0.03	0.03	0.02	0.03
Mg	0.81	0.78	0.85	0.83	0.76	0.77	0.73	0.73	0.81	0.70	0.77	0.82	0.77	0.73	0.76	0.78	0.75	0.86	0.75	0.79	0.77
Ca	0.00	0.00	0.00	0.00	0.01	0.00	0.00	0.00	0.00	0.00	0.00	0.00	0.00	0.00	0.00	0.00	0.00	0.00	0.00	0.01	0.00
Zn	0.13	0.12	0.11	0.15	0.11	0.11	0.12	0.12	0.13	0.14	0.14	0.12	0.14	0.15	0.11	0.14	0.07	0.10	0.11	0.11	0.10
Total (All)	29.52	29.51	29.54	29.53	29.49	29.49	29.50	29.48	29.53	29.41	29.50	29.49	29.53	29.49	29.46	29.53	29.45	29.52	29.49	29.55	29.51
Total (Majors ONLY)	29.39	29.38	29.43	29.38	29.38	29.37	29.37	29.35	29.39	29.27	29.37	29.37	29.39	29.35	29.35	29.39	29.37	29.42	29.37	29.44	29.40
XMg (= Mg / (Mg + Fe)	0.19	0.19	0.20	0.20	0.18	0.19	0.18	0.18	0.19	0.18	0.19	0.20	0.19	0.18	0.19	0.19	0.19	0.21	0.18	0.19	0.18

Note: Analyses conducted on the same mineral grain (e.g. 1 core analysis and 2 rim analyses on a specific staurolite grain) are highlighted in the same colour and enclosed in the same thick black box.

Staurolites cont.

Analysis Label (Specimen_mineral_grain/zone:spot number)	gb13_st_8d	gb13_st_9b	gb13_st_9a	gb13_st_9d	gb13_st_9g	gb13_st_9h	gb13_st_7a	gb13_st_7b	gb13_st_7d	gb13_st_7k	gb13_st_7h	gb13_st_7j	gb13_st_14h	ma29_st_1h	ma29_st_1i	ma29_st_1w	ma29_st_1b	ma29_st_1g	ma29_st_1l	ma29_st_1n	ma29_st_1o
Mineral Probed:	st	st	st	st	st	st	st	st	st	st	st	st	st	st	st	st	st	st	st	st	st
Core/Int/Rim:	Core	Rim	Core	Rim	Rim	Core	Core	Rim	Core	Int	Core	Core	Core	Rim	Rim	Rim	Int	Int	Core	Core	Core
EMP Initial Results:																					
Oxide conc. (wt%)																					
SiO2	28.00	27.92	27.84	27.64	27.75	27.96	28.26	28.02	27.65	27.90	27.94	27.99	27.79	27.81	27.67	27.81	27.79	27.97	27.63	27.77	27.49
TiO2	0.50	0.41	0.46	0.56	0.55	0.53	0.34	0.49	0.46	0.45	0.43	0.52	0.47	0.64	0.64	0.57	0.54	0.64	0.65	0.61	0.64
Al2O3	53.97	54.19	54.09	54.30	54.35	54.05	54.16	54.13	54.64	53.73	54.10	54.79	54.06	54.65	55.09	55.32	54.74	54.35	54.51	54.25	54.54
FeO	14.36	14.54	14.91	14.37	14.78	14.76	14.24	14.72	14.64	14.74	14.71	13.93	15.00	13.80	13.96	13.71	13.90	14.00	13.83	13.81	13.75
MnO	0.12	0.09	0.10	0.14	0.03	0.07	0.05	0.11	0.05	0.05	0.13	0.08	0.12	0.12	0.08	0.10	0.05	0.09	0.11	0.13	0.12
MgO	1.99	2.01	2.08	1.93	1.96	1.98	1.73	1.84	2.02	2.00	2.00	1.84	1.90	1.50	1.46	1.72	1.66	1.76	1.80	1.78	1.81
CaO	0.01	0.01	0.00	0.02	0.02	0.02	0.01	0.00	0.00	0.00	0.00	0.00	0.01	0.02	0.00	0.00	0.02	0.01	0.00	0.00	0.02
ZnO	0.55	0.56	0.50	0.53	0.52	0.60	0.60	0.69	0.76	0.65	0.70	0.68	0.57	0.75	0.77	0.77	0.87	0.73	0.52	0.72	0.73
Total	99.49	99.73	99.98	99.49	99.95	99.97	99.39	100.00	100.22	99.52	100.01	99.83	99.93	99.29	99.68	100.01	99.56	99.54	99.06	99.08	99.09
Cations:																					
Si	7.68	7.65	7.62	7.59	7.59	7.65	7.75	7.67	7.55	7.67	7.65	7.64	7.62	7.63	7.57	7.57	7.61	7.66	7.59	7.64	7.56
Ti	0.10	0.09	0.09	0.12	0.11	0.11	0.07	0.10	0.09	0.09	0.09	0.11	0.10	0.13	0.13	0.12	0.11	0.13	0.13	0.13	0.13
Al	17.45	17.50	17.45	17.57	17.53	17.43	17.50	17.46	17.59	17.41	17.45	17.62	17.47	17.67	17.76	17.75	17.67	17.55	17.66	17.59	17.68
Fe	3.29	3.33	3.41	3.30	3.38	3.38	3.27	3.37	3.34	3.39	3.37	3.18	3.44	3.17	3.19	3.12	3.18	3.21	3.18	3.18	3.16
Mn	0.03	0.02	0.02	0.03	0.01	0.02	0.01	0.03	0.01	0.01	0.03	0.02	0.03	0.03	0.02	0.02	0.01	0.02	0.03	0.03	0.03
Mg	0.81	0.82	0.85	0.79	0.80	0.81	0.71	0.75	0.82	0.82	0.82	0.75	0.78	0.62	0.60	0.70	0.68	0.72	0.74	0.73	0.74
Ca	0.00	0.00	0.00	0.01	0.00	0.00	0.00	0.00	0.00	0.00	0.00	0.00	0.00	0.01	0.00	0.00	0.01	0.00	0.00	0.00	0.00
Zn	0.11	0.11	0.10	0.11	0.10	0.12	0.12	0.14	0.15	0.13	0.14	0.14	0.12	0.15	0.16	0.15	0.18	0.15	0.11	0.15	0.15
Total (All)	29.49	29.52	29.56	29.51	29.53	29.52	29.43	29.51	29.56	29.53	29.54	29.45	29.55	29.40	29.42	29.44	29.44	29.43	29.44	29.44	29.46
Total (Majors ONLY)	29.38	29.40	29.46	29.40	29.43	29.40	29.31	29.37	29.41	29.40	29.40	29.31	29.43	29.25	29.27	29.28	29.27	29.29	29.33	29.29	29.32
XMg (= Mg / (Mg + Fe)	0.20	0.20	0.20	0.19	0.19	0.19	0.18	0.18	0.20	0.19	0.20	0.19	0.18	0.16	0.16	0.18	0.18	0.18	0.19	0.19	0.19

Note: Analyses conducted on the same mineral grain (e.g. 1 core analysis and 2 rim analyses on a specific staurolite grain) are highlighted in the same colour and enclosed in the same thick black box.

Staurolites cont.

Analysis Label (Specimen_mineral grain/zone:spot number)	ma29_st_1c	ma29_st_1f	ma29_st_1q	ma29_st_1s	ma29_st_1t	ma29_st_1x	ma29_st_1p	ma29_st_1u	ma29_st_2c	ma29_st_2d	ma29_st_2e	ma29_st_2f	ma29_st_2p	ma29_st_2b	ma29_st_2g	ma29_st_2j	ma31_st_10d	ma31_st_10a	ma31_st_12x	ma38(a)_st_6c	ma38(a)_st_6a
Mineral Probed:	st	st	st	st	st	st	st	st	st	st	st	st	st	st	st	st	st	st	st	st	st
Core/Int/Rim:	Core	Core	Core	Core	Core	Int	Rim	Rim	Rim	Rim	Rim	Int	Core	Int	Rim	Rim	Rim	Core	Rim	Rim	Core
EMP Initial Results:																					
Oxide conc. (wt%)																					
SiO2	27.26	27.56	27.32	27.77	27.32	27.89	27.72	27.49	27.69	27.85	27.78	27.48	27.60	27.34	27.39	27.75	28.24	27.91	27.81	27.65	27.35
TiO2	0.61	0.79	0.50	0.53	0.50	0.44	0.52	0.58	0.67	0.53	0.50	0.54	0.51	0.45	0.57	0.62	1.02	0.52	0.57	0.51	0.54
Al2O3	55.01	54.87	54.90	54.45	54.85	54.98	54.70	54.45	54.71	54.86	54.62	54.88	55.13	55.60	55.43	55.50	54.97	54.87	55.56	54.81	55.71
FeO	13.96	13.90	13.82	13.73	13.65	13.87	14.17	13.81	14.18	13.90	13.86	13.86	13.64	13.62	14.02	13.84	13.56	13.61	13.83	13.68	14.01
MnO	0.07	0.07	0.10	0.13	0.17	0.07	0.10	0.15	0.12	0.13	0.14	0.08	0.10	0.09	0.12	0.06	0.14	0.14	0.16	0.20	0.20
MgO	1.79	1.71	1.72	1.82	1.72	1.80	1.67	1.72	1.58	1.60	1.52	1.59	1.56	1.68	1.53	1.53	1.88	1.87	1.91	2.19	2.23
CaO	0.00	0.02	0.01	0.00	0.02	0.00	0.01	0.02	0.00	0.00	0.01	0.00	0.01	0.02	0.01	0.00	0.02	0.00	0.02	0.01	0.01
ZnO	0.70	0.66	0.66	0.70	0.79	0.77	0.60	0.73	0.73	0.68	0.72	0.75	0.73	0.80	0.75	0.69	0.23	0.19	0.29	0.16	0.12
Total	99.41	99.57	99.04	99.14	99.01	99.82	99.49	98.95	99.68	99.55	99.16	99.19	99.28	99.60	99.83	99.99	100.06	99.12	100.14	99.20	100.18
Cations:																					
Si	7.48	7.54	7.52	7.63	7.52	7.61	7.60	7.58	7.58	7.62	7.63	7.55	7.57	7.48	7.49	7.55	7.66	7.64	7.55	7.57	7.43
Ti	0.13	0.16	0.10	0.11	0.10	0.09	0.11	0.12	0.14	0.11	0.10	0.11	0.10	0.09	0.12	0.13	0.21	0.11	0.12	0.10	0.11
Al	17.79	17.70	17.81	17.63	17.80	17.68	17.67	17.69	17.66	17.69	17.69	17.78	17.81	17.92	17.86	17.81	17.57	17.70	17.77	17.69	17.84
Fe	3.20	3.18	3.18	3.15	3.14	3.17	3.25	3.18	3.25	3.18	3.19	3.19	3.13	3.11	3.20	3.15	3.07	3.12	3.14	3.13	3.18
Mn	0.02	0.02	0.02	0.03	0.04	0.02	0.02	0.04	0.03	0.03	0.03	0.02	0.02	0.02	0.03	0.01	0.03	0.03	0.04	0.05	0.05
Mg	0.73	0.70	0.71	0.75	0.71	0.73	0.68	0.71	0.64	0.65	0.62	0.65	0.64	0.68	0.62	0.62	0.76	0.76	0.77	0.89	0.90
Ca	0.00	0.01	0.00	0.00	0.01	0.00	0.00	0.01	0.00	0.00	0.00	0.00	0.00	0.00	0.00	0.00	0.01	0.00	0.00	0.00	0.00
Zn	0.14	0.13	0.13	0.14	0.16	0.15	0.12	0.15	0.15	0.14	0.15	0.15	0.15	0.16	0.15	0.14	0.05	0.04	0.06	0.03	0.02
Total (All)	29.50	29.44	29.48	29.45	29.48	29.46	29.46	29.46	29.45	29.42	29.42	29.45	29.42	29.47	29.47	29.41	29.35	29.40	29.45	29.48	29.54
Total (Majors ONLY)	29.35	29.31	29.34	29.30	29.32	29.30	29.34	29.31	29.30	29.29	29.27	29.30	29.28	29.31	29.32	29.28	29.31	29.36	29.39	29.44	29.51
XMg (= Mg / (Mg + Fe)	0.19	0.18	0.18	0.19	0.18	0.19	0.17	0.18	0.17	0.17	0.16	0.17	0.17	0.18	0.16	0.17	0.20	0.20	0.20	0.22	0.22

Note: Analyses conducted on the same mineral grain (e.g. 1 core analysis and 2 rim analyses on a specific staurolite grain) are highlighted in the same colour and enclosed in the same thick black box.

Staurolites cont.

Analysis Label (Specimen_mineral_grain/zone:spot number)	ma38(a)_st_6d	ma38(a)_st_5a	ma38(a)_st_5b	ma38(a)_st_5c	ma38(a)_st_7c	ma38(a)_st_7b	ma38(a)_st_7d	ma38(a)_st_4d	ma38(a)_st_4b	ma38(a)_st_4a	ma38(a)_st_1d	ma38(b)_st_2l	ma38(b)_st_2i	ma38(b)_st_2j	ma38(b)_st_2k	ma38(b)_st_2h	ma38(b)_st_2f	ma38(b)_st_2e	ma38(b)_st_2d	ma38(b)_st_2c	ma38(b)_st_2a
Mineral Probed:	st	st	st	st	st	st	st	st	st	st	st	st	st	st	st	st	st	st	st	st	st
Core/Int/Rim:	Rim	Rim	Int	Rim	Rim	Int	Rim	Rim	Int	Core	Rim	Rim	Core	Rim	Core	Rim	Int	Core	Rim	Int	Core
EMP Initial Results:																					
Oxide conc. (wt%)																					
SiO2	27.54	27.67	27.89	27.73	28.14	27.75	27.49	27.68	27.30	27.64	27.55	26.80	26.85	27.76	27.47	27.76	27.49	27.45	27.56	27.60	26.69
TiO2	0.69	0.62	0.64	0.49	0.67	0.71	0.66	0.61	0.49	0.45	0.68	0.66	0.37	0.49	0.40	0.78	0.75	0.48	0.54	0.47	0.35
Al2O3	54.67	55.05	54.75	55.13	54.69	54.41	55.51	54.97	55.67	55.43	55.07	56.05	56.30	55.44	55.53	55.16	54.86	55.36	55.70	55.11	55.94
FeO	13.85	14.06	13.95	13.75	13.73	13.87	13.70	13.68	13.89	14.01	14.16	13.87	13.64	13.66	13.71	13.53	13.97	13.75	13.78	13.77	13.77
MnO	0.18	0.16	0.10	0.18	0.20	0.20	0.19	0.20	0.20	0.20	0.20	0.18	0.20	0.16	0.17	0.14	0.21	0.18	0.16	0.17	0.20
MgO	2.21	1.85	2.13	1.92	1.89	2.03	1.71	2.09	2.13	2.14	2.13	2.10	1.96	2.00	2.11	2.21	2.02	1.98	2.03	2.08	1.95
CaO	0.02	0.00	0.00	0.00	0.01	0.00	0.01	0.00	0.00	0.01	0.01	0.01	0.01	0.01	0.00	0.01	0.01	0.00	0.00	0.00	0.00
ZnO	0.03	0.20	0.05	0.03	0.19	0.18	0.07	0.22	0.14	0.13	0.16	0.20	0.27	0.21	0.19	0.12	0.22	0.20	0.25	0.23	0.13
Total	99.19	99.61	99.51	99.23	99.53	99.15	99.34	99.46	99.83	100.01	99.96	99.86	99.60	99.74	99.58	99.71	99.52	99.40	100.02	99.43	99.03
Cations:																					
Si	7.55	7.56	7.61	7.58	7.68	7.61	7.51	7.56	7.44	7.52	7.51	7.31	7.33	7.56	7.49	7.55	7.52	7.50	7.49	7.54	7.33
Ti	0.14	0.13	0.13	0.10	0.14	0.15	0.14	0.13	0.10	0.09	0.14	0.13	0.08	0.10	0.08	0.16	0.16	0.10	0.11	0.10	0.07
Al	17.66	17.72	17.62	17.77	17.59	17.59	17.88	17.70	17.88	17.77	17.69	18.01	18.12	17.79	17.86	17.69	17.69	17.84	17.84	17.76	18.11
Fe	3.17	3.21	3.18	3.14	3.13	3.18	3.13	3.13	3.16	3.19	3.23	3.16	3.11	3.11	3.13	3.08	3.20	3.14	3.13	3.15	3.16
Mn	0.04	0.04	0.02	0.04	0.05	0.05	0.05	0.05	0.05	0.05	0.05	0.04	0.05	0.04	0.04	0.03	0.05	0.04	0.04	0.04	0.05
Mg	0.90	0.75	0.87	0.78	0.77	0.83	0.70	0.85	0.87	0.87	0.87	0.85	0.80	0.81	0.86	0.90	0.82	0.81	0.82	0.85	0.80
Ca	0.01	0.00	0.00	0.00	0.00	0.00	0.00	0.00	0.00	0.00	0.00	0.00	0.00	0.00	0.00	0.00	0.00	0.00	0.00	0.00	0.00
Zn	0.01	0.04	0.01	0.01	0.04	0.04	0.01	0.04	0.03	0.03	0.03	0.04	0.05	0.04	0.04	0.02	0.04	0.04	0.05	0.05	0.03
Total (All)	29.48	29.45	29.45	29.43	29.39	29.45	29.41	29.46	29.52	29.51	29.51	29.55	29.54	29.45	29.50	29.44	29.48	29.48	29.48	29.48	29.54
Total (Majors ONLY)	29.47	29.41	29.44	29.42	29.35	29.41	29.40	29.42	29.49	29.48	29.48	29.51	29.48	29.41	29.46	29.42	29.43	29.44	29.43	29.43	29.52
XMg (= Mg / (Mg + Fe)	0.22	0.19	0.21	0.20	0.20	0.21	0.18	0.21	0.21	0.21	0.21	0.21	0.20	0.21	0.22	0.23	0.20	0.20	0.21	0.21	0.20

Note: Analyses conducted on the same mineral grain (e.g. 1 core analysis and 2 rim analyses on a specific staurolite grain) are highlighted in the same colour and enclosed in the same thick black box.

Staurolites cont.

Analysis Label (Specimen_mineral_grain/zone:spot number)	ma38(b)_st_2b	ma38(b)_st_1e	ma38(b)_st_1b	ma38(b)_st_1d	ma38(b)_st_1a	ma38(b)_st_1c	ma40_st_1b	ma40_st_1a	ma40_st_1e	ma40_st_1d	ma40_st_1g	ma40_st_1j	ma40_st_1l	ma40_st_1n	ma40_st_1s
Mineral Probed:	st	st	st	st	st	st	st	st	st	st	st	st	st	st	st
Core/Int/Rim:	Rim	Rim	Int	Core	Core	Rim	Int	Core	Int	Core	Rim	Core	Core	Int	Core
EMP Initial Results:															
Oxide conc. (wt%)															
SiO2	27.71	28.22	27.45	27.41	27.78	28.03	28.02	27.57	27.81	27.71	27.88	27.81	27.72	27.04	27.46
TiO2	0.55	0.52	0.56	0.45	0.53	0.48	0.50	0.43	0.61	0.57	0.67	0.50	0.53	0.49	0.56
Al2O3	54.83	54.99	55.16	55.11	54.98	55.45	54.76	55.89	55.23	55.15	55.49	55.49	55.09	56.13	56.12
FeO	13.95	13.63	13.81	14.02	13.79	13.61	13.35	13.38	13.27	13.22	13.20	13.10	13.40	13.14	13.07
MnO	0.16	0.14	0.20	0.16	0.19	0.23	0.19	0.10	0.10	0.18	0.16	0.17	0.14	0.12	0.17
MgO	1.95	2.07	1.98	1.97	2.03	1.87	1.67	1.71	1.64	1.64	1.35	1.49	1.53	1.58	1.37
CaO	0.00	0.00	0.01	0.00	0.01	0.01	0.01	0.01	0.01	0.00	0.02	0.01	0.01	0.01	0.01
ZnO	0.27	0.28	0.28	0.28	0.24	0.26	0.55	0.57	0.59	0.53	0.53	0.44	0.58	0.54	0.60
Total	99.41	99.85	99.45	99.40	99.54	99.95	99.05	99.66	99.25	99.01	99.29	99.01	98.99	99.05	99.37
Cations:															
Si	7.58	7.67	7.51	7.51	7.59	7.61	7.68	7.51	7.60	7.59	7.61	7.61	7.60	7.41	7.49
Ti	0.11	0.11	0.12	0.09	0.11	0.10	0.10	0.09	0.13	0.12	0.14	0.10	0.11	0.10	0.11
Al	17.69	17.62	17.79	17.79	17.70	17.75	17.69	17.95	17.80	17.82	17.86	17.89	17.81	18.12	18.05
Fe	3.19	3.10	3.16	3.21	3.15	3.09	3.06	3.05	3.03	3.03	3.01	3.00	3.07	3.01	2.98
Mn	0.04	0.03	0.05	0.04	0.04	0.05	0.04	0.02	0.02	0.04	0.04	0.04	0.03	0.03	0.04
Mg	0.80	0.84	0.81	0.80	0.83	0.76	0.68	0.69	0.67	0.67	0.55	0.61	0.62	0.65	0.56
Ca	0.00	0.00	0.00	0.00	0.00	0.00	0.00	0.00	0.00	0.00	0.00	0.00	0.00	0.00	0.00
Zn	0.05	0.06	0.06	0.06	0.05	0.05	0.11	0.11	0.12	0.11	0.11	0.09	0.12	0.11	0.12
Total (All)	29.46	29.42	29.48	29.50	29.46	29.42	29.37	29.43	29.37	29.38	29.32	29.34	29.38	29.43	29.37
Total (Majors ONLY)	29.41	29.36	29.43	29.45	29.41	29.36	29.26	29.31	29.25	29.27	29.21	29.25	29.26	29.32	29.24
XMg (= Mg / (Mg + Fe)	0.20	0.21	0.20	0.20	0.21	0.20	0.18	0.19	0.18	0.18	0.15	0.17	0.17	0.18	0.16

Note: Analyses conducted on the same mineral grain (e.g. 1 core analysis and 2 rim analyses on a specific staurolite grain) are highlighted in the same colour and enclosed in the same thick black box.